

MANUAL FOR

**WEDGE SHEAR TESTING OF SOILS**

**T. Mirata, MSc(Eng), Ph.D, DIC, MICE**

Professor of Civil Engineering  
Middle East Technical University  
ANKARA

**March 2004**

To my wife, daughter, and son

First version: July 1998

Updated with slight revisions: June 1999

Second update with minor corrections: August 1999

Third update with minor corrections: April 2000

Fourth update with minor corrections: July 2002

Fifth update with correction of a web address in references: February 2003

Last update with minor corrections: March 2004

#### **NOTE**

All revisions and corrections since the first version can be traced from one of the following web sites

<http://www.metu.edu.tr/~mirata>

<http://www.ce.metu.edu.tr/~mirata/>

by clicking on ‘Publications in English’ and ‘corrigenda’. Possible further corrections will also be posted on the same sites.

# CONTENTS

<b>PREFACE</b> .....	vii
<b>1. INTRODUCTION</b> .....	1
<b>1.1 Development of the test</b> .....	1
<b>1.2 Fields of application</b> .....	5
1.2.1 Short term stability of slopes in stiff fissured and/or stony unsaturated clays .....	5
1.2.2 Stability of slopes in silty gravel .....	6
1.2.3 Shear strength of gravel and rockfill material .....	6
1.2.4 Compaction control and stability of clay fills .....	7
1.2.5 Residual and ultimate strength measurements .....	7
1.2.6 As an alternative to penetration tests in clays .....	8
1.2.7 For the effective stress stability analysis of jointed unsaturated clays .....	8
1.2.8 For the short term stability of saturated clays .....	8
<b>2. PRINCIPLES OF EVALUATION</b> .....	13
<b>2.1 Principles of analysis for stresses and displacements</b> .....	13
2.1.1 Analysis A .....	13
2.1.2 Analysis B .....	16
2.1.3 Analysis C .....	17
<b>2.2 Calculation of <math>Q</math> to keep <math>\sigma</math> around its value at peak strength</b> .....	18
<b>2.3 Miscellaneous calculations</b> .....	19
<b>3. COMPUTER PROGRAMS FOR DETAILED EVALUATION     OF WEDGE SHEAR TESTS</b> .....	26
<b>3.1 Introduction</b> .....	26
<b>3.2 The program IWPW77</b> .....	27
3.2.1 Input data for the program IWPW77 .....	27
3.2.2 Output of the program IWPW77 .....	32

3.2.2.1	Common data for all tests and constants for each test .....	32
3.2.2.2	Values output for each test .....	34
3.2.2.3	Values output for a series of tests when regression is possible and desired .....	37
3.2.2.4	Other values output .....	39
3.2.2.5	Values output when a check of the data is desired or due to faulty data .....	39
<b>3.3</b>	<b>The program CYLWEE88 .....</b>	<b>40</b>
3.3.1	Input data for program CYLWEE88 .....	40
3.3.2	Output of the program CYLWEE88 .....	45
3.3.2.1	Common data for all tests and constants for each test .....	46
3.3.2.2	Values output for each test .....	47
3.3.2.3	Other values output .....	48
<b>4.</b>	<b>APPARATUS, TEST PROCEDURES AND RUNNING</b>	
	<b>THE PROGRAMS .....</b>	<b>61</b>
<b>4.1</b>	<b>Introduction .....</b>	<b>61</b>
<b>4.2</b>	<b>In situ wedge shear test .....</b>	<b>61</b>
4.2.1	Apparatus for iswests without lateral load application .....	61
4.2.1.1	Equipment for supporting the sides of the test pit .....	61
4.2.1.2	Special equipment .....	62
4.2.1.3	Devices that can be easily made .....	63
4.2.1.4	Equipment available commercially .....	65
4.2.2	Additional apparatus for iswests with lateral load application .....	66
4.2.3	Test procedure .....	66
<b>4.3</b>	<b>Prismatic wedge shear test .....</b>	<b>71</b>
4.3.1	Apparatus .....	71
4.3.2	Preparation of the sample .....	71
4.3.2.1	By vibratory compaction (for clean gravels and crushed rock) ...	71
4.3.2.2	By static compaction (for clayey gravels) .....	72
4.3.3	Test procedure .....	73
<b>4.4</b>	<b>Cylindrical wedge shear test .....</b>	<b>77</b>
4.4.1	Apparatus .....	77

4.4.2 Preparation of the sample .....	77
4.4.2.1 Undisturbed samples .....	77
4.4.2.2 Compacted samples .....	78
4.4.3 Test procedure .....	80
<b>4.5 Evaluation of results .....</b>	<b>85</b>
<b>4.6 Sample data files .....</b>	<b>86</b>
<b>5. DETAILS OF THE APPARATUS .....</b>	<b>102</b>
<b>5.1 Introduction .....</b>	<b>102</b>
<b>5.2 Drawings of apparatus for the in situ wedge shear test .....</b>	<b>102</b>
5.2.1 Test moulds .....	102
5.2.2 Grooved loading plates .....	103
5.2.3 Lateral loading device .....	103
<b>5.3 Drawings of apparatus for the cylindrical wedge shear test .....</b>	<b>104</b>
<b>5.4 Drawings of apparatus for the prismatic wedge shear test .....</b>	<b>107</b>
5.4.1 General .....	107
5.4.2 High load capacity grooved plates .....	108
5.4.3 Measurement of the coefficient of friction for the grooved plates .....	110
5.4.4 Modifying test moulds for higher normal stress ranges .....	111
<b>APPENDIX 1. EQUATIONS FOR DETAILED EVALUATION OF</b>	
<b>CYLWESTS .....</b>	<b>142</b>
A1.1 Corrected area of shear .....	142
A1.2 Distribution of normal stress along the failure plane .....	142
A1.3 Co-ordinates of the centre of gravity of test mould and soil wedge .....	145
<b>APPENDIX 2. MOMENT EQUATIONS .....</b>	<b>146</b>
A2.1 For Analyses A and B .....	146
A2.2 For Analysis C .....	147
<b>APPENDIX 3. ITERATIVE CALCULATION OF <math>\bar{u}, \bar{v}</math> and <math>\beta</math> .....</b>	<b>148</b>
<b>APPENDIX 4. CALCULATION OF <math>\overline{A_1 B_1}</math> and <math>\alpha_i</math> .....</b>	<b>149</b>
<b>APPENDIX 5. DERIVATION OF CURVES IN FIG. 2.4 .....</b>	<b>150</b>
<b>APPENDIX 6. CALCULATOR PROGRAMS FOR THE SIMPLIFIED</b>	
<b>EVALUATION OF THE WEDGE SHEAR TEST AND FOR</b>	

KEEPING $\sigma \approx \sigma_f$ AFTER PEAK STRENGTH .....	151
A6.1 Introduction .....	151
A6.2 Data sheets for the simplified evaluation of the wedge shear test .....	152
A6.3 Input / Output forms for the simplified evaluation of the wedge shear test .....	153
A6.4 Input / Output forms for calculations for keeping $\sigma \approx \sigma_f$ after peak strength .....	156
Calculator program I .....	158
Calculator program II .....	159
Calculator program III .....	160
Calculator program IV .....	161
<b>REFERENCES</b> .....	162
<b>ABBREVIATIONS</b> .....	165
<b>INDEXES OF</b>	
Boxes .....	165
Definition of program variables .....	166
Definition of symbols .....	167
Equations .....	169
Figures .....	169
Forms .....	170
Notes .....	170
Tables .....	170

## PREFACE

Despite its many shortcomings the  $\phi = 0$  analysis is presented practically in all books on soil mechanics, and the method still widely used in practice for the short-term stability problems of saturated clays. For unsaturated clays, the lower the degree of saturation, the more advantage there is in treating the problem in terms of total stresses: firstly because a treatment in terms of effective stresses becomes progressively more difficult to apply; secondly because the pore water pressures become increasingly less sensitive to such factors as the changes in normal stress, the stress path, the magnitude of the intermediate principal stress, and the orientation of principal stresses at failure, all of which have a marked effect on the pore pressures developed in saturated clays. Being able to perform an analysis in terms of total stresses is particularly relieving for fissured and/or stony clays which require a larger area than in the usual laboratory tests for a representative assessment of shear strength. Besides their other possible uses, the tests described in this manual are hoped to enhance the advantageous use of the total stress analysis for unsaturated clays.

The in situ wedge shear test (iswest) was born in 1971 out of a need for a simpler test than the large-scale in situ shear box test for testing unsaturated clays. In succeeding years the test was adapted to be performed on undisturbed or compacted cylindrical samples of clay, and more recently it has been demonstrated that the cylindrical wedge shear test (cylwest) can be applied to granular soils as well. A larger version of this set-up (priswest) has been successfully applied to the testing of prismatic samples of gravel, crushed rock and clay containing particles up to 40 mm.

This manual is intended to enable the reader to have the necessary special equipment made, and to perform and evaluate all three versions of the wedge shear test. A diskette containing the relevant computer programs and typical input data is to be found in the pocket inside the back cover. For ease of reproduction, enclosed in the same pocket will be found additional copies of the data sheets devised for use both during the tests for entry of data and in the preparation of the input file for the relevant computer program.

Looking through the completed manual, it is easy to become discouraged by the amount of information that had to be given for the tests, which are claimed to be 'simple'. The fact is that, for practical purposes, the first eleven equations, and the first two calculator programs given in Appendix 6 are adequate to evaluate the tests. A possible further simplification is mentioned in Chapter 2. The detailed equations and the computer programs

would initially be preferred by the researcher who would like a more rigorous evaluation of the tests. In this latter case it may be relieving to know that, for a given set of equipment, once the basic data about the equipment is entered into an input file, these can be recovered and used for subsequent tests, with very few values to be altered in each test. As regards the sets of readings during the test, these can be kept to a minimum, depending on the purpose for which the tests are carried out. In short, once the reader becomes familiar with the given programs, their use may be preferred even to the simplest manual calculations.

The work described here is the result of research carried out at the Middle East Technical University (METU) between 1969 and 1998, entailing nearly 20 000 hours of work on the part of the Author alone. Most of the special devices were made in the General Workshops of METU, and the valuable efforts of the many technicians who have made these devices, and of those who have helped with the testing; the help of many staff members\*, administrators, research assistants, typists, and draftsmen; the contributions by the research students, who have helped apply some of the recent developments are gratefully acknowledged. For their help with difficulties encountered in composing the bulk of this manual on the PC, special thanks are due to Assistants O. Çalışan, M. Mirata, O. Sonuvar, and Ö. Yüncü, and to his daughter, E. Mirata. The research was supported at different stages by the Scientific and Technical Research Council of Turkey under project nos. MAG-277 and INTAG-702, and by the METU Research Fund under project nos. AFP-90-03-03-03, AFP-93-03-03-01, and AFP-96-03-03-03. Since the preparation of the first version of the manual in July 1998, three related papers have been published in the Electronic Journal of Geotechnical Engineering (freely accessible at <http://www.ejge.com/>), open to the criticisms and other contributions of the reader. The manual has been revised to include these and another recent reference as well as a number of minor corrections.

A 50-minute, semi-professional video film, showing the different stages of all three versions of the wedge shear test, can be viewed at the METU and ICE (London) libraries.

*19 February, 2003*

T.M.

*e-mail: mirata@metu.edu.tr*

\* The Author is indebted to Dr. Engin Karaesmen for help with the correct calculation of the coefficient of correlation for regression forced through the origin.



# CHAPTER 1

## INTRODUCTION

### 1.1 Development of the test

Instability of slopes in unsaturated clays above the water table may generally be caused by

- (a) a cut or a fill being made with no change in the water content of the soil;
- (b) the gradual infiltration of water into the mass of clay, decreasing the pore water suctions;
- (c) surface water penetrating and exerting full hydrostatic pressures in joints and fissures, while suctions may continue to exist in intact lumps of the clay (e.g., Esu, 1966).

Problems (a) and (b) may be analyzed in terms of effective stresses, or, if the stress and pore pressure conditions in the shear test are close to those in the stability problem, in terms of total stresses. For problem (c) the former approach has to be used, but if the effective cohesion  $c'$  is neglected, the knowledge of the effective angle of friction  $\phi'$  alone enables a conservative estimate of the factor of safety to be obtained.

As the degree of saturation  $S_r$  of the clay falls below about 90 %, and hence the shear strength stops being controlled primarily by the pore water pressure  $u_w$  (Bishop & Henkel, 1962), testing and analysis in terms of effective stresses become more intricate and lengthy. Nevertheless this is the more rigorous approach, and notable advances have been made in this field in recent decades (see, e.g., Fredlund & Rahardjo (1993), Khalili & Khabbaz (1998)).

That a somewhat less rigorous, but certainly simpler and more direct approach is possible for stiff, unsaturated clays can be seen by examining Fig. 1.1. The curves in Fig. 1.1(a) are examples of the variation of  $u_w$  with all-round pressure  $\sigma_3$ , measured on 36 mm diameter triaxial specimens of the stiff fissured Ankara Clay (liquid limit  $w_L = 76$  %; plastic limit  $w_P = 30$  %; clay fraction  $C_F = 56$  %;  $S_r = 96$  %) at two different moisture contents  $w$ . (To give an idea about the time involved in such determinations, it may be noted that each point on these curves has taken 3 to 5 days for the equalization of pore water pressures with the measurement system.) These curves represent the range of over

twenty similar curves obtained by the Author for undisturbed and compacted samples of plastic clays with  $90 \% < S_r < 98 \%$ . Similar curves have been presented for compacted plastic clays by Vaughan et al. (1978). Provided the scatter in test results enables an undrained shear strength envelope, such as the dotted curve in Fig. 1.1(b), to be obtained over a range of normal stresses under which  $u_w$  is negative, and the  $\sigma_3$  against  $u_w$  curve fairly flat, the following may be deduced from Fig. 1.1 for such and all drier clays:

(i)  $S_r$  will not change appreciably during the test and a linear envelope is obtainable;

(ii) the peak undrained shear strength parameters ( $c$ ,  $\phi$ ) can be measured at the natural water content in a shear box test, irrespective of the drainage conditions and the rate of testing, provided this is slow enough to minimize rheologic effects, as negative pore pressures cannot dissipate unless the soil is brought into contact with free water;

(iii) Skempton's (1954) pore pressure coefficient  $B$ , which enters the expression for pore pressure changes due to shear as a multiplier, will be so low that the contribution of  $u_w$  to shear strength will be practically constant for all points on such an envelope, so that the measured  $\phi$  will be nearly equal to, but somewhat less than,  $\phi'$  measured over a similar range of normal stresses (cf. the dotted and full envelopes in Fig. 1.1(b));

(iv) for the same reasons as at (iii), the measured  $c$ ,  $\phi$  will be applicable to a slope where the range of normal stresses are close to those in the shear test.

So stability problems such as (a) to (c) may be solved simply and reasonably accurately through undrained tests. This approach becomes even more advantageous when studying fissured and/or stony clays, which require a larger area of shear than in usual laboratory tests for representative measurement of shear strength. In fissured clays it is further desirable to measure the strength in a direction compatible with the stability problem at hand, due to the tendency of joints and fissures to concentrate around certain orientations (McGown et al., 1977). Performing such tests in situ helps to minimize the effects of sampling disturbance.

The above requirements of low stress range, large area, prescribed shear plane, and in situ testing can be met by the large in situ shear box test, or its simpler and more versatile alternative, the in situ wedge shear test (*iswest*). The *iswest* (Mirata, 1974) entails the shearing of a wedge of soil encased in a 10 mm thick steel mould TM (Fig. 1.2) by means of a single hydraulic jack HJ acting through two grooved plates LP1

and LP2 with a ball cage BC carrying thirty 12-mm dia. steel balls in between, and reacting against a steel plate through a single ball SB. By varying the mould angle  $\alpha_n$  in different tests, the normal stress can be varied, and a shear strength envelope obtained over about the same range of normal stresses as in a critical slope of the soil being tested.

Tried successfully on a number of slips in the stiff, fissured, unsaturated Ankara Clay (Mirata, 1974) and shown to yield more reliable and more consistent values of factor of safety than effective stress analyses (assuming effective stress  $\sigma' = \sigma - u_w$ ), based on the results of tests on small laboratory specimens (Mirata, 1976, 1979, 1980), the iswest has since been tried by an independent researcher in a number of soils ranging from clays to silty sands and silty gravels (Cascini, 1980, 1983, 1985, 1992). He reports good agreement between the results of iswests and 60 mm square (Cascini, 1988) shear box tests for the finer soils, and consistency with existing vertical cuts in the silty gravel, and emphasizes the "extreme simplicity" of the test.

The iswest derives its relative simplicity mainly from the fact that a single jack is used to apply both the normal and the shear stress on the failure plane, the soil itself being used to provide the necessary reaction; the need for tons of dead loading as in a large-scale in situ shear box test is thus eliminated. This simplifying feature of the test has led to a number of developments (Mirata, 1991, 1992), and although in these, and the improved version of the iswest, aimed at measuring the strength at large strains under about the same normal stress as at peak strength, a relatively small lateral load is applied, all three versions of the wedge shear test are still simpler, and the required equipment cheaper than comparable alternative tests.

The first version of the iswest was the cylindrical wedge shear test (*cylwest*), developed for enabling samples taken from boreholes to be tested without the risk of entering a test pit in an active landslide to perform an in situ test. The test can be applied either by using an available compression machine (Fig. 1.3), or by the use of a simple, portable frame (Fig. 5.5). In this test, the sample is introduced into a cylindrical mould, consisting of a stationary part TM(S) and a mobile part TM, made of a thin-walled sampling tube by cutting this at the desired angle  $\alpha_n$  to its axis. The upper part of

the shear plane of TM(S), and the lower part of the shear plane of TM are chamfered slightly\* to prevent the soil in the opposite half from bearing on the test mould wall during shear. TM(S) is clamped on the cross beam of an existing compression machine or portable frame, and the grooved loading plates LP1 and LP2 with the ball cage BC in between are mounted in position as in Fig. 1.3 or 5.5. The spacers and screws holding the two parts of the mould together are removed, dial gauges are set to record the displacements of TM, and the soil sheared as in the iswest. The double cut test mould shown in Fig. 1.4 enables compacted clays, sands or gravels, containing particles up to 10 mm, to be tested in the same mould in which they have been compacted. By replacing the removable disc RD, in the middle plate MP of the frame in Fig. 5.5, with rings of the appropriate inner diameter, this frame can be used to extrude samples from sampling tubes directly into the test mould placed between MP and the upper plate UP of the frame, or into a core cutter of the appropriate size before introduction into the test mould.

The prismatic wedge shear test (*priswest*) (Fig. 3.1), is a larger version of the cylwest, enabling prismatic specimens of gravel, crushed rock or clay containing up to 40 mm particles to be tested, using a portable frame. The 20-ton version of the frame for priswests (Figs 5.15, 5.16) and all the necessary equipment weigh about 250 kg, a quarter of the weight of a shear box apparatus with an equal shear plane area, and can be procured for about 20 % of the price of the latter.

The priswest mould is made of 10-mm thick mild steel plate, and consists of two identical halves, each with a shear plane measuring 300 mm x 300 mm internally. The mobile half TM has a removable lid; the stationary half TM(S) is bolted on the lower beam of the frame (Fig. 3.1(b)). Initially, the two halves of the mould are bolted together through four pairs of links LK with spacers SR screwed in the middle, and the lid on TM is replaced by a 70 mm high collar (Fig. 3.1(a)) while the sample is placed in the mould. In the 20-ton version of this frame (Figs 5.15, 5.16), the test mould can be easily detached, and rotated through 90° for static compaction of clayey soils. The collar is then removed, and the lid bolted on to TM. The lateral loading device, which consists of a spring loaded piston, or preferably an air piston, carrying a proving ring is mounted in position, and a small load applied. If granular material is to be tested, loading is best carried out with the frame in the horizontal position as in Fig. 4.7. For cohesive soils,

---

\* See, e.g., detail A in Fig 1.4.

the spacer on the left of Fig. 3.1(a) is removed, and the frame turned into the upright position shown in Fig. 3.1(b), if dynamic compaction has been used; otherwise, the frame is always kept in the upright position. The rest of the loading devices, identical with those in the iswest, are then assembled; the spacers are removed, and displacement dials mounted in position. The lateral load  $Q$  is gradually increased to the desired initial value, increasing the main load  $P$ , applied through the hydraulic jack, by about equal amounts.  $Q$  is then kept constant while  $P$  is gradually increased until failure occurs. Thereafter,  $Q$  is adjusted to keep the normal stress at about the value at peak strength.

The principles of evaluation of the test is given in Chapter 2, followed in Chapter 3 by the user's guide to two separate computer programs for the detailed evaluation of the test, one for iswests or priswests, the other for cylwests. The apparatus, and the detailed test procedures are given in Chapter 4, together with instructions for running the relevant computer programs, and typical data files from past applications of the tests. The detailed drawings and relevant explanations to facilitate the making of some of the special equipment are given in Chapter 5. Appendices contain equations used in the detailed evaluation, and examples of calculator programs for the simplified evaluation of the tests, and the calculations needed to adjust the lateral load to keep the normal stress at about its value at peak strength. The list of references, and abbreviations, used mostly on the forms and some tables, follow. Indexes are provided for the definitions of symbols and program variables, and for the boxes, equations, figures, forms, notes, and tables referred to in the text. Possible areas where the tests may be used advantageously is summarized in the next subsection.

## **1.2 Fields of application**

The possible fields of application of the wedge shear tests are given below, generally in the order of the degree of advantage they provide over existing methods of testing and analysis.

### **1.2.1 Short term stability of slopes in stiff fissured and/or stony unsaturated clays**

From the discussion at the beginning of section 1.1, it emerges that the ease with which the iswest can be applied and the relatively low scatter of test results offer the total stress type of stability analysis for the short term stability of slopes in unsaturated clays as an advantageous alternative to the more sophisticated effective stress approach.

Striking examples of the application of the iswest for such problems have been published (Mirata, 1974), and the results compared with estimates in terms of effective stresses using the results of triaxial tests on small laboratory specimens (Mirata, 1976, 1979, 1980). In the study of the three slips in the stiff, fissured, unsaturated Ankara Clay by the former method, the iswests were performed to conform to the change in normal stress as well as the orientation of the failure plane with depth in the actual slips, this probably contributing to the relative success of the estimates of factor of safety  $F_s$  (an average overestimate of 9 %, with a standard deviation  $s$  of 0.03). Carrying out such a study using conventional in situ shear box tests would have been practically impossible. Effective stress analyses of the same slips using the results of triaxial tests on 36-mm dia. specimens gave an average overestimate of  $F_s$  of 85 % with  $s = 0.34$ , this overestimate being 53 % for one of the slips, when 102-mm dia. specimens were used. Iswest results used in a total stress type of stability analysis clearly give more reliable and consistent estimates of factor of safety than effective stress analyses based on the results of tests on small laboratory specimens in such material.

### **1.2.2 Stability of slopes in silty gravel**

Cascini (1985) has applied the iswest to the measurement of the in situ shear strength of silty gravels, and reported good agreement with the strength exhibited in steep cuts in such material. As the strength measured in such free-draining material reflects both the undrained and the drained strength, the results can be used for short-term as well as long-term stability of such slopes.

### **1.2.3 Shear strength of gravel and rockfill material**

Priswest results on 5 mm - 10 mm gravel have been compared with those of drained triaxial tests on 102-mm dia. triaxial specimens by Mirata (1991). Further comparisons between priswests on < 38 mm gravel and crushed rock and triaxial tests on 191-mm dia. specimens have recently been published by Tosun et al. (1999). The normal stress in the priswests was generally below 200 kPa, and the degree of compaction was

about 70 %. The low range of normal stresses enabled a linear shear strength envelope to be obtained, and the relatively low degree of compaction, minimized differences arising from the fact that the priswest is more nearly a plane strain type of test. Forcing regression through the origin for comparison, the ratio  $\phi_{pw} / \phi_{tr}$  of the angle of friction  $\phi_{pw}$  measured in priswests to the corresponding value  $\phi_{tr}$  obtained from drained triaxial tests ranged between 0.96 and 1.09 for the 8 different samples tested (with an average of 1.014 and  $s = 0.043$ ). The priswests giving slightly higher values is in agreement with the findings of other investigators (see, e.g., Charles & Watts, 1980) that plane strain tests give higher strengths than triaxial tests on such materials. The advantage of the priswest over the triaxial or even the conventional shear box test of the same (300 mm x 300 mm) area of shear is that the equipment needed to perform the priswest is much lighter, portable, and much cheaper. The shear strength properties of rockfill material can thus be verified on the spot, as the material is being quarried.

#### **1.2.4 Compaction control and stability of clay fills**

The use of shear strength as a means of compaction control of clay fills has been more widely used in recent decades (e.g., Kennard et al., 1978). However, the practice so far has been to base such measurements on undrained triaxial tests under a specified cell pressure. Tests performed in collaboration with Öktem (1984), Varan (1989), Seçkin (1993), and Gün (1997) have shown that in less than the time required for a single quick triaxial test, two cylwests can be performed on site using a simple portable frame, yielding with sufficient accuracy for practical purposes (Mirata et al., 1999), both the  $c$  and  $\phi$  values, which are more meaningful for such unsaturated soils. For fills containing particles up to 38 mm and/or fissures (see, e.g., Vallejo, 1987) with spacing greater than 10 mm, the priswest can be used for a similar purpose, and the iswest can yield reliable in-situ values of shear strength. The measured parameters can be used for reliable estimates of the short-term stability of the slopes.

#### **1.2.5 Residual and ultimate strength measurements**

Cylwests performed in collaboration with Seçkin (1993) on compacted clays have shown that the measurement of residual strength is possible if re-shear tests on pre-cut planes are performed, as in similar shear box tests. The shear strength at large displacements on first loading in iswests, with an initial area of shear  $A_n$  of 900 cm<sup>2</sup>

seems to be in good agreement with re-shear cylwests ( $A_n = 100 \text{ cm}^2$ ) and shear box tests ( $A_n = 32 \text{ cm}^2$ ) with the failure surfaces smoothed and cleared of stones (Mirata, 1991).

On the other hand, there is no ambiguity about the measurement of the ultimate shear strength of gravel and crushed rock in priswests (Mirata, 1991), and of fine gravel and gravelly sand with  $< 10 \text{ mm}$  particles in cylwests (Mirata & Gökalp, 1997), provided the test is prolonged until the rate of dilation is reduced to zero.

### **1.2.6 As an alternative to penetration tests in clays**

Instead of performing penetration tests in clays and then trying to correlate these with the shear strength of the soil, it appears much more rational to take 100-mm dia. undisturbed samples, and without having to seal or ship them to a laboratory, to use the portable frame (Fig. 5.5) to extrude these into the cylwest mould, and then shear the soil along a number of different planes using different lateral loads to yield the shear strength envelope.

### **1.2.7 For the effective stress stability analysis of jointed unsaturated clays**

Based on the discussion at the beginning of section 1.1, the  $\phi$  values measured in iswests in fissured or jointed unsaturated clays may be used as the lower bound of the  $\phi'$  value in such soils, and by assuming  $c'$  as zero, a stability analysis in terms of effective stresses may be performed for the case when the joints and fissures in such material may be filled with infiltrating water. Cylwests, which enable undisturbed cylindrical borehole samples to be tested, may be used for a similar purpose (e.g., Mirata et al., 1999), using test moulds larger in size than those described here if need be.

### **1.2.8 For the short term stability of saturated clays**

So far there has been no occasion for trying the wedge shear tests in saturated clays except for a pair of cylwests on a soft marine clay from off the shore of Manavgat, southern Turkey. But there seems to be no reason why the iswest, for example, should not be advantageously used for the in situ measurement of shear strength in saturated, fissured and/or stony clays instead of large-scale shear box tests.



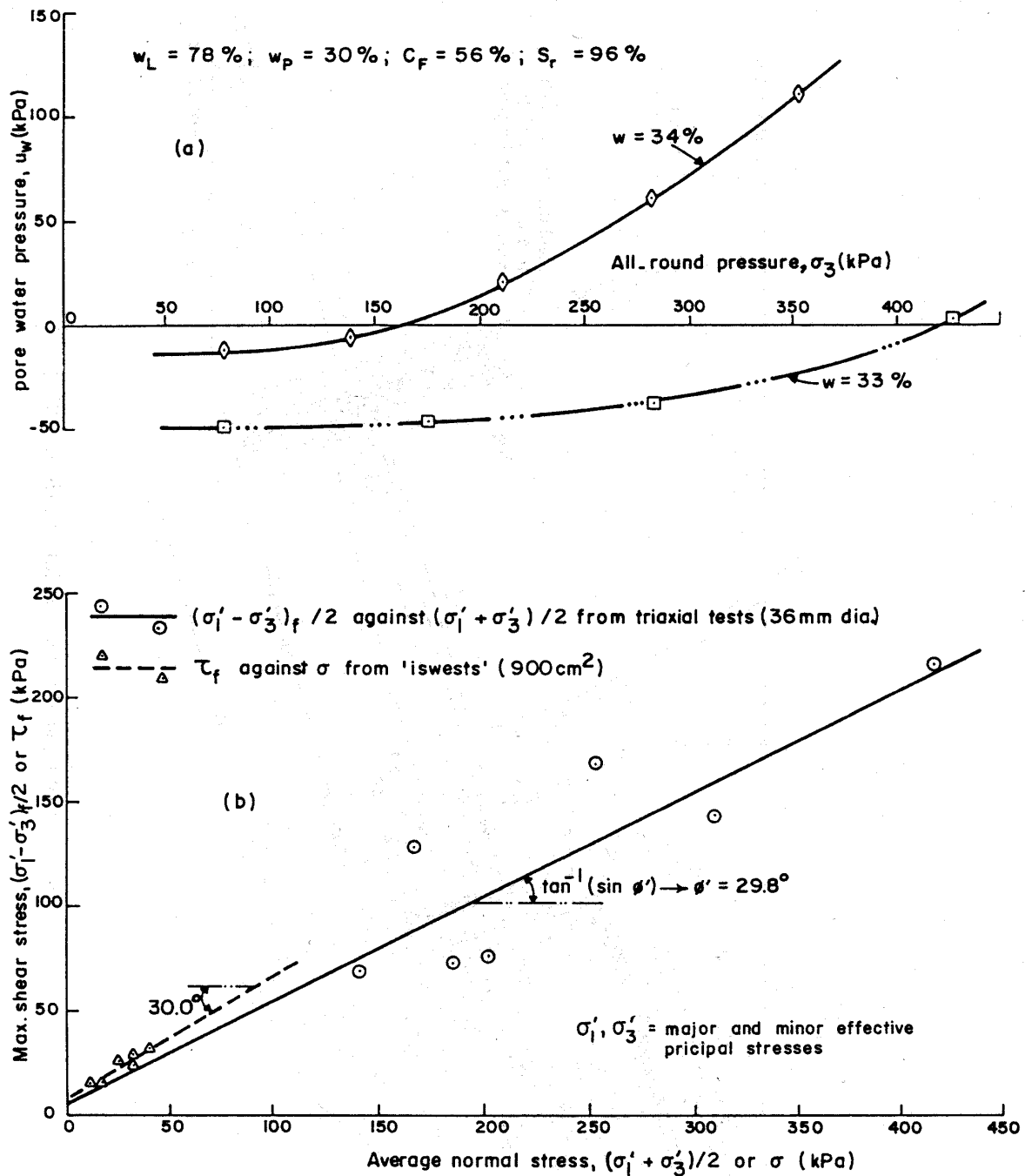


Fig. 1.1. Variation of (a) pore water pressure and (b) peak shear strength with average normal stress for a stiff fissured unsaturated clay

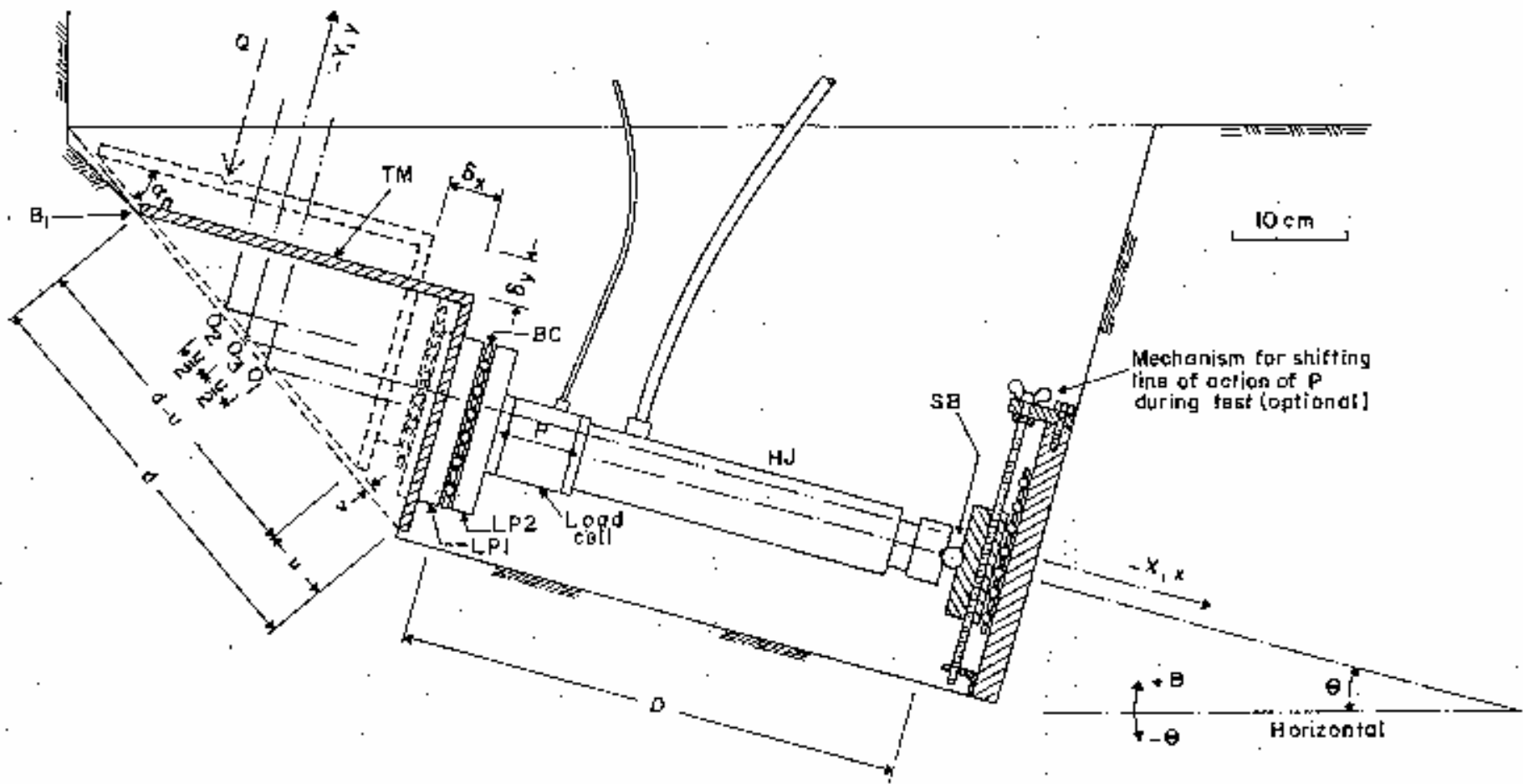


Fig. 1.2. Principle of the iswest (after Mirata, 1991)

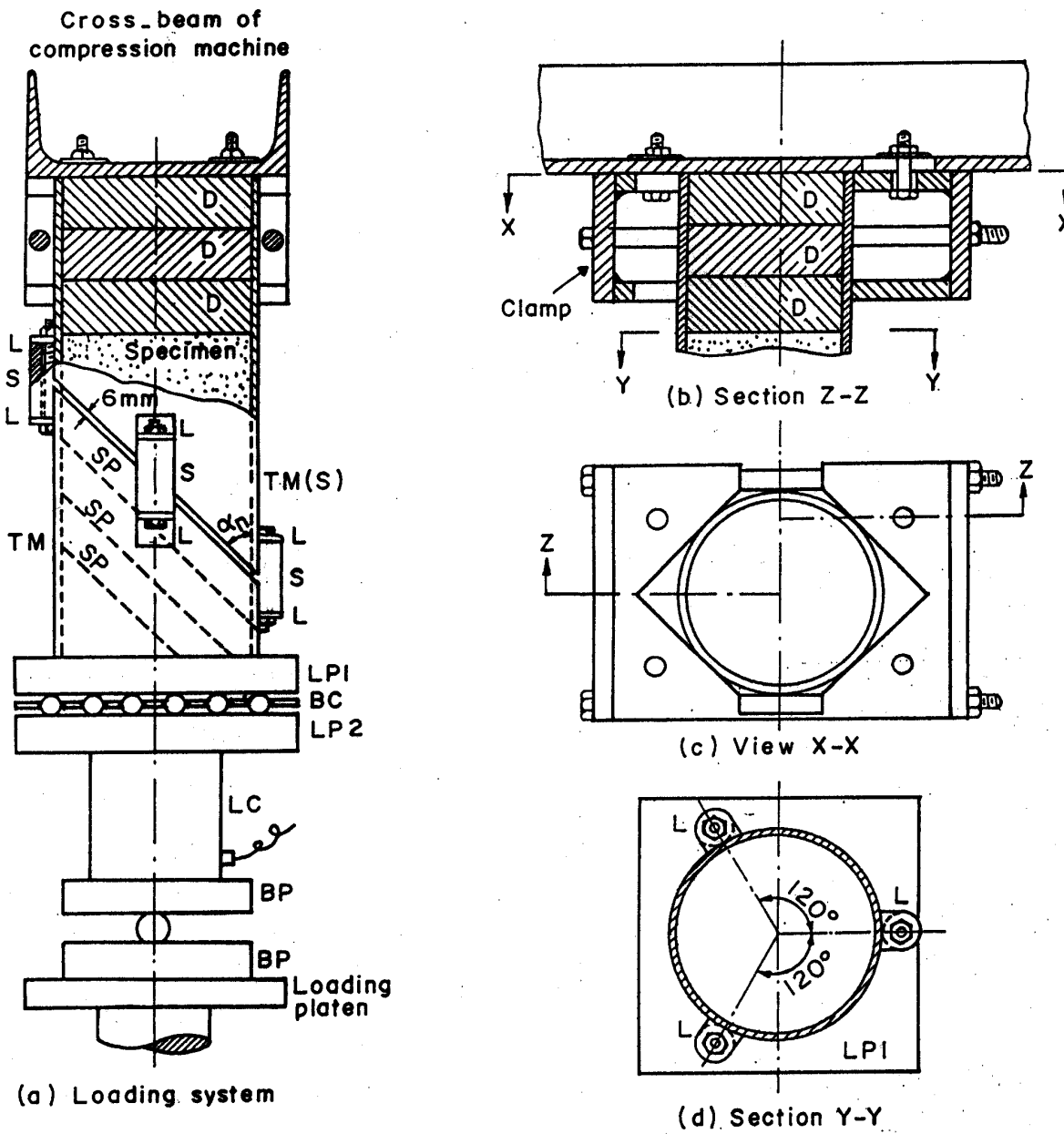
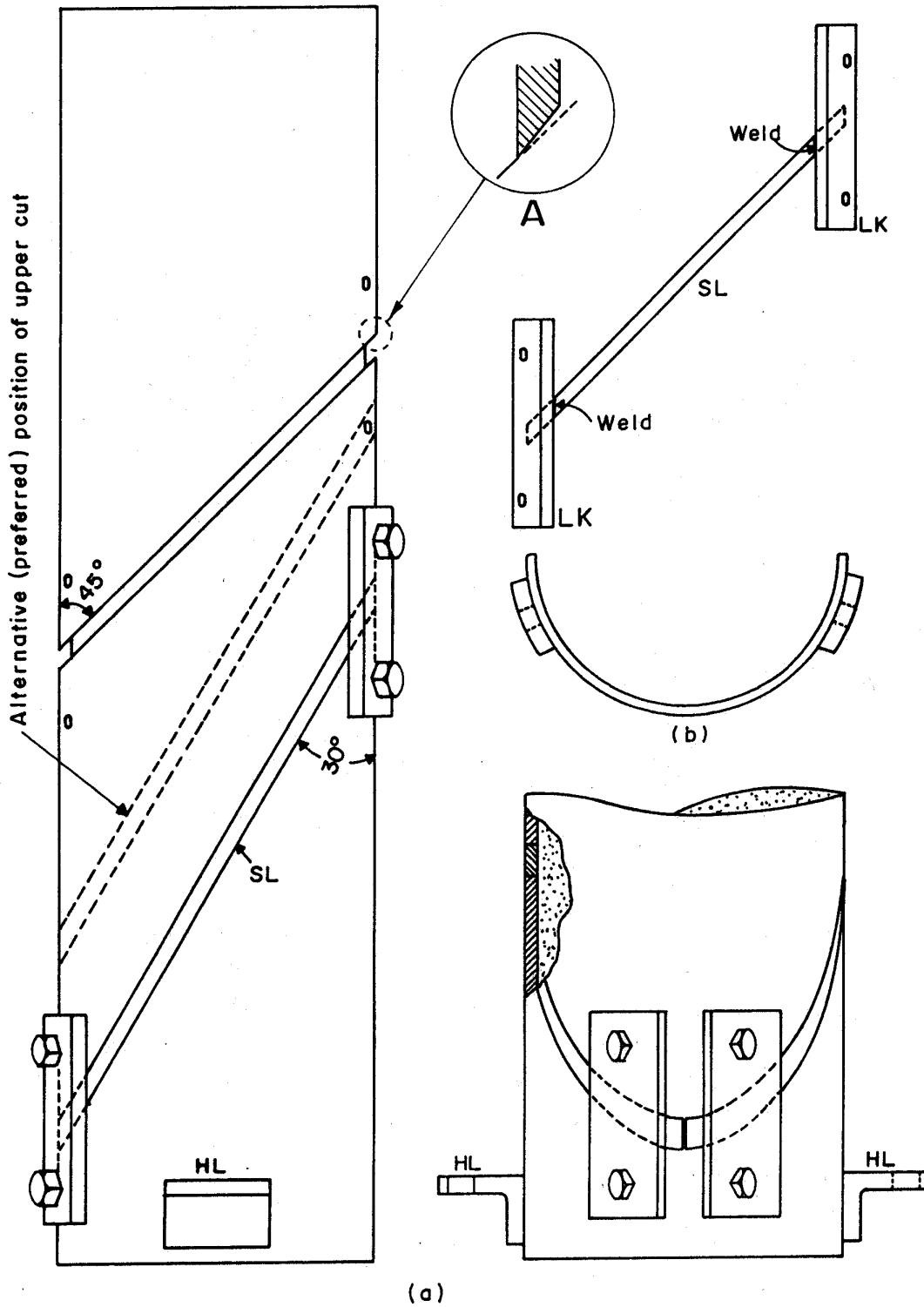


Fig. 1.3. Loading system and apparatus used in cylwests carried out in a compression machine (after Mirata, 1991)



**Fig. 1.4. Double-cut test mould for compacted samples showing (a) assembled test mould with upper coupling removed and (b) one half of upper coupling (after Mirata, 1991)**

## CHAPTER 2

### PRINCIPLES OF EVALUATION

Much of this chapter has been published (Mirata, 1991), except Appendices 1 and 2, which had been given in earlier research reports (Mirata, 1981; 1990). This information is reproduced here to facilitate the explanations given in the subsequent chapters.

#### **2.1 Principles of analysis for stresses and displacements**

Equations given here are applicable to all three versions of the wedge shear test, separate definitions being given where needed. In iswests, the displacements of the soil mass below the test wedge are assumed to be negligible relative to the displacements of the test mould, so that all the equations for priswests become applicable to iswests when the initial clearance  $n_c$  between the shearing planes of the two halves of the priswest box and the dimension  $h_m$  (Fig. 2.1) are equated to zero. For simplicity, reference will be made mostly to the diagrams for the cylwest (Fig. 2.2), similar assumptions being valid for priswests and iswests.

Basically the problem is one of summing up the normal and shear components of all forces, and dividing these by the corrected area of the shear plane. Differences in analysis arise in deciding which to take as the shear plane and whether to consider the slight rotation  $\beta$  of the test mould during the test. Distinction will be made here between three types of analysis. Equations for the more detailed analyses are given in Appendices 1 to 5.

##### **2.1.1 Analysis A**

This is the simplified analysis, which may be considered adequate for most practical purposes. The soil is assumed to break along the plane AB (Fig. 2.2(a)) midway between the stationary half TM(S) of the test mould and the initial position of the mobile half TM, and to move without rotation so that the lower part of the failure plane lies along A'B'. The average corrected shear plane is taken as CD, midway between AB and A'B'.  $O_1$ ,  $O_2$ , and  $O_3$  denote the midpoints of AB, A'B', and CD respectively. The components  $X$ ,  $Y$  of all forces parallel and normal to the force

$P$ , recorded through the load cell LC, are

$$X = P - (W + W_{BC} + W_{LP}) \sin \theta + \delta X_q \quad (2.1)$$

$$Y = (W + \frac{M_B}{D}) \cos \theta + \mu P + \delta Y_q \quad (2.2)$$

where  $\delta X_q$  and  $\delta Y_q$  are the additions to  $X$ , and  $Y$  due to the lateral load  $Q$  and are given by

$$\delta X_q = Q \cos \lambda_q - S W_{qn} \sin \lambda_q \quad (2.3)$$

$$\delta Y_q = Q \sin \lambda_q + S W_{qn} \cos \lambda_q \quad (2.4)$$

and  $D$  is the perpendicular distance between the grooves on LP1 and the single ball SB, and is constant in cylwests using the set-up shown in Fig. 2.2, but increases by  $\delta_x$  (or  $\delta_{x0}$  in analyses B and C) during the test in all wedge shear tests where a hydraulic jack is used.  $M_B$  is the sum of moments about SB of all components between the grooves of LP1 and SB when  $\theta = 0$ ;  $W$  is the total weight of the soil wedge, the test mould TM and LP1;  $W_{BC}$  and  $W_{LP}$  are the weights of the ball cage and the grooved loading plate LP2 respectively, and  $W_{qn}$  is the component normal to  $Q$  of the simply supported reaction due to the self-weight of the lateral loading device. The angle  $\theta$  between  $P$  and the horizontal can be varied conveniently between  $45^\circ$  and  $-90^\circ$  in iswests performed on the base or the side of a test pit (Fig. 4.5(b) or (a));  $\theta = 90^\circ$  in cylwests;  $\theta = -90^\circ$  in priswests performed as in Fig. 3.1(b), and  $\theta = 0$  in priswests performed with the frame in the horizontal position as in Fig. 4.7.  $\lambda_q$  is the angle between  $P$  and  $Q$ ;  $\mu$  is the coefficient of friction against the motion of LP1 relative to LP2 with the steel balls rolling in between ( $\mu$  has been found to be as low as 0.0038 for the set of plates described in section 5.4.2);  $S$  is a sign term defined by

$$S = \frac{\theta + \delta\theta}{|\theta + \delta\theta|} \quad (2.5)$$

where  $\delta\theta$  is a small angle like  $0.01^\circ$  introduced to avoid division by zero when  $\theta = 0$ .

The average normal and shear stresses ( $\sigma$ ,  $\tau$ ) are then calculated from

$$\sigma = (X \sin \alpha + Y \cos \alpha) / A_c \quad (2.6)$$

$$\tau = (X \cos \alpha - Y \sin \alpha) / A_c \quad (2.7)$$

where  $A_c$  is the corrected area of shear given by

$$A_c = b(d - u) \quad (2.8)$$

for iswests and priswests, where  $b$  is the inner width and  $d$  is the length of the shearing plane of TM, and by equation (2.9) with an underestimate of less than 0.3 % for cylwests (the exact solution is given in Appendix 1, section A1.1).

$$A_c = \pi D_i^2 / 4 \sin \alpha - D_i \cdot u \quad (2.9)$$

where  $D_i$  is the inside diameter of TM and  $u$  is the shear displacement given by

$$u = \delta_x \cos \alpha + \delta_y \sin \alpha \quad (2.10)$$

where  $\delta_x$  and  $\delta_y$  are the displacements measured in the positive directions of  $X$  and  $y$  (Figs 1.2 and 2.2) respectively. The normal displacement  $v$  is given by

$$v = \delta_y \cos \alpha - \delta_x \sin \alpha \quad (2.11)$$

where positive values of  $v$  indicate dilatation. In iswests and priswests and in those cylwests where failure takes place as in Fig. 2.2(a),  $\alpha = \alpha_n$ , the nominal angle between  $P$  and the shearing plane of TM. In cylwests performed with  $\alpha_n = 30^\circ$ , failure has sometimes been found to take place as in Fig. 2.2(b) or (c), and rarely along an intermediate plane as in Fig. 3.5(c), in which case  $\alpha$  is calculated from the geometry of the failure plane as measured after the test. The upper

half of the shear plane so determined is assumed to be stationary, and  $n_c$  taken as zero for iswests. The maximum value of  $P$  is taken as the criterion of failure when no  $Q$  is applied initially, and the maximum value of  $\tau/\sigma$  is taken otherwise.

The application of  $Q$  reduces greatly the possibility of tension developing on the failure plane, both by introducing moments, which counteract those produced by  $P$  and by preventing the reduction of direct normal stresses. So equations (2.1) - (2.11) are adequate for the simplified evaluation of test results. Examples of calculator programs for this purpose are given in Appendix 6, sections A6.1 to A6.3. A further simplification, with very little extra loss of accuracy, but not elaborated in this manual, is to do away with all dial gauges, neglect the normal displacements, and calculate the shear displacements as the appropriate component of the extension of the hydraulic jack during the test.

If it is desired to minimize moments on the failure plane, it is possible to shift the line of action of  $P$  in accordance with a set of previously calculated curves giving the amount of this shift to make the moment, given by the equations in Appendix 2, zero when  $\nu = \beta = 0$  is assumed. The moment equations can also be used to calculate the distribution of normal stress on the failure plane by assuming this distribution to be linear, and to exclude any tension zones from the corrected area of shear. Such calculations, as well as those described in sections 2.1.1 to 2.1.3, are performed by the programs described in Chapter 3.

### **2.1.2 Analysis B**

In this analysis, the average shear plane is assumed to be the same as in analysis A, except that the effect of  $\beta$  is taken into account. The average shear and normal displacements ( $\bar{u}, \bar{v}$ ) and  $\beta$  are calculated as in Appendix 3.  $\theta$  in equations (2.1) and (2.2) is then replaced by  $\theta_f = \theta + \beta$ , and  $u$  in equations (2.8) and (2.9) by  $\bar{u}$ . The value of  $\alpha$  is unaltered, implying that both  $P$  and the average shear plane rotate by  $\beta$ .

### **2.1.3 Analysis C**

The rotation  $\beta$  is calculated as in analysis B, but unless failure has taken place as in Fig. 2.2(b) or (c) or as in Fig. 3.5(c), in which case analysis B is used, shear is assumed to take place initially between the trailing tip  $A_1$  of TM and the point  $B_1$  which represents the opposite tip of TM(S) in priswests and cylwests (Figs 2.1 and 2.3) and the initial position of the leading tip of



the soil wedge in iswests (Fig. 1.2). The angle  $\alpha_i$  between  $A_1B_1$  and the initial direction of  $P$ , and the length  $\overline{A_1B_1}$  are calculated as in Appendix 4.

The angle  $\alpha_r$  between the rotated position of  $P$  and  $A_1B_1$  (Fig. 2.3), and the equivalent shear displacement  $\bar{u}_1$  are given by

$$\alpha_r = \alpha_i - \beta \quad (2.12)$$

$$\bar{u}_1 = 2d_{yb} / \sin \alpha_i - \overline{A_1B_1} \quad (2.13)$$

where  $d_{yb}$  is defined in Table 2.1 for the different wedge shear tests. Equations (2.8) and (2.9) are then replaced by equations (2.14) and (2.15) respectively, and  $\alpha$  in equations (2.6) and (2.7) is replaced by  $\alpha_r$ .

$$A_c = b(2d_{yb} / \sin \alpha_i - \bar{u}_1) \quad (2.14)$$

$$A_c = \pi \left( d_{yb} \right)^2 / \sin \alpha_i - \bar{u}_1 D_i \quad (2.15)$$

The values in the last column of Table 2.1 apply to the case when a priswest mould of original nominal angle  $\alpha_{no}$  is subjected to minor changes, described in section 5.4.4, and loaded on the lid, making the effective angle  $\alpha_n = 90 - \alpha_{no}$  (see section 5.4.1).

In analysis C, after the peak strength is reached, further movement of the soil wedge is assumed to take place in the general direction of the failure plane formed at peak strength, but any further changes in  $\beta$  to be reflected equally to the direction of  $P$  and the orientation of the failure plane. So  $\bar{u}_1$  in equations (2.14) and (2.15) is replaced by  $\bar{u}$  obtained as in analysis B, and  $\alpha_i$  and  $\alpha_r$  are assumed to remain fixed at the values at peak strength.

## 2.2 Calculation of $Q$ to keep $\sigma$ around its value at peak strength

For practical purposes, increasing  $Q$  in such a way as to keep  $P$  somewhat below its value at peak strength to account for the reduction in area as the test proceeds and the relatively small contribution of  $Q$  to  $\sigma$ , enables  $\sigma$  to be kept sufficiently close to its value  $\sigma_f$  at peak strength without any calculation. To do this more accurately, a pocket calculator may be used to perform the

following calculations.

The following equations have been derived from equations (2.1) to (2.11) assuming  $\nu = 0$ ,  $\lambda_q = 90^\circ$ , and neglecting the terms in  $\mu$ . It is assumed that a lateral load is applied from the start of the test and that  $P = C_p \delta_p$  and  $Q = C_q \delta_q$ , where  $C_p$  and  $C_q$  are the calibration constants and  $\delta_p$  and  $\delta_q$  are the gauge readings of the devices for recording  $P$  and  $Q$  respectively. Separate definitions are given for when no  $Q$  has been applied at the start. The subscript f is used to indicate the values at peak strength. The value of  $\delta_q$  required to make  $\sigma = \sigma_f$  with these assumptions, and assuming that  $\delta_p$  itself will not change upon this adjustment, is given by

$$\delta_q = K_1 F_a \left( \frac{\delta_{pf} + \delta_{qf} / K_1 - K_3}{F_{af}} - \frac{\delta_p - K_2}{F_a} \right) \quad (2.16)$$

where

$$F_a = 1 - S_a \delta_x \quad (2.17)$$

$$K_1 = (C_p \tan \alpha_n) / C_q \quad (2.18)$$

$$K_2 = \frac{1}{C_p} \left[ (W + W_{BC} + W_{LP}) \sin \theta + SW_{qn} - \frac{(W + M_B / D) \cos \theta}{\tan \alpha_n} \right] \quad (2.19)$$

and

$$K_3 = K_2 \quad (\text{for } Q_f > 0) \quad (2.20a)$$

$$K_3 = K_2 - SW_{qn} / C_p \quad (\text{for } Q_f = 0) \quad (2.20b)$$

$S_a$  is defined in Table 2.1 for the different wedge shear tests, and  $M_B/D$  can be assumed to be constant at an average value.

For convenience, the dial of the measurement device for  $P$  in cylwests is generally set to zero with the two grooved plates and the ball cage placed on top of this device; when this is done, the expression  $(W + W_{BC} + W_{LP})$  in the equation (2.19) is replaced by  $(W - W_{LP})$ .

As  $\theta$  and  $\alpha_n$  are fixed in any one test,  $K_1$ ,  $K_2$ , and  $K_3$  are constant, and the first expression in brackets in equation (2.16) need be calculated only once for the values of  $\delta_p$ ,  $\delta_q$ , and  $\delta_x$  at peak strength. So the value of  $\delta_q$  for subsequent stages of the test can be calculated easily using the  $\delta_x$  and  $\delta_p$  values recorded at that stage. When  $Q$  is changed, however,  $\delta_p$  also changes; so this calculation

may have to be repeated a number of times at any stage of the test. Examples of programs for a pocket calculator for this purpose are given in Appendix 6, section A6.4. With experience,  $Q$  may be adjusted anticipating the resultant change in  $\delta_p$ , thus reducing the number of calculations needed.

This procedure may also be used to achieve any desired normal stress level in re-shear tests or in new shear tests where the expected order of magnitude of  $\phi$  is known from previous tests on similar material. In such cases, the values of  $\delta_p$ ,  $\delta_q$ , and  $\delta_x$  at peak strength in a previous test where the desired  $\sigma$  has been reached may be used to calculate the constants  $K_1$ ,  $K_2$ , and  $K_3$ , and the rest of the procedure applied for adjusting  $Q$  during the test (see Box 4.2, file 1).

### 2.3 Miscellaneous calculations

Once the shear strength parameters  $c$  and  $\phi$  have been estimated, a number of quantities of interest in planning the test can be calculated. For instance, the curves in Fig. 2.4, derived as outlined in Appendix 5, may be used to estimate the increase  $\Delta Q$  in  $Q$  needed to ensure that the increase  $\Delta P$  in  $P$  is within the capacity of the available load cell, or to produce the required increase  $\Delta\sigma$  in normal stress. In practice, as the normal stress increases, the  $\phi$  value decreases particularly in gravels and crushed rock, so that the  $\Delta P$  or  $\Delta\sigma$  values achieved are lower than estimated by these curves. These curves are also a useful reminder of the fact that if  $(\alpha + \phi) > 89.5^\circ$  it is impossible to shear the soil in the way envisaged in the wedge shear test, and that a rapidly increasing  $P$  would be required for shear as this limit is approached (Mirata, 1974). Examples of the latter occurrence can be seen in Box 4.2, file 2.

Combining equation (22) of Mirata (1974) with equation (A5.2) yields the following equation to give an estimate of the required  $\Delta Q$  needed after peak strength to keep  $\sigma \approx \sigma_f$  in tests on clay, assuming  $\phi$  will be unchanged, cohesion will be  $c$  at peak and zero at residual strength, and neglecting terms in  $\mu$  and the change in area of shear.

$$\Delta Q = A_n \cdot c \cdot \sin \alpha_n \quad (2.21)$$

where  $A_n$  is the nominal area of the shear plane of the test mould. This equation, together with equations (A52) and (A53), can also be used for achieving a particular normal stress level in wedge

shear tests on soils whose shear strength parameters have already been measured in other types of test.

**Table 2.1. Definition of some symbols for different wedge shear tests**

Symbol	Cylwests (Fig. 2.2)	Iswests* and priswests (Fig. 2.1)	Priswests** ( $\alpha_n > 46^\circ$ )
$d_{ax}$	$D_i / \tan \alpha_n + n_c / \sin \alpha_n$	$d \cos \alpha_n$	$d \cos \alpha_n + n_c / \sin \alpha_n$
$d_{mx}$	$(D_i / 2) \cot \alpha + h_s$	$(d / 2) \cos \alpha_n + t$	$(d \cos \alpha_n + n_c / \sin \alpha_n) / 2 + t$
$d_{my}$	$D_i / 2 + t$	$(d \sin \alpha_n + n_c / \cos \alpha_n) / 2 + h_m + t$	$d \sin \alpha_n + t$
$d_{yb}$	$D_i / 2$	$(d \sin \alpha_n - n_c / \cos \alpha_n) / 2$	$(d / 2) \sin \alpha_n$
$h_{np}$	$D_i / 2$	$(d / 2) \sin \alpha_n$	$(d / 2) \sin \alpha_n$
$h_{pp}$	$D_i / 2 \tan \alpha_n$	$(d / 2) \cos \alpha_n$	$(d / 2) \cos \alpha_n$
$S_a$	$(4 \tan \alpha_n) / \pi D_i$	$1 / d \cos \alpha_n$	$1 / d \cos \alpha_n$

$t$  = wall thickness of test mould

\*  $n_c = h_m = 0$  for iswests.

\*\* See section 5.4.4.

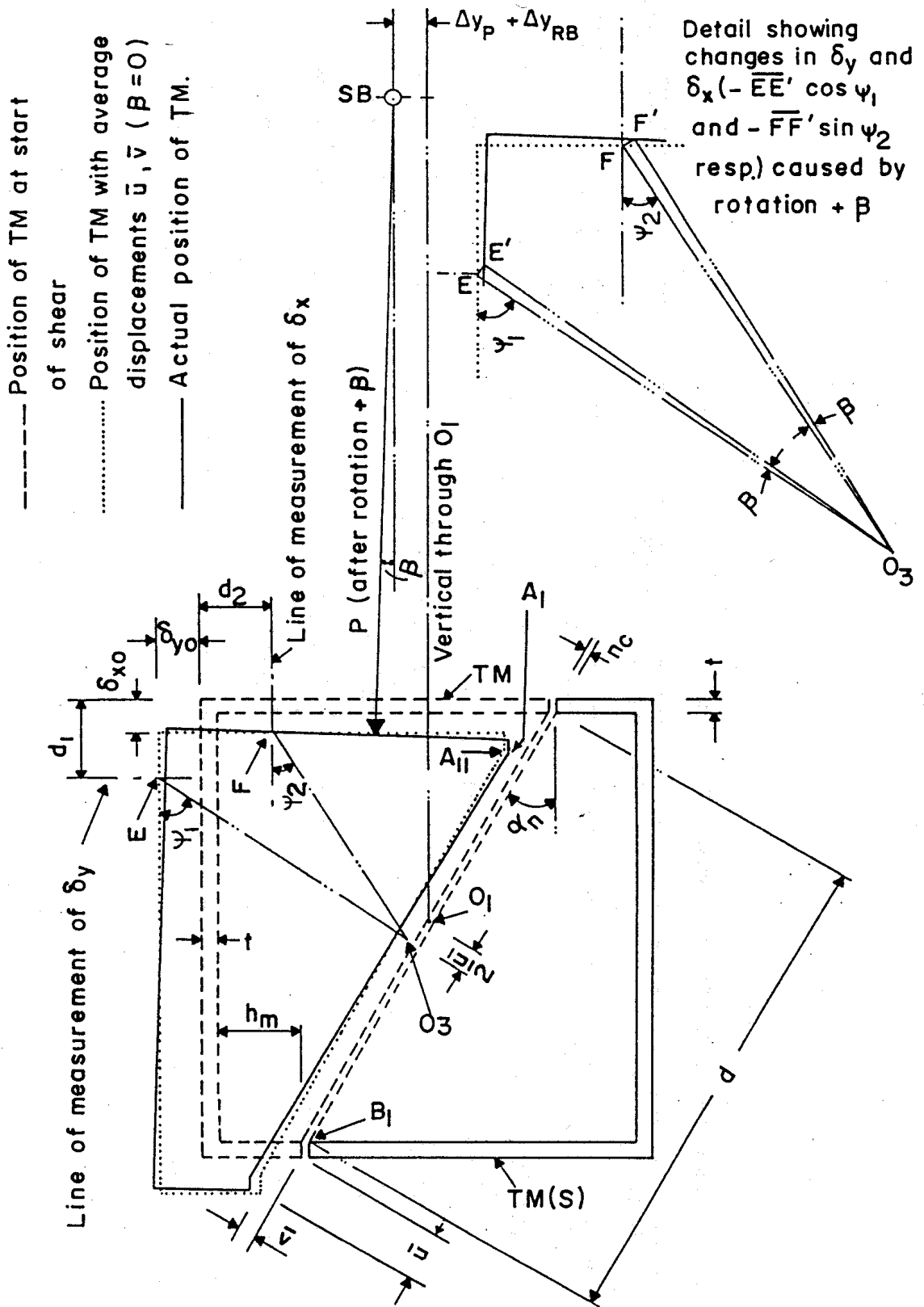


Fig. 2.1. Effect of mould rotation on the measured values of  $\delta_x$  and  $\delta_y$  in priswests (after Mirata, 1991)



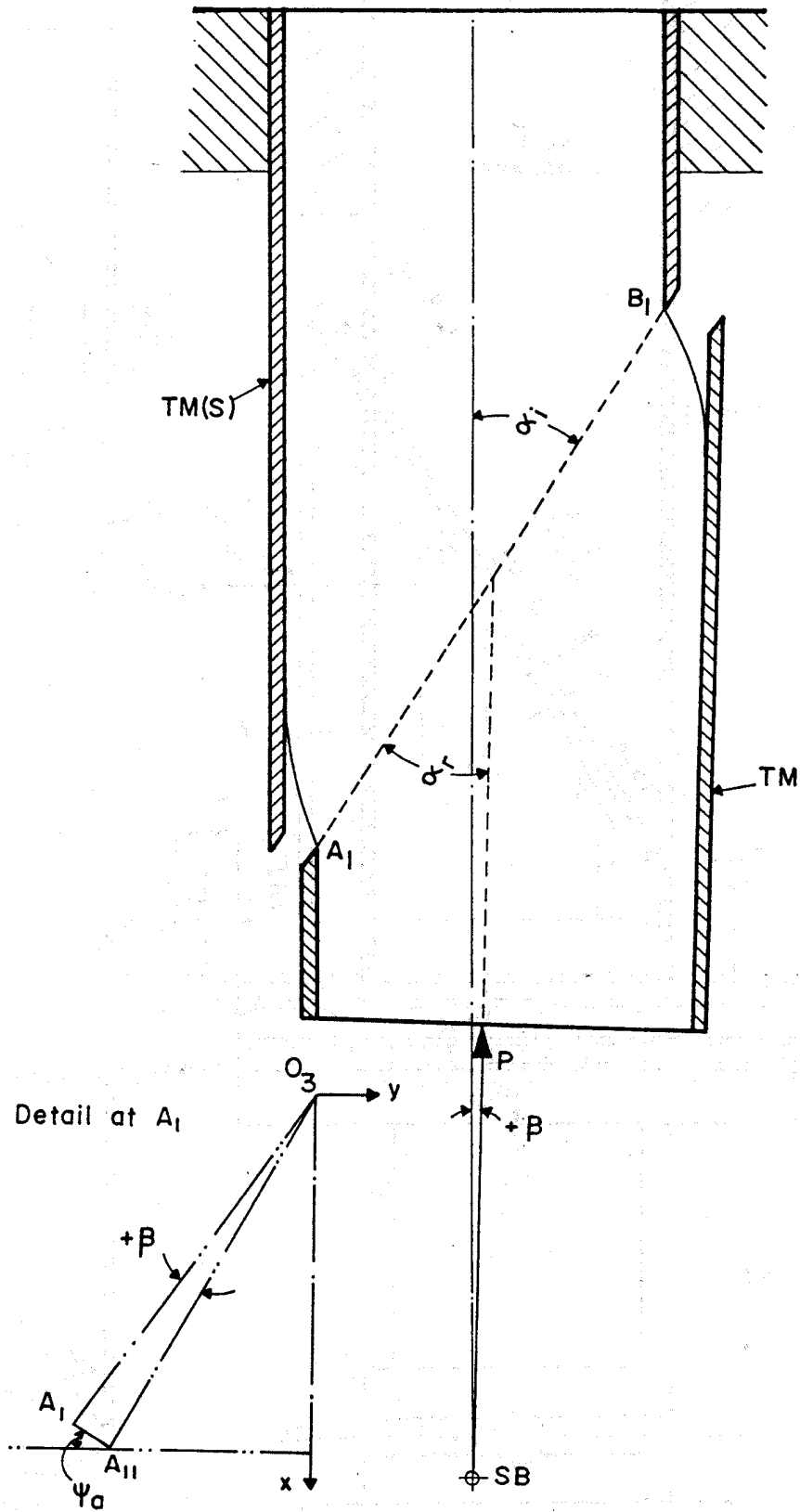


Fig. 2.3. Pre-failure deformation of a plastic clay in cylwast (after Mirata, 1991)



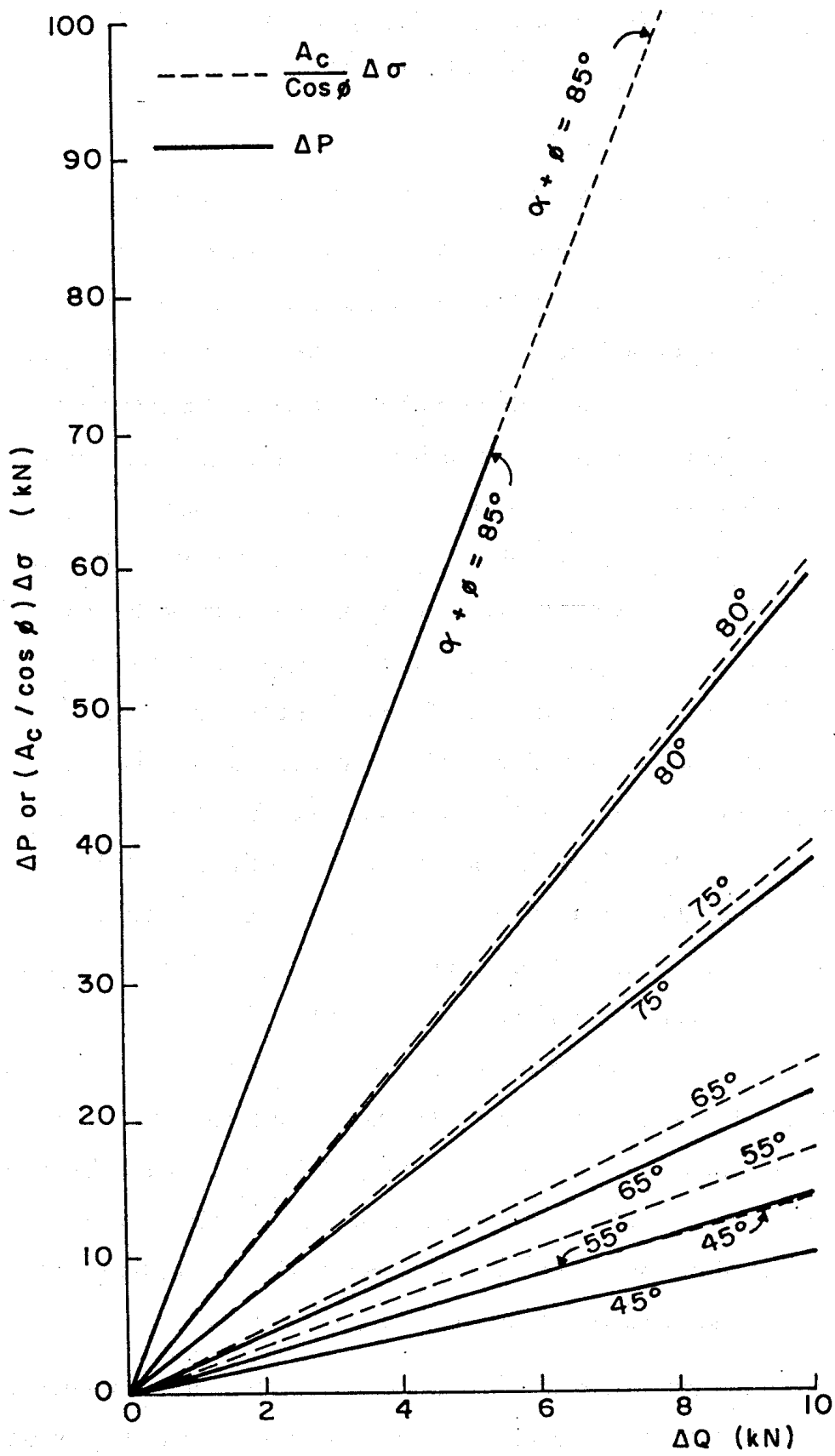


Fig. 2.4. Increase in  $P$  or  $\sigma$  produced by an increase in lateral load (after Mirata, 1991)

## CHAPTER 3

# COMPUTER PROGRAMS FOR DETAILED EVALUATION OF WEDGE SHEAR TESTS

### 3.1 Introduction

The programs IWPW77 and CYLWEE88, operating under DOS, each with over 1500 source lines, used for the detailed evaluation of iswests or priswests, and cylwests respectively are basically the same in that they both use the test data to calculate, by the three different methods of analysis outlined in Chapter 2, the stresses and displacements involved in the test, as well as the values of  $\delta\sigma/\sigma$  (the percentage difference between the normal stress at the trailing end of the soil wedge and the average normal stress), assuming a linear distribution of normal stress along the failure plane. The pairs of average normal and shear stresses at peak strength and at the end of each test are then used to obtain regressed envelopes of shear strength, depending on the type of regression specified by the user, the resulting shear strength parameters and the regression coefficients being output at the end of the output file. An optional table at the very end gives estimated values of cell pressure required to give about the same average principal stresses at failure in triaxial tests as in each of the wedge shear tests. The two programs differ only in the format of the input files, and some of the equations needed in the evaluation of the tests. As such, much of the values output are the same, and only the differences will be denoted for the output of the program CYLWEE88, following the detailed explanation of IWPW77 in the next subsection. For convenience, in both programs the data is input in kgf and cm; the stresses and displacements are output in SI units. For ease of reference, the notation  $m/n_1-n_2$  will be used to denote columns  $n_1$  to  $n_2$  of row  $m$  of the input data. Where more detailed explanation is needed than those given in the various tables, reference is made in the last column of the tables to the relevant number of the notes listed at the end of this chapter, and indexed at the end of the manual.

Utmost care has been taken in the development of these programs, and they have been tried and tested in different ways. But this is no warranty as to the accuracy of the programs and the outputs obtained through their use; it is the responsibility of the user to check the input data for conformity with this manual, and to examine the output for reasonableness.

## 3.2 The program IWPW77

### 3.2.1 Input data for the program IWPW77

Form 1 is intended for entry of data during the test and for subsequent use in preparing the input file for the program. The explanation of the entries is given in Table 3.1. All data, except those in row 12 and after, columns 8, 16, 24, 32, 40, and 48 have to be fed in floating point format.

**Table 3.1. Explanation of the entries for the input file of the program IWPW77**

Row/ column	Variable	Entry	Note
1/1-8	PDATCH	Parameter for checking the data before running the program 1.: apply data check; 0.: evaluate tests.	(1)
1/9-16	PAROUT	Parameter for specifying the type of output desired.	(2)
1/17-24	PARREG	Parameter for specifying the type of regression desired, as in the relevant footnote on Form 1.	
1/25-32	WQ	Weight of the lateral load $Q$ device excluding the end rod (kgf). 0.: no $Q$ applied <b>in any test</b> .	
1/33-40	TYPQDV	Type of device used for applying $Q$ . 0.: air piston used; 1.: spring loaded piston used.	
1/41-48	TYPTST	Type of test applied. 0.: iswests; 1.: priswests.	
1/49-56	POISNR	Poisson's ratio $\nu$ of the soil (optional).	(3)
2/1-8	TKNESS	$t$ = wall thickness of the test mould (cm). (Assumed as 1. if left blank).	
2/9-16	TLP1MN	Minimum thickness of the grooved plate LP1 (cm).	
2/17-24	WLP	$W_{LP}$ = weight of grooved plate LP2 (kgf).	
2/25-32	WBC	$W_{BC}$ = weight of ball cage BC (kgf).	
2/33-40	FRCOEF	$\mu$ = coefficient of friction defined after equation (2.4).	
2/41-48	DBPI	Distance $h_2$ between the single ball and the grooves on LP2 assuming the initial extension $d_3$ of the hydraulic jack as zero (Fig. 3.1) (cm).	
2/49-56	DENSOL	Density of the in situ soil (g/cc), needed for iswests when	

**Table 3.1. (continued)**

Row/ column	Variable	Entry	Note
		DH (defined at 8/65-72) > 0 only.	
2/57-64	APG	$A_{pg}$ in equation (3.1), for pressure gauge of hydraulic jack.	(4)
2/65-72	DPG	$D_{pg}$ in equation (3.1), for pressure gauge of hydraulic jack.	(4)
3/1-8	WHJ	Weight of the hydraulic jack HJ (Figs 1.2 and 3.1) (kgf).	(5)
3/9-16	DIASTB	Diameter of the steel balls used in the ball cage BC (cm).	(6)
3/17-24	CONDX	Factor for converting readings of dial $D_x$ (Fig. 4.7) into cm.	(6)
3/25-32	CONDY	Factor for converting readings of dial $D_y$ (Fig. 4.7) into cm.	(6)
3/33-40	CONYMP	Factor for converting readings of dial $D_{mp}$ (Fig. 4.7) into cm.	(6)
3/41-48	CONRPB	Factor for converting readings of dial $D_{rb}$ (Fig. 4.7) into cm.	(6)
3/49-56	HTQPRP	Length $h_1$ of the $Q$ device measured as in Note 7 (cm).	(7)
3/57-64	PRCONQ	Factor for converting the proving dial readings for $Q$ into kgf (kgf/division).	
3/65-72	DIVPRQ	Displacement represented by each division of the proving ring dial for $Q$ (cm). Omit if DIVPRQ = 0.000254.	
4/1-72	...	These three rows are for alphanumeric data. Any desired information can be entered in these rows. The headings appearing on the form can be altered to suit requirements.	
5/1-72	...		
6/1-72	...		
7/1-8	ALFN	$\alpha_n$ = the nominal angle between the main load $P$ and the shearing plane of the test mould (deg).	
7/9-16	TETA	$\theta$ = initial angle between $P$ and the horizontal (deg), entered as positive when $P$ is acting upwards, and negative otherwise.	
7/17-24	AL	$d$ = length of the shearing plane of test mould (Fig. 3.2(b)) (cm).	
7/25-32	B	$b$ = inner width of the test mould (cm).	
7/33-40	A	$A_r$ in equation (3.2), for indicator for $P$ .	(8)
7/41-48	D	$D_r$ in equation (3.2), for indicator for $P$ .	(8)
7/49-56	HTLC	Height of the load cell for measuring $P$ (cm).	

**Table 3.1. (continued)**

Row/ column	Variable	Entry	Note
7/57-64	WLC	Weight of the load cell for measuring $P$ (kgf).	
7/65-72	WDM	Weight of dial gauge $D_{mp}$ (Fig. 4.7) and its magnetic base (kgf).	
8/1-8	DETMDM	$d_4$ = distance from the loading face of test mould to the estimated centre of gravity of the unit at 7/65 (cm).	
8/9-16	VPI	Distance by which the jack for $P$ is shifted relative to the centre of LP1, in the positive $y$ direction (Figs 1.2, 2.1), prior to the start of loading (cm).	
8/17-24	VPTI	Hypothetical shift applied to $P$ in addition to VPI (cm).	(9)
8/25-32	D1	Distance $d_1$ defined before equation (A33) (cm).	(10)
8/33-40	D2	Distance $d_2$ defined before equation (A33) (cm).	(10)
8/41-48	D3	Extension $d_3$ (Fig. 3.1) of jack for $P$ at start of loading (cm).	
8/49-56	TO	Time elapsed (min) between the zero setting of the indicator for $P$ and the time entered at 12/1-8.	(11)
8/57-64	ZEROF	The final zero reading of the indicator for $P$ at end of test.	(11)
8/65-72	DH	Distance $\Delta h$ in iswests where failure takes place at $\alpha > \alpha_n$ .	(12)
9/1-8	PARFPL	Parameter for defining orientation of the failure plane. 1: failure has taken place along $A_1 B_1$ (Fig. 2.1); 0.: otherwise.	
9/9-16	RDGNUM	Number of rows of subscripted variables (maximum = 40.).	
9/17-24	PFIXDR	Parameter for enabling revised versions of rows 1 to 3 to be read after the end of data for the current test, and/or the optional row 10 to be read.  0.: no row 10; pass on to the alphanumeric data of the next test. 1.: no row 10; read the revised versions of rows 1 to 3. 2.: read row 10; pass on to the alphanumeric data of the next test. 3.: read row 10 and the revised versions of rows 1 to 3.	

**Table 3.1. (continued)**

Row/ column	Variable	Entry	Note
9/25-32	XSBTPQ	x co-ordinate of the pivot to $Q$ relative to the single ball (cm).	(13)
9/33-40	YSBTPQ	y co-ordinate of the pivot to $Q$ relative to the single ball (cm).	(13)
9/41-48	ANPQIN	Initial angle between the main load $P$ and $Q$ (deg).	
9/49-56	RODNUM	Number of the steel rod attached to proving ring for $Q$ .	(14)
9/57-64	SPRCON	Spring constant of the spring loaded piston for $Q$ (kgf/cm). Leave blank if an air piston is used for this purpose.	
9/65-72	CONDES	Constant for converting the readings of the dial gauge for recording the displacement of the support for the $Q$ device into cm in iswests (cm/div). Leave blank for priswests.	
10/1-72	...	<b>This row is omitted when PFIXDR = 0. or 1.</b>	
10/1-8	WINPUT	$W$ for iswests; $W_{tp}$ for priswests (kgf).	(15)
10/9-16	X1	$\bar{x}$ for iswest mould or $\bar{x}_{tp}$ for priswest mould (cm).	(15)
10/17-24	Y1	$\bar{y}$ for iswest mould or $\bar{y}_{tp}$ for priswest mould (cm).	(15)
10/25-32	X1Q	$\bar{x}_q = x$ co-ordinate of tip of rod at end of the $Q$ device relative to the centroid $O_M$ of the shear plane of the test mould (cm).	(15)
10/33-40	Y1Q	$\bar{y}_q - d_r/2 = y$ co-ordinate of tip of rod at end of the $Q$ device relative to the centroid $O_M$ of the shear plane of the test mould (cm).	(15)
10/41-48	DIAROD	Diameter $d_r$ of rod attached to proving ring for $Q$ (cm).	(14)
10/49-56	HTROD	Dimension $h_r$ of rod attached to proving ring for $Q$ (cm).	(14)
10/57-64	CGDISR	Distance $h_{cg}$ of the centre of gravity of the rod attached to the proving ring for $Q$ from point of start of threads (cm).	(14)
11/1-72	...	<b>This row is omitted for iswests.</b>	
11/1-8	HTIPWM	Dimension $h_m$ of the priswest mould, Fig. 3.2(b) (cm).	

**Table 3.1. (continued)**

Row/ column	Variable	Entry	Note
11/9-16	AMLPL	Amount by which the grooved plate <b>LP1</b> has been 'lowered' relative to the centroid of shearing plane of test mould (cm).	(16)
11/17-24	WCOMPS	Weight of soil placed in the priswest mould (kgf).	
11/25-32	WATCON	Water content of soil placed in the priswest mould (ratio).	
11/33-40	GS	Specific gravity $G_s$ of solid particles of the soil sample.	(17)
11/41-48	CLRNCE	$n_c$ = initial clearance between the shearing planes of the two halves of the priswest mould (cm).	
11/49-56	EXTASC	The initial amount by which the adjustment screw of the $Q$ device (Fig. 3.1) has been unscrewed at start of shear (cm). (Recorded for information only.)	
11/57-64	WTFLOW	Weight of soil that may have flowed out of the priswest mould at end of test. (Recorded for information only.)	
11/65-72	PGT45D	Parameter specifying whether a priswest mould with original nominal angle $\alpha_{no}$ is being loaded on the lid, making the effective mould angle, $\alpha_n = 90 - \alpha_{no}$ (see section 5.4.4). 1.: main load $P$ applied on lid; 0.: otherwise.	
12/1-3	HOUR(I)	Hour of the day at which readings have been taken (hour).	
12/4-7	MINUTE(I)	Minutes past the hour at which readings have been taken (min).	
12/8	IPARA(I)	Parameter for specifying whether the hydraulic jack is being supported. Enter '1' if supported; leave blank otherwise.	
12/9-15	DXABS(I)	Reading of dial gauge $D_x$ (Fig. 4.7) .	(18)
12/16	IPRSDX(I)	Enter '1' if dial $D_x$ has been reset; leave blank otherwise.	(19)
12/17-23	DY1ABS(I)	Reading of dial gauge $D_y$ (Fig. 4.7).	(18)
12/24	IPRSY1(I)	Enter '1' if dial $D_y$ has been reset; leave blank otherwise.	(19)
12/25-31	DTMLP2(I)	Reading of dial gauge $D_{mp}$ (Fig. 4.7).	(18)
12/32	IPRSLP(I)	Enter '1' if dial $D_{mp}$ has been reset; leave blank otherwise.	(19)
12/33-39	DRPBP(I)	Reading of dial gauge $D_{rb}$ (Fig. 4.7).	(18)
12/40	IPRSRP(I)	Enter '1' if dial $D_{rb}$ has been reset; leave blank otherwise.	(19)

**Table 3.1. (continued)**

Row/ column	Variable	Entry	Note
12/41-47	GR(I)	Indicator reading for the main load $P$ .	
12/48	IPARFL(I)	Enter '1' against the maximum value of GR(I), if PARFPL has been specified as '1.' at 9/1-8. Leave blank otherwise.	
12/49-54	SLATLD(I)	Proving ring dial reading of the lateral load $Q$ device.	
12/55-60	DEFSUP(I)	Reading of dial gauge for recording the deflection of the support for the $Q$ device in iswests. Leave blank for priswests.	
12/61-66	PGRDG(I)	Pressure gauge reading of the hydraulic jack (optional).	(4)
12/67-72	GRADQ(I)	Inclination $\lambda_1$ of the $Q$ device to the horizontal (deg) (optional).	(20)

### 3.2.2 Output of the program IWPW77

In this section, only the variables that have not been defined earlier will be explained. An index to the definition of all program variables will be found at the end of the manual. A few variables are output under a different name; such variables will be re-defined in the following tables. Units are as indicated on the outputs. (See Boxes 4.1 and 4.2 for typical outputs on the diskette.)

#### 3.2.2.1 Common data for all tests and constants for each test

The first six rows of the output contain the values applicable to all tests that follow, and fed in the first three rows of the input (Table 3.1). If any of these values have been changed before any one test (PFI XDR = 1. or 3. in the previous test), all the values are re-written. The two variables that have not been defined in Table 3.1 are given in Table 3.2. Following the common data for all tests, are the constant values applicable to the test that follows. These are also given in Table 3.2, unless previously defined.



**Table 3.2. Explanation of values output by program IWPW77 prior to each test**

Row	Variable	Explanation	Note
1	DENSTL	Density of steel.	
4	DSB	DIASTB defined in Table 3.1, 3/9-16.	
7-9	...	Alphanumeric data fed in rows 4-6 of the input, Table 3.1.	
10	THETA	TETA defined in Table 3.1, 7/9-16.	
	DELYP	$\Delta y_p$ = shift applied to $P$ in the positive $y$ direction relative to the initial centroid $O_1$ of shear plane (Figs 1.2, 2.1), before start of shear.	
10	W	Mass of mobile test mould, contained soil and grooved plate LP1 + WDM.	
	X1C	$x$ co-ordinate of W in row 10 relative to $O_M$ (Fig. 3.2(b)).	(21)
11	L	AL defined in Table 3.1, 7/17-24.	
	Y1C	$y$ co-ordinate of W in row 10 relative to $O_M$ (Fig. 3.2(b)).	(21)
12	SLRHC	A value calculated as $(A - \text{ZEROF}) / (TO + 40)$ , (div/min).	(22)
13	JTM	The number of the test mould the default data given in Fig. 3.2(b) of which have been used. JTM = 0 otherwise.	
	XBARQT	$\bar{x}_q = X1Q$ defined in Table 3.1, 10/25-32.	
	YBARQT	$\bar{y}_q = Y1Q$ defined in Table 3.1 10/33-40 plus DIAROD/2.	
15A	...	<b>Written only when DH &gt; 0 in iswests</b> (see Box 4.1, file 1, test C/4/9). ALFA (angle between $P$ and the actual failure plane) and the revised values of W, X1C, and Y1C are written..	
15B	DDENSL	The dry density of the soil.	(23)
16	HTSPCR	$h$ = height of spacers between the two halves of the priswest mould.	
	SATINL	Calculated initial degree of saturation of the soil.	(23)
	PORINL	Calculated initial porosity of the soil.	(23)
	VOIDRI	Calculated initial void ratio of the soil.	(23)
	GS(MD)	Specific gravity of solid particles (measured).	(23)
	GS(AS)	Specific gravity of solid particles (assumed).	(17)

### 3.2.2.2 Values output for each test

The degree of detail in this part of the output depends on the parameter PAROUT specified at 1/9-16, Table 3.1. The detailed output explained in Table 3.3 might be needed for research purposes, or for checking any anomalies in the test results. For most purposes, the

summary output explained in Table 3.4 is adequate. Analyses A, B, and C are those explained in sections 2.1.1 to 2.1.3.

**Table 3.3. Detailed output of program IWPW77 for each test (PAROUT = 0.)**

Col.	Variable	Explanation	Note
1	T	Time from start of shear, <b>repeated in each table of output.</b>	
2	BETABC	Calculated rotation $\beta$ of the test mould.	
3	UBAR	$\bar{u}$ = average shear displacement (Fig. 2.1).	
4	U	$u$ = shear displacement by analysis A.	
5	VBAR	$\bar{v}$ = average normal displacement (Fig. 2.1).	
6	V	$v$ = normal displacement by analysis A.	
7	SS	$\tau$ = average shear stress*.	
8	SSNB	$\tau$ = average shear stress by analysis A.	
9	TNSAVE	$\sigma$ = average normal stress*.	
10	TNNB	$\sigma$ = average normal stress by analysis A.	
11	SOVERN	The ratio $\tau/\sigma$ *.	
12	SOVRNB	The ratio $\tau/\sigma$ by analysis A.	
13	TNSMAX	$\sigma_{\max}$ = maximum normal stress on the failure plane*.	
14	TNSMIN	$\sigma_{\min}$ = minimum normal stress on the failure plane*.	
15	VPIT	Total shift applied to $P$ relative to $O_1$ in the positive $y$ direction (Figs 1.2 and 2.1).	
16	VPITT	Theoretical value of VPIT to minimize moments on failure plane.	(24)
17	INDEX	Number of iterations used in the calculation of $\beta$ (Appendix 3).	
19	P	$P$ = the main load applied through the hydraulic jack.	
21	USTRN	$\bar{u}$ expressed as a percentage of the corrected length of shear plane*.	
22	VSTRN	$\bar{v}$ expressed as a percentage of the corrected length of shear plane*.	
23	AC	Corrected area of shear*.	
24	ACNB	Corrected area of shear by analysis A.	
26	DP	Percentage difference between PGRDG, if read, and $P$ .	(4)
27	TMOMA	Moment acting on the failure plane by analysis B.	
28	TMOM	Moment acting on the failure plane*.	
29	DIFMOM	The difference (TMOMA - TMOM), columns 27, 28.	

\* By analysis C if PARFPL = 1.; otherwise, by analysis B.

**Table 3.3. (continued)**

Col.	Variable	Explanation	Note
30	DEVIBA	The value of $\delta\sigma/\sigma$ obtained by analysis B.	
31	DEVIB	The value of $\delta\sigma/\sigma$ *.	
32	DEVIBT	The value of $\delta\sigma/\sigma$ that would be obtained if the theoretical value VPITT (column 16) were applied*.	
33	DEVRPT	The value of $\delta\sigma/\sigma$ that would be obtained if the adjustment in Note 24 were done on the basis of similarly precalculated $\Delta y_{RB}$ (effect of $\beta$ and $\nu$ not eliminated)*.	
34	DEVJNR	The value of $\delta\sigma/\sigma$ that would be obtained if no shift were applied to $P$ during the test*.	
35	DEVVPI	The value of $\delta\sigma/\sigma$ that would be obtained if the hypothetical VPTI (Table 3.1, 8/17-24) were applied*.	
36	DEVNB	The value of $\delta\sigma/\sigma$ by analysis A.	
37	ERUABS	Difference between the shear displacement defined in analysis C, if used, and the average shear displacement $\bar{u}$ .	
38	RMV	The simply supported reaction $M_B/D$ in equation (2.2).	
40	DXABS	The recorded value of $\delta_x$ .	
41	DY1ABS	The recorded value of $\delta_y$ .	
42	DTMLP2	The recorded value of $\Delta y_{MP}$ .	
43	DRPB	The recorded value of $\Delta y_{RB}$ , if applied.	
44	SLATLD	$Q$ = the sub-lateral load applied.	
47	GRDQC	The calculated inclination of the $Q$ device to the horizontal.	(20)
48	ANGLQ	$\lambda_q$ = calculated angle between $P$ and $Q$ .	
49	WQNC	Calculated simply supported reaction of the $Q$ device, when horizontal, at the test mould end.	(5)
50	PWQRTI	Difference between WQNC and $(WQ + \text{weight of end rod})/2$ expressed as a percentage of the former.	
51	TNSAVP	$\sigma$ = average normal stress by analysis B.	
52	SSAVP	$\tau$ = average shear stress by analysis B.	

\* By analysis C if PARFPL = 1.; otherwise, by analysis B.

**Table 3.3. (continued)**

Col.	Variable	Explanation	Note
53	AVPRST	Average principal stress estimated by assuming $c = 0$ .	
54	DVOVDU	Rate of dilatancy.	
55	ALPHA	$\alpha_i$ in analysis C; $\alpha$ if $DH > 0$ in iswests; $\alpha_n$ if $PARFPL = 0$ .	
56	ALPHAR	$\alpha_r$ in analysis C; $\alpha$ if $DH > 0$ in iswests; $\alpha_n$ if $PARFPL = 0$ .	
57	DGR	Correction applied to the gauge reading for $P$ .	(11)
58-61	TNSAVP, SSAVP	Peak and ultimate values of the pair in columns 51 and 52.	(25)
62-65	TNSAVE, SS	Peak and ultimate values of the pair in columns 9 and 7.	(25)
66-69	TNNB, SSNB	Peak and ultimate values of the pair in columns 10 and 8. (25)	
70-73	AVPRST, DVOVDU	Peak and ultimate values of the pair in columns 53 and 54.	(25)
74	T(IMAXP)	Time at which peak strength has been reached.	(25)

**Table 3.4. Summary output of program IWPW77 for each test (PAROUT = 7.)**

Col.	Variable	Explanation	Note
1	T	Time from start of shear.	
2	UBAR	$\bar{u}$ = average shear displacement (Fig. 2.1).	
3	VBAR	$\bar{v}$ = average normal displacement (Fig. 2.1).	
4	BETABC	Calculated rotation $\beta$ of the test mould.	
5	TNSAVE	$\sigma$ = average normal stress*.	
6	SS	$\tau$ = average shear stress*.	
7	SOVERN	The ratio $\tau/\sigma$ *.	
8	P	$P$ = the main load applied through the hydraulic jack.	
9	Q	$Q$ = the sub-lateral load applied (SLATLD in Table 3.3, col. 44).	
10	XFORCE	Component of all forces in the rotated direction of $P^*$ .	(26)
11	YFORCE	Component of all forces normal to the rotated direction of $P^*$ .	(26)
12	AC	Corrected area of shear*.	

\* By analysis C if  $PARFPL = 1$ .; otherwise, by analysis B.

**Table 3.4. (continued)**

Col.	Variable	Explanation	Note
13	TMOM	Moment acting on the failure plane*.	(26)
14	DEVIB	The value of $\delta\sigma/\sigma$ *.	
15	ALPHAR	$\alpha_r$ in analysis C; $\alpha$ if $DH > 0$ in iswests; $\alpha_n$ if $PARFPL = 0$ .	
16	GRDQC	The calculated inclination of the $Q$ device to the horizontal.	(20)
17	AVPRST	Average principal stress estimated by assuming $c = 0$ .	
18	DVOVDU	Rate of dilatation.	

\* By analysis C if  $PARFPL = 1.$ ; otherwise, by analysis B.

### ***3.2.2.3 Values output for a series of tests when regression is possible and desired***

If more than one test has been carried out, and  $PARREG \neq 0$ , at the end of the output file, the following values are output for each test, followed by the regressed shear strength parameters, and the optional table of estimated cell pressures. In the first four columns, the values  $DV/DU$  ( $DVOVDU$  in Table 3.3, Column 54) and  $FI$  (angle of friction calculated as  $\tan^{-1}(\tau/\sigma)$ ) at peak strength and at the end of the test (Note 25) are listed for analysis C (or analysis B, if  $PARFPL = 0$ . has been specified). In the remaining columns, the  $(\sigma, \tau)$  pairs that are regressed are listed for analyses C, B, and A, firstly at peak strength, and then at the end of the test (Note 25). Below each pair of  $(\sigma, \tau)$  columns are given the coefficient of correlation and the regressed shear strength parameters as given in Table 3.5.

If  $POISNR$  has not been specified as  $> 0.5$  at 1/49-56, Table 3.1, the values listed in Table 3.6 are output depending on the type of regression specified.

**Table 3.5. Regression results output by program IWPW77**

PARREG	Variable	Explanation
1.	...	Coefficient of correlation for linear regression forced through the origin.
1.	PHI	Angle of friction for regression forced through the origin.
2.	COFCOR	Coefficient of correlation for ordinary linear regression.
2.	COHESN	Cohesion for ordinary linear regression.
	PHILRG	Angle of friction for ordinary linear regression.
3.	...	All values output for PARREG = 1. and 2.
4.	PHI	As for PARREG = 1.
	...	Coefficient of correlation for the logarithm of the ( $\sigma$ , $\tau$ ) pairs.
	ACONST	The value of $a$ in the relation $\tau_f = a(\sigma')^{b_1}$ , where $\tau_f$ , $\sigma'$ are in kPa.
	BEXPNT	The value of $b_1$ in the relation $\tau_f = a(\sigma')^{b_1}$ , where $\tau_f$ , $\sigma'$ are in kPa.
	SIG	Various values of $\sigma'$ (kPa), at equal intervals. The range of values output is based on the value of $\sigma'$ at peak strength in the last test in the data file.
	TAUF	Values of $\tau_f$ (kPa) calculated from $\tau_f = a(\sigma')^{b_1}$ for the $\sigma'$ values in the previous line, using the first pair of $a$ and $b_1$ values.
5.	...	All values for all three forms of regression listed above.

**Table 3.6. Estimated average principal stress and cell pressure  $\sigma_3$** 

PARREG	Columns	Output
1 or 4	1 & 2	Values of average principal stress and $\sigma_3$ based on PHI (Table 3.5).
2	3 & 4	Values of average principal stress and $\sigma_3$ based on COHESN and PHILRG (Table 3.5).
3 or 5	1 to 4	All of the above values.

#### **3.2.2.4 Other values output**

When a lateral load  $Q$  is applied in iswests, the deflection of the support for  $Q$  is assumed to take place in the direction opposite to  $Q$ . As the true position of the pivot to  $Q$  enters the calculation of the inclination  $\lambda_1$  of  $Q$ ,  $\lambda_1$  is calculated by iteration, starting with its initial value ANPQIN, fed at 9/41-48, Table 3.1, for the first set of readings involving  $Q$ , and with the value of  $\lambda_1$  last calculated, for subsequent sets of readings. The maximum number of iterations, required to make the difference between the last value of  $\lambda_1$  and the previous value less than  $0.1^\circ$  seldom exceeds 2 (see output for file 4, Box 4.1), and is output following Table 4 of the output (when PAROUT = 0. or 6.), together with the time of the readings giving this maximum.

#### **3.2.2.5 Values output when a check of the data is desired or due to faulty data**

In reading the dial gauges used for recording the various displacements, errors can sometimes occur in reading the smaller dial indicating mm, say. Major errors made in reading the dial gauges can be detected by applying a check on the data, by temporarily putting PDATCH = 1. at 1/1-8 in Table 3.1. The resulting output is explained in Table 3.7. If, as a result of the data check, no errors are detected in any one test, a message to that effect is output.

Even when the program is run with no data check (PDATCH = 0.), should negative shear displacements  $> 1.6$  mm be obtained in any test, a warning to that effect appears at the end of the output and also on the screen. Such negative shear displacements may result from misread dial gauges, or sometimes from the rapid application of the lateral load without increasing the main load by about equal amounts. Calculations are not terminated, but it is advisable to apply a data check as above when such a message appears.

Calculations are terminated if, due to missing dots, etc, the number of iterations in solving the equations in Appendix 3, or elsewhere in the program where an iterative solution is done, exceeds 16. In such cases a warning to that effect is written in the output file and on the screen. By examining the output file, the test in which such a fault exists can be located, and the data file corrected.

**Table 3.7. Values in table output when a check of the data is desired (PDATECH = 1.)**

Col.	Variable	Explanation
1	TIMACT	Actual time of reading (entered at 12/1-7, etc in Table 3.1).
2	HIGHDX	Higher $\delta_x$ than expected; otherwise, see explanation for col. 5.
3	TLOWDX	Lower $\delta_x$ than expected; otherwise, see explanation for col. 4.
4	HIGHDY	Higher $\delta_y$ than expected; otherwise, see explanation for col. 3 or 7.
5	TLOWDY	Lower $\delta_y$ than expected; otherwise, see explanation for col. 2 or 6.
6	HIGHTL	Higher $\Delta y_{MP}$ than expected; otherwise, see explanation for col. 5.
7	TLOWTL	Lower $\Delta y_{MP}$ than expected; otherwise, see explanation for col. 4.

When the data is reviewed in the light of the output explained in Table 3.7, any errors in reading the dial gauges can generally be detected. Sometimes it may be decided that there are no such errors (see end of Note 1).

### 3.3 The program CYLWEE88

#### 3.3.1 Input data for program CYLWEE88

Form 2 is intended for entry of data during the test and for subsequent use in preparing the input file for the program. The explanation of the entries is given in Table 3.8. All data, except that in row 12 and after, column 48 have to be fed in floating point format.

**Table 3.8. Explanation of the entries for the input file of the program CYLWEE88**

Row/ column	Variable	Entry	Note
1/1-8	PDATECH	See Table 3.1, 1/1-8.	
1/9-16	PAROUT	See Table 3.1, 1/9-16.	
1/17-24	PARREG	See Table 3.1, 1/17-24.	
1/25-32	TYPFRA (27)	Type of loading frame used. 1.: portable; 0.: triaxial	
1/33-40	PARLAT	1.: Lateral load $Q$ has been applied; 0.: No $Q$ applied.	
1/41-48	POISNR	See Table 3.1, 1/49-56.	



**Table 3.8. (continued)**

Row/ column	Variable	Entry	Note
2/1-8	WLP1	Weight of grooved plate LP1 (kgf).	
2/9-16	WLP2	Weight of grooved plate LP2 (kgf).	
2/17-24	WBC	See Table 3.1, 2/25-32.	
2/25-32	DIASTB	See Table 3.1, 3/9-16. (Assumed as 1.2 cm if left blank).	
2/33-40	FRCOEF	See Table 3.1, 2/33-40.	
2/41-48	TLP1MN	See Table 3.1, 2/9-16.	
2/49-56	GRINL	$A_p$ in equation (3.5), for indicator for $P$ .	(28)
2/57-64	GRSLO	$D_p$ in equations (3.5) or (3.6), for indicator for $P$ .	(28)
2/65-72	DIVPRP	Displacement represented by each division of the proving ring dial for $P$ (cm).	(29)
3/1-8	WPR	Weight of proving ring or load cell for $P$ (kgf).	
3/9-16	WHJ	Weight of hydraulic jack when TYPFRA = 1. (kgf).	
3/17-24	H2	$h_2$ = height from single ball to the grooves on LP2 (cm) (Fig. 2.2 or Fig. 3.3, with the hydraulic jack unextended).	
3/25-32	WDM	See Table 3.1, 7/65-72.	
3/33-40	TMOMDM	Moment produced by the dial gauge unit $D_{mp}$ (Fig. 3.3) about the initial centroid of the shear plane (kgf.cm).	
3/41-48	CONDX	Factor for converting readings of dial $D_x$ (Fig. 3.3) into cm.	(30)
3/49-56	CONDY	Factor for converting readings of dial $D_y$ (Fig. 3.3) into cm.	(30)
3/57-64	CONYMP	Factor for converting readings of dial $D_{mp}$ (Fig. 3.3) into cm.	(30)
3/65-72	CONRPB	Factor for converting readings of dial $D_{rb}$ (Fig. 3.3) into cm.	(30)
4/1-72	...	<b>This row is omitted when PARLAT (row 1) = 0.</b>	
4/1-8	DCLPSB	$y_{sp}$ = horizontal distance between the pivot of the spring balance and the single ball (Fig. 3.3) (cm).	
4/9-16	HTFPSB	$x_{sp}$ = height from floor to pivot of spring balance (Fig. 3.3) (cm).	
4/17-24	HTFSB	$x_b$ = height from floor to the single ball (Fig. 3.3) (cm). (Just before start of $P$ application when a compression machine is used.)	

**Table 3.8. (continued)**

Row/ column	Variable	Entry	Note
4/25-32	LYOK	$L_y$ = initial length of the yoke for $Q$ (Fig. 3.4) (cm).	(31)
4/33-40	WYK	Half the weight of the devices for applying $Q$ (kgf).	
4/41-48	ASPBL1	$A_{s1}$ = constant used in converting spring balance 1 readings into kgf.	(32)
4/49-56	DSPBL1	$D_{s1}$ = factor for converting spring balance 1 readings into kgf.	(32)
4/57-64	ASPBL2	$A_{s2}$ = constant used in converting spring balance 2 readings into kgf.	(32)
4/65-72	DSPBL2	$D_{s2}$ = factor for converting spring balance 2 readings into kgf.	(32)
5/1-72	...	These three rows are for alphanumeric data. Any desired information can be entered in these rows. The headings appearing on the form can be altered to suit requirements.	
6/1-72	...		
7/1-72	...		
8/1-8	ALFN	$\alpha_n$ = nominal angle between the axis and the current shearing plane of the test mould (deg).	
8/9-16	DIAIN	$D_i$ = inside diameter of test mould (cm).	
8/17-24	ALFNOC	$\alpha_n$ angle for the other cut in the double-cut mould (deg). Leave blank for single-cut moulds.	(33)
8/25-32	PARCUT	1.: shear along lower cut; 2.: shear along upper cut. Leave blank for single-cut moulds.	(33)
8/33-40	WSPPTM	Weight of specimen plus test mould (kgf).	
8/41-48	EMPTY	Height of empty portion of mould above specimen (cm).	
8/49-56	HDISC	Height of wooden disc, if any, at bottom of mould (cm).	
8/57-64	D1	Distance $d_1$ in Fig. 3.3 (cm).	(34)
8/65-72	D2	Distance $d_2$ in Fig. 3.3 (cm).	(34)
9/1-8	D3	$d_3$ = initial amount by which the hydraulic jack (Fig. 3.3) is extended (cm), when TYPFRA = 1.; leave blank otherwise.	
9/9-16	CLRNCE	$n_c$ = initial clearance between the shearing planes of the two halves of the test mould for the current cut (cm).	

**Table 3.8. (continued)**

Row/ column	Variable	Entry	Note
9/17-24	VPI	Distance by which LP2 is shifted relative to LP1, in the positive $y$ direction (Fig. 2.2), prior to start of loading (cm).	
9/25-32	DH	Dimension $\delta h$ , $\delta h_1$ , or zero, depending on mode of failure.	(35)
9/33-40	DH2	Dimension $\delta h_2$ , or zero, depending on mode of failure.	(35)
9/41-48	PARFPL	Parameter for defining orientation of the failure plane. 1: failure has taken place along $A_1B_1$ (Fig. 2.3); 0.: otherwise.	
9/49-56	PFIXDR	Parameter for enabling revised versions of rows 1 to 4 to be read after the end of data for the current test, and/or the optional row 11 to be read.  0.: no row 11; pass on to the alphanumeric data of the next test.  1.: no row 11; read the revised versions of rows 1 to 4.  2.: read row 11; pass on to the alphanumeric data of the next test.  3.: read row 11 and the revised versions of rows 1 to 4.	
9/57-64	PSPBDL	1.: Lateral load, $Q = Q_1 + Q_2$ , given by equations (3.7), (3.8). 2.: Lateral load, $Q = 2Q_1$ , given by equation (3.7).	(36) (36)
9/65-72	RDGNUM	Number of rows of subscripted variables (maximum = 40.).	
10/1-72	...	<b>This row is omitted when RDGNUM (row 9) &lt; 41.</b>	
10/1-8	RDGNUM	True number of rows of subscripted variables (maximum = 40.).	
10/9-16	GS	Specific gravity of solid particles.	
10/17-24	WATCON	Water content of soil placed into the cylwtest mould (ratio).	
11/1-72	...	<b>This row is omitted when PFIXDR (row 9) &lt; 2.</b>	
11/1-8	DIAOUT	$D_o$ = outside diameter of the test mould (cm).	(37)
11/9-16	HTLOWR	Dimension $h_L$ of mobile half of test mould (Fig. 3.3) (cm).	(37)
11/17-24	XBARQT	$x$ co-ordinate $\bar{x}_q$ of point of application of $Q$ relative to the centroid $O_M$ of shearing plane of the mobile half TM of	

**Table 3.8. (continued)**

Row/ column	Variable	Entry	Note
		the test mould (Fig. 3.3) (cm). (Negative if above $O_M$ .)	(37)
11/25-32	YBARQT	y co-ordinate $\bar{y}_q$ of point of application of $Q$ relative to the centroid $O_M$ of the shearing plane of TM (Fig. 3.3) (cm).	(37)
11/33-40	HTMOLD	Overall height of test mould (cm).	(37)
11/41-48	WTMEMP	Weight of assembled test mould while empty (kgf).	(37)
11/49-56	WADDTM	Weight $W_a$ of any lugs or links left on TM (Figs 1.3, 1.4)(kgf).	(37)
11/57-64	TMOMAV	Moment $M_{av}$ of $W_a$ about the centroid $O_M$ of shear plane of TM, with the axis held vertically (kgf.cm).	(37)
11/65-72	TMOMAH	Moment $M_{ah}$ of $W_a$ about the centroid $O_M$ of shear plane of TM, with the axis held horizontally (kgf.cm).	(37)
12/1-4	HOUR(I)	Hour of the day at which readings have been taken (hour).	
12/5-8	MINUTE(I)	Minutes past the hour at which readings have been taken (min).	
12/9-16	DXABS(I)	Reading of dial gauge $D_x$ (Fig. 3.3).	(38)
12/17-24	DY1ABS(I)	Reading of dial gauge $D_y$ (Fig. 3.3).	(38)
12/25-32	DTMLP2(I)	Reading of dial gauge $D_{mp}$ (Fig. 3.3).	(38)
12/33-40	DRPBP(I)	Reading of dial gauge $D_{rb}$ (Fig. 3.3).	(38)
12/41-47	GR(I)	Indicator reading for the main load $P$ .	(39)
12/48	IPARFL(I)	Enter '1' against the maximum value of GR(I), if PARFPL has been specified as '1.' at 9/41-48. Leave blank otherwise.	
12/49-56	SPBAL1(I)	$G_{y1}$ = reading of spring balance No. 1.	(32)
12/57-64	HTFYKS(I)	$x_h$ = height from floor to spring balance end of yoke (Fig. 3.3).	
12/65-68	DECLYK(I)	Total amount by which the effective length of yoke has been decreased during the test (cm).	(40)
12/69-72	SPBAL2(I)	$G_{y2}$ = reading of spring balance No. 2, <b>if used</b> , and PSPBDL (at 9/57-64) = 1.; leave blank otherwise.	

**Table 3.9. Default values in the program CYLWEE88 regarding the test moulds**

Mould No.	:	1	2	3	4		
Number of cuts	:	Single	Single	Double	Double		
Cut	:	...	...	Lower	Upper	Lower	Upper
Input value of $\alpha_n$	(deg):	29.6	45.0	30.34	46.0	30.00	29.74
Input value of $D_i$	(cm):	8.56	10.24	10.08	10.08	10.44	10.44
Input $\alpha_n$ for the other cut	(deg):	...	...	46.0	30.3	29.74	30.00
Outside diameter, $D_o$	(cm):	8.90	10.75	10.84	10.84	11.30	11.30
Dimension $h_L$ of mould	(cm):	5.53	3.96	6.10	22.73	5.16	11.95
Dimension $\bar{x}_q$ of mould	(cm):	-0.49	0.24	-1.46	-2.08	-2.29	-0.39
Dimension $\bar{y}_q$ of mould	(cm):	5.38	6.30	5.82	5.83	6.12	6.12
Overall height of mould	(cm):	34.1	27.4	48.0	48.0	44.0	44.0
Weight of empty mould	(kgf):	1.935	2.288	5.197	5.197	5.375	5.375
Weight $W_a$ of lugs, etc	(kgf):	0.113	0.109	0.100	0.445	0.150	0.460
Moment $M_{av}$ of mould	(kgf.cm):	0.270	0.311	0.00	0.00	0.00	0.00
Moment $M_{ah}$ of mould	(kgf.cm):	0.240	0.211	0.49	6.39	1.64	4.43

### 3.3.2 Output of the program CYLWEE88

As in section 3.2.2, only the variables that have not been defined earlier will be explained here; the rest can be quickly traced through the index to such variables. Much of the detailed output for CYLWEE88 is the same as that given in Table 3.3; only the differences will be given. Tables 3.4 to 3.7 are equally applicable for the output of CYLWEE88. The units are as indicated on the outputs. (See Box 4.3 for typical outputs on the diskette.)

#### 3.3.2.1 Common data for all tests and constants for each test

The first five rows of the output contain the values applicable to all tests that follow, and fed in the first four rows of the input (Table 3.8). If any of these values have been

changed before any one test (PFI<sub>XDR</sub> = 1. or 3. in the previous test), all the values are re-written. The four variables that have not been previously defined are given in Table 3.10. Following the common data for all tests, are the constant values applicable to the test that follows. These are also given in Table 3.10, unless previously defined.

**Table 3.10. Explanation of values output by program CYLWEE88 prior to each test**

Row	Variable	Explanation	Note
1	RMLC	The simply supported reaction $M_B/D$ in equation (2.2), for the load cell and attached equipment used by the Author.	(41)
2	DENSWD	Density of wood assumed in the program.	
2	RMPR	The simply supported reaction $M_B/D$ in equation (2.2), for the proving ring and attached equipment used by the Author.	(41)
3	DVRP	DIVPRP defined in Table 3.8, 2/65-72.	
10	ALFA	The actual inclination $\alpha$ of the shear plane (Fig. 3.5(a) to (c)), or the initial value of $\alpha_i$ (Fig. 3.5(d)).	
	HTLOWS	The dimension $h_s$ of the sheared soil wedge (Fig. 3.5).	
	WTM	Mass of mobile part of test mould, excluding WADDTM.	
	WS	Mass of mobile half of sheared soil wedge (Fig. 3.5).	
11	XBARTM	$x$ co-ordinate of centre of gravity of WTM relative to $O_M$ (Fig. 3.3).	
	XBARS	$x$ co-ordinate of centre of gravity of WS relative to the initial centroid of the shear plane.	
	WD	Mass of wooden disc, if used, at bottom of mould.	
12	DH	The dimension $\delta h$ if failure has taken place as in Fig. 3.5(a) or (b); 88.: implies failure as in Fig. 3.5(c).	
	YBARTM	$y$ co-ordinate of centre of gravity of WTM relative to $O_M$ (Fig. 3.3).	
	YBARS	$y$ co-ordinate of centre of gravity of WS relative to the initial centroid of the shear plane.	
	RM	Actual value of the simply supported reaction $M_B/D$ in equation (2.2).	
13	WTMC	Mass of mobile part of test mould, including WADDTM.	
	XBRTMC	$x$ co-ordinate of centre of gravity of WTMC relative to $O_M$ (Fig. 3.3).	

**Table 3.10. (continued)**

Row	Variable	Explanation	Note
13	YBRTMC	$y$ co-ordinate of centre of gravity of WTMC relative to $O_M$ (Fig. 3.3).	
	SW	The sum WTMC + WS + WDM + WD.	
14	PARINC	0.: triaxial frame used, no $Q$ applied; 1.: portable frame used; 2.: triaxial frame used; $Q$ capable of being applied.	
	DOITRM	Distance between the grooves on LP1 and the initial centroid of the shear plane.	
	WCINL	WATCON = initial water content of the specimen, if fed in row 10.	
17	XTMO1	$x$ co-ordinate of centre of gravity of WTM + WS + WD + WLP1 relative to the initial centroid of the shear plane.	
	YTMO1	$y$ co-ordinate of centre of gravity of WTM + WS + WD + WLP1 relative to the initial centroid of the shear plane.	
18	X1C	Value of XTMO1 relative to $O_M$ in Fig. 3.3.	
	Y1C	Value of YTMO1 relative to $O_M$ in Fig. 3.3.	
	VOIDR	Initial void ratio of specimen, if row 10, Form 2 has been fed.	
19	DH1	The dimension $\delta h_1$ when failure has taken place as in Fig. 3.5(c).	

**3.3.2.2 Values output for each test**

The detailed output of the program CYLWEE88 is the same as that given in Table 3.3 for iswests and priswests, except for the differences listed in Table 3.11.

**Table 3.11. Differences in detailed output of program CYLWEE88 for each test**

Col.	Variable	Explanation	Note
25	SECMOM	$I$ = moment of inertia of the corrected area of shear*.	
26	PERSMA	Percentage error in $I$ if calculated by approximating failure plane to an 'equivalent rectangle' defined before Eq (A15).	

\* By analysis C if PARFPL = 1.; otherwise, by analysis B.

**Table 3.11. (continued)**

Col.	Variable	Explanation	Note
30	DEVREC(I)	The value of $\delta\sigma/\sigma$ obtained by approximating failure plane to an 'equivalent rectangle' defined before Eq (A15).	
47	GRSBAL	The inclination of the spring balance to the horizontal.	(42)
58	XFC	XFORCE defined in Table 3.4, column 9.	

### 3.3.2.3 Other values output

The regression results and the values output when a check of the dial gauge readings is desired is as given in sections 3.2.2.3 and 3.2.2.5 respectively, except that the limit for the negative shear displacements for the warning in the latter section is in this case 0.4 mm, and the limit of the number of iterations for terminating calculations in case of faulty data is 8.

A further table, now almost obsolete because of the lack of occurrence of negative stresses on the failure plane with the application of  $Q$  after failure, gives a set of values related with the solution of stresses using equations (A9) to (A17), Appendix 1. The more significant of these values are DCOMPU =  $D_u$ , calculated by equation (A9), and INXDU = number of iterations applied in solving for  $D_u$ .

**NOTE 1.** Errors of the order of  $500 \times 10^{-2}$  mm can sometimes be made in reading the smaller dial registering mm of the gauges  $D_x$ ,  $D_y$ , and  $D_{mp}$  (Fig. 4.7). The program provides a means of detecting such errors by comparing the ratio of the differences between consecutive readings. By examining the output explained in section 3.2.2.5, the user can easily detect whether such errors have been made, or whether the error messages are the result of an abnormal rotation of the test mould or a rapid application of the lateral load. After correcting any such errors, the parameter at 1/1-8 is changed to '0.' to enable the tests to be evaluated.

**NOTE 2.** Outputs of differing degree of detail are obtainable from the program as follows.

0.: All the details listed in Table 3.3 are output.

6.: A summary of the calculated values, listed in Table 3.4, is output together with a table of normal and shear stresses at peak strength and at the end of each test (Table 3.3, columns 58-74). All but the last of the values in the latter table are output collectively, when any type of regression is desired; so, option '7.' may be preferred in most cases.

7.: The summary table for each test is output as for option '6.', together with the results of the regression as explained in section 3.2.2.3.



8.: Only the identifying information about each test, and the results of regression is output. This option may be used to quickly view the differences in the final results due to changes made to the test data, where an output has already been obtained by one of the earlier options.

**NOTE 3.** A recent facility added to the program is the calculation of the approximate average principal stress at peak strength in each test, assuming the angle between the failure plane and the plane on which the major principal stress acts to be equal to  $45 + \phi/2$ . The regressed values of cohesion  $c$  (if any) and  $\phi$  are used for these calculations. The intermediate principal stress is also estimated by assuming the soil to be an elastic material, and as such the value of Poisson's ratio  $\nu$  is needed in this calculation. A good average value of  $\nu$  for unsaturated clays and gravels, as measured by the Author, is 0.3, and this value is assumed in the calculations, if the actual value of  $\nu$  is not specified at 1/49-56. Such calculations are omitted altogether if any value greater than 0.5 for  $\nu$  is entered at 1/49-56.

**NOTE 4.** The values of  $A_{pg}$  and  $D_{pg}$  to be entered in these sections, are those needed to convert the hydraulic jack pressure gauge readings  $G_{pg}$ , if entered in 12/61-66 and subsequent rows, into a force  $P_{pg}$  (kgf) given by the following equation.

$$P_{pg} = (G_{pg} - A_{pg}) \cdot D_{pg} \quad (3.1)$$

The values of  $P_{pg}$  calculated by equation (3.1) are not used in the evaluation of the tests, but for comparison with the  $P$  values measured using the load cell, as a rough check on the proper functioning of this cell. Entering the values of  $A_{pg}$  and  $D_{pg}$ , and any value of  $G_{pg}$  is optional.

**NOTE 5.** If this space is left blank, the value is assumed as 10.44 kgf. In the program, the simply supported reaction of the devices for applying  $P$  is calculated, using the actual equipment used by the Author, making allowance for such details as the change in the position of the estimated centre of gravity of the hydraulic jack during the test. For general use, the values of  $M_B/D$  so calculated are multiplied by the ratio of the sum of the actual weights of the hydraulic jack, the load cell, the grooved plate, and the ball cage to the sum of the weights of those used by the author. A similar procedure is applied in the calculation of WQNC, Table 3.3, column 49.

**NOTE 6.** If any of the values in 3/9-48 happen to coincide with the default values of 1.2 cm for the diameter of the steel balls, and 0.001 cm for each of the other four values, the corresponding spaces may be left blank, in which case the default values will be assumed. The dial gauge constants are taken as positive when the gauges are arranged as in Fig. 4.7, and indicate an increase in reading when the tips are depressed. Thus, the readings of dial gauges  $D_x$  and  $D_{mp}$  (for determining  $\delta_x$  and  $\Delta y_{MP}$ , the movement of grooved plate LP2 in the negative  $y$  direction (Figs 1.2, 2.1) relative to the initial centroid  $O_1$  (Fig. 2.1) of the shear plane prior to the start of loading, plus the additional movement of LP2 in the same direction relative to LP1 during the test) should normally be decreasing during the test; those of dial gauges  $D_y$  and  $D_{rb}$  (for determining  $\delta_y$  and  $\Delta y_{RB}$ , the amount of shift, if any, applied to the pivot to  $P$  in the positive  $y$  direction (Figs 1.2, 2.1) during the test) should be increasing. **If the opposite is true for any one dial, the corresponding dial gauge constant should be entered as negative.**

**NOTE 7.** The dimension  $h_1$  is defined as the distance between the ball joint of the lateral loading device (Fig. 3.1) and the test mould end of the proving ring, with the adjustment screw completely screwed in its housing, and with the spring loaded piston under zero load (or the ram of the air piston in its most extended position).

**NOTE 8.** The values of  $A_r$  and  $D_r$  to be entered are those needed to convert the indicator readings  $G_r$  of the device for measuring the main load  $P$  into kgf using the following equation.

$$P = (G_r - A_r) \cdot D_r \quad (3.2)$$

**NOTE 9.** This value is fed just to see how the  $\delta\sigma/\sigma$  values would be modified, if a shift (such as 1.0 cm) had been applied to the jacking equipment in addition to the shift actually applied before the start of loading.

**NOTE 10.**  $d_1$  and  $d_2$  (Fig. 2.1) are the respective distances from the right angled corner of the test mould at which independently supported dial gauges for the measurement of  $\delta_y$  and  $\delta_x$  contact the test mould before any displacement of the mould has taken place. **If the dial for  $\delta_y$  contacts a central bracket BR (Fig. 4.7),** screwed on the test mould, to minimize errors that may arise from the slight transverse rotation of the mould during the test,  **$d_1$  must be entered as negative.**

**NOTE 11.** Especially when the electrical load cell has not been allowed to warm up sufficiently before the zero adjustment, the final reading of the gauge under zero load at the end of the test may differ slightly from the initial setting. The program applies a correction to the calculated load  $P$ , by assuming this difference in zero reading to build up uniformly with time after the zero adjustment. **If the initial reading  $A_r$  of the gauge under zero load (entered at 7/33-40) is not zero, the final value must definitely be entered at 8/57-64 irrespective of whether it is different from the initial value or not.**

**NOTE 12.** This situation may arise in iswests, if the angle of friction  $\phi$  of the soil is below certain limits depending on the angle  $\alpha_n$  of the test mould and the loading configuration used. These limits have been discussed by Mirata (1974). The distance  $\Delta h$  applicable to such cases is shown in Fig. 3.2(b)(i). (See Box 4.1, file 1 for the only test in which this condition has been encountered.) If failure occurs along the shearing plane of the test mould, this section should be left blank.

**NOTE 13.** These co-ordinates ( $x_{sp}$ ,  $y_{sp}$ ), Fig. 3.1, should be measured while the grooved plates LP1 and LP2 are concentric.

**NOTE 14.** If the dimensions  $d_r$ ,  $h_r$ , and  $h_{cg}$  are within a few mm of the default values listed in Fig. 3.2(a), and the relevant rod number in this list is entered at 9/49-56, then, if row 10 is at all needed, 10/41-64 can be left blank. If any of the values are different, then all three values must be entered at 10/41-64; in this case, 9/49-56 may be left blank, or filled with any one-digit number, which will be output without affecting computations.

**NOTE 15.** If the dimensions of the test moulds used are the same as those presently in use at METU (iswests moulds with an inner width of 250 mm, and priswest moulds with an inner width of 300 mm, Fig. 3.2(b)), and row 10 is at all needed, sections 10/1-40 may be left blank. In this case, the mould number JTM will be determined from the mould angle  $\alpha_n$  specified at

7/1-8, the AL value specified at 7/17-24, and the type of test specified at 1/41-48, and the corresponding default values (Fig. 3.2(b)), based on an assumed soil density of 1.85 g/cc for the iswest moulds, taken. If any of the values are different, all the values in this section should be entered (the weight  $W$  of the test mould with LP1 attached and the enclosed soil in the case of iswests **or** the weight  $W_{tp}$  of the mobile half of the empty test mould with LP1 attached in the case of priswests; the co-ordinates  $(\bar{x}, \bar{y})$  **or**  $(\bar{x}_{tp}, \bar{y}_{tp})$  of the centre of gravity of these weights relative to the centroid  $O_M$  of the shearing plane of the test mould; and the co-ordinates  $(\bar{x}_q, (\bar{y}_q - d_r/2))$  of the rounded tip of the rod at the end of the lateral loading device (when in the recess on the test mould) relative to  $O_M$ ).

**NOTE 16.** To prevent the steel balls rolling in between the grooved plates LP1 and LP2 from approaching the edge of these plates by more than about 6 mm at the larger shear displacements, LP1 is screwed on to the priswest mould TM at a finite distance to the right, as viewed in Fig. 3.1(b), of the centroid  $O_M$  of the shearing plane of TM (Fig. 3.2(b)). The amount AMLP1L by which **LP1** has been 'lowered' (Fig. 4.7) when used with the moulds (JTM = 8 to 11 in Fig. 3.2(b)) with  $\alpha_n = 35^\circ, 40^\circ, 45^\circ$ , and with the 40-degree mould loaded on the lid with the equivalent  $\alpha_n = 50^\circ$  (PGT45D = 1. at 11/65-72) was 11.5 mm, 23.2 mm, 28.0 mm, and 24.0 mm respectively.

**NOTE 17.** If this space is left blank, the program assumes  $G_s = 2.70$ , if PARREG at 1/17-24 has been specified as '2.', and  $G_s = 2.65$  otherwise.

**NOTE 18.** The initial readings of the dial gauges  $D_x, D_y, D_{mp}$ , and  $D_{rb}$  (Fig. 4.7) do not have to be zero. The displacements are calculated, by taking the difference between each reading and the corresponding initial reading, until the dials are reset (see Note 19), in which case the reading immediately after such resetting is taken as the basis for the additional displacements.

**NOTE 19.** For cases where the test is prolonged in order to measure the strength at the larger shear displacements, and the capacity of the dial gauges used are likely to be exceeded, provision is made in the program for resetting the desired dial gauge. For this purpose, one final set of readings is taken immediately before resetting; loading is temporarily stopped while the dials are reset; the reset readings are entered in the next row, together with the rest of the data in the previous row; and a '1' is entered in the 7th column following that at which each reset reading has started to be entered.

**NOTE 20.** The inclination  $\lambda_1$  of the  $Q$  device to the horizontal, taken as positive when acting downwards, is calculated from the initial co-ordinates given at 9/25-40, and the calculated displacements of the test mould, and written in column 47 of the detailed output (Table 3.3). As a check on such calculations, if desired,  $\lambda_1$  can occasionally be measured directly during the test, and entered in columns 67-72 of Form 1. Such measured values are written in column 46 of the detailed output and can be easily compared with the corresponding calculated values in the next column. When no such measurements are taken, the relevant rows in column 46 are left blank. An ambiguous situation may arise in measuring  $\lambda_1$  and interpreting its calculated value, when the direction of the main load  $P$  is close to the horizontal. To avoid such ambiguity it needs to be known that  $\lambda_1$  is calculated within the program from these equations, depending on the initial inclination  $\theta$  of  $P$  to the horizontal:

$$\text{when } \theta \geq 0, \quad \lambda_1 = \lambda_q - \theta_r \quad (3.3)$$

$$\text{when } \theta < 0, \quad \lambda_1 = 180^\circ - (|\theta_r| + \lambda_q) \quad (3.4)$$

where,  $\theta_r$  is the inclination of the rotated direction of  $P$  to the horizontal (Fig. 1.2);  $\lambda_q$  is the angle between  $P$  and  $Q$ . Thus, for an initial value of  $\lambda_q = 92^\circ$ , initially, if  $\theta = 5^\circ$ , by equation (3.3),  $\lambda_1$  will be  $87^\circ$ ; if  $\theta = 1^\circ$ ,  $\lambda_1$  will be  $91^\circ$ ; if  $\theta = -5^\circ$ , by equation (3.4),  $\lambda_1$  will be  $83^\circ$ .

**NOTE 21.** The values of X1C and Y1C are the same as X1 and Y1 defined in Table 3.1, 10/9-24 for iswests, but for the slight effect of the dial gauge unit  $D_{mp}$  (Fig. 4.7); they include, in addition, the effect of the contained soil for priswests.

**NOTE 22.** The value of SLRHC (the rate of change of the indicator reading for  $P$  under zero load with time (min) starting from the instant this indicator was set to zero), used for the calculations within the program, is based on the actual duration of the test.

**NOTE 23.** The values in rows 15B - 17 of the output are written only for priswests.

**NOTE 24.** The value of VPITT is the total shift that would have to be applied to the pivot to  $P$  if  $\Delta y_{MP}$  were to be adjusted continuously and exactly in accordance with a set of precalculated curves, based on equations (A24) - (A26), giving the theoretical value of  $\Delta y_{MP}$  to make the moments on the shear plane zero, assuming  $\nu = \beta = 0$ . Note that when  $\Delta y_{MP}$  is adjusted in this way during the test, the alteration to  $\Delta y_{MP}$  due to the slight mould rotation  $\beta$  and the actual value of  $\nu$  is automatically compensated, thus bringing the eccentricity of  $P$  closer to the true theoretical value required to minimize moments.

**NOTE 25.** The values output as 'end of test' has a significance only when the test has been prolonged with the intention of measuring the ultimate strength. The values in the last set of readings are generally taken, but as in some tests the strength sometimes increases temporarily during shear, the previous two sets of readings are also checked to see if the  $P$  value in tests where no  $Q$  has been applied, or the  $\tau/\sigma$  value in tests where a  $Q$  is applied is smaller, and the pair corresponding to the lowest of these values is output. So if the test has been curtailed directly on reaching the peak strength, the values output as 'end of test' may represent values two rows before the peak strength. All values output as 'peak' and 'at end of test' are those corresponding to the set of readings giving such values by analysis C if PARFPL = 1., or by analysis B if PARFPL = 0.; apart from exceptional conditions as noted in Box 4.2, file 2, this way of fixing such values is also mathematically true for analyses A and B; physically, it is always the more correct choice.

**NOTE 26.** These values are output for the benefit of those who may be interested in the finite element solution of stresses within the test wedge.

**NOTE 27.** The purpose of this parameter is to indicate whether the single ball is displaced during the test as when a compression machine is used (Fig 1.3), or whether its position is fixed as in the use of a portable frame and a hydraulic jack as (Fig. 5.5).

**NOTE 28.** The values of  $A_p$  and  $D_p$  to be entered are those needed to convert the indicator readings  $G_r$  of the device for measuring the main load  $P$  into kgf using the following equations.

$$\text{If } A_p \neq 0, \quad P = (A_p - G_r) \cdot D_p \quad (3.5)$$

If  $A_p = 0$ , as when a proving ring is used,

$$P = G_r \cdot D_p \quad (3.6)$$

**NOTE 29.** This value may be omitted if it is equal to 0.000254 cm/div. If, however, a load cell is used, a small value like 0.000001 must be fed, otherwise the default value of 0.000254 will be assumed.

**NOTE 30.** These values are fed as positive when the dial gauges are positioned as in Fig. 3.3, and the readings increase when the tips are depressed. If the opposite is true for either of these conditions, the relevant value has to be fed as **negative**. If any of the spaces in 3/41-72 is left blank, the default value of 0.001 cm/div is assumed.

**NOTE 31.** This dimension can be set to a constant value by adjusting the distances  $D_1$ ,  $D_2$  and  $D_3$  (Fig. 3.4) to fixed values at the beginning of each test.

**NOTE 32.** The program allows for the use of two identical spring balances in parallel when desired, as explained in section 4.4.3(1). The values of  $A_{s1}$ ,  $D_{s1}$ ,  $A_{s2}$ , and  $D_{s2}$  are those required to convert the readings  $G_{y1}$ ,  $G_{y2}$  of the spring balances 1 and 2 into lateral forces  $Q_1$  (kgf) and  $Q_2$  (kgf) respectively by

$$Q_1 = A_{s1} + D_{s1} G_{y1} \quad (3.7)$$

$$Q_2 = A_{s2} + D_{s2} G_{y2} \quad (3.8)$$

If only one spring balance is being used, or the total load  $Q$  applied through two such devices is  $2Q_1$  (**in this latter case, 2. must be entered at 9/57-64**), the spaces for  $A_{s2}$ , and  $D_{s2}$  (4/57-72) may be left blank.

**NOTE 33.** This information is used within the program to read the relevant default test mould data given in Table 3.9. If this data is to be independently fed in Row 11, the space 8/17-32 may be left blank.

**NOTE 34.**  $d_1$  and  $d_2$  are the distances from the edge C of the test mould at which the independently supported dial gauges ( $D_y$  and  $D_x$  in Fig. 3.3) for recording the displacements  $\delta_y$  and  $\delta_x$  respectively contact the test mould. As for physical reasons and for evening out the effect of any slight transverse rotation of the test mould, dial gauge  $D_x$  bears on a central bracket screwed on the grooved loading plate LP1, that is, at a point beyond the test mould,  $d_2$  has to be entered as a **negative** value.

**NOTE 35.** If the mode of failure is as in Fig. 3.5(a) or (b), the dimension  $\delta h$  is entered at 9/25-32 as a positive or negative value respectively; 9/33-40 is left blank. If failure has taken place as in Fig. 3.5(c),  $\delta h_1$  is entered at 9/25-32, and  $\delta h_2$  at 9/33-40. If failure has taken place along the plane  $A_1B_1$  as in Fig. 3.5(d), or along an intermediate plane between the two halves of the test mould, 9/25-40 is left blank.

**NOTE 36.** Note that if a single spring balance is being used, and so  $Q_2$  is zero, this parameter is still to be fed as '1.'. Only when two spring balances are used and the calibration factors are identical, is this parameter fed as '2.'.

**NOTE 37.** If these quantities match those given in Table 3.9, row 11 may be omitted, in which case the relevant data will be read from the default values within the program (see Note 33).

**NOTE 38.** The initial readings of the dials for recording  $\delta_x$ ,  $\delta_y$ ,  $\Delta y_{MP}$ , and  $\Delta y_{RB}$  do not have to be zero. The displacements are calculated by taking the difference between each reading and the corresponding initial reading.

**NOTE 39.** The program assumes that the device for recording  $P$  has been set to zero with the loading plates LP1, LP2 and the ball cage BC resting on it. So, after each reading is converted into kgf by equations (3.5) or (3.6) within the program, the weights of these components are added on to the result to convert it into the  $P$  value defined before equation (2.1). The values in column 19 of the detailed output are the latter values in N.

**NOTE 40.** After the yoke is set to the initial length entered at 4/25-32, so long as the lateral load  $Q$  is increased by means of the turnbuckle, this space may be left blank. Once the turnbuckle reaches its limit of travel, further increase in  $Q$  is effected by means of the fly nuts on the yoke. The total amount by which the effective length of the yoke is decreased in this way has to be entered in each row starting with and following such adjustment, until this length is re-adjusted, when the new value of the total decrease has to be entered in each new row.

**NOTE 41.** The true value  $M_B/D$  is estimated by direct proportion of the total weight of the devices used for applying  $P$  in the current test to the total weight of those used by the Author.

**NOTE 42.** The inclination  $\lambda_1$  of the yoke to the horizontal is taken as positive, when  $Q$  is acting downwards towards the test mould, as in Note 20. For consistency, the values of GRSBAL are also taken as positive, when the force exerted by the spring balance acts downwards towards the test mould. In determining  $Q$  from the spring balance readings, the component of the load recorded by the spring balance in the direction of the yoke is taken.

**Form 1. Test and computer input data sheet for the in situ and prismatic wedge shear tests (see Table 3.1)**

1	9		17		25		33		41		49		57		65							
	PDATCH (0.: no; 1.: yes)		PAROUT(0.:detl.;7.:sum.)		PARREG*		WQ (kg) (0.: Q = 0.)		TYPQDV (0.:air; 1.:spring)		TYPTST (0.:iswest;1.: p/w)		POISNR (optional)									
1																						
2	TKNESS (cm)		TLP1MN (cm)		WLP (kgf)		WBC (kgf)		FRCOEF, $\mu$		DBPI (cm)		DENSOL (g/cc)		APG DPG							
3	WHJ (kgf)		DIASTB (cm)		COND $\times$ ( $\neq$ .001 cm)		CONDY ( $\neq$ .001 cm)		CONYMP ( $\neq$ .001 cm)		CONRPB ( $\neq$ .001 cm)		HTQPRP (cm)		PRCONQ (kgf/div) DIVPRQ ( $\neq$ .000254 cm)							
4	PROJECT :																					
5	TEST NO. :																					
6	SOIL TYPE :																					
	FILE PAGE :																					
	INCL. OF FL. PL. TO HORIZ. :																					
	DATE :																					
	STRAIN RATE :																					
	TEMPERATURE :																					
	TIME OF ZERO SETTING :																					
7	ALFN (deg)		TETA (deg)		AL (cm)		B (cm)		A = GRINL		D = GRSLO		HTLC (cm)		WLC (kgf) WDM (kgf)							
8	DETMDM (cm)		VPI (cm)		VPTI (cm)		D1 (cm)		D2 (cm)		D3 (cm)		TO (min)		ZEROF DH (cm)							
9	PARFPL <sub>(1.:A; B; ; 0.: o/w)</sub>		RDGNUM <sup>#</sup>		PFIXDR		XSBTPQ (cm)		YSBTPQ (cm)		ANPQIN (deg)		RODNUM		SPRCON (kgf/div) CONDES							
10**	WINPUT (kgf)		X1 (cm)		Y1 (cm)		X1Q (cm)		Y1Q (cm)		DIAROD (cm)		HTROD (cm)		CGDISR (cm)							
11***	HTIPWM (cm)		AML1L (cm)		WCOMPS (kgf)		WATCON (ratio)		GS		CLRNCE (cm)		EXTASC (cm)		WTFLOW (kgf) PGT45D (0.: $\alpha_n < 46$ ; 1.: $\alpha_n = 50$ )							
	IPARA(I)		IPRSDX(I)		IPRSY1(I)		IPRSLP(I)		IPRSRP(I)		IPARFL(I)											
	HOUR(I) MINUTE(I)		DXABS(I)		DY1ABS(I)		DTMLP2(I)		DRPBP(I)		GR(I)		SLATLD(I)		DEFSUP(I) PGRDG(I) (optional) GRADQ(I) (optional)							
12																	#					
13																	1					
14																	2					
15																	3					
16																	4					
17																	5					
18																	6					
19																	7					
20																	8					
21																	9					
22																	10					
23																	11					
24																	12					
25																	13					
26																	14					
27																	15					
28																	16					
	1		4		9		17		25		33		41		49		55		61		67	

\* 0.: no regression desired; 2.: ordinary linear regression; 4.: option 1 plus power curve fit; \*\* Row 10 needed only when PFIXDR (Row 9) > 1.  
 1.: regression forced through origin; 3.: both of options 1 and 2; 5.: all three options. \*\*\* Row 11 needed for priswests only.

**Form 2. Test and computer input data sheet for the cylindrical wedge shear test (see Table 3.8)**

1		9		17		25		33		41		49		57		65	
	PDATCH (0.: no; 1.: yes)	PAROUT(0.:detl.;7.:sum.)	PARREG*	TYPFRA(1.:port.;0.:triax.)	PARLAT (1.:Q > 0; 0.:Q = 0)	POISNR (optional)											
1																	
2	WLP1 (kgf)	WLP2 (kgf)	WBC (kgf)	DIASTB (cm)	FRCOEF, $\mu$	TLP1MN (cm)	GRINL	GRSLO	DIVPRP ( $\neq$ 0.000254)								
3																	
4**	WPR (kgf)	WHJ (kgf)	H2 (cm)	WDM (kgf)	TMOMDM (kgf.cm)	CONDX ( $\neq$ .001 cm)	CONDY ( $\neq$ .001 cm)	CONYMP ( $\neq$ .001 cm)	CONRPB ( $\neq$ .001 cm)								
	DCLPSB (cm)	HTFPSB (cm)	HTFSB (cm)	LYOK (cm)	WYK (kgf)	ASPBL1	DSPBL1	ASPBL2	DSPBL2								
5	PROJECT :				SOIL TYPE :				FILE PAGE :								
6	TEST NO. :				INCL. OF FL. PL. TO HORIZ. :				DATE :								
7	STRAIN RATE :				TEMPERATURE :												
8	ALFN (deg)	DIAIN (cm)	ALFNOC (deg)	PARCUT(1.:lower;2.:upper)	WSPPTM (kgf)	HEMPTY (cm)	HDISC (cm)	D1 (cm)	D2 (cm)								
9																	
10***	D3 (cm)	CLRNCE (cm)	VPI (cm)	DH (cm)	DH2 (cm)	PARFPL(1.:A,B.; 0.: o/w)	PFIXDR	PSPBDL(1.:Q-Q+Q;2.:Q-2Q)	RDGNUM <sup>#</sup>								
	RDGNUM <sup>#</sup>	GS	WATCON (ratio)														
11 <sup>#</sup>																	
12	HOUR(I)	MINUTE(I)	DXABS(I)	DY1ABS(I)	DTMLP2(I)	DRPBP(I)	GR(I)	IPARFL(I)	SPBAL1(I)	HTFYKS(I)	DECLYK(I)	SPBAL2(I)					
13																	
14																	
15																	
16																	
17																	
18																	
19																	
20																	
21																	
22																	
23																	
24																	
25																	
26																	
27																	
28	1	5	9	17	25	33	41	49	57	65	69	77	85	93	101	109	117

\* 0.: no regression desired, 1.: regression forced through origin; 2.: ordinary linear regression; 3.: both of options 1 and 2; 4.: option 1 plus power curve fit; 5.: all three options. \*\* Row 4 needed only when PARLAT (Row 1) = 1. \*\*\* Row 10 needed only when RDGNUM (Row 9) > 1. # Row 11 needed only when PFIXDR (Row 9) > 1.



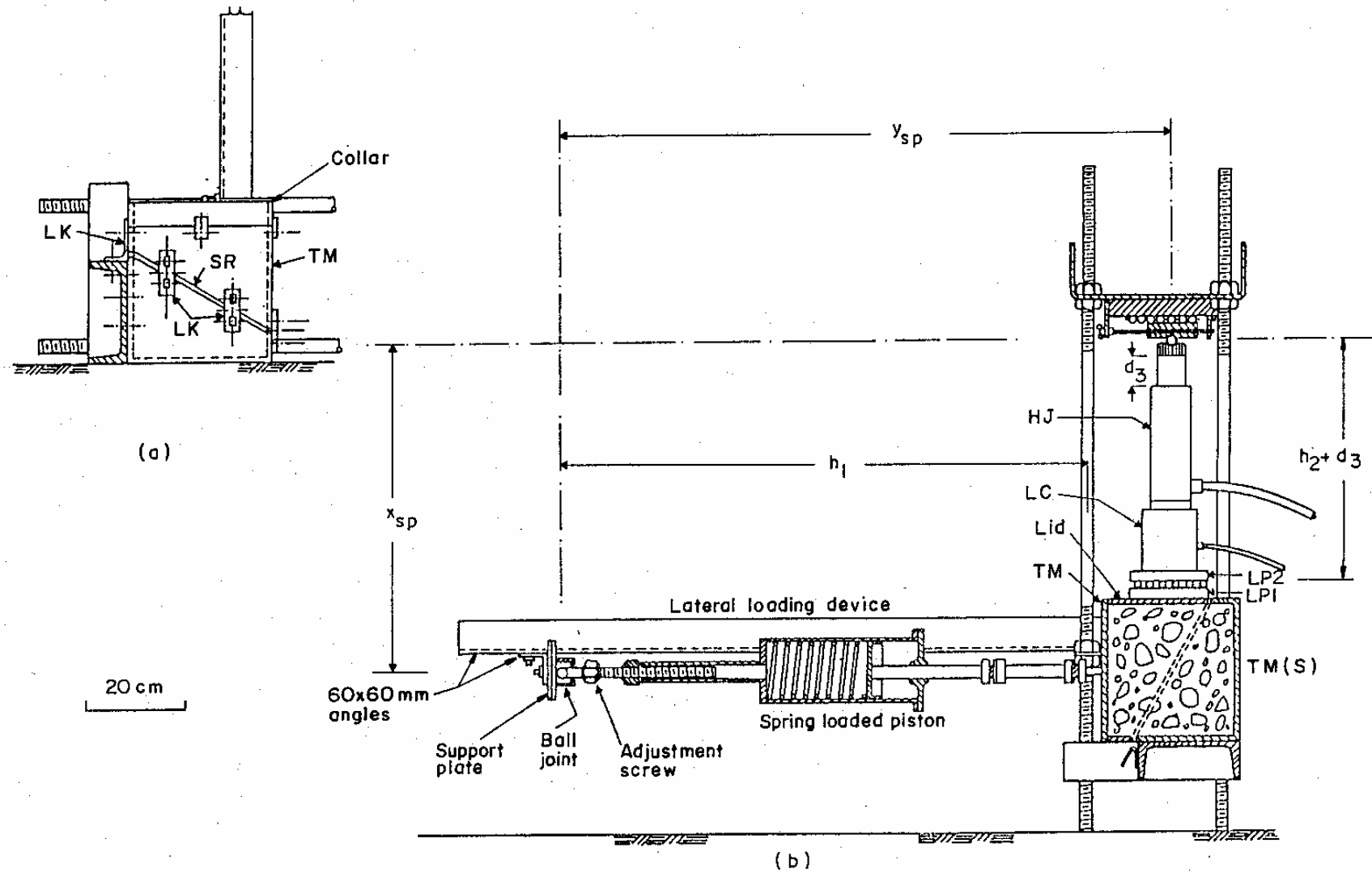
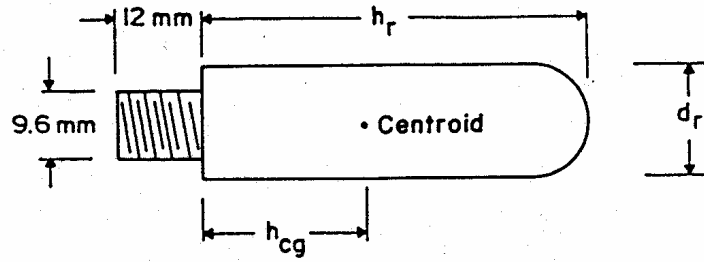
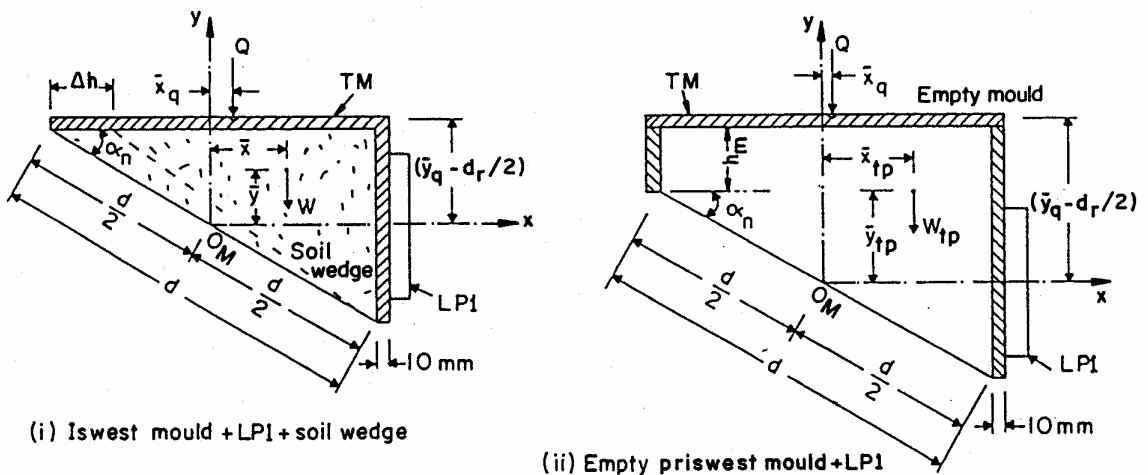


Fig. 3.1. Priswest set-up showing (a) test mould in position for placement of sample and (b) at start of shear using 5-ton loading frame (after Mirata, 1991)



Dimension	$d_r$	$h_r$	$h_{cg}$
Rod no.	(cm)	(cm)	(cm)
1	1.58	2.50	0.95
2	1.56	4.61	2.05
3	1.62	7.62	3.53
4	1.60	2.10	0.18

(a) Default data regarding the rod at the end of the lateral loading device



(i) Iswest mould + LP1 + soil wedge

(ii) Empty priswest mould + LP1

Identifying values					Default values					
$\alpha_{no}$ ( $^\circ$ )	Mould type	$h_m$ (cm)	$b$ (cm)	$d$ (cm)	JTM	$W/W_{tp}$ (kgf)	$\bar{x}/\bar{x}_{tp}$ (cm)	$\bar{y}/\bar{y}_{tp}$ (cm)	$\bar{x}_q$ (cm)	$\bar{y}_q - d_r/2$ (cm)
25	(i)	0	25	36	1	29.51	7.14	3.33	-3.29	8.33
30	(i)	0	25	36	2	31.67	6.97	3.68	-3.36	9.67
35	(i)	0	25	36	3	33.72	6.74	4.07	-3.36	10.98
40	(i)	0	25	36	4	34.57	6.49	4.34	-3.01	12.29
45	(i)	0	25	36	5	34.83	6.16	4.57	-3.07	13.45
30	(i)	0	25	54	6	58.86	9.21	5.42	-4.82	14.22
30	(ii)	5	30	30	7	18.27	5.33	6.53	-0.01	12.80
35	(ii)	5	29.6	30	8	22.69	5.38	6.80	0.05	14.10
40	(ii)	4	30	30	9	21.99	5.53	6.44	0.00	14.20
45	(ii)	4	30	30	10	22.14	5.51	6.50	0.00	15.24
50*	(ii)	4	30	30	11	21.99	9.11	3.24	0.00	12.17

\* $\alpha_{no} = 40^\circ$  mould modified as in section 5.4.4.

(b) Default data for test mould TM + soil wedge + LP1 for iswests and for TM + LP1 for priswests

**Fig. 3.2. Default values of rod and test mould data in program IWPW77**

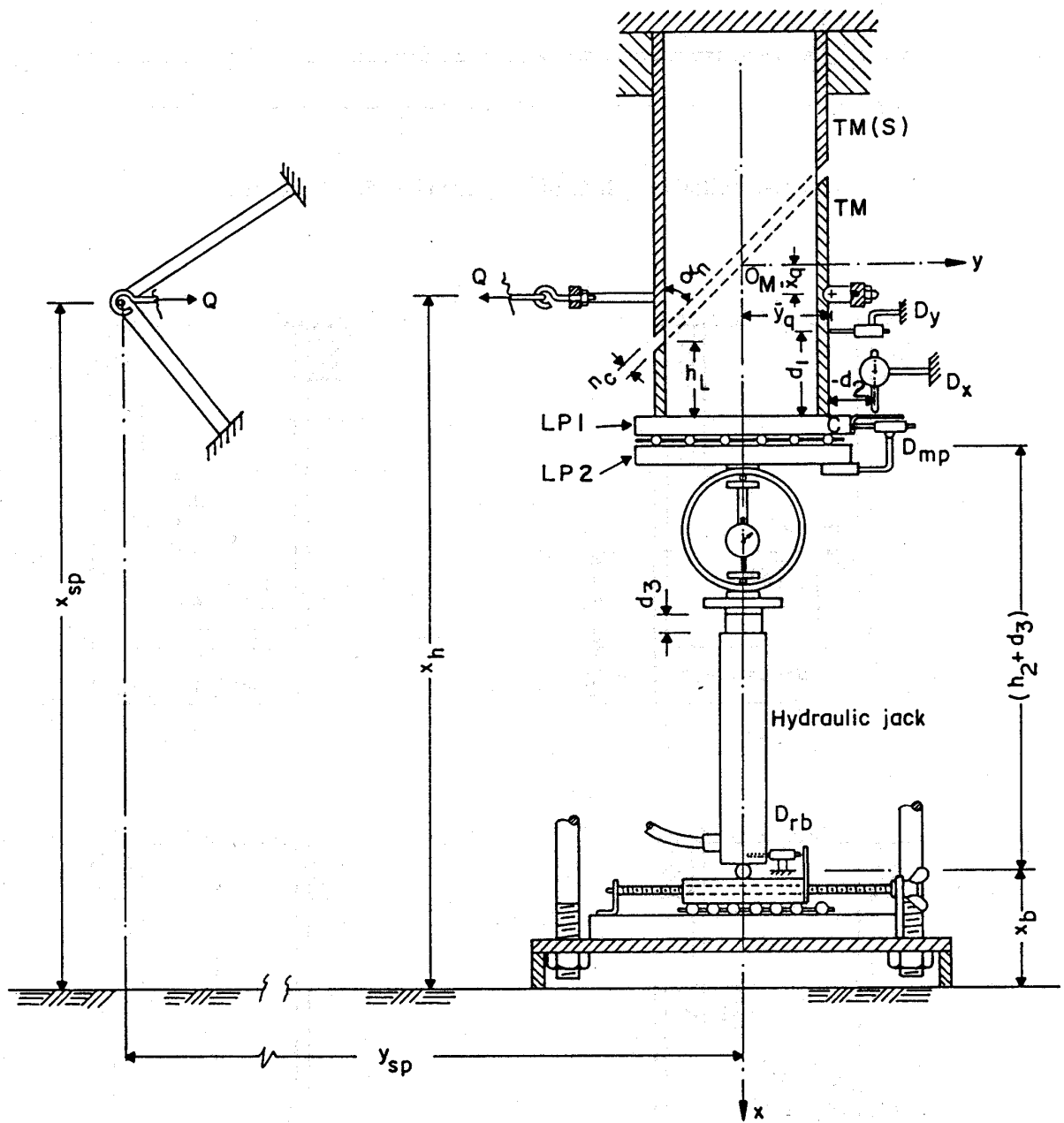


**Fig. 3.3. Distances involved and layout of dial gauges in cylwrests using a portable frame**

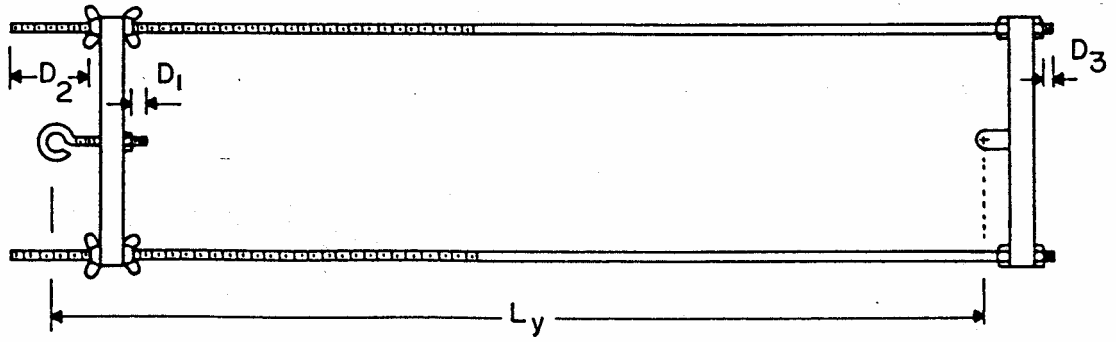


Fig. 3.4. Initial length  $L_y$  of the yoke (Fig.5.6) for cylwests

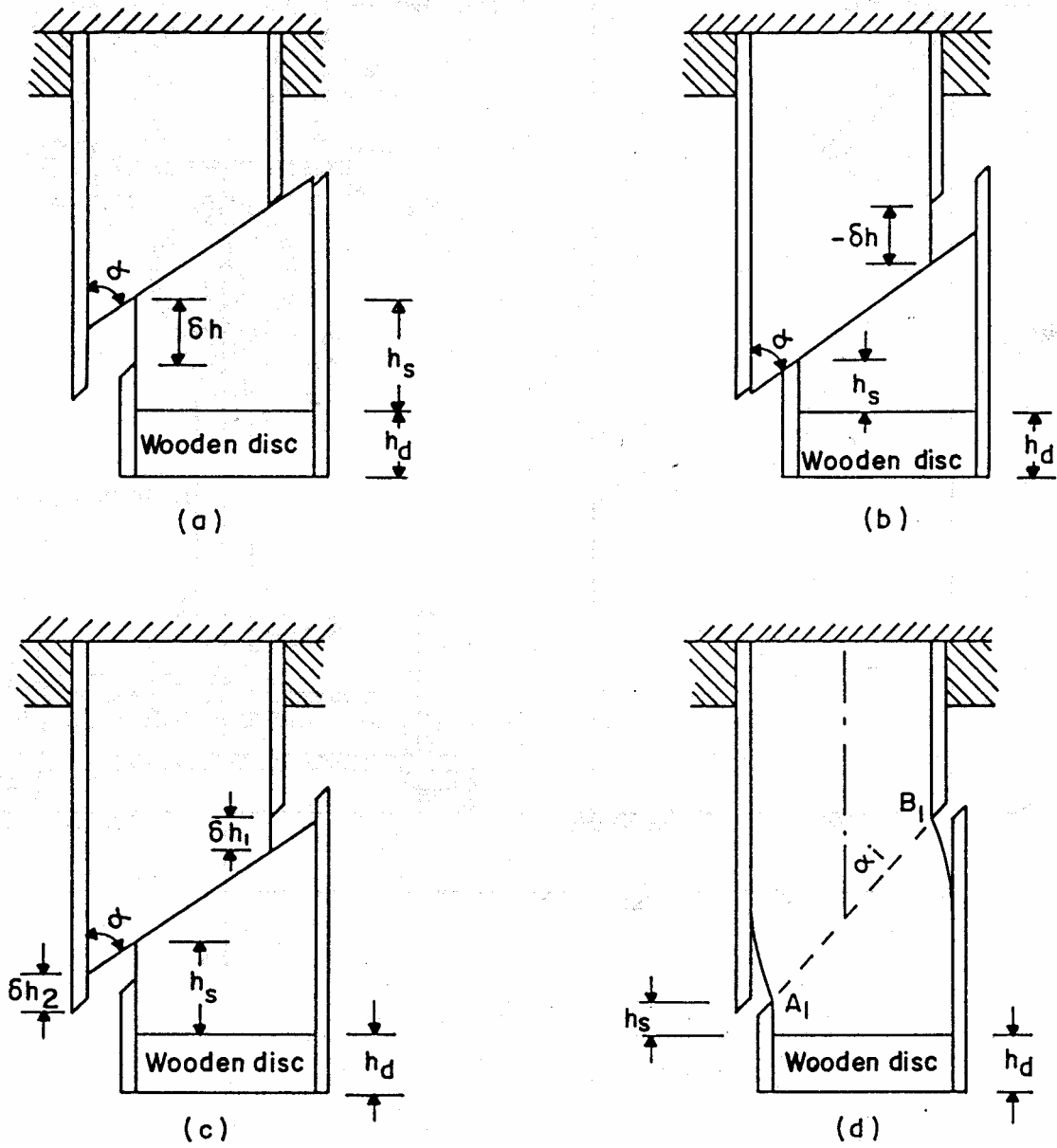


Fig. 3.5. Possible modes of failure in cylwests

## CHAPTER 4

# APPARATUS, TEST PROCEDURES AND RUNNING THE PROGRAMS

### **4.1 Introduction**

The essential features of the apparatus, and the detailed test procedures for the three versions of the wedge shear test will be given here; the detailed drawings of some of the equipment are given in Chapter 5. As values are read during the test, which part of the forms explained in Chapter 3 these are to be entered is stated using the notation given at the end of section 3.1. Instructions for checking the data and running the programs is given in section 4.5.

### **4.2 In situ wedge shear test**

As an in situ test may have to be carried out where it may not be possible to readily procure certain devices and materials, a full list is given below of the apparatus and materials to be checked before embarking on such field work.

#### **4.2.1 Apparatus for iswests without lateral load application**

##### ***4.2.1.1 Equipment for supporting the sides of the test pit***

1. If the test is to be carried out at the bottom or on the side of a test pit, an efficient and practical means of supporting the sides of such a pit is provided by the 400-mm high expansible steel rings described by Mirata (1975, 1976). These are made of 3-mm thick mild steel plate, and have a vertical slit, which can be expanded by two turnbuckles of the type shown in Fig. 4.1(b). Fitted at each end of a diameter perpendicular to the one through the slit, is a dual purpose steel bar, 8 mm in diameter, bent to the shape shown in Fig. 4.1(a). This acts as a handle when in the vertical position, and as a step when horizontal. A rotatable catch helps to hold the handle in the vertical position during transport, and when one ring is to be passed through the other.

Eight such rings with minimum diameters ranging from 1033 mm to 1255 mm at about 30-mm intervals have been successfully used to support the sides of a test pit in a fairly soft clay up to a depth of 4 m. For each size, a separate guide ring, about 25 mm larger in minimum diameter than the corresponding expansible ring, bent out of a 30-mm wide strip of 1.5-mm thick lamina and reinforced by two orthogonal, 8-

mm dia. steel bars, aids in excavating the pit to the right diameter. For every 400 mm that the pit is deepened, the next smaller ring is contracted to its minimum diameter, lowered through the rings already placed, and expanded in position. Removal of the rings, as the pit is back-filled is a reversal of this procedure. The rings are so dimensioned as to fit into each other up to the level of the handles, thus occupying a minimum of space during storage and transport. Each ring is light enough to be hauled and mounted in position comfortably by two men. A length of rope, and some five posts to be placed around the top of the pit, aid in the lowering and extraction of the rings, and can be used as a safety barrier around the pit.

2. A two-tier shelf (made of two 250-mm wide, 30-mm thick boards, one side measuring 640 mm the other 900 mm, connected together by four 450-mm long, 8-mm dia. steel bars near the corners), suspended in the side of the pit is useful for mounting the hand pump of the hydraulic jack, and for placement of data sheets, etc.

#### **4.2.1.2 Special equipment**

1. Test moulds. Two test moulds, of the type described in detail in section 5.2.1, one having  $\alpha_n = 30^\circ$ , the other with  $\alpha_n = 45^\circ$  are sufficient for testing most unsaturated clays.

2. Grooved loading plates and the ball cage. The grooved plates, having five grooves and the ball cage housing thirty 12-mm dia. steel balls (Fig. 5.2) are adequate for iswests and cylwests. If these are to be made for the first time, a set of plates and balls, as described in section 5.4.2 may be used for all three versions of the test.

3. Pivoting and jacking frame. This is a steel frame (Fig. 4.2), having levelling screws LS, clamp screws CS, a jacking screw JS with the tip a sliding fit in the hole D on the test mould (Fig. 5.1), and set screws SS a sliding fit in the holes B on this mould. It aids in passing the test mould over the soil wedge squarely and without undue disturbance to the soil.

4. Apparatus for raising the jacking equipment during the test. (Optional.) This device, described by Mirata (1974, 1976) and illustrated at the right of Fig. 1.2, aids in aligning the jacking equipment, and in shifting this equipment during the test in order to minimize moments on the failure plane if the strength at higher shear displacements is to be measured.

#### ***4.2.1.3 Devices that can be easily made***

1. *Adjustable guide frame*. Made by cutting two pieces of 1.5-mm thick steel laminae to the shape shown in Fig. 4.3(a), and then bending these to form a rectangular frame as in Fig. 4.3(b), this frame enables the loading pit (Fig. 1.2) to be excavated rapidly and accurately. Its length can be adjusted to suit possible alterations in the loading equipment.

2. *Inverted gauging stool*. (Optional.) This is a simple wooden stool with four legs on which lines have been inscribed to denote the depth of the loading pit for each test mould. By a similar means as shown in Fig. 4.3, its length can be made adjustable to suit different loading equipment. It provides a rapid means of checking the dimensions of the loading pit.

3. *L-plates*. Bent out of 1.5-mm thick rectangular laminae to the shape of an L in cross-section, one such plate is needed for each test mould used. Each has a width of 253 mm; the length of one limb is equal to the length of the inner loading face of the corresponding test mould, and that of the other limb is equal to the length of the other inner rectangular face of the same mould.

4. *Ball pads and reaction plate*. (Needed only when item (4), section 4.2.1.2 is not available.) Two 100 mm x 100 mm x 20 mm mild steel plates, each with a central conical recess of depth 5 mm, base width 20 mm, and a mild steel plate measuring 270 mm x 250 mm x 20 mm.

5. *Centralizer*. (Needed only when item (4), section 4.2.1.2 is not available; otherwise, a simpler frame for temporary support of the hydraulic jack (Fig. 5.23) is adequate.) This is a wooden frame with cross-pieces so shaped as to enable the load cell LC, the hydraulic jack HJ (Fig. 1.2) and the two ball pads (item 4 above) to lie concentrically when placed in their appropriate positions. The overall length of the frame is slightly less than the length of the equipment to be aligned; its width is about 240 mm and height 70 mm. The frame rests on and is reinforced by a 2-mm thick steel lamina close to the corners of which four nuts have been welded. Through these pass 8-mm dia., 150-mm long fly-bolts with rotatable cup washers at the lower tips, forming the levelling screws.

6. *Wooden wedges*. If an adjustable spirit level is not available for levelling the various surfaces at the desired inclination, an ordinary spirit level may be used together with the required combination of five wooden wedges, measuring about 40 mm across

the triangular faces, and about 200 mm in length, with the smallest angles ranging from  $5^\circ$  to  $25^\circ$  at 5-degree intervals.

7. Wooden blocks. Two 250 mm x 100 mm x 100 mm, two 250 mm x 100 mm x 50 mm, and two 250 mm x 50 mm x 15 mm wooden blocks.

8. Wooden strut and wedge. A 150-mm wide, 15-mm thick wooden strut measuring slightly less than the length of the loading pit minus 20 mm, and a 100-mm wide wooden wedge, tapering from about 30 mm to 2 mm in a length of 150 mm. One end of the strut is also cut so that one of the longer edges measures about 30 mm shorter than the other.

9. Steel bars. If loading is to be in directions other than the horizontal, two 300-mm long and one 600-mm long steel reinforcement bars of about 10 mm diameter.

10. Stabilizing plate. A 460 mm x 240 mm x 1.5 mm lamina for placing on the base of the loading pit to prevent the levelling screws of the pivoting frame and of the centralizer from sinking into the ground in cases where ground water seeps into and softens the base of this pit.

11. Raising boards. Three or four 360 mm x 300 mm x 20 mm boards are sometimes useful in rapid adjustment of the elevation of the loading equipment.

12. Gauging board. When the test is to be performed on the side of a test pit, loading in directions close to the vertical, a gauging board is useful in clamping the pivoting frame (Fig. 4.2) into position, before mounting the test mould on this frame. This is a 280 mm x 250 mm x 15 mm board, enlarged to a width of 270 mm at the end where holes are drilled at the sides, for the set screws SS on the pivoting frame to engage, and is marked with a set of lines at the distances  $h_b$  (Fig. 5.1) from these holes.

13. Reinforcing strips. Eight 320 mm x 20 mm x 2 mm brass strips bent to the cross-section of a right-angled channel with two 100-mm long limbs.

14. Supports for dial gauges. Slotted angle bars, about 60 mm x 40 mm x 2 mm in cross-section for the independent support of dial gauges on magnetic bases. Two sets, each consisting of a length of about 500 mm on to which a shorter length of about 250 mm can be screwed at the desired angle are required.

15. Support for reaction plate. When the test is to be performed on the side of a test pit, loading in directions close to the vertical, two 600-mm long slotted angle bars, 60 mm x 40 mm x 2 mm in cross-section are needed to be driven into the side of the test pit to support the reaction plate.



#### **4.2.1.4 Equipment available commercially**

1. A flat faced electrical load cell. An electrical load cell of 50-kN capacity is satisfactory for iswests in most soils. If the same load cell is intended for use in priswests on gravel or rockfill material, a 150-kN capacity one is recommended. The lower sensitivity of the latter is not likely to affect test results to any significant extent.

2. A hydraulic jack. A hydraulic jack with the jacking cylinder connected to the hand pump by a flexible hose. One of 100-kN capacity is adequate for in situ tests; a second cylinder of 150-kN or 200-kN capacity that can be used in conjunction with the same hand pump can be used for priswests.

3. Dial gauges on magnetic bases. Depending on the type of analysis envisaged (see Chapter 2), and whether the jacking unit is to be shifted during the test, two to four 50-mm travel dial gauges, mounted on adjustable supports with magnetic bases. The number of turns applied to the lifting screw for the device in section 4.2.1.2(4) may be used instead of the fourth dial gauge.

4. An adjustable spirit level or an ordinary spirit level. An adjustable spirit level is very useful in levelling the various surfaces, especially when loading is in directions other than the horizontal. If this is not available, an ordinary spirit level may be used with a selection of wooden wedges (4.2.1.3(6)).

5. Miscellaneous devices and materials. A stop-watch; a 50-mm steel rule graduated in mm; a 2-m long steel measuring tape; a carpenter's square; tools for scraping, excavating, and cutting for shaping the loading pit and the soil wedge; a screw driver; a small container of vaseline; a small can of light grade oil; an 18-mm dia. steel ball (for ease in transport and handling, this may be pasted to the ball pad next to the reaction plate); four 40-mm long wood screws; three 6.3-mm dia. 18-mm long screws; four 4.8-mm dia. 15-mm long screws with fly-nuts; two cellophane sheets, measuring about 1.5 m x 1.0 m, for covering the test area if left temporarily for some hours, and for placing instruments on; means of evacuating any water seeping into the test pit; a thermometer; moisture content boxes; cellotape; cloth or similar material for cleaning purposes; a carrying case measuring about 540 mm x 380 mm x 140 mm for all the smaller items.

#### 4.2.2 Additional apparatus for iswests with lateral load application

1. Lateral loading device. A lateral loading device consisting of a spring loaded piston, Fig. 5.3 (if a compressed air source is not available), or an air piston, at one end of which is attached a 10-kN capacity proving ring with exchangeable rods (Fig. 3.2(a), H in Fig. 5.4) ), at the other end, an adjustment screw and a ball joint welded on a mounting plate (Fig. 5.3(a)), with holes matching the screws welded on the support plate (Figs 3.1(b) and 4.4).

2. Supports for lateral loading device. Two 1800-mm long, 60 mm x 60 mm angle bars, tapered at one end to facilitate driving, and having a driving head of 100-mm dia. steel plate welded at the other end. These should have some seven 18-mm dia. holes at 50-mm intervals drilled close to the driving head (Fig. 4.4). A third angle bar, of the same size and length, with a 100-mm long, 18-mm wide slot, 25 mm from each end on one limb, and central slotted holes on the other. The latter holes are for attaching the 120-mm dia. support plate, on which have been welded four 25-mm long flat-head screws on to which the lateral loading device can be fastened through fly-nuts.

3. Support for dial gauge for the deflection of the support of the Q device. About 2 m length of 30 mm x 30 mm x 1 mm slotted angle bar, with two others of the same size but about 800 mm and 600 mm in length for driving into the ground and holding the long bar.

4. A 10-kg hammer for driving the angle bars for supporting the Q device, and spanners for tightening the 16-mm dia. nuts and bolts holding these bars as in Fig. 4.4.

#### 4.2.3 Test procedure

Whichever of the modes of loading shown in Fig. 4.5 is to be applied, the procedure is essentially as follows.

1. A shallow pit, about 500 mm wide, is formed as in Fig. 4.6(a) such that AB is parallel to the proposed failure plane, DB is parallel to the direction of loading and equal to the combined length of the top of the soil wedge and the jacking equipment, and DE is at least 80 mm.

2. Using the adjustable frame (Fig. 4.3) as a guide, a loading pit is dug to a depth equal to the height of the loading face of the soil wedge plus about 10 mm (Fig. 4.6(b)). The guide frame is then removed, and the loading face of the test wedge accurately trimmed perpendicular to the upper face, the L-plate (section 4.2.1.3(3)) being used to facilitate this procedure. The sides of the loading pit are then cut by a further 20 to 30

mm for a distance of about 80 mm from the test wedge end. The dimensions of the loading pit are finally checked using the gauging stool (section 4.2.1.3(2)).

3. The reaction plate RP, or if the adjustable unit in section 4.2.1.2(4) is to be used, one of the boards in section 4.2.1.3(11) is placed at the end of the pit, and the L-plate held in position by a wooden strut and wedge (section 4.2.1.3(8)), while the sides of the soil wedge are trimmed using the L-plate as a guide (Fig. 4.6(b)). If the soil is soft, a stabilizing plate (section 4.2.1.3(10)) is placed on the base of the loading pit.

4. The electrical load cell is switched on, and allowed to warm up. The inner walls of the mould are smeared with vaseline (see Note 43). The pivoting and jacking frame is mounted on the test mould through the set screws SS (Fig. 4.2) engaging the holes B on the mould (Fig. 5.1). The set screws are adjusted until the jacking screw JS is coaxial with the hole D on the mould, when the pivoting frame is held perpendicular to the loading face of the mould. The levelling screws LS and the clamp screws CS on the pivoting frame, together with the wooden blocks placed along the sides and at the rear of the loading pit, are used to clamp the frame in the position shown in Fig. 4.6(c), with the marks M, on the chamfered edges of the test mould level with the top of the soil wedge. *If the mode of loading shown in Fig 4.5(a) is to be used, the pivoting and jacking frame is clamped in position by means of the gauging board (section 4.2.1.3(12)), before mounting the test mould on this frame.*

5. The test mould is rotated about the set screws SS (Fig. 4.2) until the upper inner face of the mould just touches the upper face of the soil wedge. During this rotation, the cutting edges of the mould trim off the excess soil on the two sides of the test wedge. The jacking screw JS (Fig. 4.2) is then screwed forward until it engages the hole D on the test mould (Fig. 5.1). The sets screws SS are unscrewed until they are clear of the mould. The hydraulic jack is inserted between the upper part of the loading face of the mould and the reaction plate. The mould is jacked forward by the simultaneous operation of the jacking screw and the hydraulic jack until resistance is felt on both these units. If the mould tends to slide back when left unsupported, temporary support is provided by a steel reinforcement bar bearing on the handle of the mould and held by two other bars (section 4.2.1.3(9)) driven into the soil on either side of the mould, before the pivoting frame and the hydraulic jack are removed.

6. The section AB (Fig. 4.6(a)) is trimmed back as in Fig. 1.2. This is to avoid ambiguity about the area correction applied in the evaluation of the test. In the softer soils it is advisable to reinforce the trimmed section AB by some eight reinforcing strips (section 4.2.1.3(13)), with the two limbs driven at 30-mm intervals into the soil, and the tops lying along AB. This is to minimize the possibility of local passive failure in this zone.

7. If a lateral load  $Q$  is to be applied, the two tapered angle bars (section 4.2.2(2)) are driven at about 800 mm from either side of the test mould to a sufficient depth to sustain the proposed lateral load (Fig. 4.4). The cross-bar (section 4.2.2(2)), is then bolted through such a pair of holes on the previous two bars that, when the  $Q$  device is mounted in position, with the adjustment screw unscrewed by about 100 mm, the tip of the steel rod of suitable length at the end of this device just touches the test mould. (*If the mode of loading shown in Fig. 4.5(a) is being used, the opposite side of the pit can be used to provide the necessary reaction for the supporting plate (Fig. 4.4) screwed on to a suitably dimensioned board, either suspended from the top or driven in the bottom of the test pit.*) The mounting plate of the  $Q$  device is then secured on the supporting plate with fly-nuts, and the adjustment screw turned until the tip of the rod lies about 50 mm from the test mould.

8. The grooved loading plate LP1 (Fig. 5.2(a)) is screwed on to the test mould using the plates GP (Fig. 5.1) as a guide. The grooves are cleaned and lubricated with a light grade oil. The ball cage BC (Fig. 1.2) and the cleaned and lubricated second grooved plate LP2 (Fig. 5.2(b)) are placed on the rotatable brackets BR of the LP1, and fastened by means of the swivel catches K on LP1 engaging the screws S on LP2. The load cell indicator is set to zero, and the time of this adjustment entered at 6/68-72 of Form 1. If the adjustable ball pad unit (section 4.2.1.2(4)) is to be used, this is placed at the reaction end of the loading pit, *supporting it by two slotted angle bars (section 4.2.1.3(15)) driven into the soil if the mode of loading in Fig. 4.5(a) is being used.* The load cell LC, the hydraulic jack HJ, and the two ball pads with an 18-mm dia. steel ball in between are then placed in their appropriate positions on the centralizing frame (section 4.2.1.3(5)); the whole is introduced into the loading pit, and the levelling screws on the centralizer adjusted until the jacking equipment is coaxial with the brass disc BD on LP2 (Fig. 5.2(b)). *Alternatively, if the adjustable ball pad (Fig. 1.2) is being used, the jack can be placed on the simple frame shown in Fig. 5.23, and the load cell introduced*

to engage the discs on LP2 and on the adaptor (A in Fig. 4.10) at the base of the hydraulic jack. The ball pad can then be shifted by turning the actuating screw AS (Fig. 4.7) to align the jacking equipment. The co-ordinates  $x_{sp}$ ,  $y_{sp}$  of the ball joint of the  $Q$  device relative to the single ball (Fig. 3.1) are measured and entered at 9/25-40 of Form 1 (see Note 13).

9. (This step is omitted if the mode of loading in Fig. 4.5(a) is used.) A dial gauge is mounted on independent supports, and set to zero, ready to gauge the deflection of the cross-beam of the  $Q$  device, in the direction opposite to  $Q$ . The factor for converting the divisions of this dial into cm is entered at 9/65-72 of Form 1 (as positive if readings increase as the tip is depressed); e.g., for a dial gauge calibrated in  $10^{-3}$  inch, 0.00254 is entered.

10. Unlike the configuration shown in Fig. 4.6(d), suitable for analysis A only, two dial gauges (for convenience, all dial gauges will be referred to with the same designations as in Fig. 4.7) on magnetic bases are mounted on supports consisting of two slotted angle bars, each with a transverse bar screwed on, driven into the soil well clear of the soil wedge. These are positioned similarly to  $D_x$  and  $D_y$  in Fig. 4.7 to measure the displacements  $\delta_x$  and  $\delta_y$  of the mould, the distances  $d_1$  and  $d_2$  (Fig. 2.1) being about 120 mm and 10 mm respectively, and the tip of the dial gauge  $D_y$  bearing on the mould as close to the line of symmetry as possible, to even out the effect of the slight transverse rotation of the mould during the test. The dial gauge  $D_y$  is set to a reading of about  $300 \times 10^{-2}$  mm; the distance  $d_1$  (Fig. 2.1), is measured and entered at 8/25-32 of Form 1. The tip of the dial gauge  $D_x$  is fully depressed until it registers a value around  $5000 \times 10^{-2}$  mm. The distance  $d_2$  (Fig. 2.1) and the initial extension  $d_3$  of the hydraulic jack are measured and entered at 8/33-40 and 8/41-48 of Form 1, respectively.

11. For enabling the slight rotation  $\beta$  of the test mould to be recorded, a dial gauge is mounted in a similar position to  $D_{mp}$  in Fig. 4.7, and is set to measure the relative displacement between LP1 and LP2, with an initial reading of about  $3000 \times 10^{-2}$  mm. The distance  $d_4$  of the estimated centre of gravity of the  $D_{mp}$  unit from the edge of TM (Fig. 4.7) is measured and entered at 8/1-8 of Form 1. If the jacking system is to be shifted during the test, a fourth dial gauge is set similarly to  $D_{tb}$  in Fig. 4.7 to bear on a bracket screwed on the adjustable ball pad, and to read about  $500 \times 10^{-2}$  mm. (Instead of this dial gauge, the number of turns of the screw AS (Fig. 4.7) actuating the ball pad can be used, entering the total number of turns for 'raising' (for the layout in Fig. 4.7) the jack as positive at 12/33-39 and in

subsequent rows, and entering 1/(turns per cm) at 3/41-48 of Form 1.)

12. A small load of about 150 N is applied through the hydraulic jack. The initial reading of the dial  $D_{mp}$  is noted, and if desired, an initial shift  $\Delta y_p$  is applied to the jacking system in the positive  $y$  direction (Fig. 1.2), the change in the reading of  $D_{mp}$  being entered in cm at 8/9-16 of Form 1. The initial readings of the dials  $D_x$  and  $D_y$ , and the new readings of  $D_{mp}$  and  $D_{rb}$  are entered at 12/9-15, 17-23, 25-31, and 33-39 respectively. The hour of the day and the minutes past the hour are entered at 12/1-3 and 4-7; the time in minutes elapsed from the time entered at 6/68-72 is entered at 8/49-56. The initial reading of the load cell gauge is entered at 12/41-47.

13.  $P$  is then gradually increased to produce a displacement rate of about 0.5 mm/min in the direction of  $P$ . If  $P$  is being applied close to the horizontal, directly  $P$  reaches a value of about 2 kN, sufficient to enable the jacking system to stand unsupported, the levelling screws on the supporting frame are unscrewed until the support is well clear of the jacking unit, this clearance being occasionally checked throughout the test. For all readings during which the hydraulic jack is supported, '1' should be entered in column 8 of row 12 and after; otherwise this column is left blank. Readings are taken at about 2-minute intervals. On reaching the peak value of  $P$ , '1' is entered in column 48. If the test is to be prolonged for the measurement of the strength at large shear displacements, the adjustment screw on the  $Q$  device is unscrewed until the tip of the rod just seats itself in the recess on the mould. The initial angle between  $P$  and  $Q$  is entered at 9/41-48. Calculator programs such as III and IV in Appendix 6 may be used to adjust the value of  $Q$  to keep  $\sigma \approx \sigma_f$  (see Note 44). At this stage, the rate of loading may be increased between readings, provided it is restored to the original value during the readings to minimize rheologic effects.

14. If at any stage of the test, any of the dial gauges needs re-setting, see Note 19. To check the calculated values of the inclination of  $Q$ , see Note 20. To check the values of  $P$  measured through the load cell roughly against the load obtained through the pressure gauge of the hydraulic jack, see Note 4.

15. At the end of the test, the dial gauges are removed. If  $P$  was being applied *nearly in the vertical direction*,  $P$  is reduced to zero, keeping an eye on the jacking equipment; the grooved plates are fastened together through the brackets and swivel catches, and the hydraulic jack and the load cell removed. The final reading of the load cell indicator is entered at 8/57-64, and the unit switched off.  $Q$  is then reduced to zero,

and the  $Q$  device detached from its support. If  $P$  was being applied *closer to the horizontal*, the  $Q$  device is removed first, and the jacking unit subsequently, the rest of the preceding procedures being applied.

16. The grooved plates and the ball cage are stored in a dust-proof container. Moisture content specimens are taken from the failure plane; the mould is emptied, cleaned and smeared with machine oil to minimize oxidation.

17. Steps (1) to (16) are repeated using a test mould with a different angle, or by applying a finite  $Q$  from the start of the test. For each test, the readings have to be entered on a new data sheet (Form 1), but unless there are any changes in the data in the first three rows, these are omitted, feeding PFIXDR at 9/17-24 in the previous test as zero (if row 10 is not to be read) or as '2'.

### **4.3 Prismatic wedge shear test**

#### **4.3.1 Apparatus**

As it is presumed that this test will initially be performed in a laboratory, no list of equipment as for iswests is given here. When needed to be performed on site, such a list can be prepared from past experience in the laboratory.

#### **4.3.2 Preparation of the sample**

##### **4.3.2.1 *By vibratory compaction (for clean gravels and crushed rock)***

1. The loading frame is brought to the horizontal position as in Fig. 4.7 and kept in that position throughout the test. To facilitate the various operations, the cross-bar of the support for the lateral load  $Q$  device is removed. The lower half of the priswest mould is bolted on the cross-beam of the loading frame through the four hooks ( $P_1$  and  $P_2$  in Fig. 5.21). The links, with spacers of suitable height depending on the compressibility of the soil screwed in the middle, are bolted on the lower half of the box, using spring washers to prevent slackening during vibration. The upper half is laid on the spacers, and the upper bolts of the links, also carrying spring washers, are tightened evenly.

2. The lid is removed, and to prevent grit blocking the tapped holes at the top of the box, these are temporarily plugged by headless screws. The bracket BR (Fig. 4.7) in front of the upper half of the box is removed temporarily, and the collar S (Fig. 5.19) is screwed on top of the box through the four lugs.

3. The material to be tested is placed in the mould in layers, and compacted in the desired way. An efficient way of compacting clean gravels and crushed rock is to apply the vibrating hammer directly on to the levelled surface of 75-mm thick layers for about 100 minutes, with additional vibration applied for about 10 seconds on a 95 mm x 95 mm x 10 mm steel plate placed at each corner in turn (*the last operation may be unnecessary if a square or rectangular tamping head is used*), this procedure giving a degree of compaction of about 92 % of the vibrating hammer method of compaction given in BS 1377 (British Standards Institution, 1975). Higher degrees of compaction can be obtained by reducing the thickness of each layer. Applying the vibrating hammer for about 1 minute on a 20-mm thick steel plate, smaller by about 6 mm than the inner dimensions of the mould, placed on the surface of each of three layers of about equal height produces degrees of compaction around 83 %.

4. The collar is then removed, the surplus material scraped off, and the surface smoothed. The weight, water content and specific gravity of solid particles of the soil placed in the mould are entered at 11/17-40 of Form 1. The temporary plugging screws are removed, and the lid secured in position by fly-bolts. The cross-bar of the support for the  $Q$  device is mounted in such a position as to enable the tip of the short rod at the end of this device to just touch the test mould when the adjustment screw (Fig. 3.1(b)) has been unscrewed by about 20 mm if a spring loaded piston is used, or when the air piston has been depressed by a few mm from its outermost position, with the adjustment screw unscrewed by about the same amount.

#### **4.3.2.2 *By static compaction (for clayey gravels)***

1. The 20-ton priswest frame (Figs 5.15, 5.16) is brought to the vertical position. The test mould, assembled as in 4.3.2.1(1), is detached from the lower beam, and turned through 90°. The collar is mounted instead of the lid, as at 4.3.2.1(2), and the mould located centrally on the lower beam. As the links holding the two halves of the mould are not strong enough to prevent the tendency of the upper half TM of the mould being forced in the direction of shear during static compaction, TM must be restrained by inserting suitably sized steel channels between it and the strain rods of the loading frame (see Mirata et al. (1998), Fig.3).

2. The amount of soil, calculated to give the desired bulk density when compacted to just fill the mould (the weight, water content and specific gravity of solid particles of the soil are entered at 11/17-40 of Form 1) is placed in the mould in batches,



and lightly compacted by ramming with a metal rod, about 30 mm in diameter and 400-mm long. A cellophane sheet is placed on top of the soil to prevent sticking, followed by a 50-mm thick hardwood block (Fig. 5.22(a)), some 6 mm smaller than the inner dimensions of TM, and a 20-mm thick steel plate of the same size (R in Fig. 5.19).

3. If an adjustable ball pad (Fig. 1.2) is in use, the ball cage in this unit is temporarily replaced by a 100 mm x 100 mm x 10 mm steel plate to prevent overstressing of the grooves. Then the 150-kN hydraulic jack, also used during the test, but with the adaptor A (Fig. 4.10) removed so that the base can bear firmly on the steel plate, is mounted centrally between this plate and the single ball pasted on the ball pad.

4. The load is increased gradually until the top of the steel plate is level with the top of the collar. Since the soil generally rebounds on removing the load, the load is re-applied a number of times, applying a slight over-compression, until the rebounded surface of the plate does not protrude above the top of the collar. Because of slight non-uniformities in the compressibility of the sample, it is generally not possible to ensure all four corners of the plate to be level with the top of the collar. In such cases, the compaction can be carried out to make the volume of the sample equal to the inner volume of the mould, and the surface of the sample smoothed after compaction.

5. The collar is removed together with the steel plate, wooden block, and cellophane sheet. The top of the sample is smoothed level with the top of the mould. The plugging screws are removed, and the lid screwed in position. The mould is then turned through 90°, and bolted on the lower beam through the four hooks ( $P_1$  and  $P_2$  in Fig. 5.21).

### 4.3.3 Test procedure

1. The electrical load cell is switched on, and allowed to warm up. The lateral load  $Q$  device is mounted in position; the proving ring dial is set to zero before the tip contacts the test mould. The initial extension of the adjustment screw when the tip of the  $Q$  device just sits in the recess on the test mould (and if an air piston is being used, the piston is depressed by a few mm) is entered at 11/49-56 of Form 1 for information purposes, and a lateral load of about 150 N is applied.

2. The grooved loading plate LP1 (Fig. 5.24(a)), with the brackets BR and swivel catches K removed, is screwed on to the mobile half TM of the mould, and the grooves are cleaned and lubricated with a light grade oil. The link bolts next to the grooved plate are removed. The ball cage (Fig. 5.25), housing sixty-four 12-mm dia. steel balls, and the cleaned and lubricated second grooved plate LP2 (Fig. 5.24(b)) are placed on top of LP1, making sure that the edges are in one line, and held together temporarily by two wooden clasps reinforced by steel laminae at the corners (Fig. 4.8).

3. For tests with the loading frame in the horizontal position, the wooden frame (Fig. 5.23), carrying a pulley M for supporting the hydraulic jack temporarily, is placed in position (Fig. 4.7). The load cell indicator is set to zero, and the time of this adjustment entered at 6/68-72 of Form 1. The adaptors A and B shown in Fig. 4.10 are fitted to the base and the ram of the hydraulic jack. The load cell is placed between LP2 and the hydraulic jack, with its central recesses engaging the discs on LP2 and the adaptor A. The hydraulic jack is operated until the recess on adaptor B engages the single ball carried by the adjustable pad or the reaction plate (Fig. 4.7).

4. The wooden clasps are removed. The hydraulic jack is aligned perpendicular to the test mould, with the two grooved plates concentric, by means of the screw AS for shifting the single ball and, for the frame in the horizontal position, by adjusting the levelling screws LS (Fig. 5.23) on the frame supporting the jack. A load of about 200 N is applied.

5. The bracket BR (bent out of a 100 mm x 40 mm x 2.5 mm steel bar, similar to J in Fig. 4.9) for the dial gauge  $D_y$  (Fig. 4.7) to bear on, is screwed back on to the test mould TM, with the outer smoothed face of the 70-mm long limb level with the relevant surface of TM. The link bolts are slackened evenly and removed, leaving the spacers in position. The support S for  $D_y$  is placed in position; this consists of a 120 mm x 80 mm x 2 mm steel plate welded on the middle of a 12-mm dia. steel bar, at the ends of which have been welded two 80-mm long 30 mm x 30 mm angles so spaced as to enable them to tightly engage the strain rods of the loading frame. The magnetic base of  $D_y$  is placed on this support, and the tip of the dial gauge adjusted to bear on the smoothed face of the bracket BR (Fig. 4.7) at as close a point as possible to TM. (Minimizing this distance has been found to reduce the number of iterations needed for the solution of equations (A33) to (A45)). This dial is set to a reading of about  $400 \times 10^{-2}$  mm; the

distance  $d_1$  in Fig. 4.7 is measured\* and entered **as a negative value** at 8/25-32 of Form 1.

6. With its support fixed on the strain rod of the loading frame, the tip of the dial gauge  $D_x$  (Fig. 4.7) is adjusted to bear on TM, and fully depressed until it registers a value close to  $5000 \times 10^{-2}$  mm. The distance  $d_2$  in Fig. 4.7, and the initial extension  $d_3$  of the hydraulic jack are measured\*, and entered at 8/33-40 and 8/41-48 of Form 1, respectively.

7. For enabling the slight rotation  $\beta$  of the test mould to be recorded, the dial gauge  $D_{mp}$  (Fig. 4.7) is set to measure the relative displacement between LP1 and LP2, and adjusted such as to register a value of about  $4800 \times 10^{-2}$  mm, when the hydraulic jack is 'raised' (for the layout in Fig. 4.7) by the amount required to account for the initial eccentricity of LP1, as explained in Note 16, plus a few mm to make  $\Delta y_{MP}$  about 6 mm. The distance  $d_4$  of the estimated centre of gravity of the  $D_{mp}$  unit from the edge of TM\* is entered at 8/1-8 of Form 1. If the jacking system is to be shifted during the test (this procedure has not been applied in recent priswests (see Note 45)), the dial gauge  $D_{tb}$  (Fig. 4.7) is set to bear on a bracket screwed on the adjustable ball pad, and to read about  $100 \times 10^{-2}$  mm. (Instead of this dial gauge, the number of turns of the screw AS (Fig. 4.7) actuating the ball pad can be used, registering turns for 'raising' (for the layout in Fig. 4.7) the jack as positive at 12/33-39 and in subsequent rows, and entering 1/(turns per cm) at 3/41-48 of Form 1.)

8. The initial angle between  $P$  and  $Q$  is entered at 9/41-48 of Form 1. The spacers are removed and the clearance  $n_c$  between the shearing planes of the two halves of the mould measured on either side of the mould; the average value is entered at 11/41-48.

9. The reading of the dial  $D_{mp}$  (Fig. 4.7) is noted, and by actuating the screw AS and, if  $P$  is being applied in the horizontal direction, the levelling screws of the wooden frame, the line of action of  $P$  is shifted by the amount  $AMLPI_L$  to be entered at 11/9-16 of Form 1 (see Note 16) plus a few mm to make  $\Delta y_{MP}$  about 6 mm. The total change in the reading of  $D_{mp}$  is entered as the VPI value in cm at 8/9-16 of Form 1. The initial readings of the dials  $D_x$  and  $D_y$ , and the new readings of  $D_{mp}$ , and  $D_{tb}$  are entered at 12/9-15, 17-23, 25-31, and 33-39 respectively. The hour of the day and the minutes past the hour are entered at 12/1-3 and 4-7; the time elapsed (min) from the time entered at 6/68-

---

\* See Note 48.

72 is entered at 8/49-56. The initial readings of the load cell gauge and the proving ring of the  $Q$  device are entered at 12/41-47 and 12/49-54 respectively.

10.  $P$  and  $Q$  are increased simultaneously by about equal increments until  $Q$  reaches the desired value. This value of  $Q$  is retained until the peak strength is reached.  $P$  is then gradually increased to produce a displacement rate of about 0.5 mm/min in the direction of  $P$ . If  $P$  is being applied in the horizontal direction, directly  $P$  reaches a value of about 2 kN, sufficient to enable the jacking system to stand unsupported, the levelling screws on the supporting frame are unscrewed until the pulley is well clear of the hydraulic jack, this clearance being occasionally checked throughout the test. For all readings during which the hydraulic jack is bearing on the pulley, '1' should be entered in column 8; otherwise this column is left blank. Readings are taken at about 2-minute intervals. On reaching the peak value of  $P$ , '1' is entered in column 48. Calculator programs such as III and IV in Appendix 6 may then be used to adjust  $Q$  to keep  $\sigma \approx \sigma_f$  (see Note 44). At this stage, the rate of loading may be increased between readings, provided it is restored to the original value during the readings to minimize rheologic effects.

11. If at any stage of the test any of the dial gauges needs re-setting, see Note 19. To check the calculated values of the inclination of  $Q$ , see Note 20. To check the values of  $P$  measured through the load cell roughly against the load given through the pressure gauge of the hydraulic jack, see Note 4.

12. At the end of the test, the dial gauges are removed. Any granular material that may have flowed out of the mould is collected and weighed, this value being entered at 11/57-64 of Form 1, for information purposes. If  $P$  was being applied *in the vertical direction*,  $P$  is reduced to zero, keeping an eye on the jacking equipment. The wooden clasps are then fitted on the grooved plates, and the hydraulic jack and the load cell are removed. The final reading of the load cell indicator is entered at 8/57-64, and the unit switched off.  $Q$  is then reduced to zero, and the  $Q$  device removed. If  $P$  was being applied *in the horizontal direction*, the  $Q$  device is removed first, and the jacking unit subsequently, the rest of the preceding procedures being applied.

13. The grooved plates and the ball cage are stored in a dust-proof container. Moisture content specimens are taken from the failure plane to check the value at 11/17-24 of Form 1; the mould is emptied, cleaned and smeared with machine oil to minimize oxidation.

14. Steps (1) to (13) are repeated for a larger initial  $Q$  to increase the normal stress. If the normal stress needs to be increased beyond that obtainable by the maximum  $Q$  that can be applied, the test is carried out using moulds with larger effective values of  $\alpha_n$ .

For each test, the readings have to be entered on a new data sheet (Form 1), but unless there are any changes in the data in the first three rows, these are omitted, feeding PFIXDR at 9/17-24 in the previous test as zero (if row 10 is not to be read) or as '2.'.

#### **4.4 Cylindrical wedge shear test**

##### **4.4.1 Apparatus**

As explained in Chapter 1, the cylwtest can be performed either by using an available compression machine such as one used for the triaxial test (Fig. 1.3), or by using a simple, portable frame (Fig. 5.5). A loading capacity of 10 kN has been found sufficient for the size of test moulds used so far (Table 3.9). By the use of simple attachments (ZC to ZX in Box. 5.2) and slight modifications to earlier devices, a lateral load can also be applied when an available compression machine is used. The portable frame enables the test to be easily performed in the field as well, in which case, as for priswests, the required list of apparatus can be prepared from past experience in the laboratory.

##### **4.4.2 Preparation of the sample**

###### **4.4.2.1 Undisturbed samples.**

To test the soil along planes relevant to the stability problem at hand, it is advisable to have the orientation of samples marked on the sampling tubes during sampling.

1. The removable disc RD (Fig. 5.5) closing the central opening of the middle plate of the portable frame, held in position by its recesses (Fig. 5.10) engaging the tongues T (Fig. 5.8) screwed on this plate, is temporarily replaced by a ring of the appropriate diameter (Fig. 5.10), and the sampling tube clamped below this ring, with the cutting edge pointing downwards.

2. Using suitable dolly bars and the hydraulic jack also used during the shear tests, the sample is extruded by about 3 mm from the top of the ring. If available, a

cylwest mould of the same inside diameter as the sampling tube is assembled, making sure that the fixing bolts of the single cut moulds are so oriented as to enable their removal after the mould is clamped in position (Fig. 1.3). This mould is positioned over the extruded part of the sample in such a way as to make the orientation of the eventual shear plane as close to the relevant in situ shear plane as possible. The upper plate UP of the frame (Figs 5.5 and 5.7), having a 30-mm dia. central hole, is lowered to touch the top of the mould. The sample is then extruded directly into this mould. If such a mould is not available, in the first instance the sample has to be extruded into a core cutter of the same inside diameter  $D_i$  as the next smaller sized test mould, before introduction into this mould. If the height of the sample is limited, a wooden disc, of slightly smaller diameter than  $D_i$  and about 10 mm less in thickness than the dimension  $h_L$  (Fig. 3.3) of the mould, can be pressed into the bottom of the mould.

3. The mould is weighed together with the enclosed specimen and any wooden disc in the bottom, the result being entered, together with the height of the empty portion at the top of the mould, and the height of the wooden disc, if used, at 8/33-40, 8/41-48, and 8/49-56 of Form 2 respectively. If no disc has been used, the last space is left blank. The space between the top of the specimen and the top of the mould is then packed completely with wooden or perspex discs of slightly smaller diameter than  $D_i$ .

4. The removable disc RD in the middle plate of the portable frame is replaced.

#### **4.4.2.2 *Compacted samples.***

The double cut test mould (Fig. 1.4) enables compacted clays, sands and gravels with finer particles than 10 mm to be tested in the same mould in which they have been compacted. It is formed by cutting a thin-walled sampling tube along four planes (preferably along the dashed lines rather than the upper cut to enable the area and orientation of the shear plane to remain constant, the normal stress being altered by applying a lateral force from the outset in one of the tests), then cutting the 6-mm thick slices SL along the uppermost and lowermost points, and welding a pair of links LK on each half as shown in Fig 1.4(b), thus forming two pairs of couplings. During compaction, the mould is secured on the base plate of a standard compaction apparatus through hooked lugs HL, with both couplings screwed in position through tapped holes in the mould. The sample is compacted as follows.

1. To prevent granular soils from flowing out during handling or to reduce the volume of clayey soils to be compacted, a tightly fitting wooden disc, about 25 mm thick (this thickness is entered at 8/49-56 of Form 2), is inserted in the bottom of the mould. The mould is secured on the base plate.

2. From the standard compaction test results, the bulk density  $\rho$  (g/cc) of the soil at the desired moisture content is read off, and the mass  $M_1$  (g) of wet soil to give the same height  $h_c$  of layer after compaction in the cylwtest mould as in the standard test is calculated from the following equation.

$$M_1 = \pi(D_i)^2 h_c \rho / 4 \quad (4.1)$$

3. (a) *If dynamic compaction is to be applied.* The number  $n_d$  of drops of the rammer to be applied to each layer to keep the compactive effort equal to that applied in the standard test is calculated from the following equation.

$$n_d = n_s (D_i / D_{is})^2 \quad (4.2)$$

where,  $n_s$  is the number of drops used in the standard test, and  $D_{is}$  is the inside diameter of the standard mould. The  $M_1$  grams of soil is placed in the cylwtest mould, and compacted by  $n_d$  drops of the rammer. This procedure is repeated until the top of the specimen is about 40 mm above the upper cut.

(b) *If static compaction is to be applied.* The mass of wet soil for each layer is calculated using equation (4.1), and this amount of soil is placed in the cylwtest mould. Then a cylindrical plunger of hardwood, 1 mm smaller in diameter than  $D_i$ , and of sufficient height is introduced above the soil, having marked the required level to which it has to be forced down to give the required height  $h_c$  of the layer, and the necessary load applied to compact the soil. This procedure is repeated until the top of the specimen is about 40 mm above the upper cut.

4. The mould is detached from the base plate and weighed, entering this weight at 8/33-40 of Form 2. The space between the top of the specimen and the top of the mould, the height of which is to be entered at 8/41-48 of Form 2, is packed completely with wooden or perspex discs of slightly smaller diameter than  $D_i$ .

### 4.4.3 Test procedure

The procedure is very similar whether the test is carried out using an available compression machine or a portable frame. The procedure below is given for the latter case, with separate explanations given in italics for the former, where needed.

1. If a lateral load  $Q$  is to be applied, the length  $L_y$  of the yoke is adjusted to the constant value explained in Note 31, and this value entered at 4/25-32 of Form 2. The turnbuckle TB (Fig. 5.5) is attached at the hooked end of the yoke, and a 1000-N capacity spring balance (or, two 500-N capacity ones, by using two adaptors of the type H shown in Fig. 4.9) is attached at the other end of the turnbuckle. The unit is hooked on one of the cross-bars of the supporting angles  $S_1$  and  $S_2$  (Fig. 5.5); then swung around, and hung on the hook HK (Figs 5.8, 5.12) screwed on the middle plate MP of the frame in Fig. 5.5, (*or the hook ZH welded on the channel used as the cross-beam of the compression machine (Fig. 5.14(c))* under a tension of about 100 N.

2. The test mould is passed between the jaws of the clamp (Fig. 5.13) on the middle plate, and held in position temporarily by the rotatable steel bar BR (Fig. 5.12), about 40 mm x 3 mm in cross-section, and of sufficient length to just support the test mould though one of the lugs, while the rest of the equipment is assembled.

3. An adaptor such as E in Fig. 4.10, carrying a 70 mm x 70 mm x 10 mm steel plate as a tight fit, is screwed at the lower end of a 10-kN capacity proving ring (see Note 46), and the whole placed vertically on any plate having a central recess to house the stud on this adaptor. The grooved plate LP2 is attached to the upper end of the proving ring using an adaptor such as C in Fig. 4.10. The grooves on LP2 are cleaned and lubricated with a light grade oil. The ball cage BC and the cleaned and lubricated grooved plate LP1 are placed on top of LP2, and fastened by the brackets and catches on LP1 (Fig. 5.2). The proving ring is set to zero (see Note 39).

4. The adjustable ball pad (Fig. 3.3) (or if this is not available, an ordinary ball pad), carrying an 18-mm dia. steel ball in its central recess, is placed on the lower plate of the portable frame (Fig. 5.5) (*or on the loading platen of the compression machine*). The hydraulic jack, carrying the adaptor A (Fig. 4.10) at its base and the adaptor B at the top is placed on the single ball, and kept nearly vertical by means of a wooden restraining board (shown by dashed lines in Fig. 5.12), having an oval hole in the middle, and held tightly against the strain rods of the portable frame.



5. Holding the proving ring by the sides to avoid its passing into tension, the assembled unit is placed on the hydraulic jack, with the stud on the bottom adaptor, engaging the central hole in the adaptor at the top of the jack (*or on the second ball pad with a similar central hole, placed on the single ball*).

6. By actuating the hydraulic jack (*or operating the compression machine*), the loading unit is raised until LP1 contacts the test mould, and the top of the mould touches the disc RD (Fig. 5.5) in the middle plate (*or the channel used as cross-beam of the compression machine*). The supporting bar BR (Fig. 5.12) is then turned out of the way, the test mould is rotated until the shear plane is normal to the plane of Fig. 5.5, and clamped into position, tightening the vertical screws on the clamp lightly first, then tightening the horizontal screws evenly, and finally tightening the vertical screws.

7. Using the concentric dots punched on the non-grooved face of LP1 (section 5.4.2(3d)) as a guide, the grooves on LP1 are adjusted concentrically with the test mould (see Note 47), the guide plates G (Fig. 4.10) are pushed to touch the test mould, and their fixing screws tightened. The axial load is increased to about 100 N.

8. The spacers and screws holding the two halves of the single cut mould, or just the fixing bolts of one pair of the couplings of the double cut mould are removed. If fine gravel or gravelly sand is being tested, only one test is possible on each sample; so, to impose lower moments on the stationary part TM(S) of the test mould when a lateral load  $Q$  is applied, the upper cut only is used for the shear test, if this is inclined at  $30^\circ$  to the axis, the  $45^\circ$  inclination being unsuitable for such material because of the limitation explained in section 2.3. If higher  $Q$  than about 300 N is to be applied, the rigidity of TM(S) is increased by inserting a cross-bar (*or a bar shaped as shown in Fig. 5.14(b) for the use of a compression machine*) and suitable packing between its lower tip and the strain rods of the loading frame.

9. The supports of the dial gauges  $D_x$  and  $D_y$  (Fig. 3.3) are fixed on the strain rods of the loading frame, and an extension piece of the type D in Fig. 4.10 is screwed at the tip of each dial gauge. The bracket J (Fig. 4.9) is screwed centrally on the side of LP1, and the dial gauge  $D_x$  adjusted to bear on this, reading a value around zero. The dial gauge  $D_y$  is adjusted to bear on the side of the movable part TM of the test mould, reading about  $400 \times 10^{-2}$  mm. The distances  $d_1$  and  $d_2$  (Fig. 3.3) are measured, and entered at 8/57-64 and 8/65-72 of Form 2, the **latter as a negative value**. The initial

extension  $d_3$  of the hydraulic jack is measured and entered at 9/1-8 of Form 2. (*This space is left blank when a compression machine is used.*)

10. For enabling the slight rotation  $\beta$  of the test mould to be recorded, the magnetic base of the support for the dial gauge  $D_{mp}$  (Fig. 3.3) is mounted on the underside of LP2, with the tip of the gauge bearing on LP1, and adjusted to read about  $2000 \times 10^{-2}$  mm. The magnetic base of this dial gauge is secured by a piece of resistance wire on to the screws on LP2 for safety against an accidental drop. If the single ball is to be shifted during the test, the dial gauge  $D_{rb}$  (Fig. 3.3) is set to bear on a bracket screwed on the adjustable ball pad, reading about  $3000 \times 10^{-2}$  mm. (Instead of this dial gauge, the number of turns of the screw actuating the ball pad can be used, registering turns for shifting to the right (for the layout in Fig. 3.3) as **negative** at 12/33-40 and in subsequent rows, and entering  $1/(\text{turns per cm})$  at 3/65-72 of Form 2.)

11. The spacers S (Fig. 1.3) or one of the couplings (Fig. 1.4) are removed, and the average clearance  $n_c$  between the shearing planes of the two halves of the mould determined and entered at 9/9-16 of Form 2. The distances  $h_2$ ,  $y_{sp}$ ,  $x_{sp}$ , and  $x_b$  (Fig. 3.3) are measured and entered at 3/17-24, and 4/1-8, 9-16 and 17-24 respectively.

12. The catches and brackets on LP1 are turned free of LP2, and the two grooved plates aligned by shifting the single ball. If desired, an initial shift  $\Delta y_p$  may be applied to the single ball towards the right in Fig. 3.3, and this value entered at 9/17-24 of Form 2. If  $Q$  is to be applied from the start of the test, the  $Q$  device is released from the hook HK (Fig. 5.12) on the middle plate (*or the hook ZH (Fig. 5.14(c)) on the channel cross-beam*), and the rounded tip of the rod is lodged in the recess closest to the centroid of the proposed shear plane as in Fig. 3.3.

13. The initial readings of dials  $D_x$ ,  $D_y$ ,  $D_{mp}$ , and  $D_{rb}$  in Fig. 3.3, of the proving ring, and if  $Q$  has been applied, of the spring balance(s) and the height  $x_h$  are entered on Form 2 at 12/9-16, 17-24, 25-32, 33-40, 41-47, 49-56 (if two spring balances of different calibration are being used, the reading of the second at 12/69-72), and 12/57-64 respectively. The hour and the minutes past the hour are entered at 12/1-4, 5-8. If the length  $L_y$  of the yoke has been decreased relative to the value noted at step 1, the amount of this decrease is entered at 12/65-68, and repeated in every succeeding row until the total decrease relative to  $L_y$  is changed, when the new value has to be likewise entered.

14. If  $Q$  is to be raised to a particular value, as  $Q$  is increased, about equal increments are applied to  $P$ ;  $Q$  is then kept constant until the peak strength is reached.

Axial loading is continued at an axial displacement rate of about 0.3 mm/min, and readings taken at about 2-minute intervals. For undisturbed soils, a gradual decrease in the value of  $P$  indicates failure. In compacted clays, the friction between the soil and the inner wall of the mould, which prevents compression of the sample initially, can sometimes be overcome before the peak strength is reached; the soil then begins to compress resulting in a temporary drop in  $P$ . This can be distinguished from a true failure by the continued axial displacement accompanied by practically zero movement on the lateral displacement dial  $D_y$ . In such cases, axial loading is continued until  $P$  starts rising again and then begins to drop.

15. In the row containing the maximum value of  $P$ , '1' is entered in column 48, if the mode of failure is as in Fig. 3.5(d). After the peak strength is reached, if the test is to be prolonged to measure the ultimate strength of granular soils or the strength at large displacements in clays, calculator programs such as III and IV in Appendix 6 may be used to adjust  $Q$  to keep  $\sigma \approx \sigma_f$  (see Note 44). The rate of displacement may be increased between readings, provided it is restored to the original value during the readings to minimize rheologic effects. Loading is continued until  $P$  stops changing appreciably. If no  $Q$  is being applied, in brittle clays it is almost impossible to continue the test after the peak strength is reached, as  $P$  starts to drop very rapidly, almost to zero in some cases, and the whole set-up may fall apart. In such cases, the test should be stopped soon after the peak strength is reached, and step 16 applied. In plastic clays, loading may be continued until the shear plane becomes distinct, taking care not to let the equipment collapse. When  $Q$  is being applied, there is no danger of such sudden collapse.

16. Dial gauges  $D_x$ ,  $D_y$  (Fig. 3.3) are removed by detaching from their supports; dials  $D_{mp}$  and  $D_{rb}$ , if used, are removed together with their magnetic bases. The two grooved plates are fastened together using the swivel catches and brackets. If  $Q$  was being applied, this is decreased to about 100 N, and the yoke stretched and hung on to the hook HK (Fig. 5.12) (or the hook ZH in Fig. 5.14(c)). The vertical screws holding one jaw of the clamp are slackened. The horizontal screws of the clamp are slackened evenly. The mould is rotated until it can be supported by means of the bar BR (Fig. 5.12) through one of the lugs. The jacking unit is lowered. The proving ring and the attached grooved plates are removed, and placed on the plate with a central recess. Holding its two parts together, the mould is removed.

17. If granular soil is being tested, the soil in the upper half of the mould flows out, and a second test is impossible. For clayey soils, measurements are taken to enable the true inclination of the failure plane to be calculated, the section 9/25-48 of Form 2 being completed in accordance with Table 3.8.

18. In clayey soils, to enable the two shear surfaces to match, the irregularities are trimmed off.

(a) *For the double cut mould*, the couplings are bolted on to the lower half of the mould, and the bolts tightened. The upper half is then placed on top, and the upper bolts are tightened evenly. An additional disc, slightly smaller in diameter than  $D_i$ , is placed on top, and the two parts of the specimen are pressed together under the maximum load recorded during the previous test. The additional disc is replaced by one with the right height to just fill the space that may have appeared at the top of the mould.

(b) *For the single cut mould*. The two parts of the mould are screwed together; a wooden disc D (Fig. 1.3), slightly smaller in diameter than  $D_i$  and  $20/\sin \alpha_n$  mm thick is placed on top, and the two parts of the specimen are pressed together under the maximum load recorded during the previous test. The additional disc is then jacked down completely, pushing the specimen and the previous shear plane SP downwards; the extruded soil is cut flush with the bottom of the mould.

19. Steps 1 - 17 are repeated, this time applying a higher  $Q$  from the outset, and in the case of the double cut mould, applying the shear test on the second cut. The readings have to be entered on a new data sheet (Form 2), but unless there are any changes in the data in the first four rows, these are omitted, feeding PFIXDR at 9/49-56 in the previous test as zero (if row 11 is not to be read) or as '2.'. The two shear tests can be completed within an hour, and enable the shear strength parameters of homogeneous unsaturated soils to be determined with sufficient accuracy for practical purposes (see Box 4.3, files 5 to 8, and Mirata et al., 1999).

(20) The grooved plates and the ball cage are stored in a dust-proof container.

#### **4.5 Evaluation of results**

Having completed the tests of any one series, the rest of Form 1 for iswests or priswests, or Form 2 for cylwests is completed using the information given in Chapter 3, for the first test. The rest of the data sheets need not be completed, except for the

changed values. At this stage it is best to prepare the data file for the first test, and copy the appropriate lines of this test for the succeeding tests, applying the necessary corrections. As a starting point in preparing the data file, the typical data files on the diskette inside the back cover can be used, choosing the desired files and lines from the information summarized in Table 4.1, and given in more detail in section 4.6. The procedure will be explained for cylwests, and is similar for the other types of test.

1. A new data file is opened, and saved as DCWFIRST.DAT, say, using a filename of maximum 8 characters. This will be referred to as the *current file*. The lines corresponding to rows 1 to 12 of Form 2 are copied on to the current file from the appropriate file on the diskette, selected on the basis of the information given in Table 4.1. The necessary corrections or additions are applied to these lines, saving the current file frequently throughout this procedure. The subscripted data, which follow row 12 on Form 2, may best be entered using the tabulator key.

2. In entering the values for the second test, unless there has been any change to the values in the first 4 rows of Form 2, lines 5 - 12 of the first test can be copied at the end of the current file, and the necessary corrections applied. The rest of the readings are once again entered using the tabulator key.

3. Step 2 is repeated for all the tests in the series. If in any test, the values in the first four rows of Form 2 have changed, depending on whether row 11 is being read or not, '3.' or '1.' respectively is entered in the line corresponding to 9/49-56 of Form 2 for the last test before such a change; rows 1 - 4 of the current file are copied at the end of the data for this last test, and the necessary corrections applied to these, before proceeding with the rest of step 2 for the new test.

4. Having completed the data file, it is saved with '1.' at 1/1-8 of Form 2 (and at all other rows, where this row may have been inserted (see step 3 above)) if a check on the dial gauge readings is desired (see section 3.2.2.5). The program is run by entering its name: CYLWEE88. The filename is asked. For the example given above, DCWFIRST.DAT is entered. Then the output filename is asked. This may be entered as DCWFIRST.OUT. The program runs and is terminated, the output being saved in the output file named. After examining the output on the lines outlined in section 3.2.2.5, and applying any necessary corrections, the current data file is re-saved this time with '0.' at 1/1-8 of Form 2 (and at all other rows, where this row may have been inserted (see step 3 above)), and the program re-run as above. The test results now appear in the same

output file; at the end of this, are the regressed values of the shear strength parameters for the series of tests evaluated (Table 3.5) and the optional results explained in Table 3.6.

5. Having prepared a data file for a series of tests using a particular set of equipment, this can be used in step 1, for subsequent series of tests using the same equipment.

6. If re-shear tests have been performed on smoothed failure planes in order to determine the residual strength of clayey soils, a separate data file can be prepared for such tests. In this case, only the values output under the heading 'end of test' do have any significance.

#### **4.6 Sample data files**

On the diskette in the pocket inside the back cover, in addition to the executable files of the programs IWPW77 and CYLWEE88, will be found a number of data files. Some of these are the original files used for the evaluation of the tests. Others are duplicates of these, with the parameter PAROUT changed to '7.' to output summary tables only, and some lines added as examples of how the test mould and/or rod data, etc can be specified, or of how the values in the first few rows of Forms 1 and 2 can be changed for the subsequent tests. The lines where such changes have been made are summarized in Table 4.1. Here will be given some details about these files, and reference will be made to some of the results which substantiate the remarks in the earlier chapters.

The first three letters of the filenames indicate the type of test; thus, filenames starting with DIW, DPW, and DCW indicate files for iswests (Box 4.1), priswests (Box 4.2), and cylwests (Box 4.3) respectively. The next 2 to 3 letters denote the location of the tests or samples, or the initials of the research student in collaboration with whom the tests have been performed; the last 2 to 3 letters generally denote the original and the modified versions of the same set of data, identified by the preceding letters.

The data files for iswests and priswests were initially prepared using a transformation program for converting the input format from that of the earlier versions of the program to that of IWPW77. To make such files look more like how they would appear when prepared afresh, the first few lines at the top of each file, the whole of the data for the first test, and the first few lines, including the first line of the subscripted

data for the subsequent tests have been aligned manually. The rest of the data has been left as prepared by the transformation program.

In the iswests and some of the cylwests, the line of action of the main load was tried to be adjusted during the test in accordance with a set of pre-calculated curves as explained at the end of section 2.1.1. No such attempt was made in the priswests (see Note 45), only an initial shift being applied to the main load, before the start of shear. All data files could be run on the relevant programs, following section 4.5, step 4, and the outputs obtained; for convenience, and to enable quick reference to these in the text, these outputs have also been given on the diskette with the same filename, but with the extension 'OUT' instead of 'DAT'. At the end of each output file is given the shear strength parameters obtained by all three methods of analysis explained in Chapter 2. Examining these will give an idea about the differences resulting from the type of analysis used.

#### **Box 4.1. Explanations regarding the iswest data files on the diskette**

- 1. DIWC4DEF.DAT.** This contains 8 of the 10 iswests, the results of which have been summarized in the Addendum by Mirata (1974), and given in more detail by Mirata (1976). These tests were performed in a test pit supported by the steel segments described in section 4.2.1.1, five of the tests by using the mode of loading in Fig. 4.5(a), the rest using that in Fig. 4.5(b). The tests using different modes of loading were found to give very close results (cf. outputs DIWC4DEF.OUT and DIWC4DE4.OUT). Test C/4/9 was the only test in which  $DH > 0$  has been observed so far. See also Note 43.
- 2. DIWC4DE4.DAT.** This contains the four tests using the mode of loading in Fig. 4.5(a) of the tests in DIWC4DEF.DAT (file 1).
- 3. DIWC4TMS.DAT.** This is a duplicate of DIWC4DEF.DAT (file 1), except for the following modifications introduced both to test the program IWPW77, and as illustration in preparing data files: PAROUT was changed to 7. in lines 1 and 146; PFIXDR (at 9/17-24 of Form 1) was altered to 2. in line 9, and line 10 inserted to specify the test mould data; similar changes were applied in lines 129 and 130, but here PFIXDR was specified as 3., implying that the first three lines of Form 1 are to be re-read after the end of the current test; these lines were therefore inserted as lines 146-148, without any

**Box 4.1 (continued)**

changes, as there were none to apply. If the output DIWC4TMS.OUT of this file is compared with that of file 1 (DIWC4DEF.OUT), it will be seen that JTM in lines 24 and 233 of the former are both zero, instead of 4 and 2 in lines 24 and 609 for the corresponding tests in the latter, showing that the test mould data (unaltered in this instance) are the ones specified in the former, and the default values in the latter. Also, the 'common data' have been re-printed in lines 260-267 of the former.

**4. DIWTKDEF.DAT.** This contains the only five iswests so far performed with a lateral load  $Q$  applied after the peak strength was reached, to keep the normal stress at about its value at peak strength. These were reported as test series IW/TK by Mirata (1991). In the last test, using a test mould with  $\alpha_n = 30^\circ$ ,  $Q$  was applied from the outset, to see if the normal stress range could be varied sufficiently; as can be seen from lines 527-531 of DIWTKDEF.OUT, this aim was achieved. Line 24 of this file is an example of all four dial gauges being re-set as explained in Note 19. Note also that, the 20-ton hydraulic jack and the proving ring used for measurement of the main load being unduly heavy, the jacking system had to be supported throughout most of these tests, IPARA(I) in column 8 of row 12 and after (Form 1) being fed as 1.

**5. DIWTKROD.DAT.** This is a duplicate of DIWTKDEF.DAT (file 4), except for the following modifications: PAROUT was altered to 7. in lines 1, 29, and 93; in line 9, PFIXDR was altered to 3., and RODNUM to zero; line 10 was inserted to specify the test mould and rod data; the first three lines of Form 1, to be re-read after the end of the current test, were inserted as lines 29-31, without any changes. In line 56, PFIXDR was altered to 2., and RODNUM to zero, and the test mould and rod data specified in the next line. In line 78, PFIXDR was altered to 1., and the first three lines of Form 1, to be re-read after the end of the current test, were inserted as lines 93-95, without any changes. If the output DIWTKROD.OUT of this file is compared with that of file 4 (DIWTKDEF.OUT), it will be seen that JTM in lines 24 and 108, as well as RODNUM in lines 25 and 109 are all zero, instead of 2 and 3 respectively in lines 24, 25, 235, and 236 of the latter, showing that the test mould and rod data are the ones specified in the former, and the default values in the latter. Also, the 'common data' have been re-printed in lines 54-61, and again at 171-178 of the former.



#### Box 4.2. Explanations regarding the priswest data files on the diskette

**1. DPWGW38H.DAT.** This file contains tests, performed in collaboration with Gökalp (1994), on well graded clean gravel with  $< 38$  mm particles and a degree of compaction of 92 % achieved by the method given in section 4.3.2.1(3). In this series of tests, a 45-degree mould was used for the first time, enabling normal stresses of up to 952 kPa to be reached in test GWVD/3. The data for this test has been placed at the end of the data file, because the range of SIG, for which TAUF values are output (Table 3.5), is based on the maximum normal stress reached in the last test in the data file. An air piston was used for applying  $Q$  in these tests. The output of this file (DPWGW38H.OUT) may be used to feed information into Program III in Appendix 6, to obtain desired stress ranges in priswests on similar material, using Program IV in Appendix 6 during the test. For example, if a normal stress of about 200 kPa is desired at peak strength, from line 498 of this output the third test in the output file (Test GWVD/4) may be used for this purpose: from line 309, last figure, it is seen that peak strength in this test has occurred at  $T = 16$  min; so, if a 35-degree test mould is used, and from the values in line 240, table column 19 and line 288, columns 40 and 44,  $\delta_{qf}$ ,  $\delta_{pf}$ , and  $\delta_{xf}$  are fed as 30 kgf, 3087 kgf, and 0.82 cm respectively to Program III, adjusting  $Q$  using Program IV during the test, the desired normal stress level may be achieved.

**2. DPWMSHGC.DAT.** This file contains tests, performed in collaboration with Şakar (1997), on 19 mm - 38 mm gravel to which 20 % of  $< 1$  mm fines ( $w_L = 58$  %;  $w_P = 26$  %;  $C_F = 53$  %) were added. As the proving ring for recording  $Q$  was changed after test GC/4, PFIHDR was specified as 1. in line 65, and the corrected versions of lines 1 to 3 inserted as lines 81 to 83. A spring loaded piston was used for applying  $Q$  in these tests. Because of the relatively low angle of friction compared to that of clean gravel, higher values of mould angle than  $45^\circ$  were required to increase the normal stress range. The procedure described in section 5.4.1 was applied for the first time in tests GC/5 and 6. From the table of  $\sigma$  versus  $\tau_f$  values, lines 664 and 666 of the output file (DPWMSHGC.OUT), it can be seen that in test GC/6 in which  $Q$  was 2025 N at peak strength, the normal stress  $\sigma$  was more than doubled compared to that obtained by using the 45-degree test mould. Another interesting observation in tests GC/5 and 6, was the continued rise in  $P$  after the peak strength was reached (see column 19, lines 438-461, and 585-590). This was a coincidental, experimental proof of the statement that “a rapidly increasing  $P$  would be required for shear” as the limit of  $(\phi + \alpha) = 89.5^\circ$  is

#### **Box 4.2 (continued)**

approached, quoted in section 2.3. (From column 56, lines 513-537, and 630-636, it is seen that the  $\alpha_r$  values increased from  $49.0^\circ$  and  $49.4^\circ$  at peak strength to  $50.0^\circ$  in both of these tests, making the sum  $(\phi + \alpha_r) = 87.5^\circ$  when the tests were stopped because the capacity of the load cell had been approached.) This is also another verification (Mirata, 1992) of the fact that, analysis C (Chapter 2) is the most rigorous analysis; this continued rise in  $P$  would not have been explained otherwise, and as seen from column 12, lines 438-462, and lines 585-590, the  $\tau/\sigma$  ratio would have appeared to be continuously rising after the peak, correctly fixed by analysis C. (The difficulty of approaching the limit of  $(\phi + \alpha_r) = 89.5^\circ$  in a subsequent test on gravel, containing 15 % of fines and having  $\phi = 40.3^\circ$ , was overcome by using all three spacers (Box 5.3, item T) on top of each other, thus reducing the effective angle between the main load and the true shear plane (Mirata et al., 1998).)

**3. DPWMSHTR.DAT.** This is a duplicate of file 2, except for the following modifications: in lines 1 and 83, PAROUT was altered to 7.; in line 44, PFIXDR was altered to 2., and RODNUM to zero, and the test mould and rod data specified in the next line; in line 66, RODNUM was altered to zero, and PFIXDR was altered to 3., enabling the corrected versions of lines 1 to 3 to be re-read after the end of the current test (in lines 83-85) as well as specifying the test mould and rod data in line 67. If the output DPWMSHTR.OUT of this file is compared with that of file 2 (DPWMSHGC.OUT), it will be seen that JTM in lines 95 and 134, as well as RODNUM in lines 96 and 135 are all zero, instead of 10 and 4 respectively in lines 207, 208, 309 and 310 for the corresponding tests in the latter, showing that the test mould and rod data (unaltered in this instance) are the ones specified in the former, and the default values in the latter.

#### **Box 4.3. Explanations regarding the cylwtest data files on the diskette**

*NOTE. The tests contained in files 1 to 4 have been performed using the portable frame in Fig. 5.5, and the rest using a 5-ton triaxial compression machine as in Fig. 1.3, with modifications (Fig. 5.14) for applying a lateral load.*

**1. DCWC2USC.DAT.** This contains four of the twenty-three cylwtests performed on ten undisturbed samples of the stiff, fissured, unsaturated Ankara Clay, the results of seven of which have been reported by Mirata (1991) as cylwtest series CW/C2/Q.

**Box 4.3 (continued)**

These were performed using the single-cut moulds 1 and 2 in Table 3.9. The original data has been adjusted manually to the input format of CYLWEE88, and the number of sets of readings has been reduced. Note that PFIXDR in line 22 has been specified as 1., implying the use of the default data for the test mould, but that corrected versions of lines 1 - 4 are to be read after the end of the current test (lines 31 - 34).

**2. DCWC2TMS.DAT.** This is a duplicate of file 1, with the following modifications: PAROUT was altered to 7. in lines 1 and 33; PFIXDR was altered to 2. in lines 9 and 41, and to 3. in line 23, the test mould data being specified in lines 10, 24, and 42.

**3. DCWPFDEF.DAT.** The data in this file has been prepared by adjusting the format, and reducing the number of sets of readings, as for file 1. Each of the two pairs of tests were performed in collaboration with Seçkin (1993) on a plastic clay, compacted dynamically as in section 4.4.2.2(3(a)), directly in the double-cut mould 4 ( Table 3.9).

**4. DCWPFINR.DAT.** This is a duplicate of file 3, with the following modifications: PAROUT was altered to 7. in lines 1 and 25; PFIXDR was altered to 1. in line 19, and lines 1 - 4 inserted at 25 - 28, with no change.

**5. DCWTXSTA.DAT.** This is one of a set of tests performed by Gün (1997) on different clays to compare the peak strength parameters of statically and dynamically compacted specimens (Mirata et al., 1999). In this file, the specimens were compacted in the double cut mould 4 (Table 3.9), using static compaction as in section 4.4.2.2(3(b)). During the tests, the data was recorded on Form 2; so no adjustment of format was necessary. Two cylwests were performed on each of two similarly compacted specimens. The tests were performed using a 5-ton triaxial compression machine, with the attachments described in Box 5.2, items ZC to ZS. In line 3 of this file, the constants CONDX and CONDY of the dial gauges  $D_x$  and  $D_y$  (Fig. 3.3) were fed as negative, for their readings decreased as the tips were depressed.

**6. DCWTXDYN.DAT.** The tests in this file have been performed on the same sample as in file 5, the specimens this time having been compacted dynamically as in section 4.4.2.2(3(a)).

**7. DCWTXST2.DAT.** This file consists of the first two tests in file 5, and as file 8, has been included here as an example of the reproducibility of the cylwest. The proximity of the results given at the end of the output of this file (DCWTXST2.OUT) and that at the end of DCWTXSTA.OUT are typical of the 27 series of cylwests (Mirata et

**Box 4.3 (continued)**

al., 1999) so far performed by Varan (1989), Seçkin (1993), and Gün (1997) on clays compacted at different water contents, and in three series of cylwests on gravelly sand by Gökalp (1994) (Mirata & Gökalp, 1997).

**8. DCWTXDY2.DAT.** This file consists of the first two tests in file 6, included here for the same purpose as file 7.

**9. DCWTXDGS.DAT.** This is a duplicate of file 6, with PAROUT altered to 7. in line 1, and the following modification made to enable the specific gravity and water content of the specimen to be specified: RDGNUM in line 35 was specified as 44. (a number > 40.), and line 36 inserted with the correct value of RDGNUM, followed by GS and WATCON. Thus in the output of this file (DCWTXDGS.OUT), WCINL = WATCON, GS, and the initial degree of saturation (SATINL), dry density (DDENSL), and void ratio (VOIDR) are printed in lines 95, 97, and 99, whereas the corresponding spaces for the same test (AB/D/3) are blank in the output of file 6 (DCWTXDYN.OUT), lines 197, 199, and 201.

**NOTE 43.** Neglect in lubricating the inner walls of the test mould has resulted in difficulty in jacking the test mould to fully contact the soil wedge in Test C/4/5, file 1, Box 4.1, the test eventually being performed with the mould 12 mm short of touching the loading face of the soil wedge; hence the value of  $L = 34.4$  cm in line 242 of the output for this file.

**NOTE 44.** For practical purposes,  $\sigma \approx \sigma_f$  may be achieved sufficiently accurately by adjusting  $Q$  to keep  $P$  somewhat below its value at peak strength, to account for the decrease in the area of shear and the relatively small contribution of  $Q$  to  $\sigma$ .

**NOTE 45.** No attempt has been made to shift the line of action of the main load  $P$  during the recent priswests, as the high loads involved require higher load capacity grooved plates in the device on the left of Fig. 4.7, and this is hardly warranted as the  $\delta\sigma/\sigma$  values on the failure plane can be kept to within about  $\pm 15\%$  at peak strength and to less than about  $35\%$  at the end of the test, with just an initial eccentricity  $\Delta y_P$  of about 6 mm applied to  $P$  (see outputs for files 1 and 2 in Box 4.2, noting that the  $\Delta y_P$  value of 28 mm inadvertently applied in test GWVD/5 of file 1 is unnecessarily high).

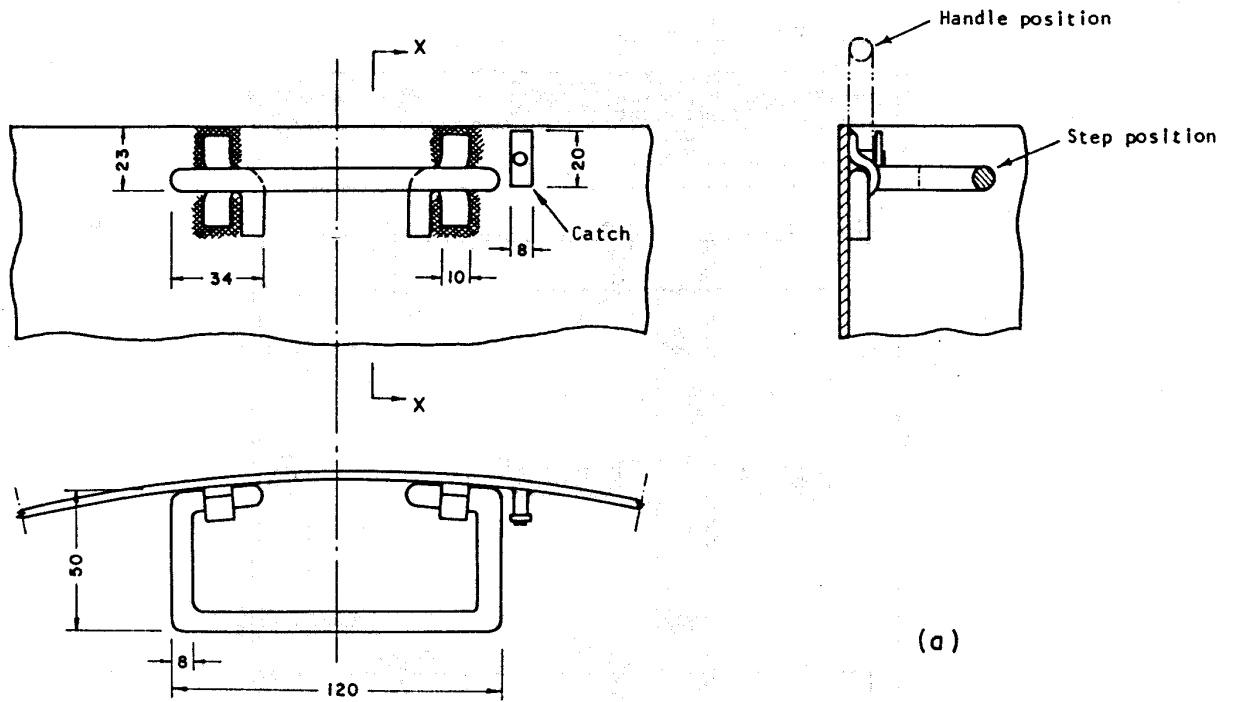
**NOTE 46.** Alternatively, a load cell may be used, particularly if very brittle material like marl is to be tested, as the abrupt release of load in a proving ring can suddenly thrust the movable half of the test mould, and damage the dial gauges. For the use of a load cell, simple discs, a sliding fit to the end recesses are adequate as adaptors.

**NOTE 47.** As explained in section 5.4.2(2), in the making of the grooved plates, the two plates are clamped side by side on a milling machine, and each groove cut in one continuous operation. To ensure that the grooves cut in this way always face each other when the plates are assembled for the test, one side of the plate is trimmed 3 mm shorter from the nearest groove than the other. Incorrect placement of the plates thus becomes quickly apparent due to the side of one plate protruding by 3 mm beyond the side of the other, but the outer dimensions of the plate are not symmetrical with respect to the grooves.

**NOTE 48.** By inscribing lines on the bracket BR, and on the test mould, indicating the points at which the dial gauges  $D_y$  and  $D_x$  respectively contact these components, and by marking the position of the dial gauge  $D_{mp}$  on the mould, the need to measure the distances  $d_1$ ,  $d_2$ ,  $d_3$  and  $d_4$  in every test using any particular test mould can be eliminated.

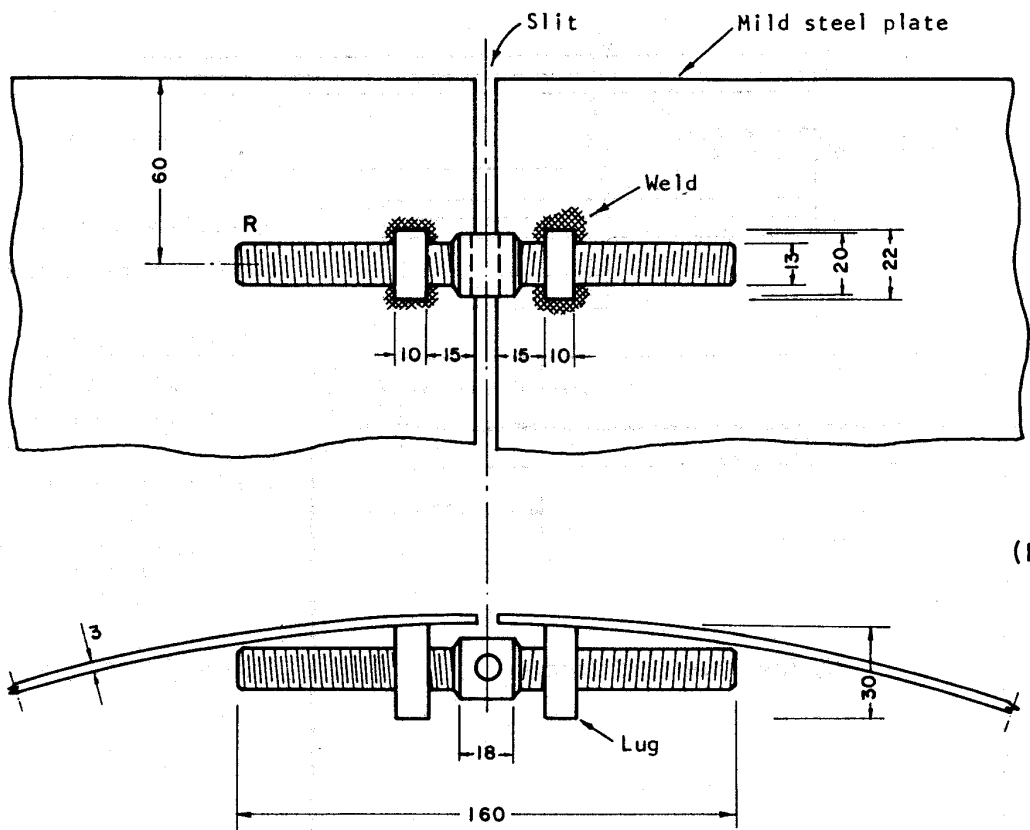
**Table 4.1. Lines of data files on diskette for use in preparing new data files for different wedge shear tests**

Type of data to be prepared	Iswest data files		Priswest data files		Cylwest data files	
	Filename	Lines	Filename	Lines	Filename	Lines
$Q = 0$ in all tests; default values used for test mould.	DIWC4DEF	1-10	...	...	...	...
$Q = 0$ in all tests; test mould data specified; first few lines unaltered for the next test.	DIWC4TMS	1-11	...	...	...	...
$Q = 0$ in all tests; test mould data specified; first few lines altered for the next test.	DIWC4TMS	1-3; 124-131; 146-148	...	...	...	...
$Q > 0$ in any of the tests; default values used for test mould.	DIWTKDEF	1-10	DPWMSHGC DPWGW38H	1-11 1-11	DCWC2USC DCWPFDEF	1-10 1-10
$Q > 0$ in any of the tests; default values used for test mould (and rod); first few lines altered for the next test .	DIWTKROD	1-3; 73-79; 93-95	DPWMSHGC	1-3; 60-67; 81-83	DCWC2USC	1-4; 18-23; 31-34
$Q > 0$ in any of the tests; test mould (and rod) data specified; first few lines unaltered for the next test.	DIWTKROD	1-3; 51-58	DPWMSHTR	1-3; 39-47	DCWC2TMS	1-11
$Q > 0$ in any of the tests; test mould (and rod) data specified; first few lines altered for the next test.	DIWTKROD	1-11; 29-31	DPWMSHTR	1-3; 61-69; 83-85	DCWC2TMS	1-4; 19-25; 33-36
Specifying specific gravity and water content in cylwests; available compression machine used.	...	...	...	...	DCWTXDGS	1-4; 31-37



(a)

All dimensions in mm



(b)

Fig. 4.1. Details of expansible rings for support of test pit walls showing (a) combined step and handle and (b) turnbuckle (after Mirata, 1976)

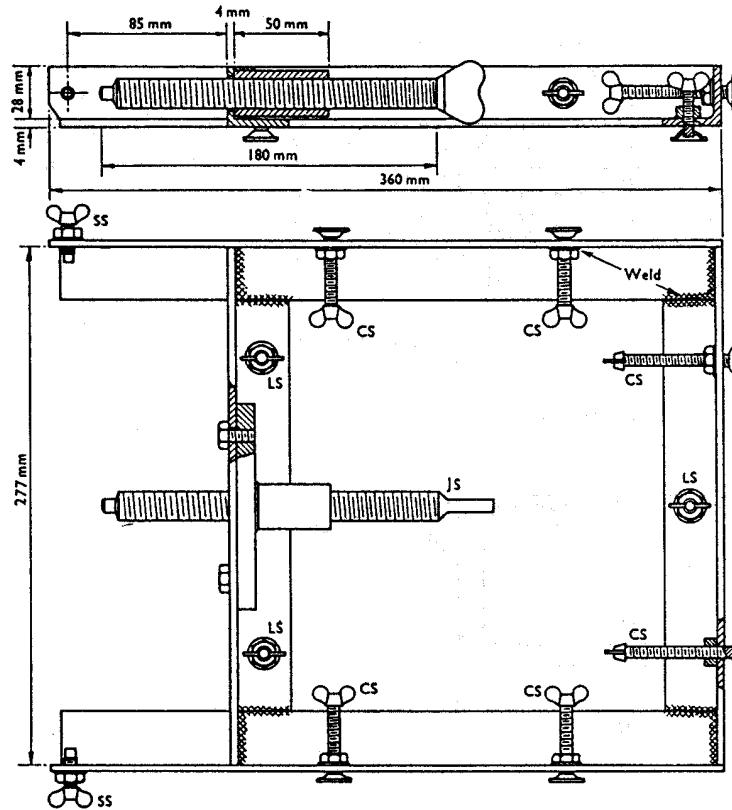


Fig. 4.2. Pivoting and jacking frame used in iswests (after Mirata, 1974)

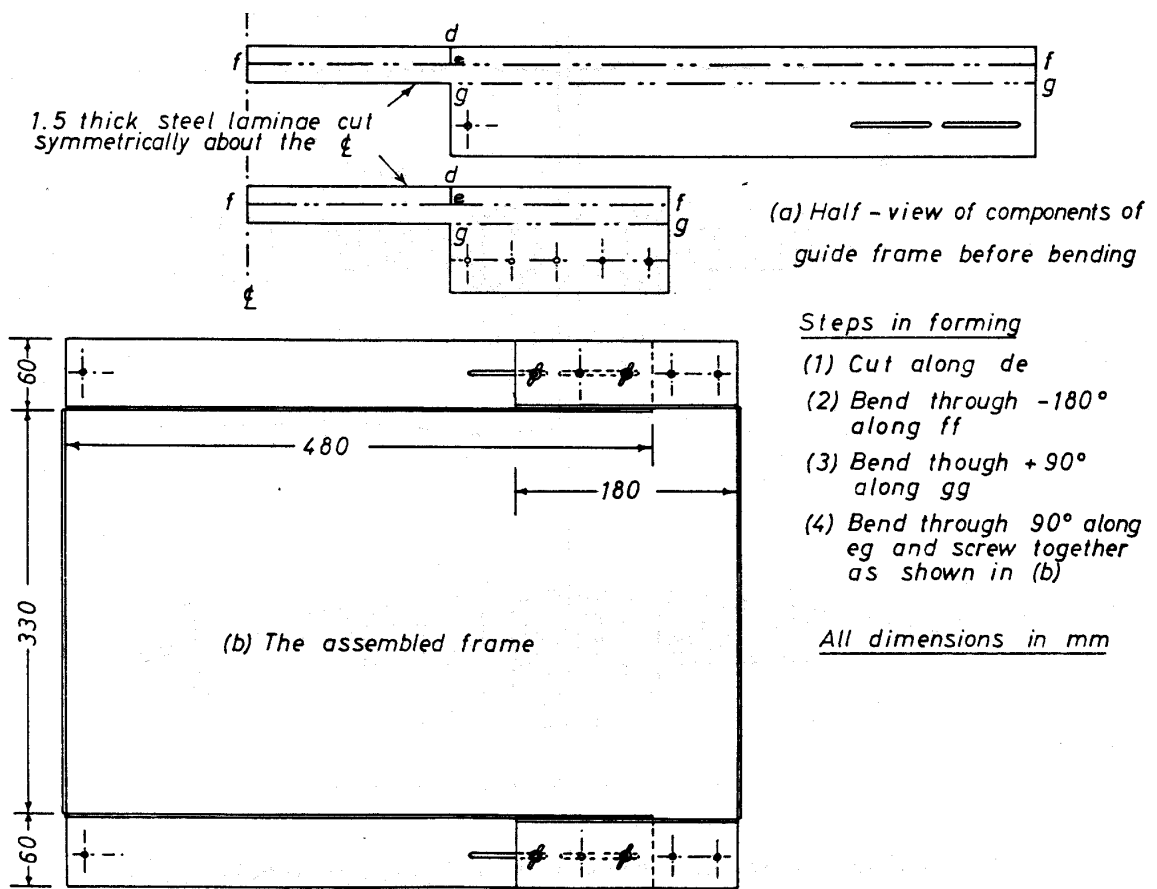


Fig. 4.3. Adjustable guide frame used in iswests (after Mirata, 1976)



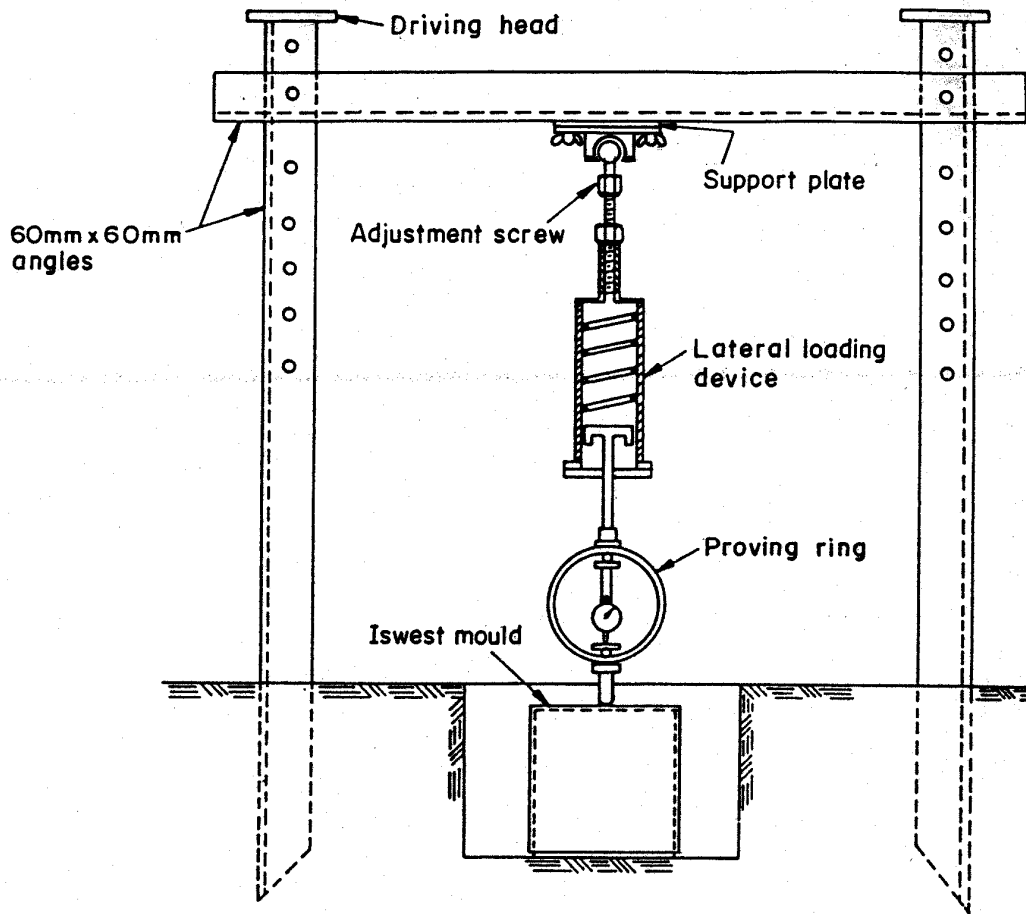


Fig. 4.4 Lateral load application in iswests (after Aybak, 1988)

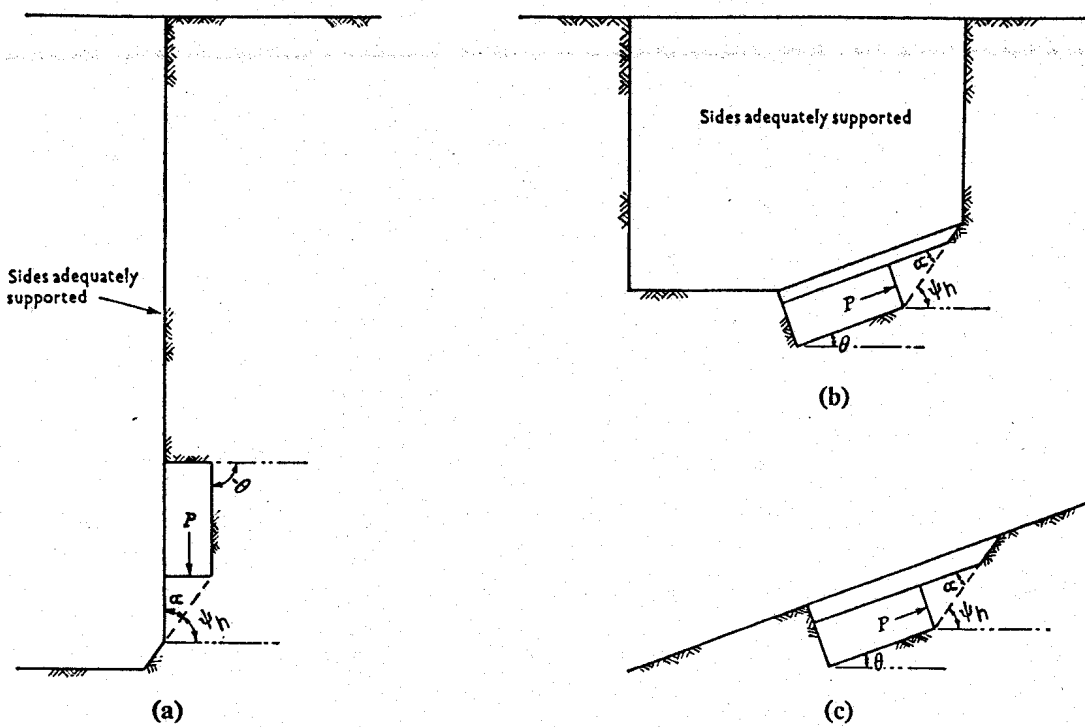
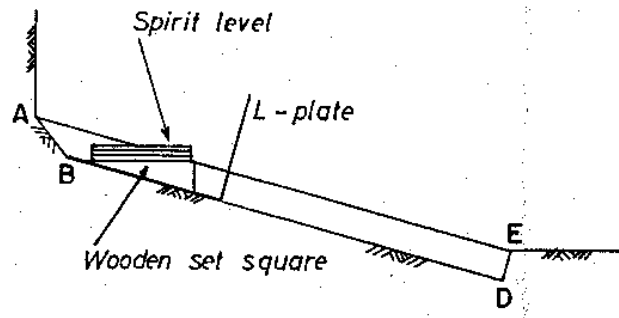
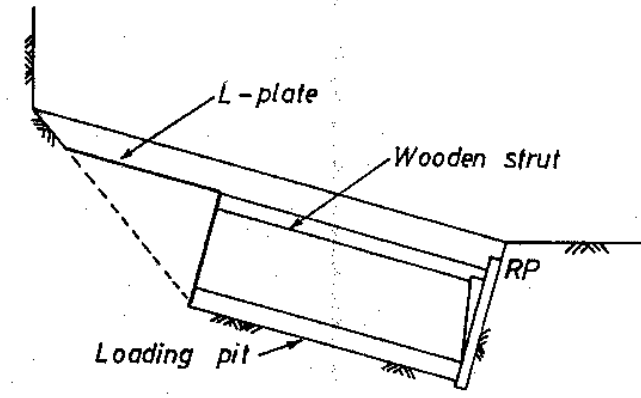


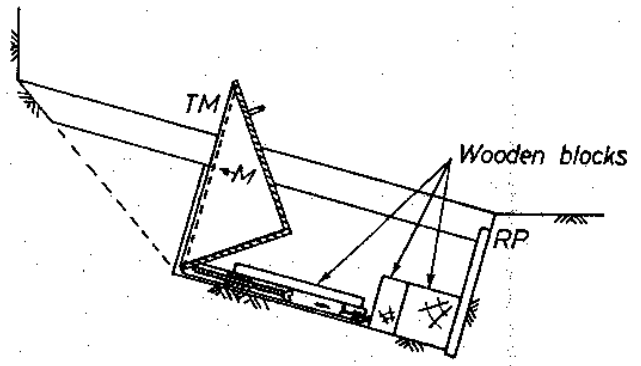
Fig. 4.5. Different ways of measuring shear strength on a given plane by iswests: (a) on side of test pit, (b) on base of test pit; (c) on an incline (after Mirata, 1974)



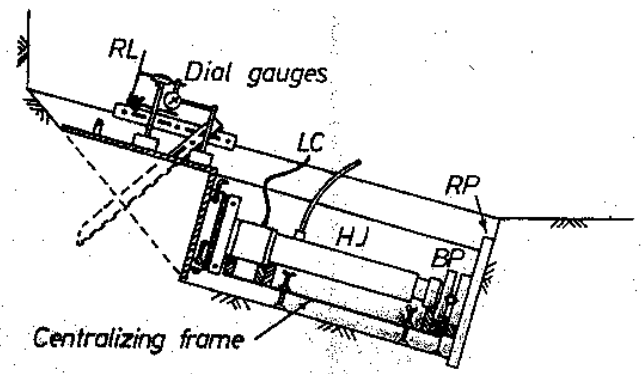
(a) Preparation of test area  
(in a test pit)



(b) Cutting sides of soil wedge



(c) Test mould ready for pivoting into position



(d) Loading

Fig. 4.6. Stages in performing an iswest (after Mirata, 1974)

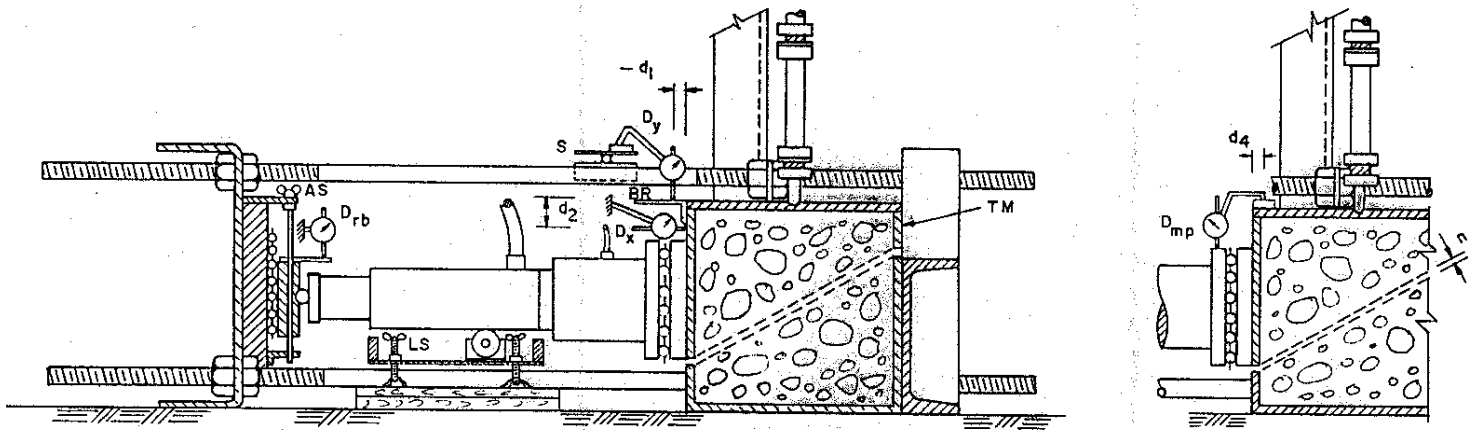


Fig. 4.7. Layout of dial gauges used in the priswest

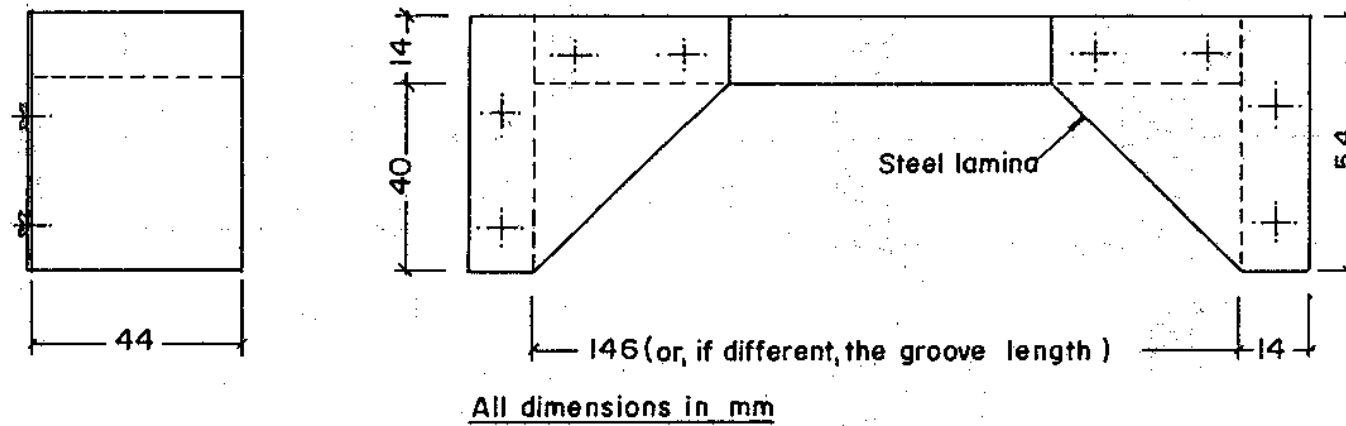
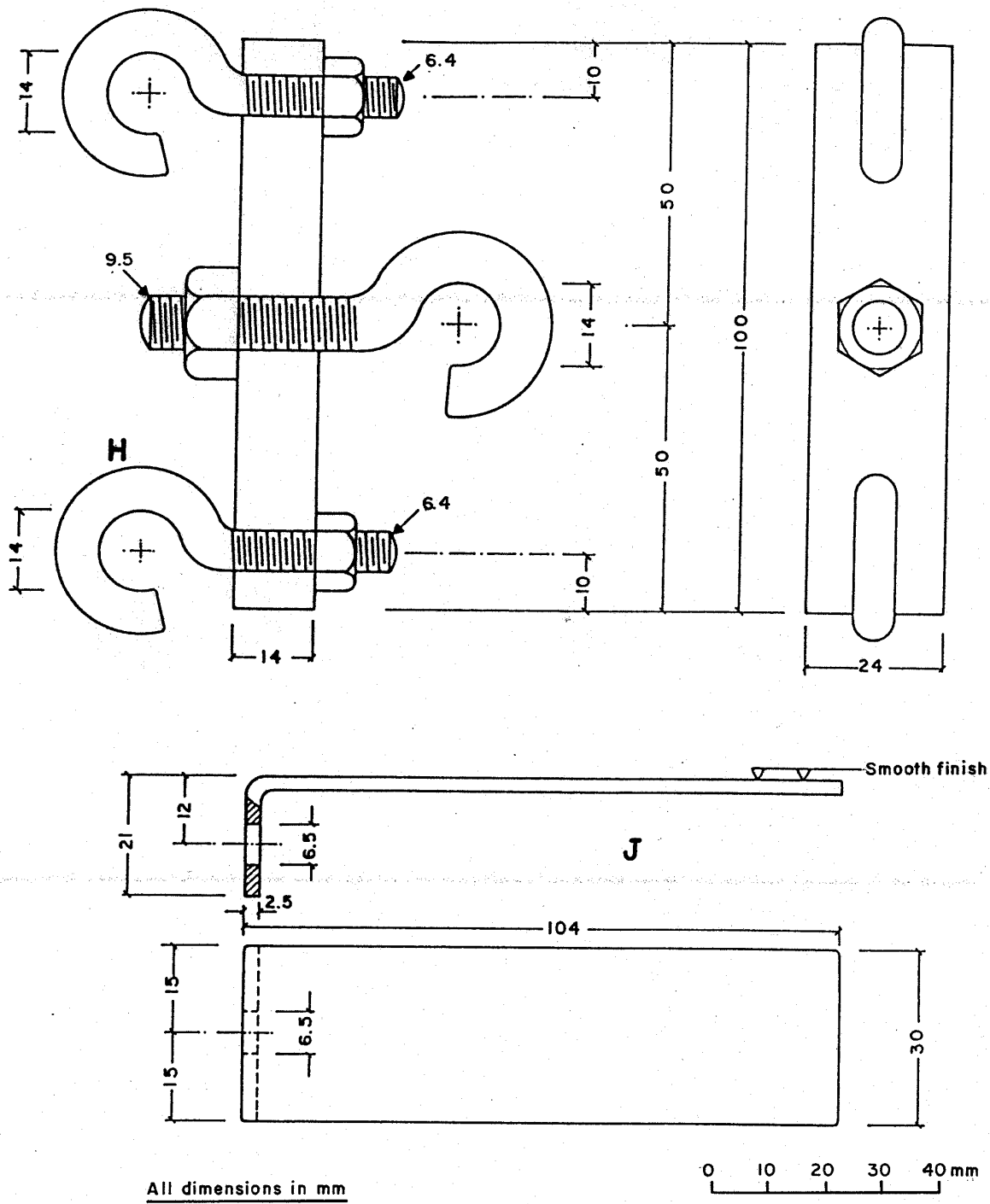
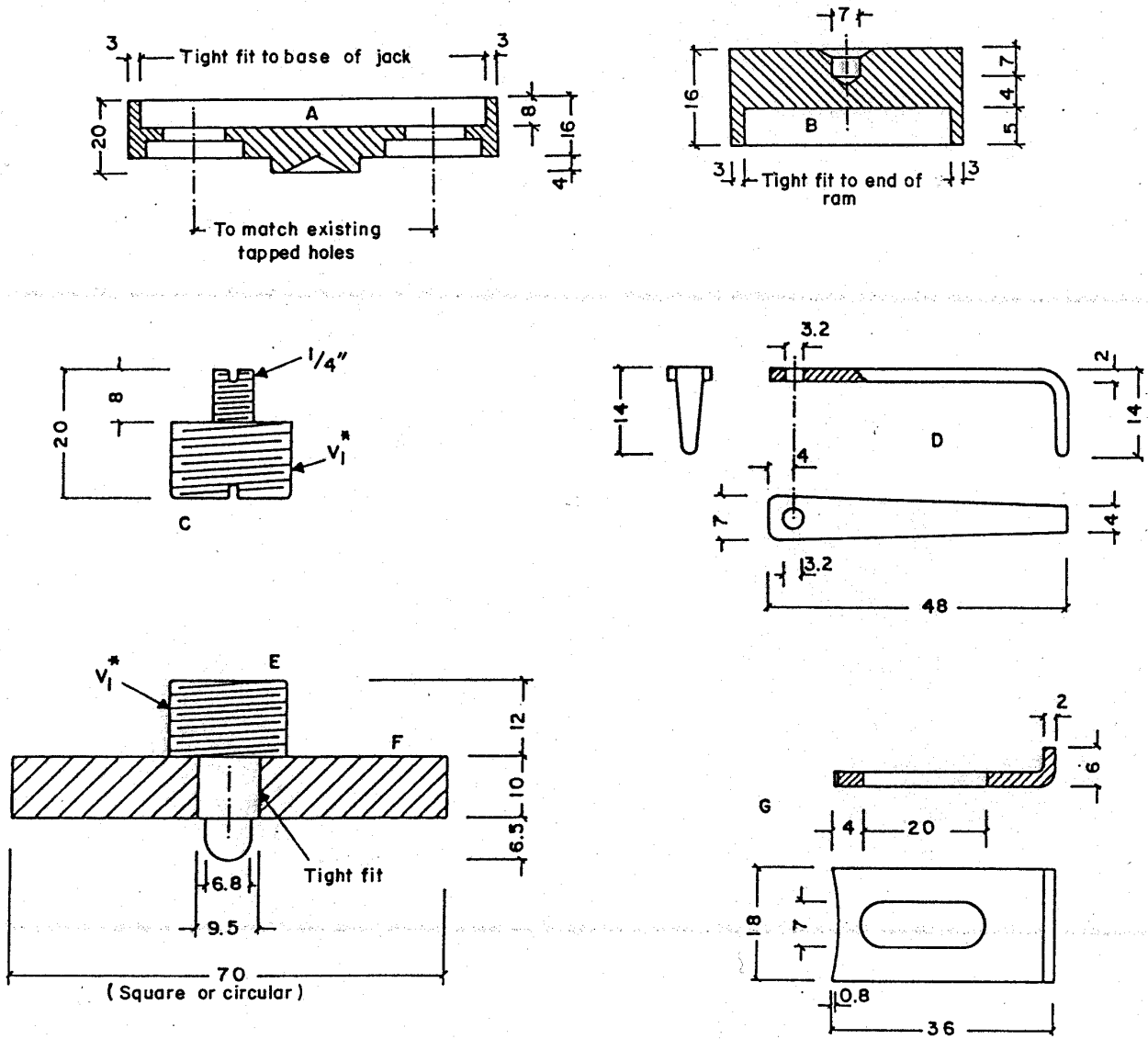


Fig. 4.8. Reinforced wooden clasps used in the priswests



Part	Number required	Material
H	2	Mild steel
J	1	Mild steel

Fig. 4.9. Hook assembly for use of two spring balances and bracket used in cylwests



All dimensions in mm

Part	Number	Material
A	1	Stainless steel
B	1	Stainless steel
C	1	Brass or stainless steel
D	2	Brass
E	1	Brass or stainless steel
F	1	Mild steel
G	3	Brass

\* Threads to fit the available 10-kN proving ring.

Fig. 4.10. Various adaptors used in cylwests

## CHAPTER 5

### DETAILS OF THE APPARATUS

#### 5.1 Introduction

The special devices needed for the different versions of the wedge shear test are so simple that the various diagrams in the published papers (Mirata, 1974, 1991, 1992), mostly reproduced in the earlier chapters, are almost the ‘working drawings’; Cascini (1980), for example, has had the relevant devices for the iswest made on the basis of such drawings. To facilitate the making of some of such equipment, the detailed drawings used in the making of the prototypes are given here with explanations where necessary. Otherwise, it is expected that the information given in the earlier chapters is sufficient to understand the various drawings.

#### 5.2 Drawings of apparatus for the in situ wedge shear test

##### 5.2.1 Test moulds

Fig. 5.1 shows the details of a typical iswest mould. It is made out of four, 10-mm thick mild steel plates, cut to size and welded. At least two moulds with as widely different angles  $\alpha_n$  as possible are adequate for most unsaturated soils encountered in practice. Moulds with  $\alpha_n$  ranging between  $25^\circ$  and  $45^\circ$  in steps of  $5^\circ$  have been used by the Author (Fig. 3.2(b)).

Except for the mould with  $JTM = 6$  in Fig. 3.2(b), each mould has an inside width of 250 mm and the length of the open end is 360 mm, giving a constant initial area of shear of  $900 \text{ cm}^2$ . The other dimensions are determined by the angle  $\alpha_n$ . Each mould has the following additional features.

- (a) The long sides of the open end are chamfered at  $45^\circ$  to form cutting edges.
- (b) The three tapped holes A for 6.3-mm dia. screws enable the mounting of the grooved loading plate LP1 (Fig. 5.2(a)), with the grooves central relative to the loading face of the test mould (see Note 47).
- (c) On either side of the mould are two holes B, 6.2 mm in dia. and 5 mm deep. For moulds with the smaller angles  $\alpha_n$  the chamfer of the sides of the mould may be back-filled with weld sufficiently to enable the holes B to be drilled.

(d) On the loading face, in a position identified by the procedure at step 4, section 4.2.3, there is a hole D, 7.5 mm in dia. and 5 mm deep.

(e) The outer rectangular faces of the mould have a smooth finish.

(f) Two 40 mm x 15 mm x 3 mm guide plates GP are screwed and adjusted to enable rapid centralizing of the grooves on LP1 (Fig. 5.2(a)) in screwing this on to the mould.

(g) On each of the chamfered sides of the mould, a mark M is inscribed at a distance  $h_b$  from the centre of the hole B, equal to the perpendicular distance between this hole and the opposite inner rectangular face of the mould.

(h) If the same mould is intended for use on soils with low or zero angles of friction, the effective value of  $\alpha_n$  may be increased up to  $65^\circ$  by duplicating the features (b) to (d), (f), and (g) for the other rectangular face as well.

(j) A handle is welded in such a position as not to interfere with possible usage as at (h) above.

### **5.2.2 Grooved loading plates**

If the plates described in section 5.4.2 are to be needed anyway, these can also be used for iswests and cylwests. Otherwise, the plates shown in Fig. 5.2, and a ball cage similar to that in Fig. 5.25, but having thirty 12-mm dia. steel balls, are adequate for iswests, and certainly so for cylwests. The procedure to be followed in the making of these components is similar to that given in 5.4.2.

### **5.2.3 Lateral loading device**

An optional item for iswests, this device is a vital part of priswests if cohesionless material is to be tested. If a compressed air source is not available, a spring loaded piston, illustrated in Fig. 5.3, can be used for this purpose. Loads up to 4.5 kN have been applied using this device; the load capacity may be increased by using a stiffer spring.

If a compressor is available, replacing the components in Figs 5.3(b) and (d) by a commercially available air piston using a frame similar to that shown in Fig. 5.4 (designed for an air piston of dimensions as shown by dashed lines) results in a more versatile device not needing continual adjustment during the test. The explanations related with Fig. 5.4 are given in Box 5.1 in alphabetical order of the designations of the

different parts, followed by the number of components required in parentheses. Unless otherwise stated, all parts are of mild steel. An air piston, providing a force of about 7 kN under an air pressure of 850 kPa, with a piston travel of at least 70 mm is suitable.

#### **Box 5.1. Explanations regarding the components in Fig. 5.4**

*NOTE. The dimensions given may be modified to suit the available air piston.*

**A (one).** A 180-mm dia., 14-mm thick disc with holes of the size and spacing shown in Fig. 5.4(d).

**B (one).** A 180-mm dia., 14-mm thick disc with a central tapped hole to fit the threads at the end of the adjustment screw housing shown in Fig. 5.3(c), and four holes of the size and spacing shown in Fig. 5.4(e).

**C (four).** Brass spacers with inside and outside diameters of 11 mm and 17 mm, and a length of 72 mm.

**D (four).** Brass spacers with inside and outside diameters of 11 mm and 17 mm, and length to suit the available bolts.

**E (four).** 16-mm dia., 450-mm long rods, threaded along 60 mm at one end and along 50 mm at the other.

**F (sixteen).** Nuts fitting the threads at the ends of rods E.

**G (one).** Brass adaptor for the air piston rod to screw at one end, and the 10-kN proving ring at the other.

**H (one).** Rod with a rounded tip, to be screwed on the 10-kN proving ring.

### **5.3 Drawings of apparatus for the cylindrical wedge shear test**

The details of the various devices required for performing a cylwtest using an available compression machine or a portable frame are given in Figs 5.5 - 5.14. Explanations regarding these are given in Box 5.2, in alphabetical order of the designations used on the drawings, followed in parentheses by the Fig. no(s) in which they appear, and the number of components required. In Fig. 5.14 are given the simple components, recently tried successfully in collaboration with Gün (1997), for enabling a lateral load to be applied in cylwtests using an available compression machine, without harming the original construction of such a machine. Unless otherwise stated, all parts are of mild steel.



## **Box 5.2. Explanations regarding the components in Figures 5.5 - 5.14**

**BR** ( Fig. 5.12; one). A 300 mm x 40 mm x 3 mm bar, with a 24.2-mm dia. hole at one end, used to support the test mould temporarily while this is being mounted in position, and capable of being turned out of the way after use. The nuts above and below BR are furnished with lock nuts. A 280 mm x 50 mm x 4 mm version of this bar with a 38.4-mm dia. hole has been used on the 38-mm dia. strain rods of an available compression machine.

**C** (Figs 5.5, 5.13; one). The clamp used for fixing the upper part of the test mould either to the middle plate MP of a portable frame (Fig. 5.5) or to the channel replacing the cross-beam of an available compression machine (Fig. 5.13). Although initially drawn to scale, some dimensions have subsequently been changed to suit requirements; the numerical values are the revised ones.

**D** (Fig. 5.5; three for moulds with  $\alpha_n = 30^\circ$ ; five for moulds with  $\alpha_n = 45^\circ$ ). Wooden discs of dia. 2 mm smaller than the inside dia. of the mould and height  $20/\sin\alpha_n$  mm. These are varnished to prevent swelling, and are used with the single-cut moulds. For the double-cut moulds, one 44-mm high and two 64-mm high discs have been used.

**HK** (Figs 5.8, 5.12; one). A hook bent out of 6-mm dia. stainless steel bar.

**LP** (Figs 5.5, 5.9, 5.12; one). The lower plate of the frame in Fig. 5.5. Cut out of 15-mm thick plate and welded.

**MP** (Figs 5.5, 5.8, 5.12; one). The middle plate of the frame in Fig. 5.5. Cut out of 15-mm thick plate and welded. It has a central opening to enable the frame to be used for extruding samples when needed, and slotted holes to enable the clamping of different diameter test moulds.

**RB** (Fig. 5.12; one). A 20-mm thick wooden restraining board, having an oval hole in the middle, large enough not to touch the hydraulic jack during the test, and held tightly against the strain rods of the portable frame.

**RD** (Figs 5.5, 5.10; one of each type or size). These are the removable disc used during the test (Fig. 5.5) or rings, designed for use together with sampling tubes, while the sample is extruded from such tubes. These are kept in position by the recesses at the sides being pushed past the tongues T screwed on the middle plate MP in Fig. 5.8, and then rotating them slightly.

**SR** (Figs 5.5, 5.11(a), 5.12; four). The strain rods of the frame in Fig. 5.5, with the

**Box 5.2. (continued)**

portions shown in Fig. 5.11(a) having 23.8-mm threads. The threaded portion on one rod is extended by 170 mm to support BR (Fig. 5.12).

**S1** (Figs 5.5, 5.11(b); one). This support is made of two angle bars measuring 25 mm x 25 mm x 1550 mm, held together at one end by a 12-mm dia., 410-mm long rod. The opposite end is attached in a rotatable way to the lower plate LP of the frame in Fig. 5.5, or to the lower pair of hinged clamps ZC (Fig. 5.14(a)), attached to the strain rods of an available compression machine. Starting from 1265 mm from the frame attachment end are three pairs of slots, 14 mm wide.

**S2** (Figs 5.5, 5.11(c); one). This support is made of two pairs of angle bars measuring 25 mm x 25 mm x 1020 mm, each pair being welded together as in Fig. 5.11(c), held together at one end by a 12-mm dia., 460-mm long rod. The opposite end is attached in a rotatable way to the middle plate MP of the frame in Fig. 5.5, or to the pair of lugs ZL (Fig. 5.14(c)) welded on the channel replacing the cross-beam of an available compression machine.

**T** (Fig. 5.8; two). Brass tongues screwed on the middle plate MP of the frame in Fig. 5.5 (see RD above).

**TB** (Fig. 5.5; one). This is a turnbuckle consisting of two 9-mm dia. bars, bent to the shape of a U, 20 mm in height and 140 mm wide, which are welded on the opposite flats of two nuts, one with left-hand the other with right-hand threads. Fitting these nuts are two 10-mm dia. 128-mm long hooks, the threaded portions being about 78 mm long.

**UP** (Figs 5.5, 5.7, 5.12; one). The upper plate of the frame in Fig. 5.5. Cut out of 10-mm thick plate, it carries a central hole to enable checking the height of the specimen extruded into the test mould or core cutter.

**YK** (Figs 5.5, 5.6; one). The yoke is made out of two 10-mm dia. steel bars and two 16 mm x 24 mm x 200 mm cross-pieces. On one of the cross-pieces is screwed a hook, with a nut acting as reinforcement as well as a lock nut for the hook. On the other is a central rod with a rounded tip.

**ZC** (Fig. 5.14(a); four). These are hinged clamps, designed to be easily fitted on the 38-mm dia. strain rods of the available 5-ton compression machine, with paper packing in between to prevent damage to the threads on the strain rods. Two are used to support the angle bars S1; the other two hold a rotatable arm similar to BR (Fig. 5.12) in between.

**Box 5.2. (continued)**

**ZD** (Fig. 5.14(b); one). Formed by cutting and welding a 24 mm x 24 mm x 560 mm steel bar, this is fixed (using hose clamps) to the strain rods of the compression machine, and used to give extra support to the upper part of the test mould when relatively large lateral loads are applied.

**ZH** (Fig. 5.14(c); one). A hook bent out of 8-mm dia. steel bar and welded on to the channel replacing the cross-beam of the compression machine.

**ZL** (Fig. 5.14(c); two). These are lugs welded on the channel replacing the cross-beam of the compression machine, and used to support the angle bars S2 (Fig. 5.5).

**ZS** (Fig. 5.14(c); two). Two short pieces of pipe, spot-welded on the channel replacing the cross-beam of the compression machine, to act as spacers to enable the upper nuts, with side knobs, of the strain rods to press on the channel.

## **5.4 Drawings of apparatus for the prismatic wedge shear test**

### **5.4.1 General**

The details of the 20-ton capacity loading frame, the supports for the lateral loading device (Figs 5.3, 5.4), and the prismatic mould are given in Figs 5.15 - 5.26. The variable dimensions for four test moulds with different angles  $\alpha_n$  have been shown by symbols on the drawings; the numerical values are given in Table 5.1. It is recommended that for each size of mould, which is to be made, a separate set of photocopies of these drawings be prepared, and the symbols replaced by the dimensions given in Table 5.1 for the particular  $\alpha_n$ . Indicating the original angles  $\alpha_n$  on the drawings by  $\alpha_{no}$ , with the simple modifications explained in section 5.4.4, for the moulds with  $\alpha_{no} < 45^\circ$  it is possible when desired, to apply the main load  $P$  on the lid, thus making the effective angle  $\alpha_n$  between  $P$  and the shear plane =  $(90 - \alpha_{no})^\circ$ . For clayey gravels and the like which have lower angles of friction than clean gravel, the range of normal stresses can thus be extended as much as the capacity of the loading equipment permits. This procedure, first proposed by Mirata (1992), has been successfully tried for the  $\alpha_{no} = 40^\circ$  mould (see Box 4.2, file 2, and Mirata et al., 1998).

The scales in Figs 5.15 - 5.22 are valid for the  $\alpha_n = 35^\circ$  mould, except that after the frame was made, the numerical values for its width have been changed to give an extra clearance of 30 mm between the test mould and the strain rods on either side, to facilitate the tightening and removal of the link bolts in future productions of the equipment.

Explanations regarding the components in Figs 5.15 - 5.22 are given in Box 5.3, in alphabetical order of the designations used on the drawings, followed in parentheses by the Fig. no(s) in which they appear, and the number of components required (in the case of the components of the test mould, for one mould only). Unless otherwise stated, all parts are of mild steel.

The details of the simple frame used to support the jack temporarily in iswests and priswests when loading is in the horizontal direction are given in Fig. 5.23, together with the necessary explanations.

The grooved plates shown in Fig. 5.2, and a ball cage with thirty 12-mm dia. steel balls have been found satisfactory for loads up to about 80 kN. For higher loads in priswests, the version of these components that have been successfully tested up to 145 kN are shown in Figs 5.24 and 5.25; the procedures followed in making these, and in determining the coefficient of friction  $\mu$  are given in sections 5.4.2 and 5.4.3. These plates are designed to be used for iswests and cylwests as well. For use in priswests, the brackets and catches are replaced by the clasps shown in Fig. 4.8. The simple alterations to existing moulds with  $\alpha_{no} < 45^\circ$ , to enable the main load  $P$  to be applied on the lid when desired, making the angle  $\alpha_n$  between  $P$  and the shear plane  $= (90 - \alpha_{no})^\circ$ , are explained in section 5.4.4, for the example of the  $\alpha_{no} = 40^\circ$  mould.

#### **5.4.2 High load capacity grooved plates**

This is a description of the procedure followed and the materials used in the making of the grooved plates and the ball cage housing sixty-four 12-mm dia. steel balls to be used between these (Figs 5.24 and 5.25). Note that, what is important regarding the groove diameter is that it should be the same as the diameter of the steel balls. If 12-mm dia. balls are not available, the groove diameter should be adjusted to the nearest size of ball that can be acquired.

1. A 304 mm x 164 mm plate was sawed out of a 25-mm thick plate of steel with an initial hardness of about 20 Rockwell C. This plate was then sawed into two

equal parts, close to the dimensions shown in Fig. 5.24. These were hardened by heating and quenching, and tempered to produce a hardness of about 30 Rockwell C.

2. The surfaces of the plates were machined parallel to each other. One of the surfaces was ground to a smooth finish, and three of the edges smoothed to produce a width of 146 mm; one of the shorter edges being left untreated initially. These plates were then clamped side by side on a milling machine with the 146-mm wide smoothed edges in one line, and lying on their smoothed surfaces. Starting at 24 mm from the smoothed 146-mm edges and spaced at 16 mm between the centres, eight 12-mm dia., 1-mm deep grooves were cut, each by one continuous motion of the cutting tool along the 292 mm combined length of the two plates. Finally, the fourth edge of each plate was machined at a distance of 21 mm from the centre of the last groove.

3. The details shown in Fig. 5.24 and explained below were added.

(a) Three two-stage holes H were drilled in plate LP1, at the points shown in Fig. 5.24(a). At each side of this plate were fitted two swivel catches K, cut out of 1-mm thick brass plate and having brass bushings to prevent over-tightness or loosening during use.

(b) On the sides of LP2 (Fig. 5.24(b)) were fitted four 5-mm dia. screws S, with the heads clear of the sides by about 3 mm, for the swivel catches K to engage. On the non-grooved face of this plate, a brass disc BD, 21.8 mm in dia. (to be a sliding fit to the recesses at the ends of the available load cell), was screwed centrally relative to the grooves.

(c) On the upper edge (Fig. 5.24) of each plate, a 6.4-mm dia., 10-mm deep tapped hole TH was drilled.

(d) To enable these plates to be used for cylwests as well, on the non-grooved face of LP1, in positions shown in Fig. 5.24(a), two 6.4-mm dia., 8-mm deep tapped holes A were drilled for attaching the sliding guide plates G shown in Fig. 4.10. On this same face, centrally relative to the grooves, were punched a series of dots marking the outer diameter of the different cylwest moulds to be used. In the lower edge of the same plate, were fitted two brackets of 3-mm thick steel plate with brass bushings to prevent over-tightness or loosening during use.

4. The ball cage shown in Fig. 5.25 was made as follows. Two 1-mm thick steel plates and a 5-mm thick aluminium plate were cut and brought to the dimensions of 146 mm x 157 mm. At the nodes of the grid shown in Fig. 5.25(a) with 14 mm x 16 mm

cells, 64 holes were drilled and shaped as in Fig. 5.25(b), to enable free rotation of 12-mm dia. steel balls within. To ensure this, the plates were initially held together by means of bolts and nuts; having made sure that each of the 64 balls could rotate freely, the bolts were replaced, one at a time, by rivets. Three extra balls of the same size as that used for the ball cage were kept for the determination in the next sub-section.

### **5.4.3 Measurement of the coefficient of friction for the grooved plates**

In determining the coefficient of friction  $\mu$  against the motion of one grooved plate relative to the other with the steel balls rolling in between, the following were observed.

(1) The grooved plate LP1 (Fig. 5.24(a)) was placed on a rigid surface with the grooves facing upwards, and perfect horizontality of the upper surface was ensured. (Note that  $\mu = 0.0038$  measured on such plates is equivalent to an inclination of  $0.22^\circ$  to the horizontal as regards the motion of LP2 relative to LP1.)

(2) The grooves of both plates were cleaned and lubricated by a light grade oil. Three steel balls of the same diameter as those used for the ball cage in Fig. 5.25 were placed in the grooves of LP1, at the corners of an equilateral triangle of side about 110 mm. An eye bolt was screwed in the tapped hole TH on LP2, and this plate placed on the steel balls, with the edges in line with those of LP1.

(3) A string tied on the eye bolt on LP2 was passed horizontally over a pulley with ball bearings, and a 1-litre capacity plastic pail suspended from the end.

(4) Precautions were taken to limit the motion of the 50-kg weights to be placed centrally on LP2, seeking the assistance of at least two other persons to prevent inadvertent toppling over of these weights. As  $\mu$  was very low, LP2 with a 50-kg weight on top was set in motion under the self weight of the pail; so the load was increased to 100 kg. Sand was slowly added to the pail, while occasionally giving a slight push to LP2. At the point when the motion of the plate continued under the weight of the pail and its contents, but without acceleration, the pail and its contents were weighed; another 50-kg weight was added, and the test continued up to a total load of 350 kg. An additional weight was placed on the pile momentarily, and then removed, repeating the determination under each load during unloading. The values of the average frictional force were plotted against the corresponding normal load; the slope gave  $\mu$ .

#### 5.4.4 Modifying test moulds for higher normal stress ranges

The following simple modifications have been applied to the  $\alpha_{no} = 40^\circ$  test mould (Fig. 5.26) to enable the main load  $P$  to be applied on the lid when desired, making the angle  $\alpha_n$  between  $P$  and the shear plane =  $50^\circ$ .

(1) The prisms ABC and A'B'C' were ground off. The handles H and H' were bent as shown by dashed lines, parallel to the shear plane.

(2) A conical recess was made at point R, for the lateral load device to engage.

(3) To screw the grooved loading plate LP1 (Fig. 5.24(a)) on the lid, three 6.4-mm dia., 8-mm deep tapped holes were formed at points D, and the 40 mm x 15 mm x 3 mm guide plates screwed in such positions as to centralize the grooves on LP1 relative to the loading face of the mould, with the lower edge 28 mm above the lower face of the mould.

(4) On either side of the mould at point N, a 6.4-mm dia., 8-mm deep tapped hole, and at point E on the centre-line of the lid, a 4.8-mm dia., 8-mm deep tapped hole was formed.

**Table 5.1. Values of the variable dimensions in Figures 5.15 - 5.22**

Angle $\alpha_n$ of the test mould (deg):		30	35	40	45
Fig. no(s)	Symbol	Numerical value (mm)			
5.17, 5.19	L <sub>1</sub>	279.8	265.8	249.8	232.1
5.17, 5.19, 5.20	L <sub>2</sub>	200.0	222.1	232.8	252.1
5.17, 5.19	L <sub>3</sub>	50.0	50.0	40.0	40.0
5.17, 5.19	L <sub>4</sub>	15.0	14.0	13.0	12.0
5.17	L <sub>5</sub>	129.9	122.9	114.9	106.1
5.17	L <sub>6</sub>	65.0	60.0	48.0	44.0

**Table 5.1. (continued)**

Angle $\alpha_n$ of the test mould (deg):		30	35	40	45	
Fig. no(s)	Symbol	Numerical value (mm)				
5.17	L <sub>7</sub>	25.0	25.0	20.0	20.0	
5.17	L <sub>8</sub>	11.0	11.0	11.0	17.0	
5.18, 5.19	L <sub>9</sub>	75.0	70.0	58.0	56.0	
5.18	L <sub>10</sub>	139.9	132.9	124.9	116.0	
5.19	L <sub>11</sub>	259.8	245.8	229.8	212.1	
5.19	L <sub>12</sub>	37.5*	37.5	48.2	67.5	
5.19	L <sub>13</sub>	25.0*	25.0	45.7	55.0	
5.19	L <sub>14</sub>	254.0	240.0	224.0	206.0	
5.19	L <sub>15</sub>	139.9	132.9	124.9	116.1	
5.20	L <sub>16</sub>	0.0	1.5	0.2	5.1	
5.20	L <sub>17</sub>	7.5	9.0	7.7	12.6	
5.20	L <sub>18</sub>	138.5	140.0	138.7	143.6	
5.20	L <sub>19</sub>	73.0	74.5	73.2	78.1	
5.22	L <sub>20</sub>	254.0	240.0	224.0	206.0	
5.20	L <sub>21</sub>	for E <sub>1</sub>	15.0	15.0	15.0	15.0
		for E <sub>2</sub>	10.0	10.0	10.0	...
5.20	L <sub>22</sub>	for E <sub>1</sub>	14.0	14.0	14.0	14.0
		for E <sub>2</sub>	10.5	10.5	10.5	...

\* The  $\alpha_n = 30^\circ$  test mould, originally used on the 5-ton loading frame (Fig. 3.1), has to be raised by 22 mm above the floor level when the frame is horizontal, for use on the 20-ton frame.



**Table 5.1. (continued)**

Angle $\alpha_n$ of the test mould (deg):		30	35	40	45	
Fig. no(s)	Symbol	Numerical value (mm)				
5.18	$h = 5 \text{ mm}$	$h \cos \alpha_n$	4.33	4.10	3.83	3.54
		$h \sin \alpha_n$	2.50	2.87	3.21	3.54
		$a_1$	76.3	74.7	64.3	64.0
5.18	$h = 8 \text{ mm}$	$h \cos \alpha_n$	6.93	6.55	6.13	5.66
		$h \sin \alpha_n$	4.00	4.59	5.14	5.66
		$a_1$	77.1	75.5	65.2	65.1
5.18	$h = 12 \text{ mm}$	$h \cos \alpha_n$	10.39	9.83	9.19	8.49
		$h \sin \alpha_n$	6.00	6.88	7.71	8.49
		$a_1$	78.1	76.7	66.5	66.5

**Box 5.3. Explanations regarding the components in Figures 5.15 - 5.22**

**A** (Figs 5.15, 5.17 - 5.19; four). Of these four parts constituting the trapezoidal sides of the test mould, unlike those of the opposite half, to those of the mobile half ( $A_1, A_2$ ) the tapped holes  $a$  and  $d$  (Figs 5.17, 5.18), and to those of the stationary half ( $A_3, A_4$ ) the tapped holes  $c$  (Figs 5.17, 5.19) are drilled.  $A_1$  and  $A_2$  are welded on  $B_1$  and  $D_1$  only;  $A_3$  and  $A_4$  are welded to  $B_2$  and  $D_2$  as well as to  $C_2$ .

**B** (Figs 5.15, 5.17; two). The narrower rectangular sides of the test mould. To that of the mobile half of the mould ( $B_1$ ), the tapped holes  $d$  and  $e$ , to those of the stationary half ( $B_2$ ), the tapped holes  $f$  are drilled. A handle is welded on each, for ease during handling.

**C** (Figs 5.15, 5.17, 5.18; two). The removable lid ( $C_1$ ) of the mobile part of the mould, and the fixed base ( $C_2$ ) of the stationary half. Along each edge of  $C_1$ , two 5-mm dia. holes  $g$  are drilled to enable this plate to be screwed on  $A_1, B_1, A_2$  and  $D_1$ . At the centre of  $C_1$ , is a conical recess as in Fig. 5.18.  $C_2$  is welded on  $A_3, D_2, A_4$  and  $B_2$ .

**Box 5.3. (continued)**

**D** (Figs 5.15, 5.17, 5.20; two). The wider rectangular sides of the test mould. To that of the mobile half of the mould ( $D_1$ ), the tapped holes  $f$  (Fig. 5.17) and  $g$  (Fig. 5.20), and three tapped holes  $j$  are drilled. Holes  $j$  are for screwing the grooved plate LP1 (Fig. 5.24(a)) on the mould. To enable rapid positioning of LP1, two 40 mm x 15 mm x 3 mm guide plates  $k$  are screwed on  $D_1$  as shown in Fig. 5.20. On  $D_2$ , two tapped holes are drilled opposite to holes  $e$  on  $B_1$ . Both  $D_1$  and  $D_2$  are welded on the adjoining parts.

**E<sub>1</sub>** (Fig. 5.20; six or eight). These are the links holding  $A_1$  and  $A_3$ ,  $A_2$  and  $A_4$ ,  $D_1$  and  $B_2$ , and, for the mould with  $\alpha_n = 45^\circ$ ,  $B_1$  and  $D_2$  together temporarily, with spacers in between, while the sample is placed in the mould.

**E<sub>2</sub>** (Fig. 5.20; two or nil). These are the links holding  $B_1$  and  $D_2$  together temporarily with spacers in between while the sample is placed in the moulds with  $\alpha_n = 30^\circ$ ,  $35^\circ$ , and  $40^\circ$ , for the first two, used during static compaction only.

**E<sub>3</sub>** (Fig. 5.20; two or nil). These are needed for the  $\alpha_n = 30^\circ$  and  $35^\circ$  moulds only, and are used for connecting  $B_1$  on to the channel  $K_2$ .

**F** (Figs 5.15, 5.16, 5.20; two). These plates are for attaching the angles  $N_1$ ,  $N_2$  (Fig. 5.15) on to the loading frame.

**G** (Figs 5.15, 5.16; two). These are the 380-mm long, 160 mm x 65 mm channels  $G_1$ ,  $G_2$  (Fig. 5.15). On these, holes are drilled for the 40-mm dia. strain rods, and the wide sides are welded on to the channels  $K_1$  and  $K_2$ . *Although not shown in Figs 5.15 and 5.16, for aesthetic reasons and extra reinforcement, the open sides of these channels have been closed by welding 5-mm plates, in making the prototype.*

**H** (Figs 5.15, 5.16; four). The 1280-mm long, 40-mm dia. strain rods, threaded along 450 mm at each end.

**I<sub>1</sub>** (Figs 5.15, 5.16; eight). The end nuts, each able to sustain a shear force of 50 kN.

**I<sub>2</sub>** (Figs 5.15, 5.16; sixteen). The intermediate nuts, which need merely be able to hold the relevant parts tightly together.

**J** (Figs 5.15, 5.16, 5.21; one). A 580-mm long, 400 mm x 110 mm channel to which holes are drilled for the strain rods  $H$ , and tapped holes drilled for screwing the plates  $L$  (Fig. 5.21) which hold the 250 mm x 250 mm x 21 mm plate in position.

**K** (Figs 5.15, 5.16; two). These are the 410-mm long, 220 mm x 80 mm channels  $K_1$ ,  $K_2$ , which are welded to each other along the tips, and to  $G_1$ ,  $G_2$  at the two ends. The tapped holes  $m$  are drilled on  $K_2$ .

**Box 5.3. (continued)**

**L** (Fig. 5.21; four). Clamping pieces cut and bent out of 3-mm thick plate.

**M** (Fig. 5.16; one). A 680-mm long, 60 mm x 60 mm x 10 mm angle bar.

**N** (Figs 5.15, 5.16, 5.21; two). These are the 1540-mm long, 60 mm x 60 mm x 10 mm angle bars, shown as  $N_1$ ,  $N_2$  in Fig. 5.21.

**P** (Figs 5.19, 5.21; four). Hooks  $P_1$ ,  $P_2$  formed out of 3-mm thick plate. These are welded on channel  $K_2$ , enabling the bolts  $V_{11}$  screwed in tapped holes  $c$  on  $A_3$  and  $A_4$  to engage, and thus the test mould to be easily mounted on and removed from the loading frame.

**R** (Fig. 5.19; one). A 20-mm plate of length 294 mm and width  $L_{14}$  defined in Table 5.1. Two hooks are screwed on this as in Fig. 5.19, for ease of handling.

**S** (Fig. 5.19; one). A collar for increasing the effective depth of the test mould by 70 mm when mounted in place of the lid  $C_1$ . Its inner dimensions and wall thickness are the same as those of the mould. At the middle of each edge, there is a lug, through which it can be screwed on to  $A_1$  and  $A_2$  through the tapped holes  $a$  (Fig. 5.17), and to  $B_1$  and  $D_1$  through tapped holes  $d$  and  $g$  (Figs 5.17 and 5.20).

**T** (Fig. 5.18; twelve). Spacers for adjusting the height  $h$  between the two halves of the mould to three different values (5 mm, 8 mm, and 12 mm). Two spacers are required of each of the two types  $T_1$  and  $T_2$ .

**V<sub>1</sub>** (Fig. 5.18; eight). Round head screws; 3.2-mm dia., 11-mm long (for connecting spacers to the links).

**V<sub>2</sub>** (Fig. 5.18; eight). Headless screws; 4.8-mm dia., 14-mm long (for plugging the holes  $d$  during sample placement).

**V<sub>3</sub>** (Figs 5.17, 5.20; sixteen). Fly-bolts with spring washers; 6.4-mm dia., 11-mm long (for connecting the links on to the test mould).

**V<sub>4</sub>** (Fig. 5.17, 5.18; eight). Fly-bolts; 4.8-mm dia., 24-mm long (for fixing the lid).

**V<sub>5</sub>** (Fig. 5.19; four). Fly-bolts; 4.8-mm dia., 11-mm long (for fixing the collar).

**V<sub>6</sub>** (Fig. 5.19; two). Hooked screws; 4.8-mm dia., 12-mm long.

**V<sub>7</sub>** (Fig. 5.20; four). Hexagonal head bolts; 4.8-mm dia., 11-mm long (for the guide plates  $k$ ).

**V<sub>8</sub>** (Fig. 5.21; four). Round head screws; 3.2-mm dia., 11-mm long (for the clamping pieces  $L$ ).

**V<sub>9</sub>** (Fig. 5.15, 5.20; four). Hexagonal head bolts with nuts and washers; 9.5-mm dia., 30-

**Box 5.3. (continued)**

mm long (for fixing the angle bars N on to the plates F).

**V<sub>10</sub>** (Fig. 5.16; two). Hexagonal head bolts with nuts and washers; 16-mm dia., 30-mm long (for fixing M on to N).

**V<sub>11</sub>** (Fig. 5.19; four). Hexagonal head bolts; 6.4-mm dia., 11-mm long (for fixing the TM(S) on to the hooks P).

**Y** (Fig. 5.22; one). Varnished hardwood block of width  $L_{20}$  defined in Table 5.1, length 294 mm, and thickness 50 mm.

**Z** (Fig. 5.22; one). Varnished wooden box for storing the spacers, links, screws, etc when not in use.

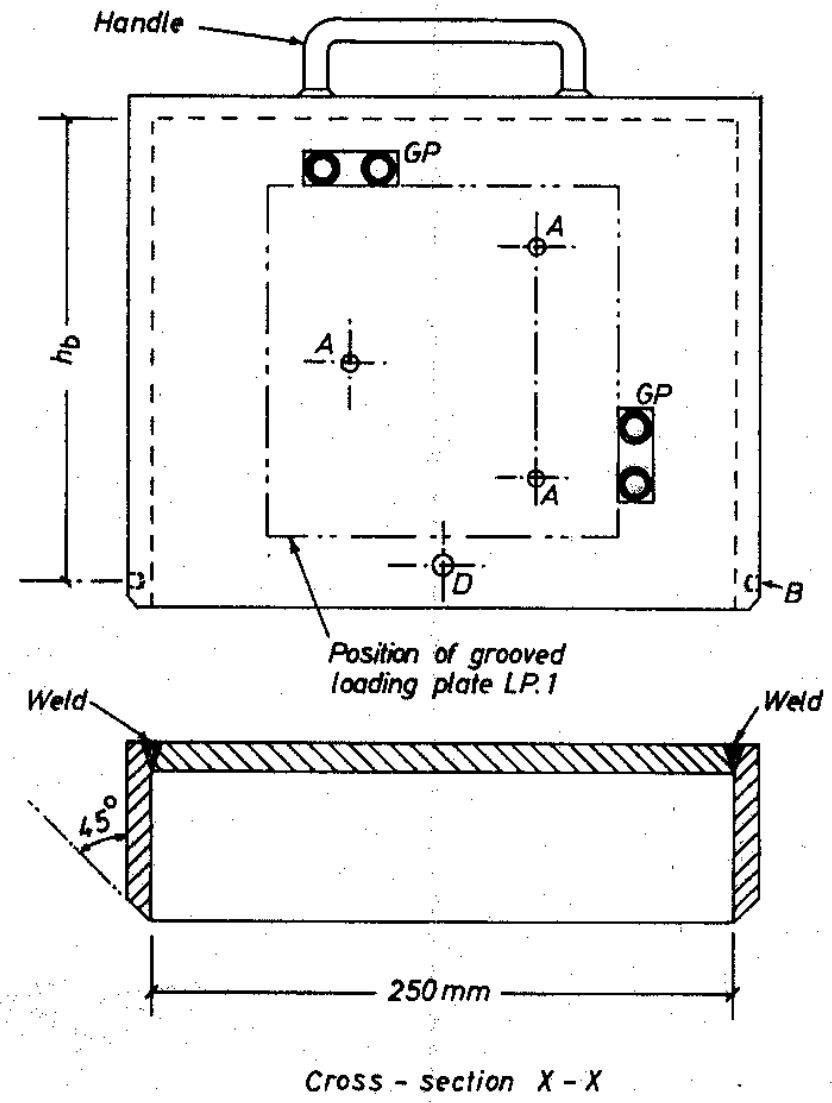
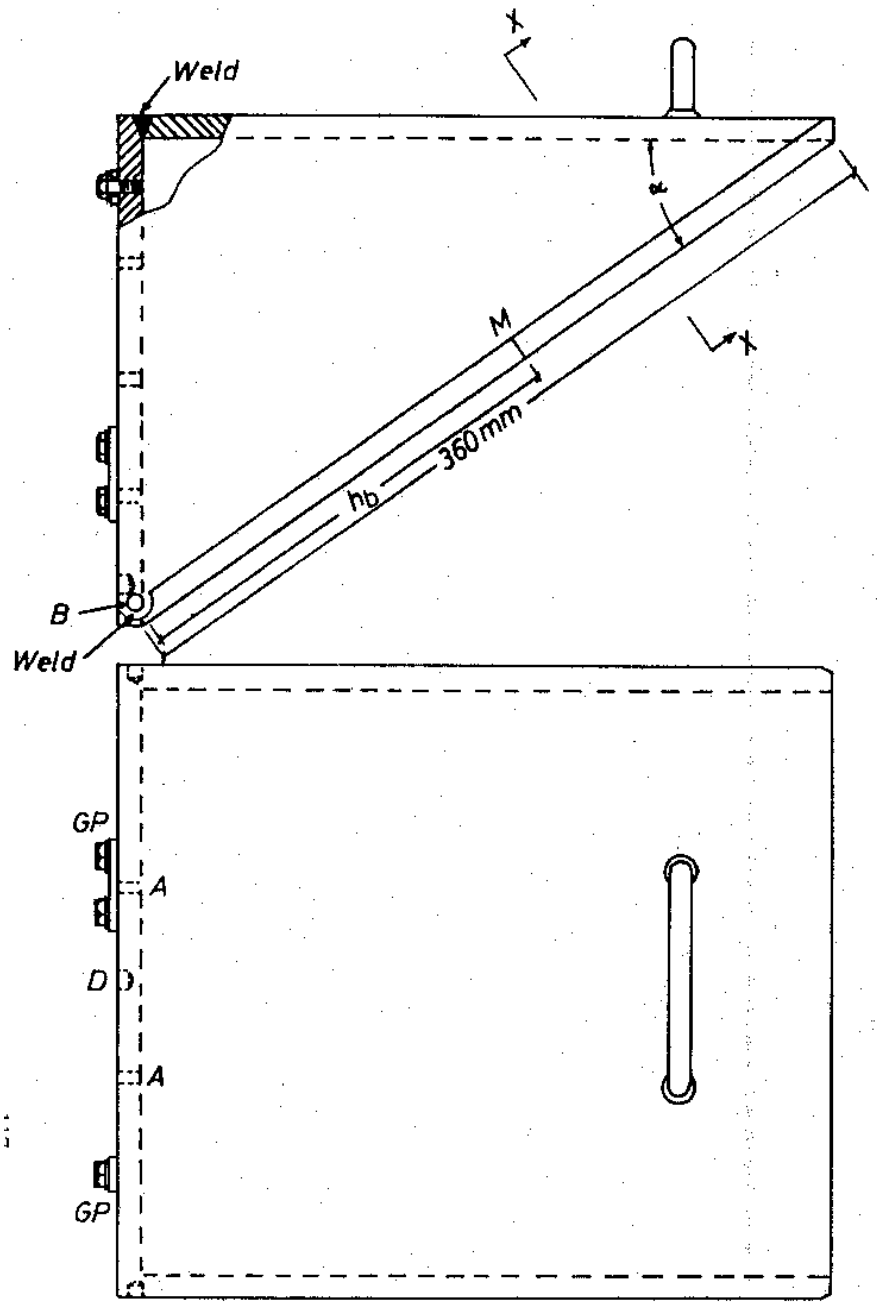


Fig. 5.1. Test mould used in iswests (after Mirata, 1976)

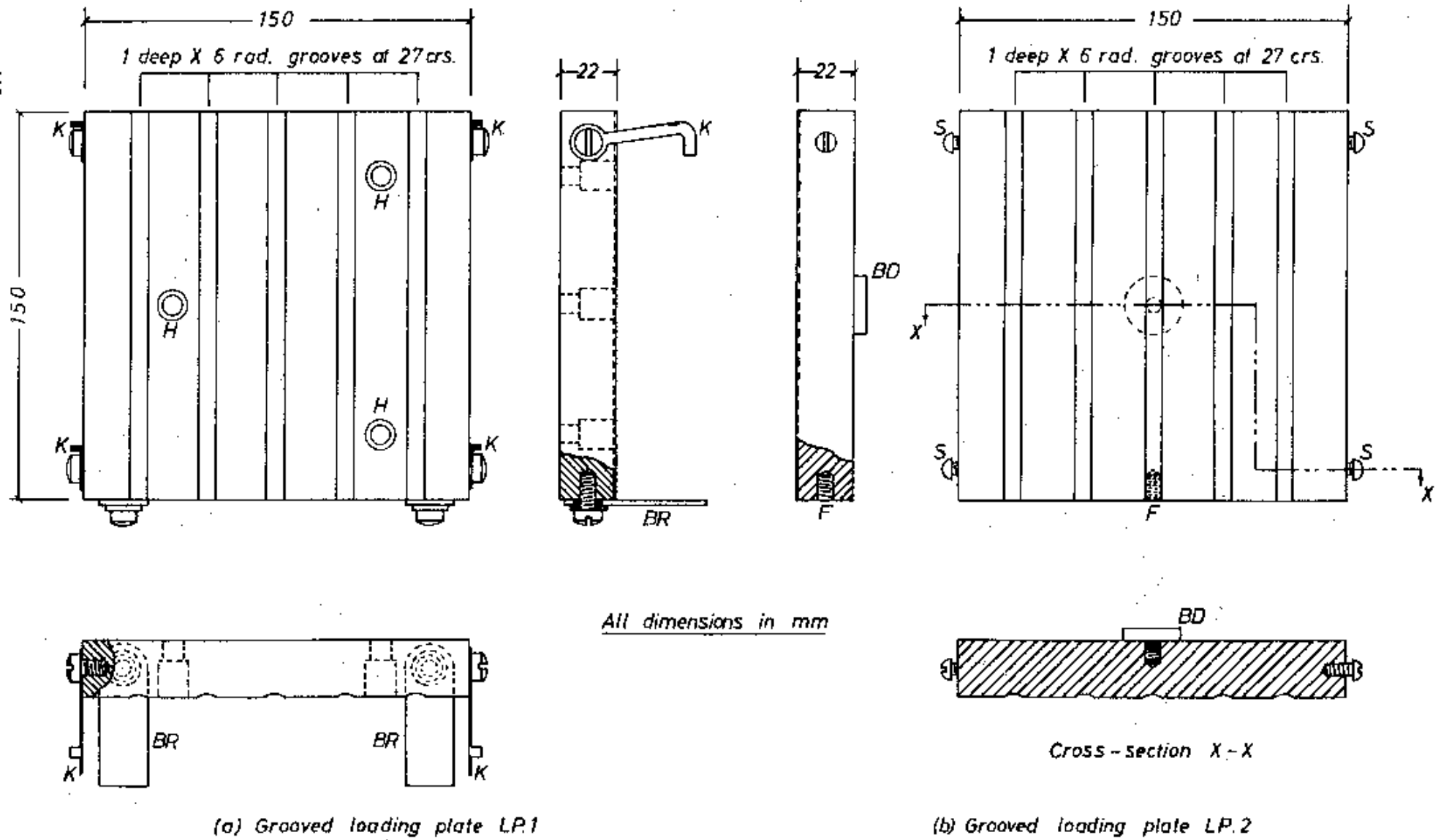


Fig. 5.2. Details of grooved loading plates suitable for iswests and cylwests (after Mirata, 1976)

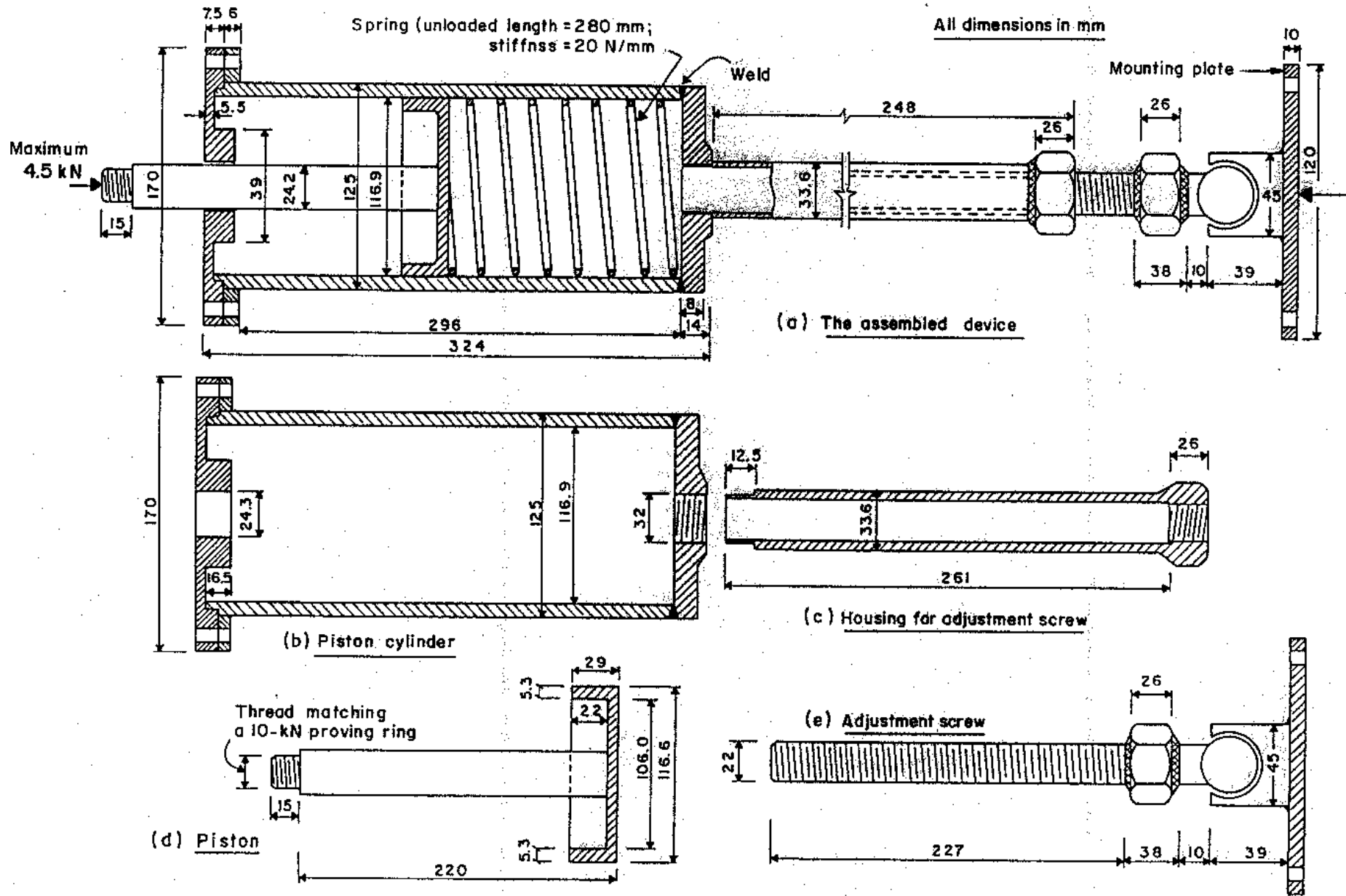


Fig. 5.3. Details of the spring loaded piston used for lateral load application in iswests or priswests (after Aybak, 1988)

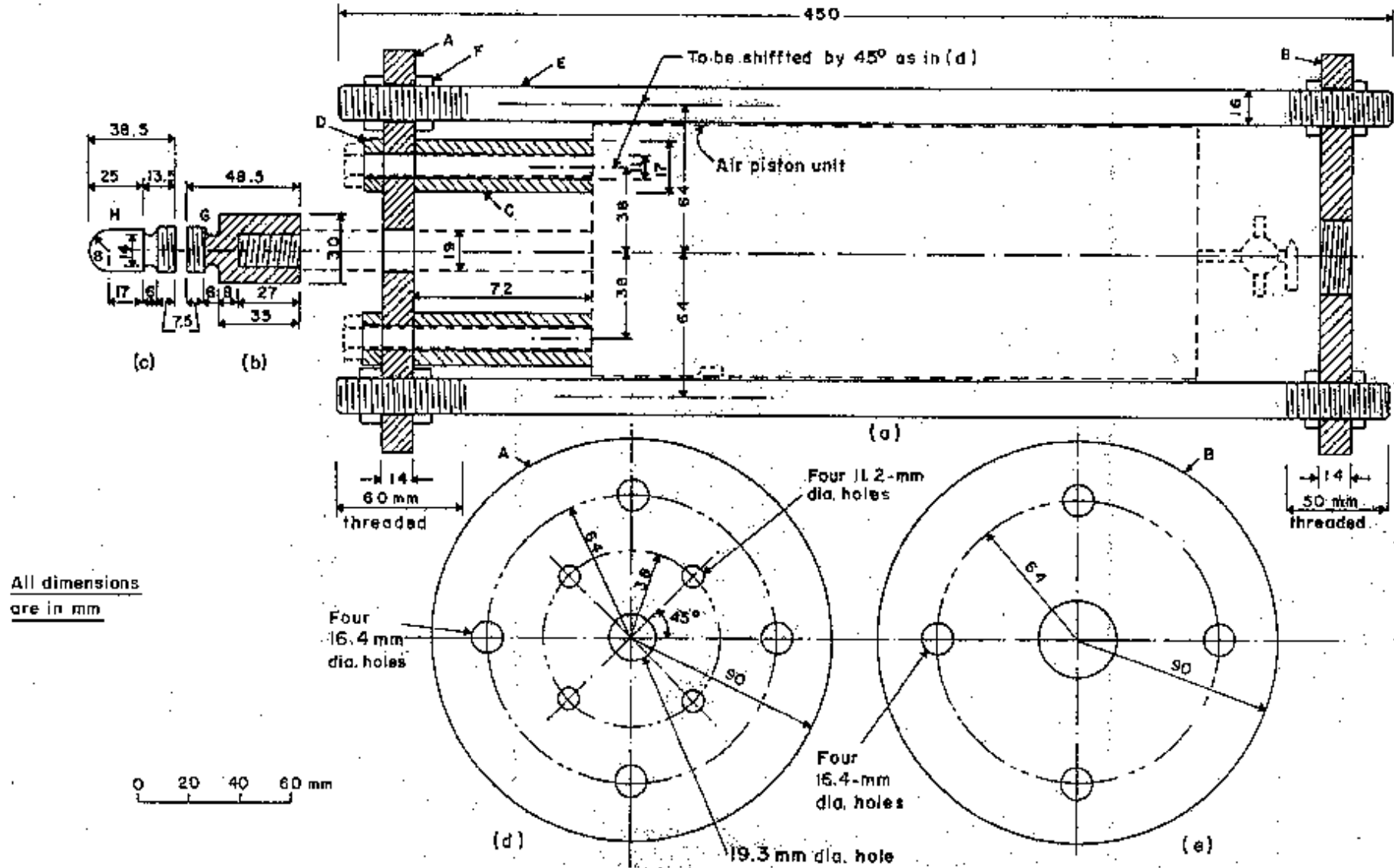
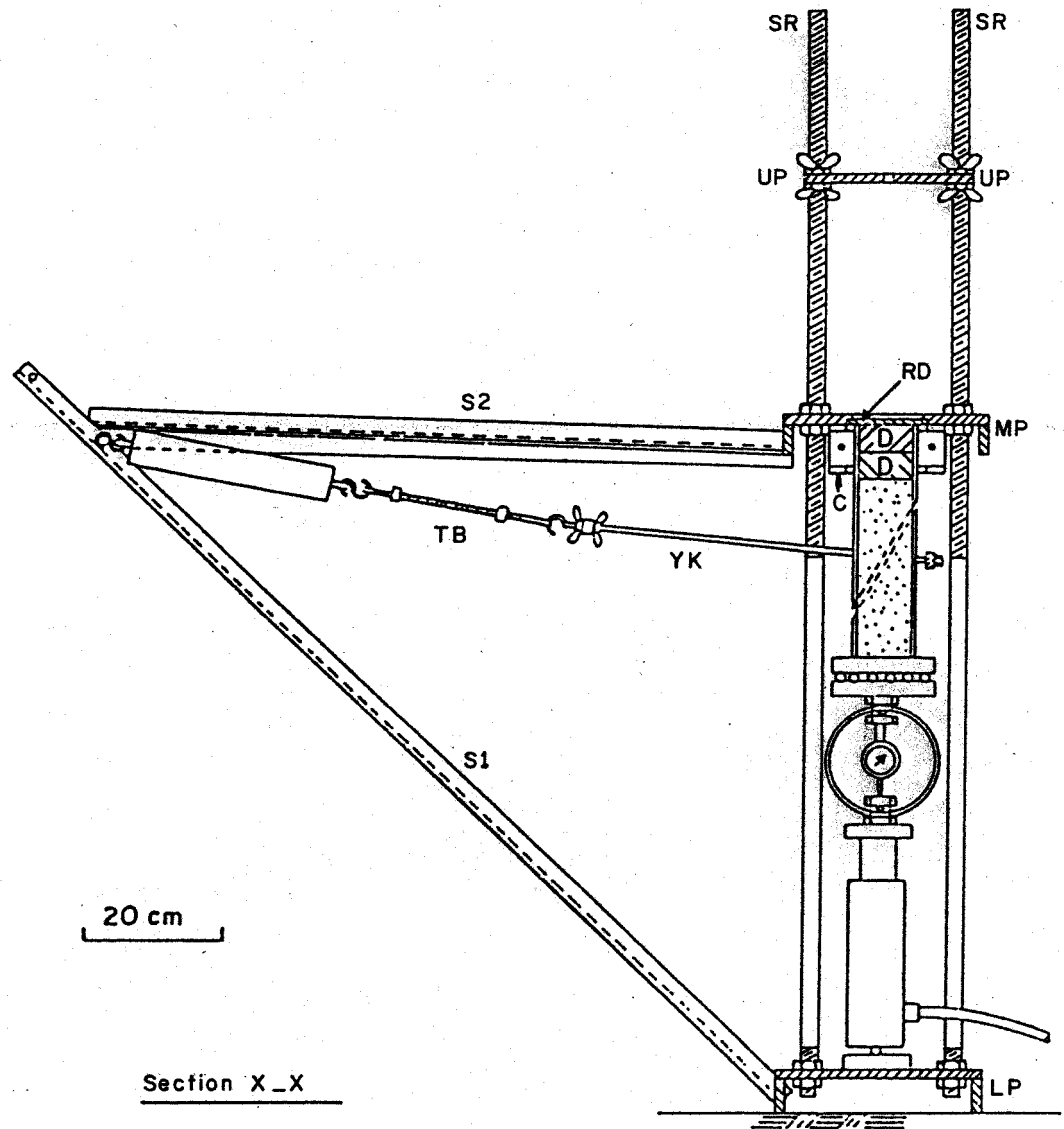


Fig. 5.4. Components for adapting an available air piston for use in place of those in Fig. 5.3(b) and (d)





All dimensions in mm

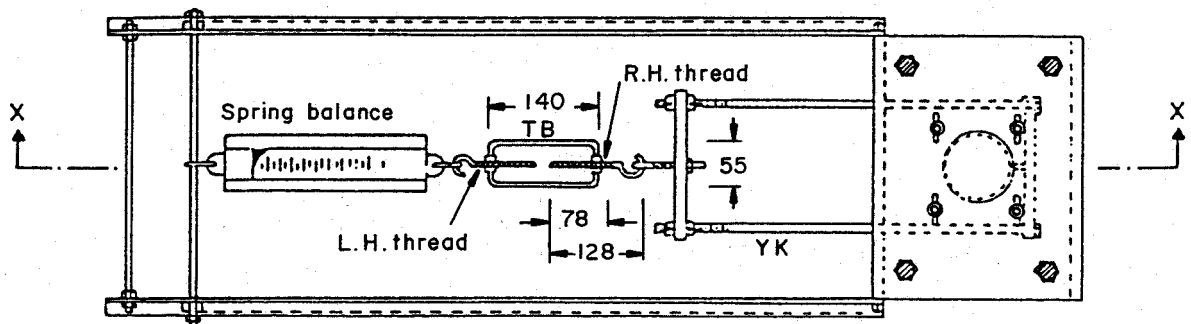


Fig. 5.5. Set-up for performing a cylwast using a portable frame

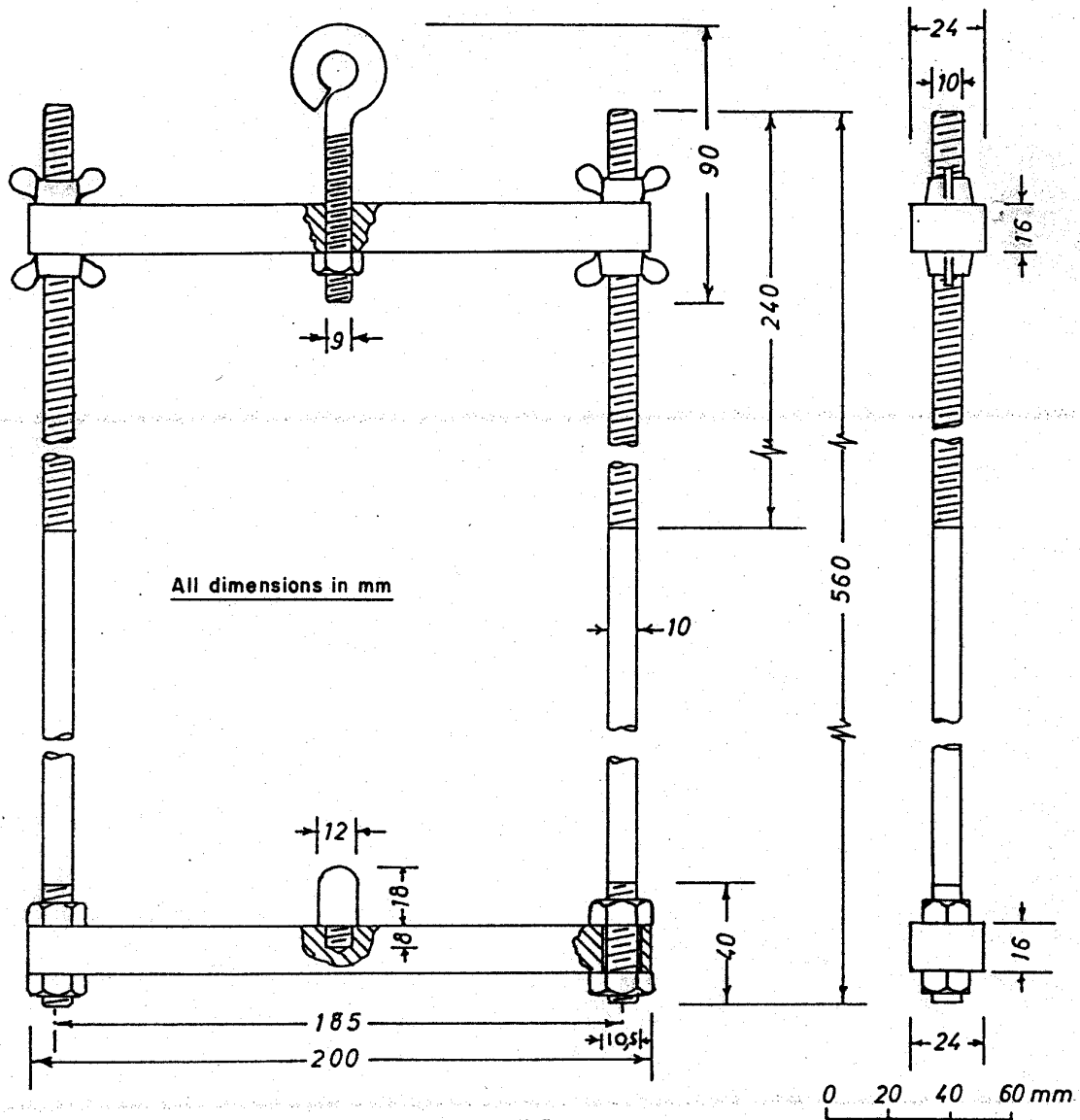


Fig. 5.6. Details of the yoke YK in Fig. 5.5

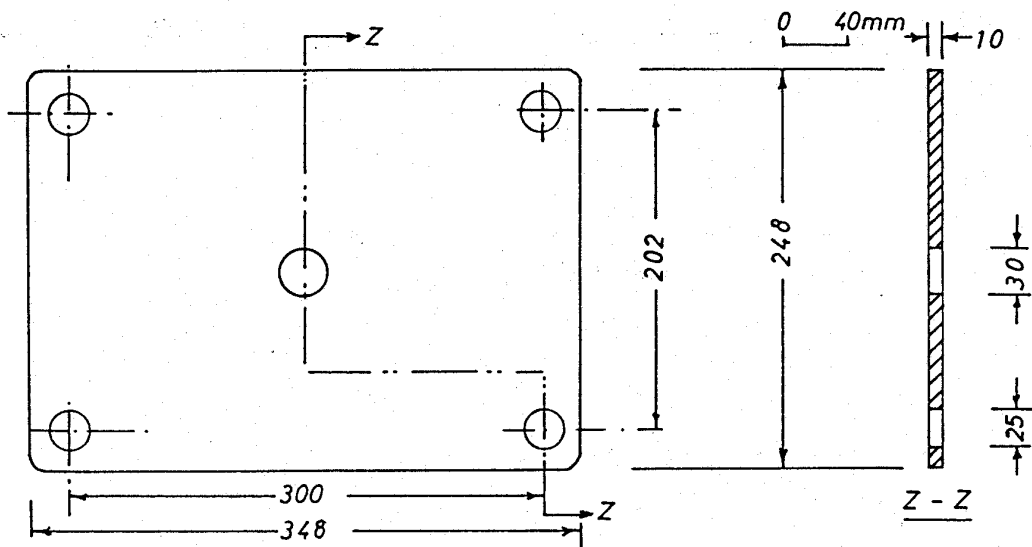


Fig. 5.7. Upper plate UP in Fig. 5.5

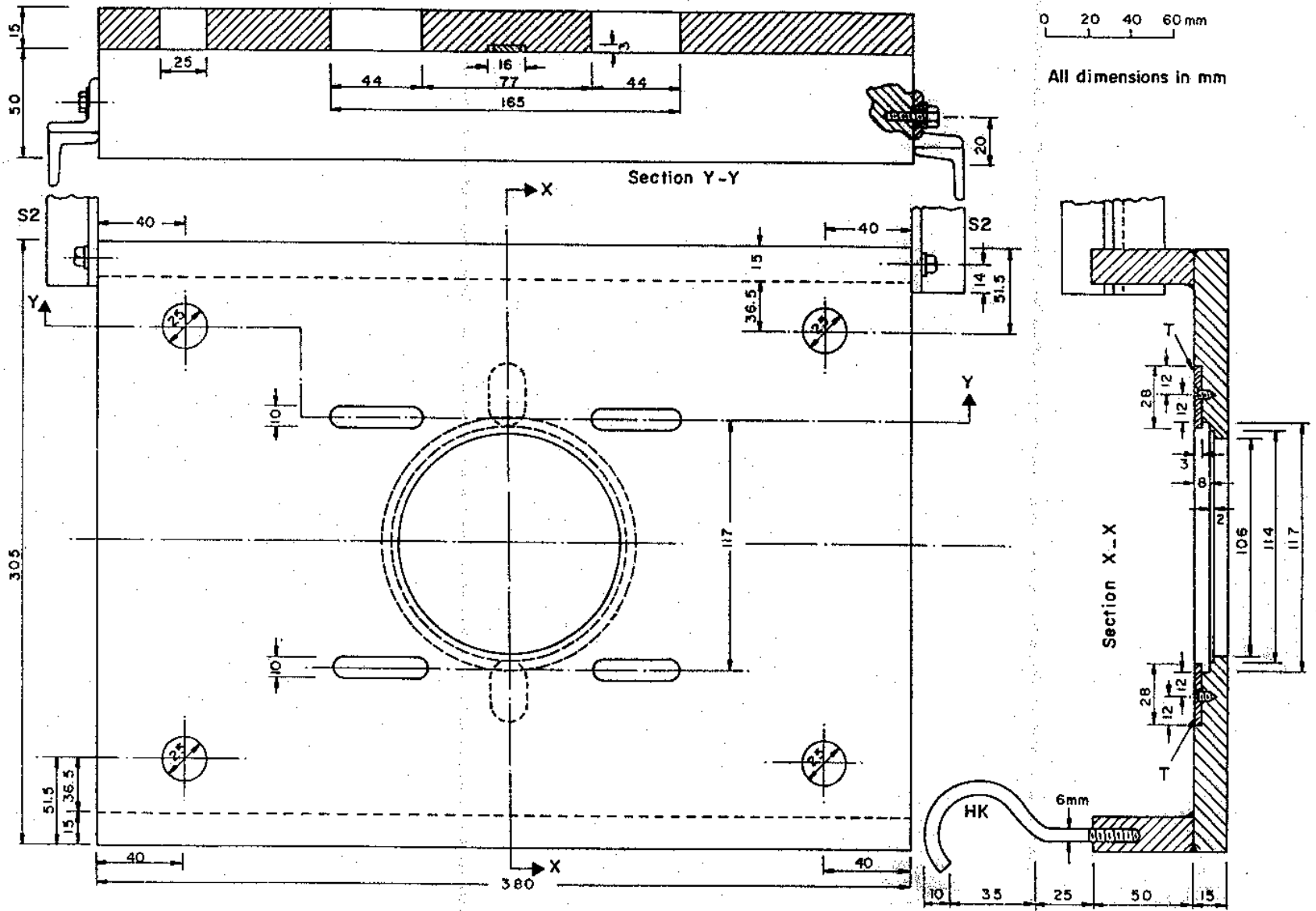


Fig. 5.8. Details of the middle plate MP in Fig. 5.5

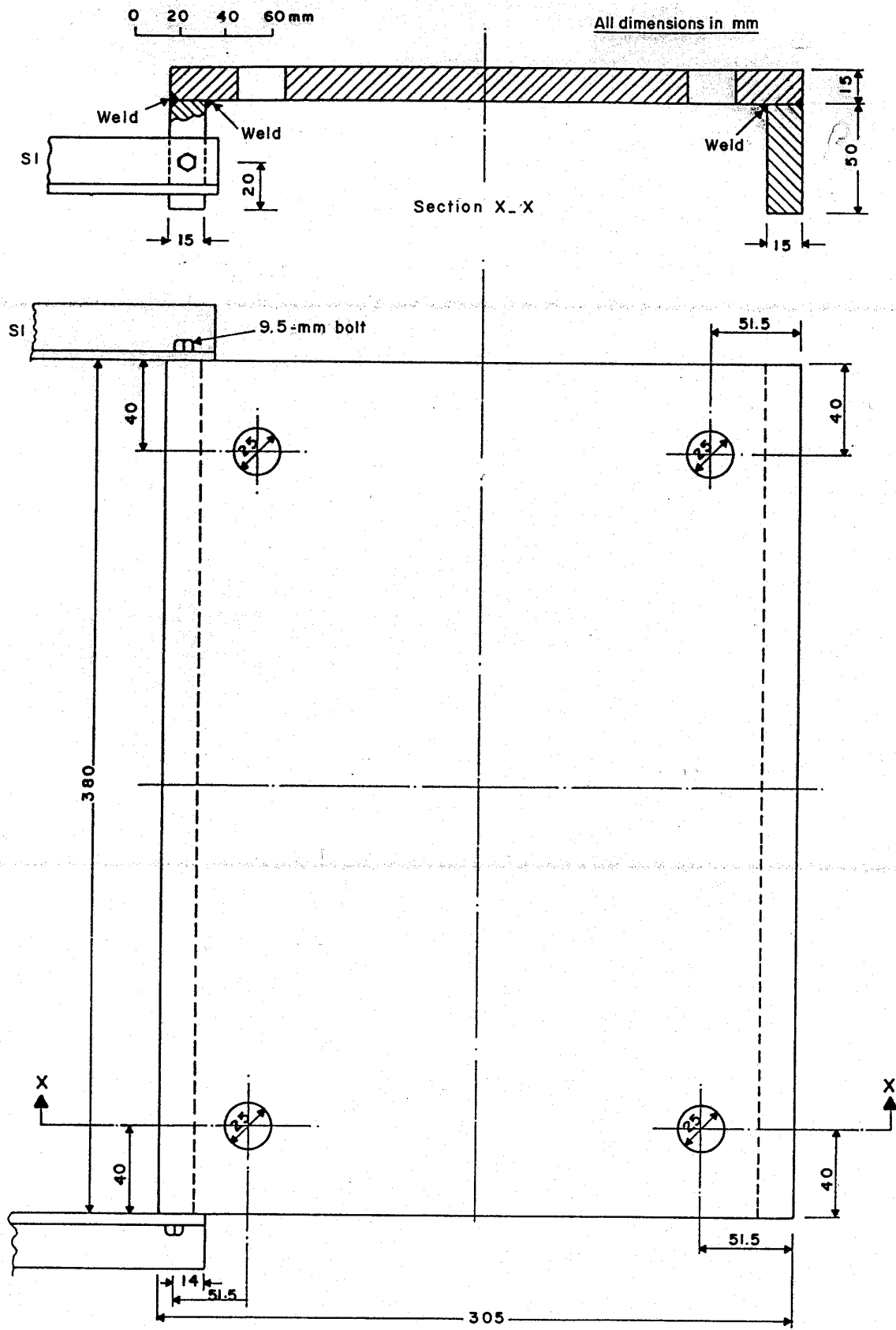
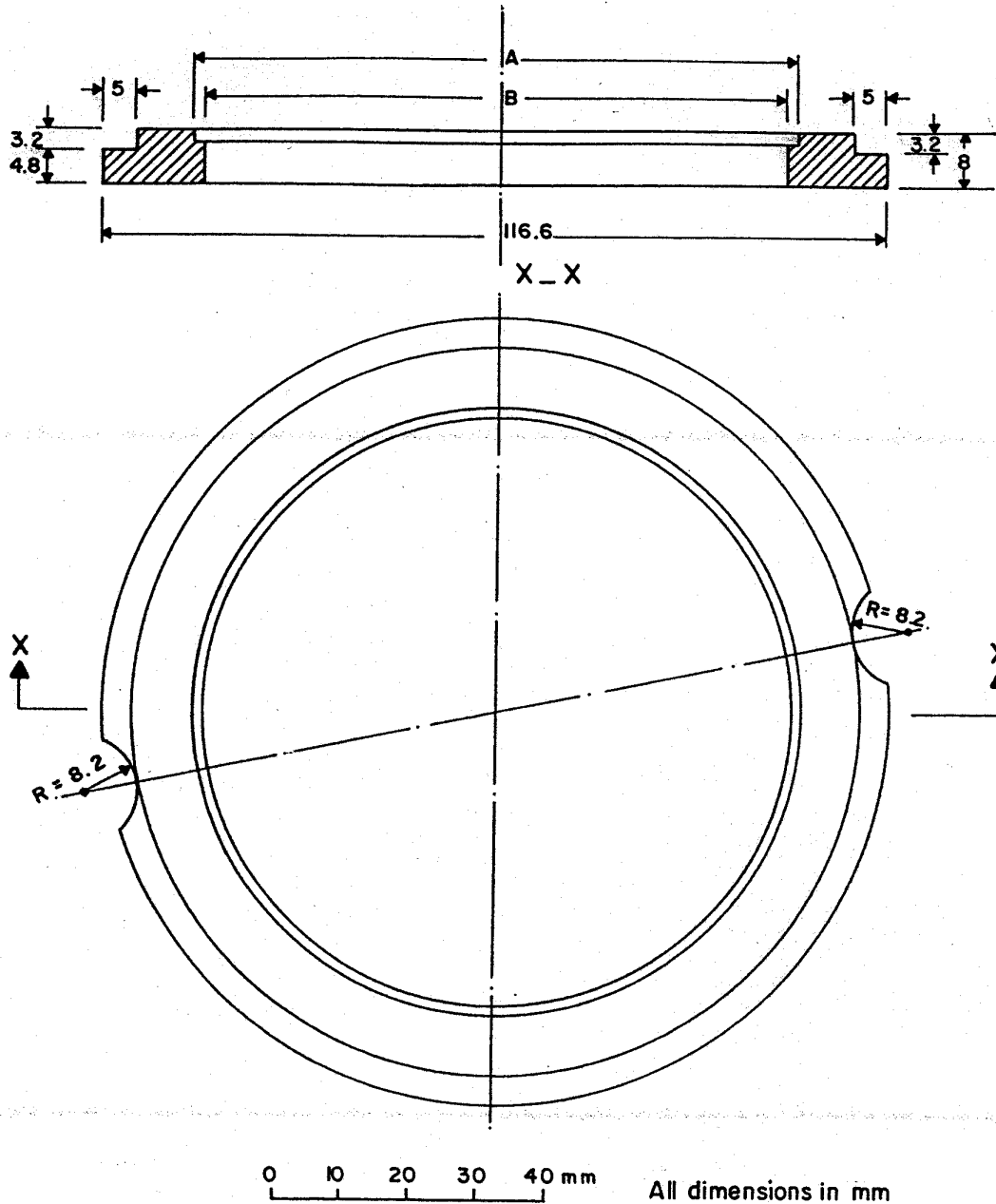


Fig. 5.9. Details of the lower plate LP in Fig. 5.5



#### VARIABLE DIMENSIONS

Number required	A (mm)	B (mm)	Remarks
1	102.7	95.5	Example
1	90.3	86.6	Example
1	0	0	Solid disc
1	Outside dia. of sampling tube+1mm	Inside dia. of sampling tube+1mm	In general

**Fig. 5.10.** The removable disc RD in Fig. 5.5 and typical rings to replace this during sample extrusion

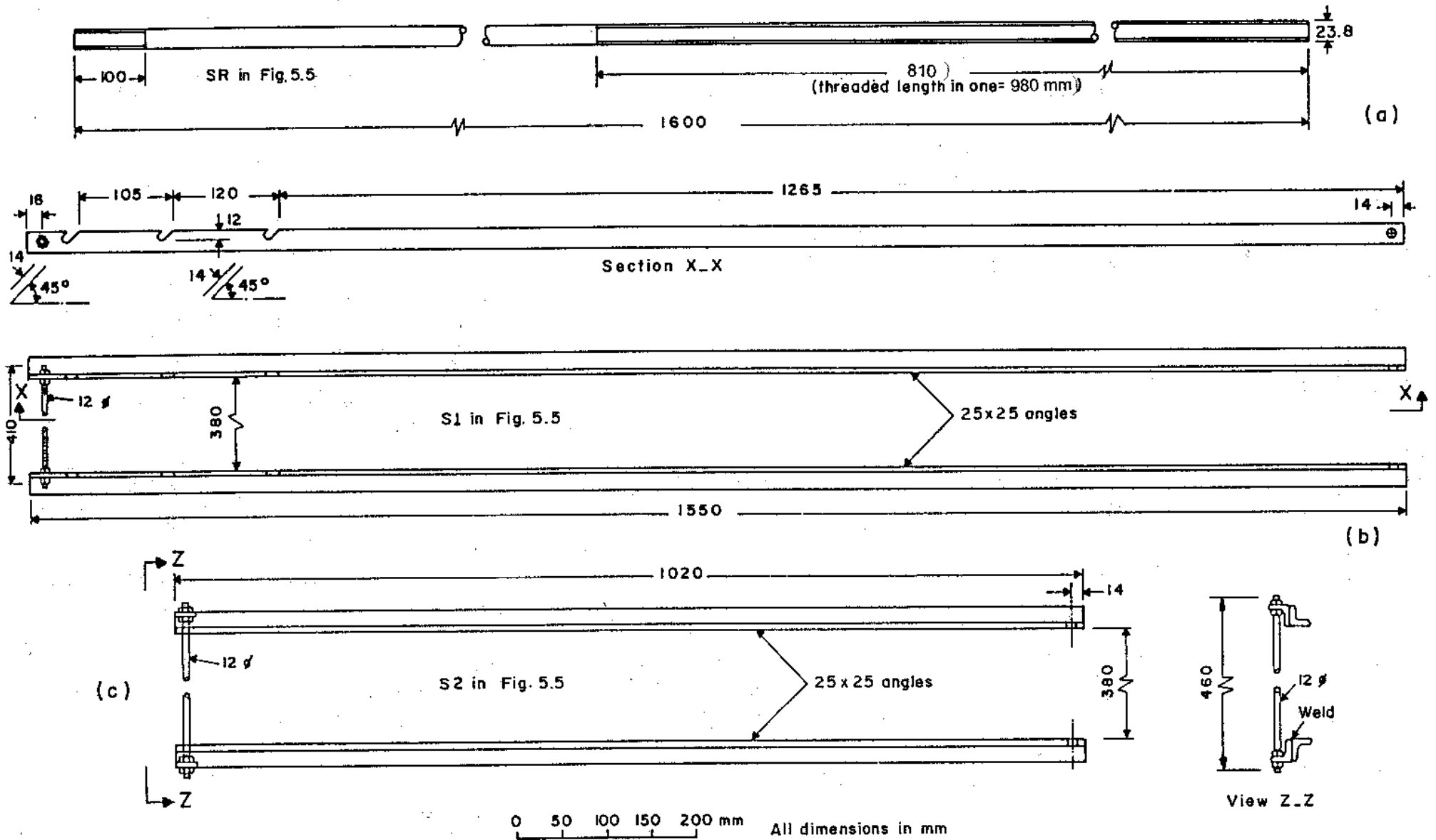


Fig. 5.11. Details of (a) strain rods SR, (b) lateral support S1, and (c) lateral support S2

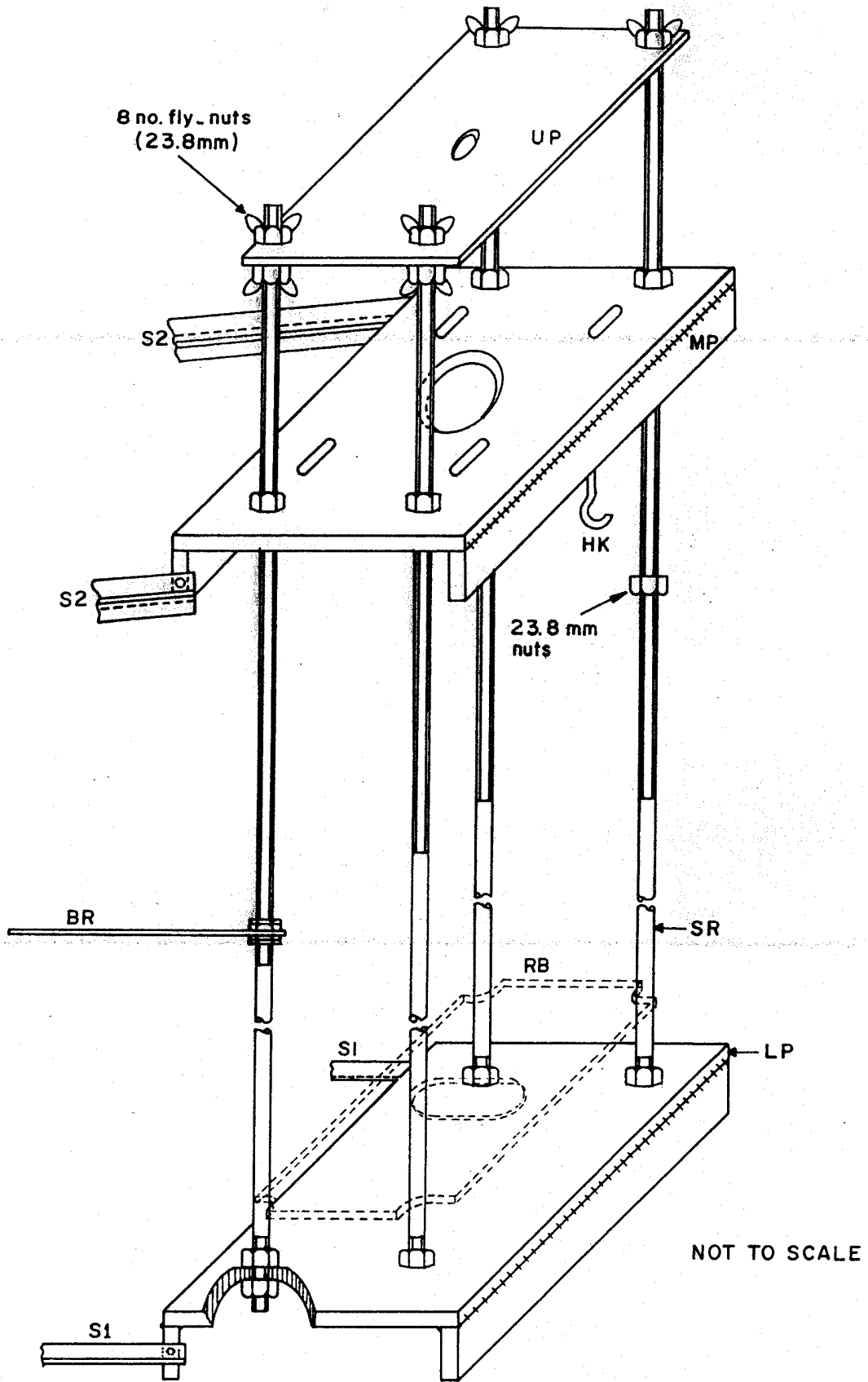
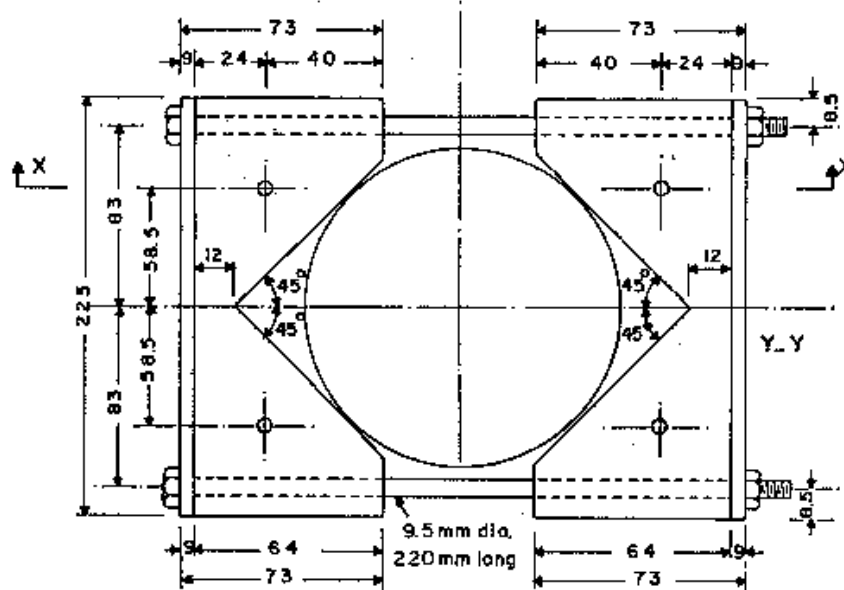
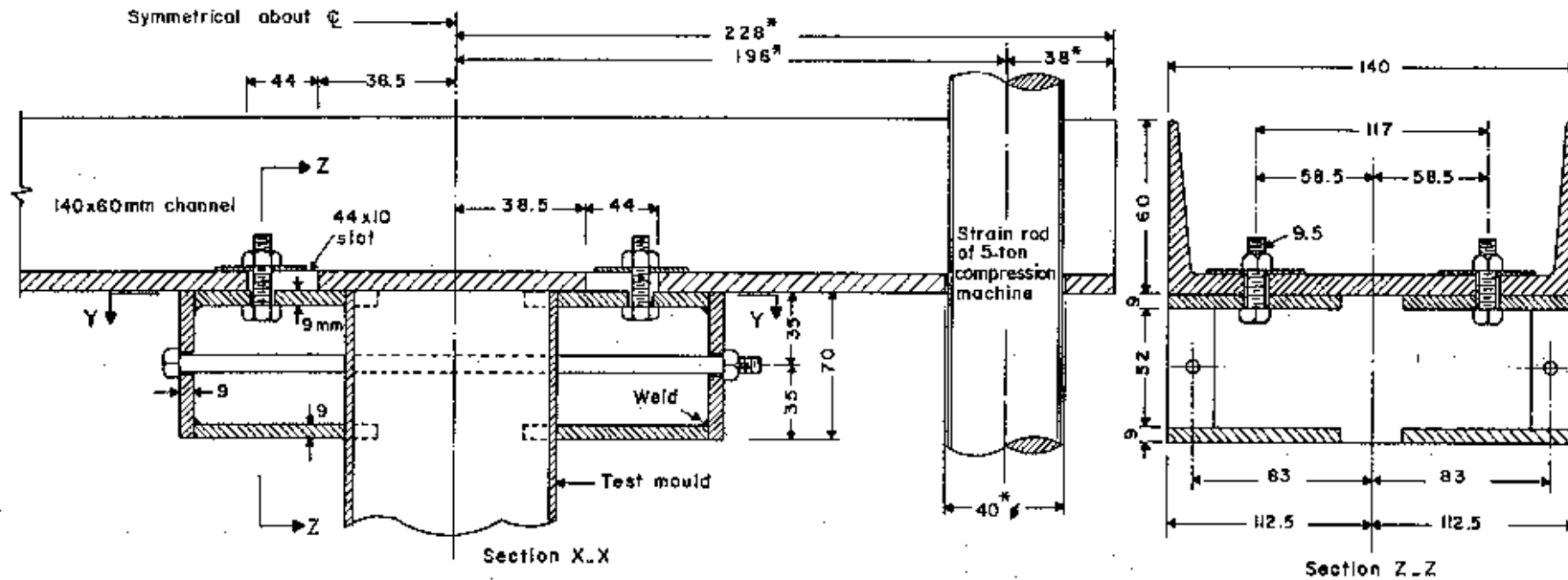


Fig. 5.12. Isometric view of the portable frame shown in Fig. 5.5



\* To be varied to suit the spacing between the strain rods of the available compression machine.

All dimensions in mm (NOT TO SCALE)

All bolts 9.5 mm in dia.; holes for these 10.5 mm in dia.

Fig. 5.13. Details of the clamp C in Fig. 5.5 and the channel for replacing the upper cross-beam of an existing compression machine to adapt this for cylwests



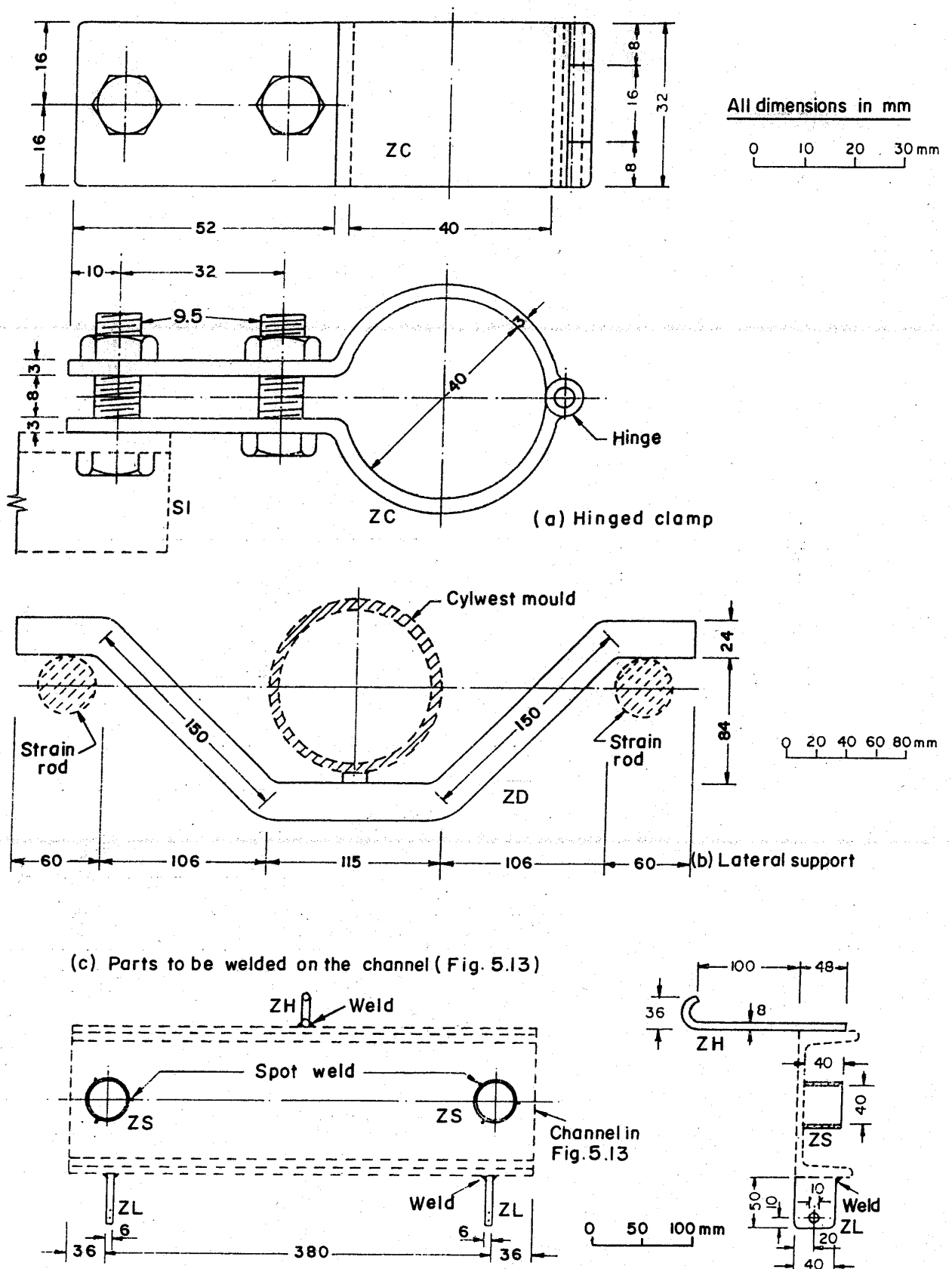


Fig. 5.14. Additional components needed to enable lateral load to be applied in cylwests using an available compression machine

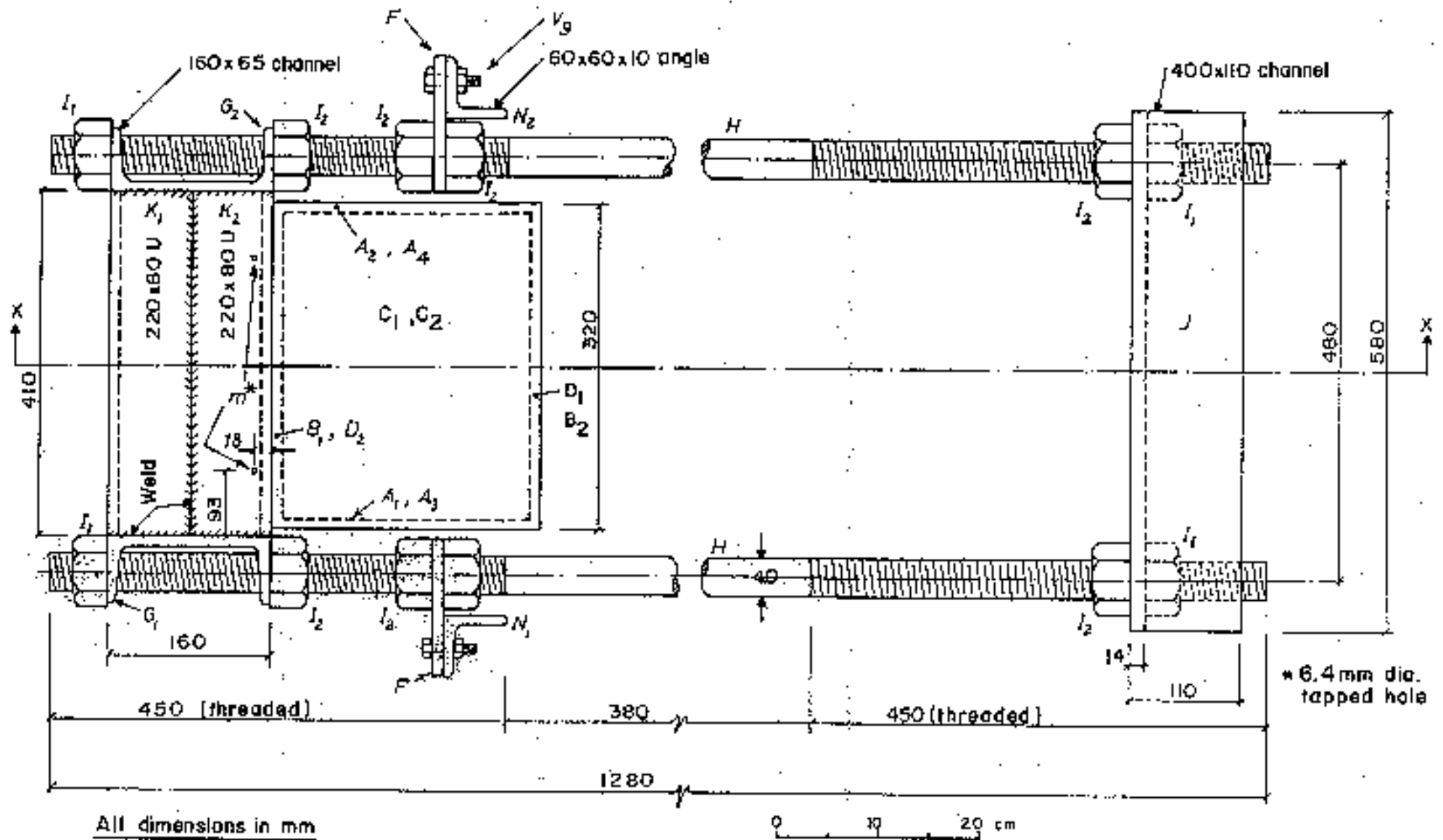


Fig. 5.15. Top view of the 20-ton loading frame for prisvests





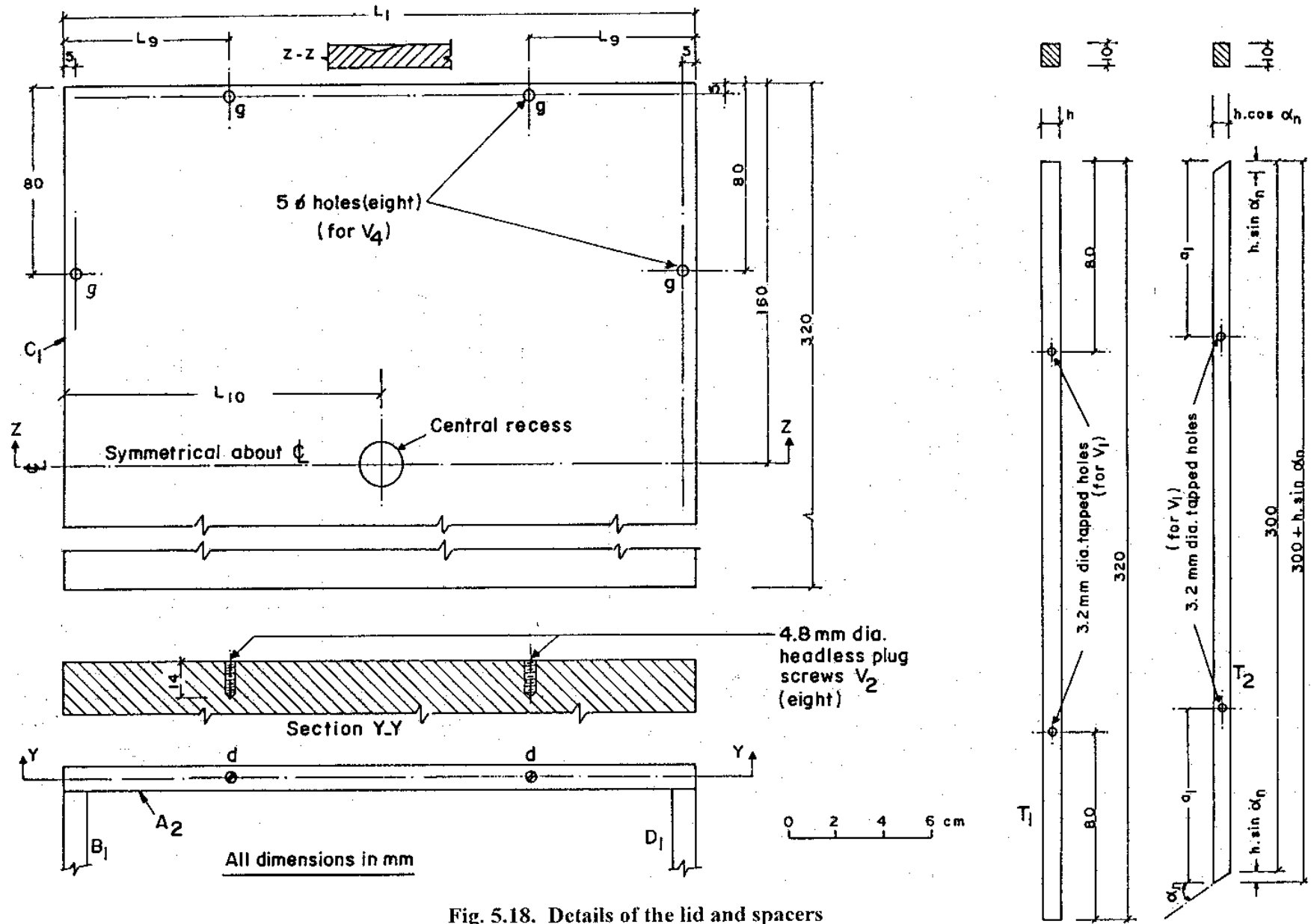


Fig. 5.18. Details of the lid and spacers

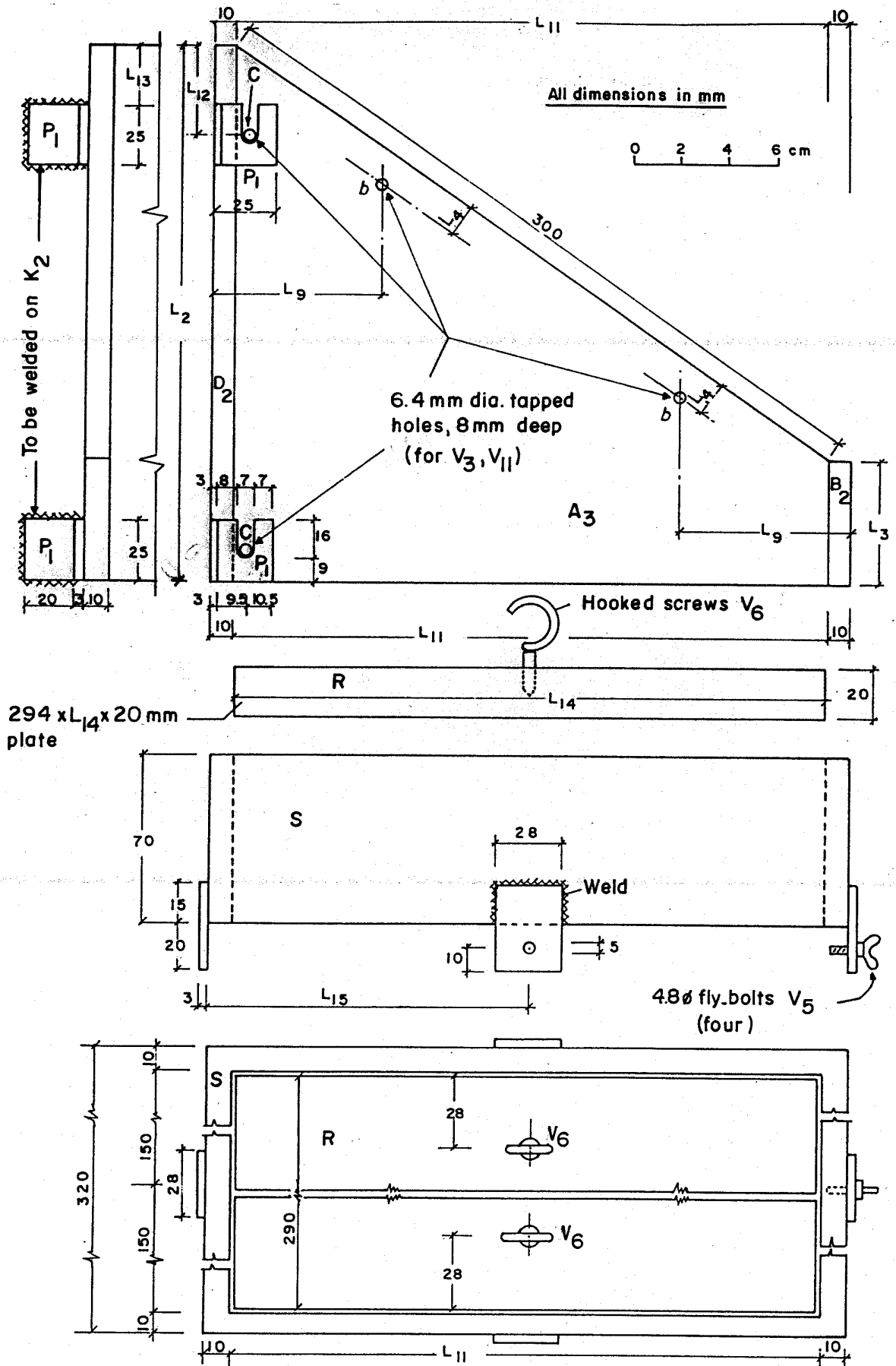
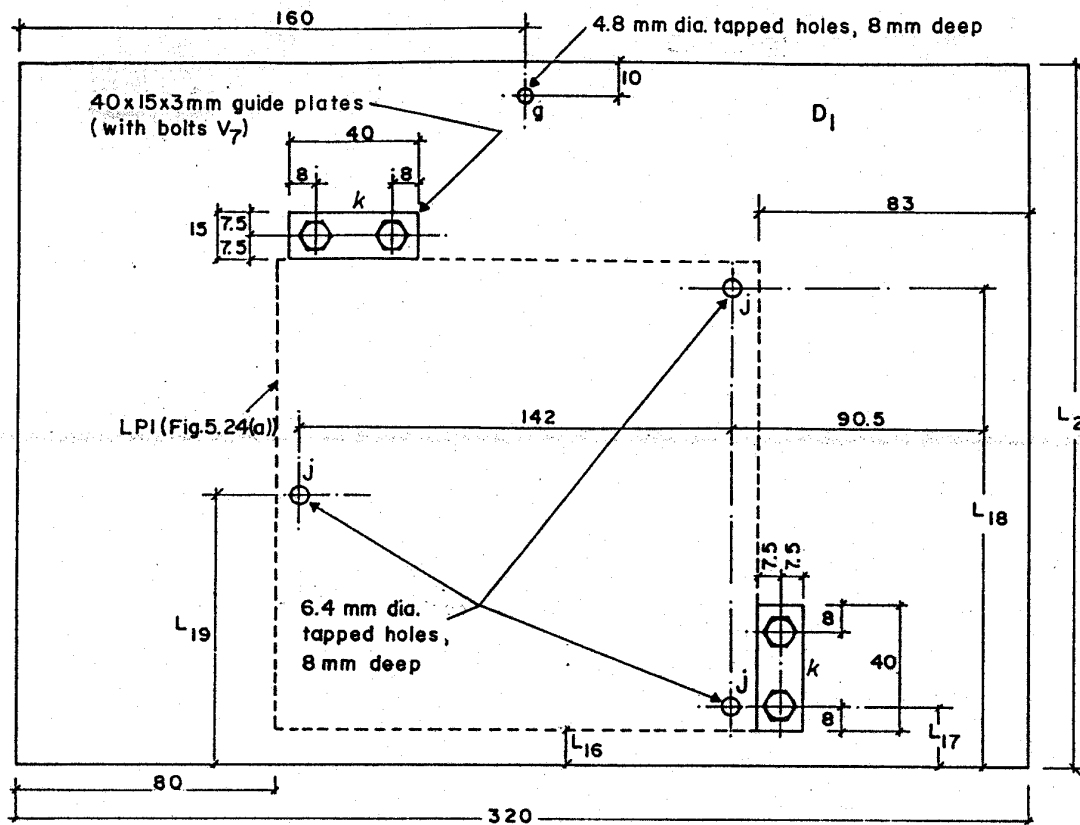


Fig. 5.19. The priswest mould, collar and compaction plate



All dimensions in mm

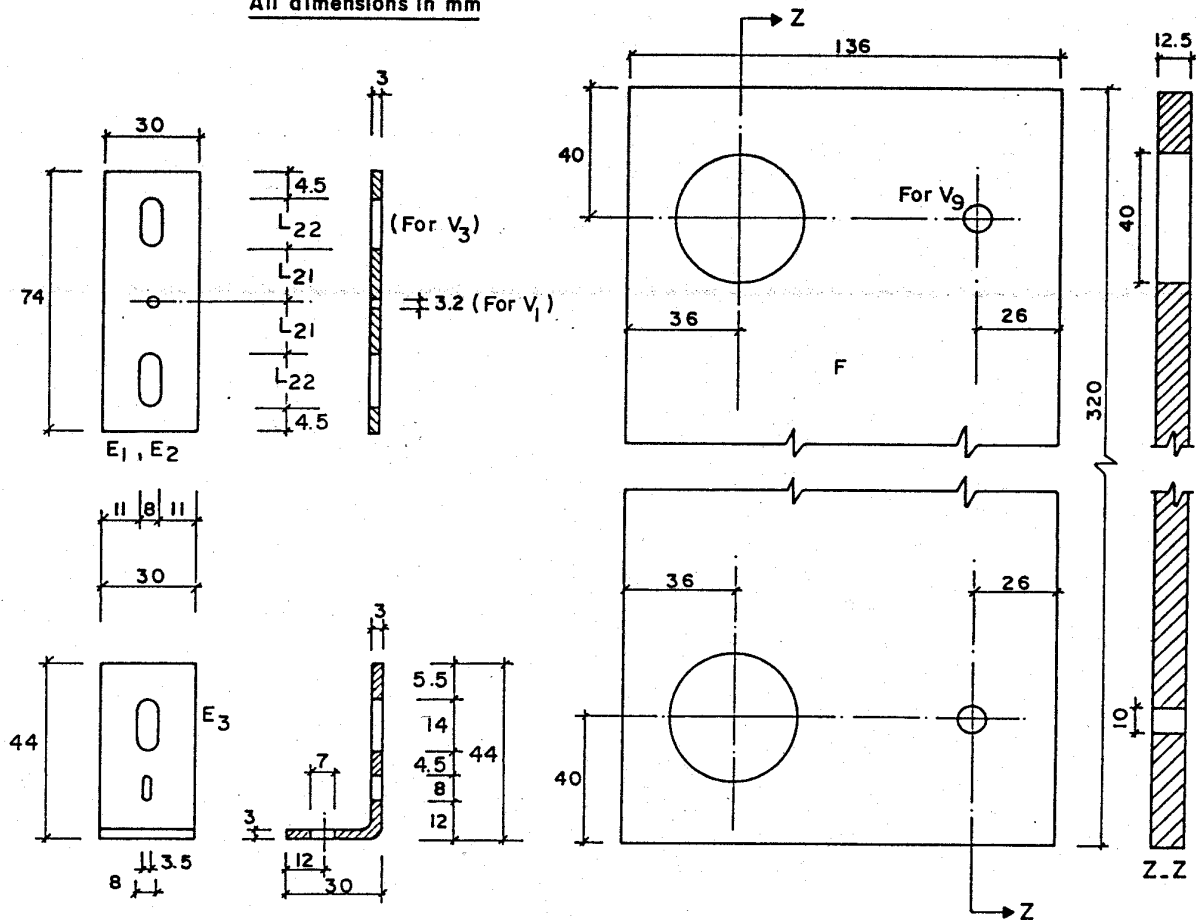
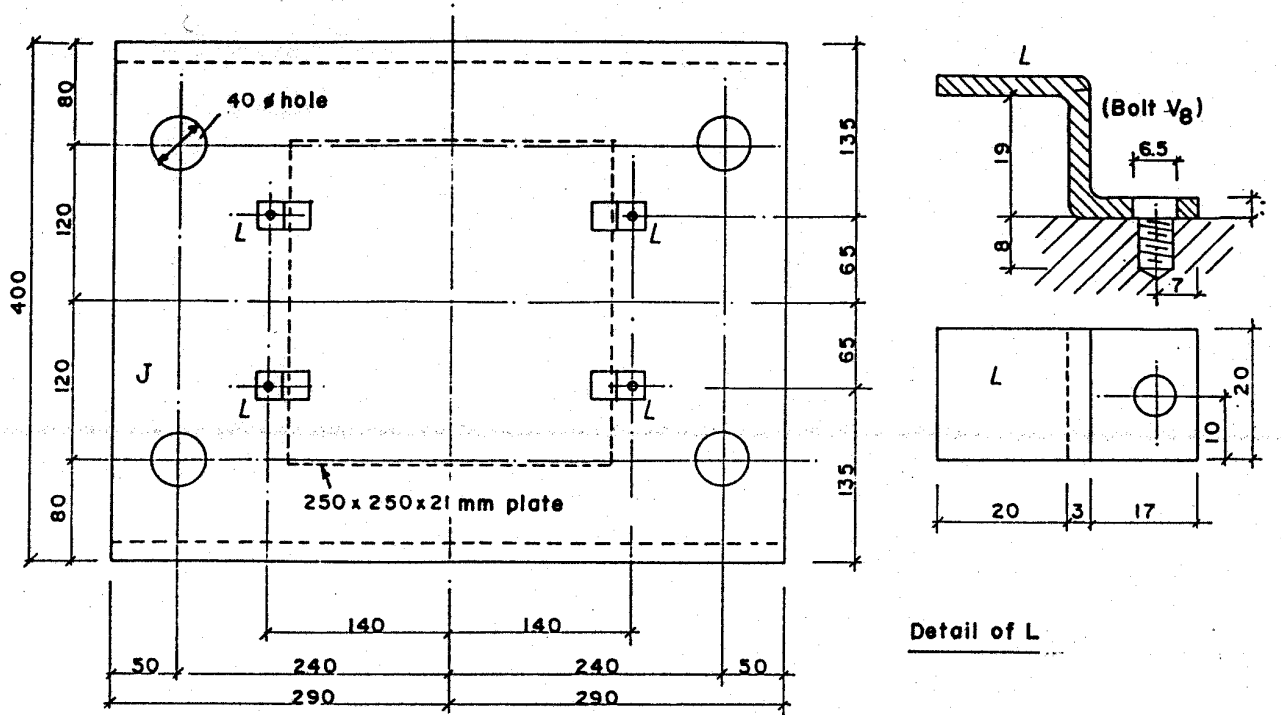


Fig. 5.20. Details of the links E, guide plates, and support plates F



Channel J viewed from left as in Fig. 5.16

All dimensions in mm

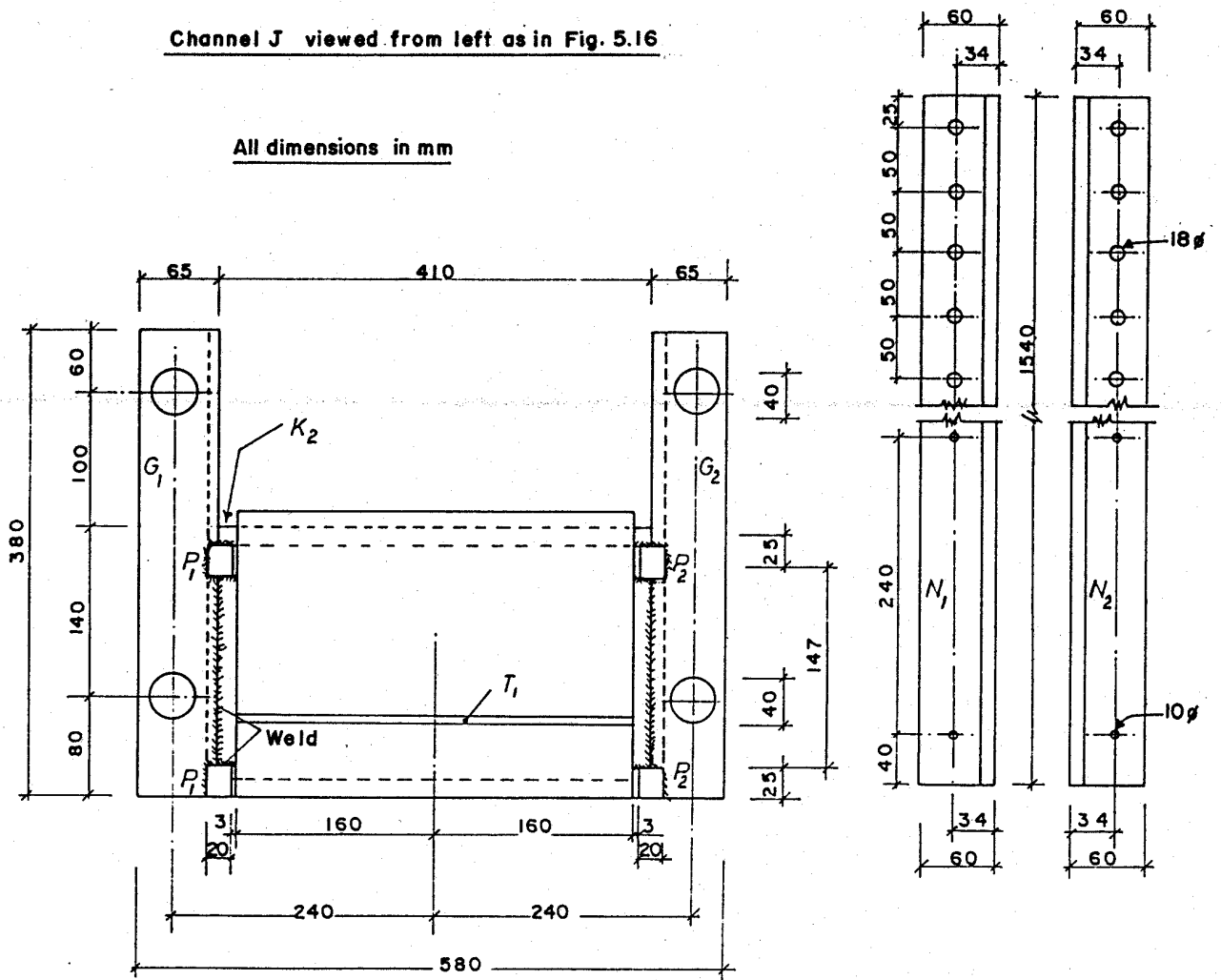


Fig. 5.21. Layout of the hooks P, details of the clamping pieces L and angles N



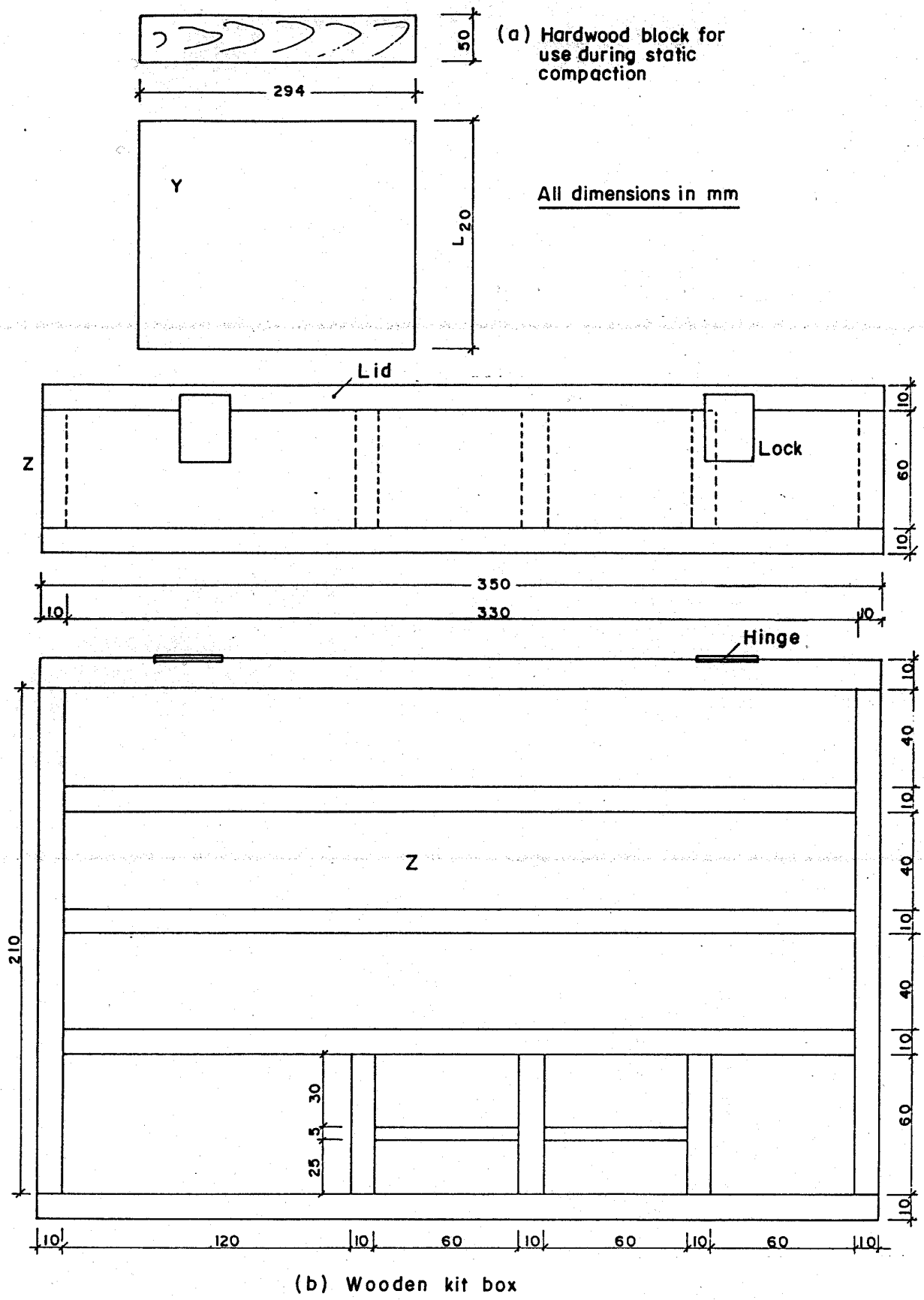
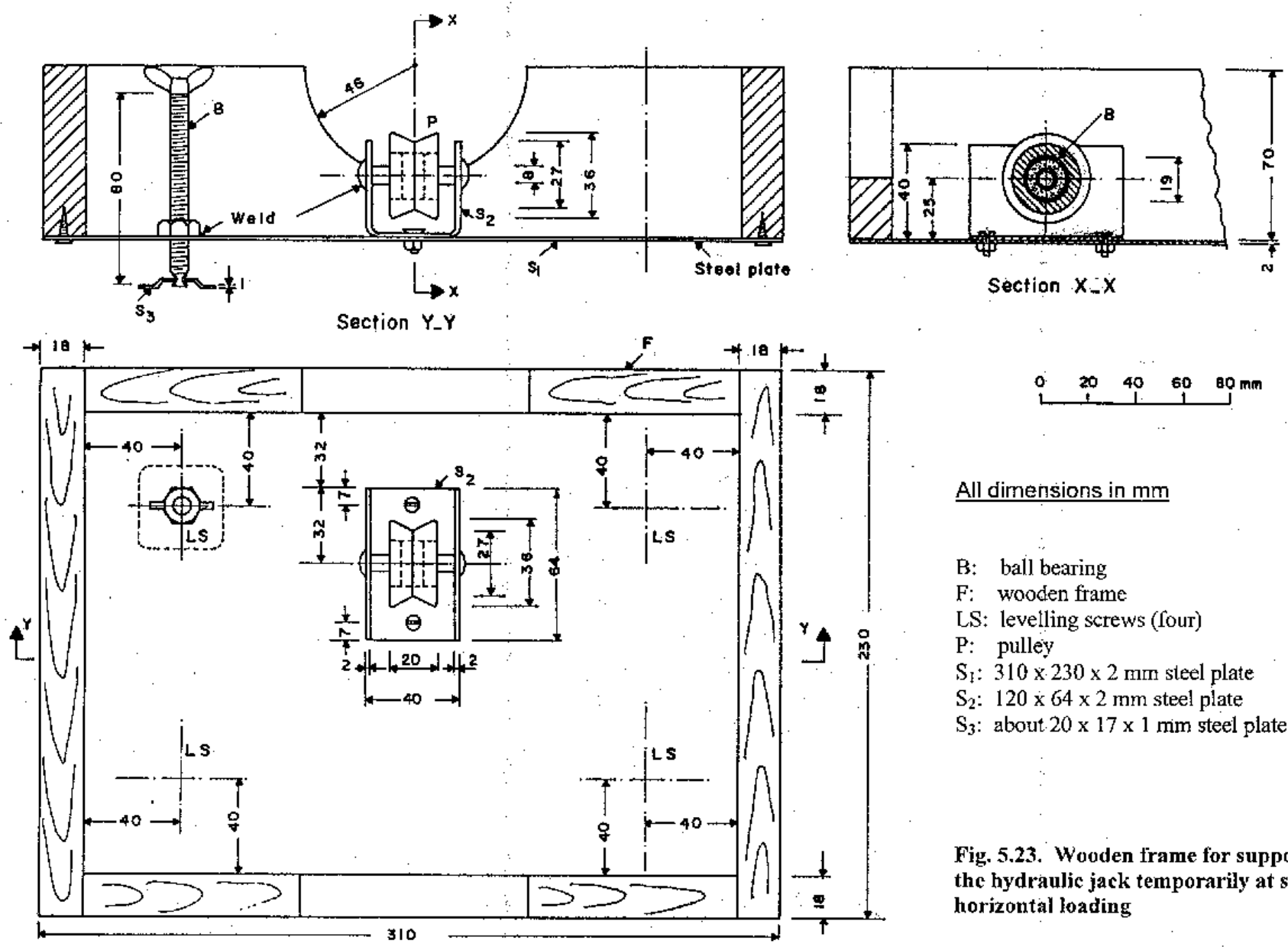


Fig. 5.22. Hardwood block Y and wooden kit box Z



All dimensions in mm

- B: ball bearing
- F: wooden frame
- LS: levelling screws (four)
- P: pulley
- S<sub>1</sub>: 310 x 230 x 2 mm steel plate
- S<sub>2</sub>: 120 x 64 x 2 mm steel plate
- S<sub>3</sub>: about 20 x 17 x 1 mm steel plate (four)

Fig. 5.23. Wooden frame for supporting the hydraulic jack temporarily at start of horizontal loading

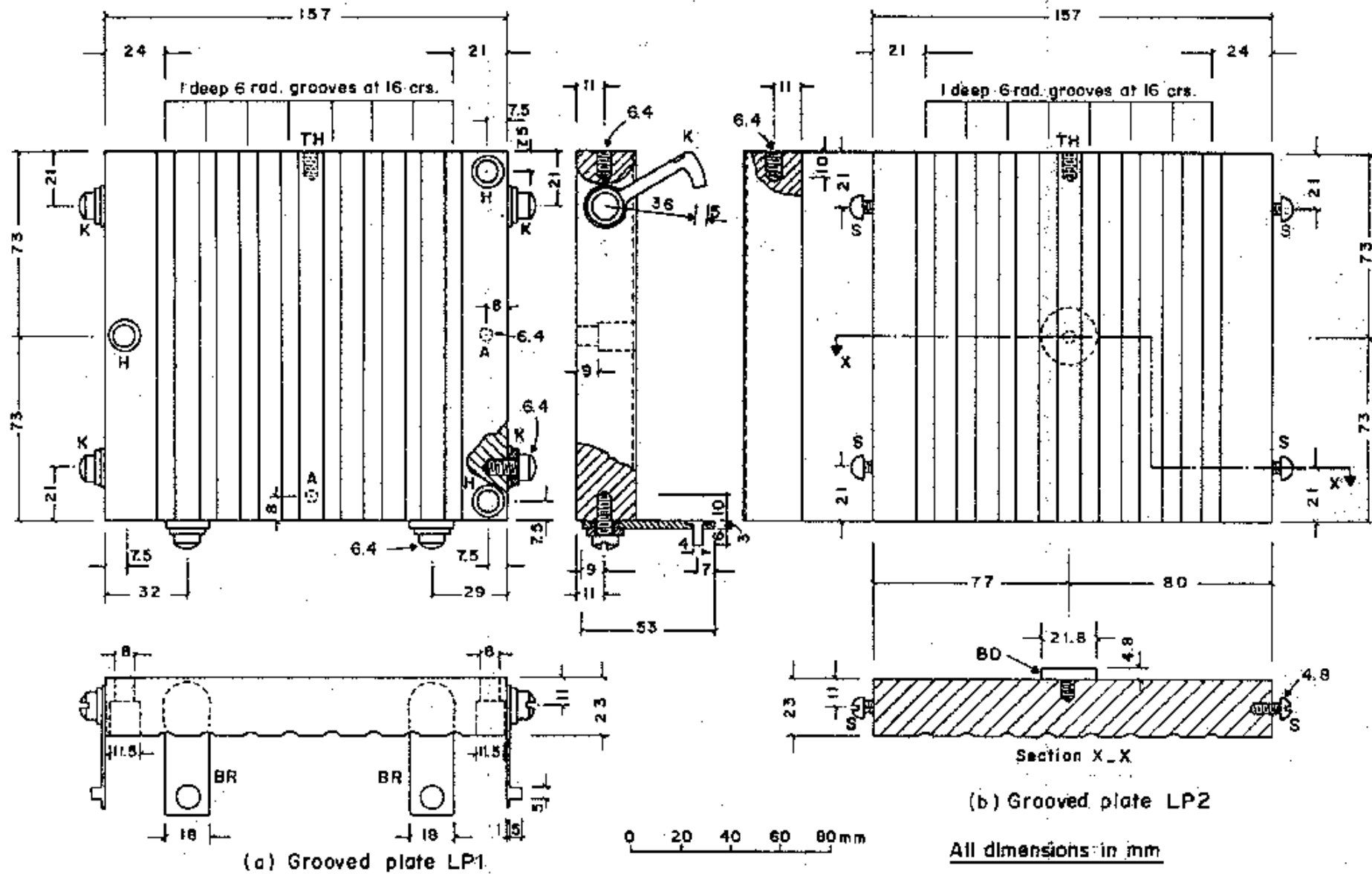
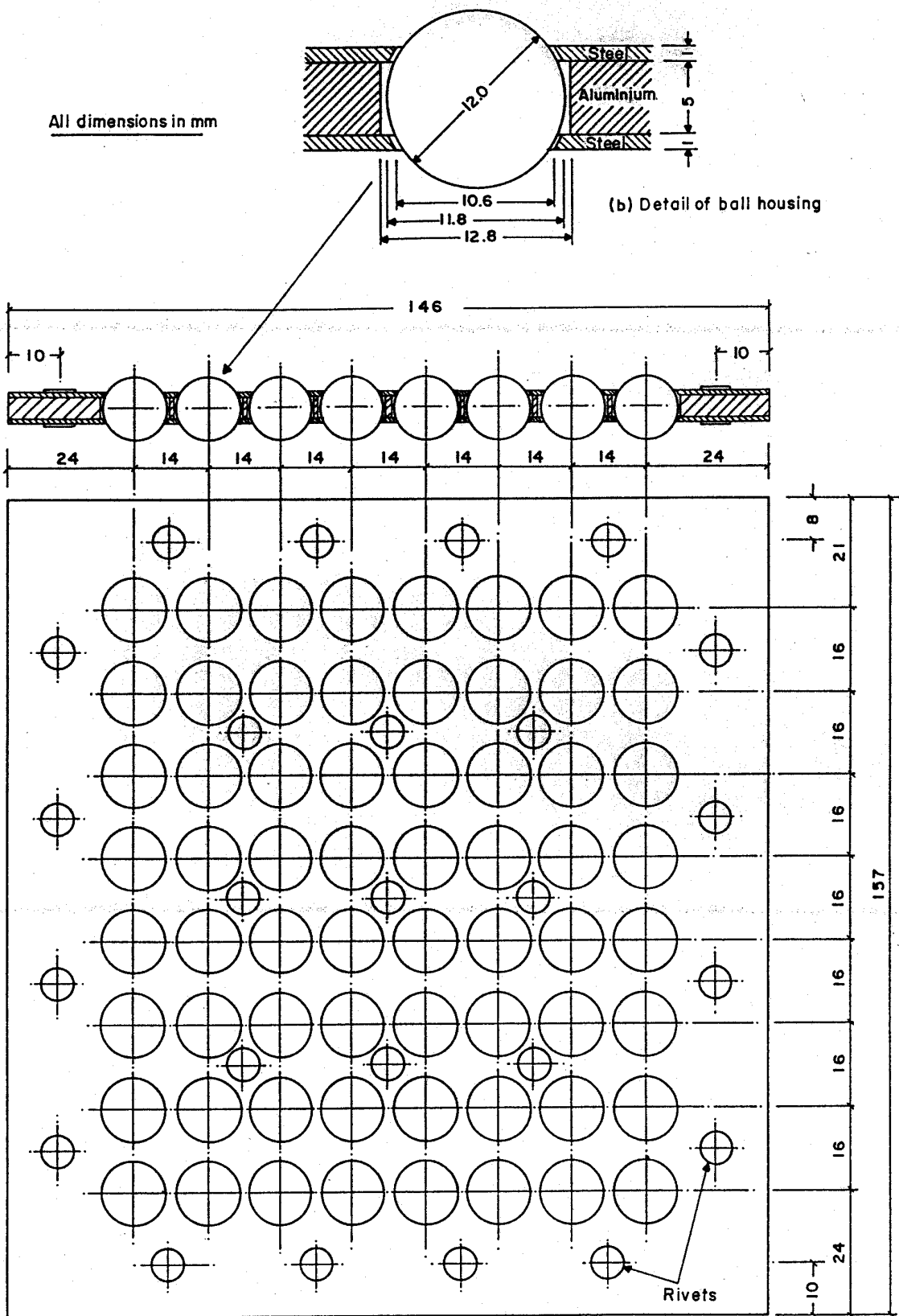
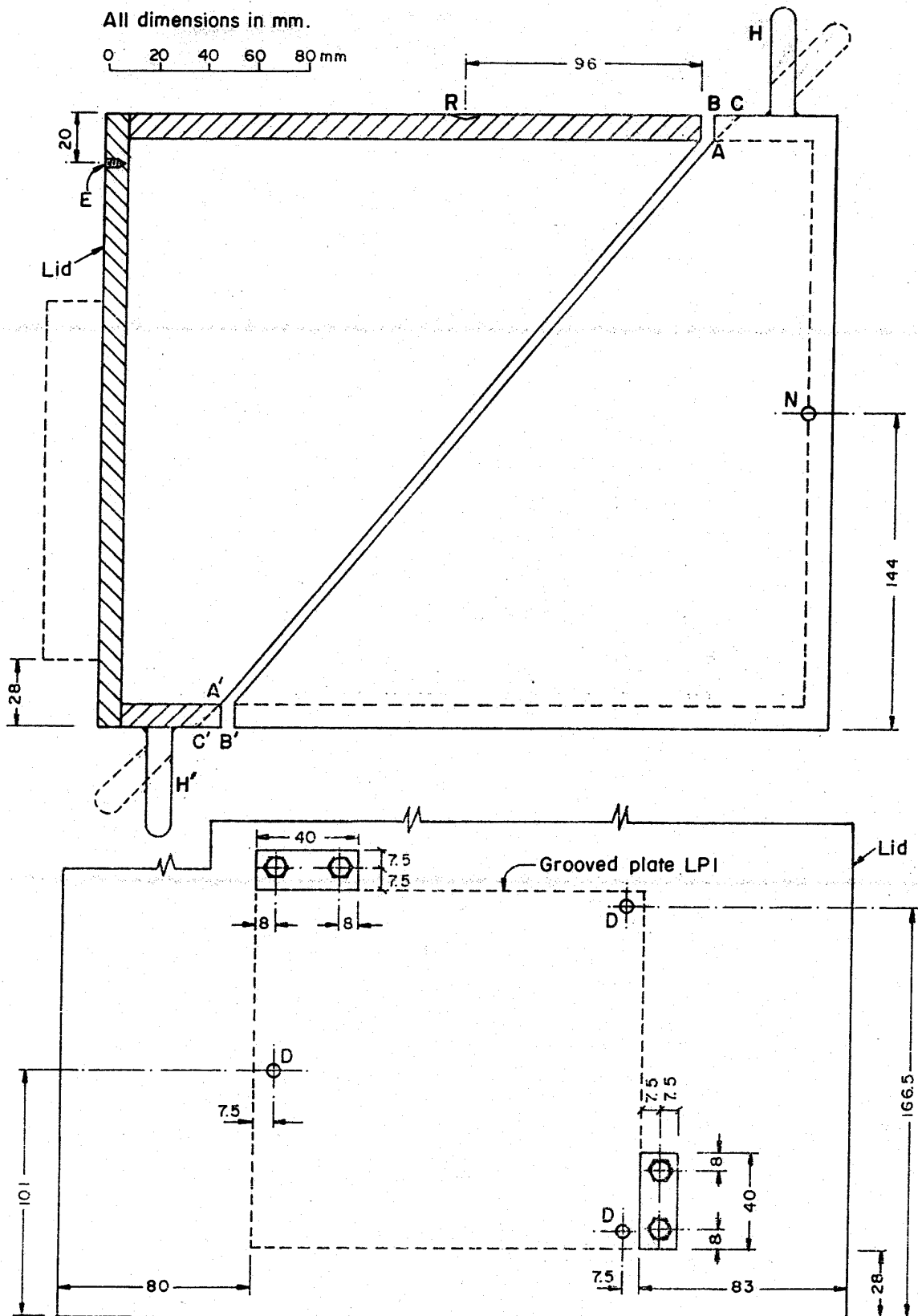


Fig. 5.24. Details of the 15-ton capacity grooved loading plates



**Fig. 5.25. The ball cage for use between the grooved plates in Fig 5.24**



**Fig. 5.26. Modifications applied to the 40-degree test mould to enable its use as a 50-degree mould when desired**

## APPENDIX 1. EQUATIONS FOR THE DETAILED EVALUATION OF CYLWESTS

Equations given in this appendix have been derived by suitable integration, outlined elsewhere (Mirata, 1981) from the geometry of Figs 2.2 and A1. In these equations, when Analysis B (Chapter 2) is used,  $u$  has to be replaced by  $\bar{u}$ , and when Analysis C is used,  $\alpha$  and  $u$  have to be replaced by  $\alpha_i$  and  $\bar{u}_i$  respectively.

### A1.1 Corrected area of shear

The corrected area of shear, without any tension zones, can be calculated from the following equation, as the area of an ellipse, axes  $2f$  and  $D_i$  with a strip of width  $u$  removed from the central portion.

$$A_c = f_{2s}(\pi - \psi_{2s}) \quad (\text{A1})$$

where

$$f = D_i / 2 \sin \alpha \quad (\text{A2})$$

$$f_{2s} = f^2 \sin \alpha \quad (\text{A3})$$

$$\psi_{2s} = 2\psi + \sin 2\psi \quad (\text{rad}) \quad (\text{A4})$$

$$\psi = \sin^{-1}(u / 2f) \quad (\text{rad}) \quad (\text{A5})$$

### A1.2 Distribution of normal stress along the failure plane

Assuming the distribution of normal stress along the failure plane to vary linearly, the maximum and minimum values of normal stress are given by the following equations.

$$\sigma_{\max} = \sigma + |M|(f - u/2) / I \quad (\text{A6})$$

$$\sigma_{\min} = \sigma - |M|(f - u/2) / I \quad (\text{A7})$$

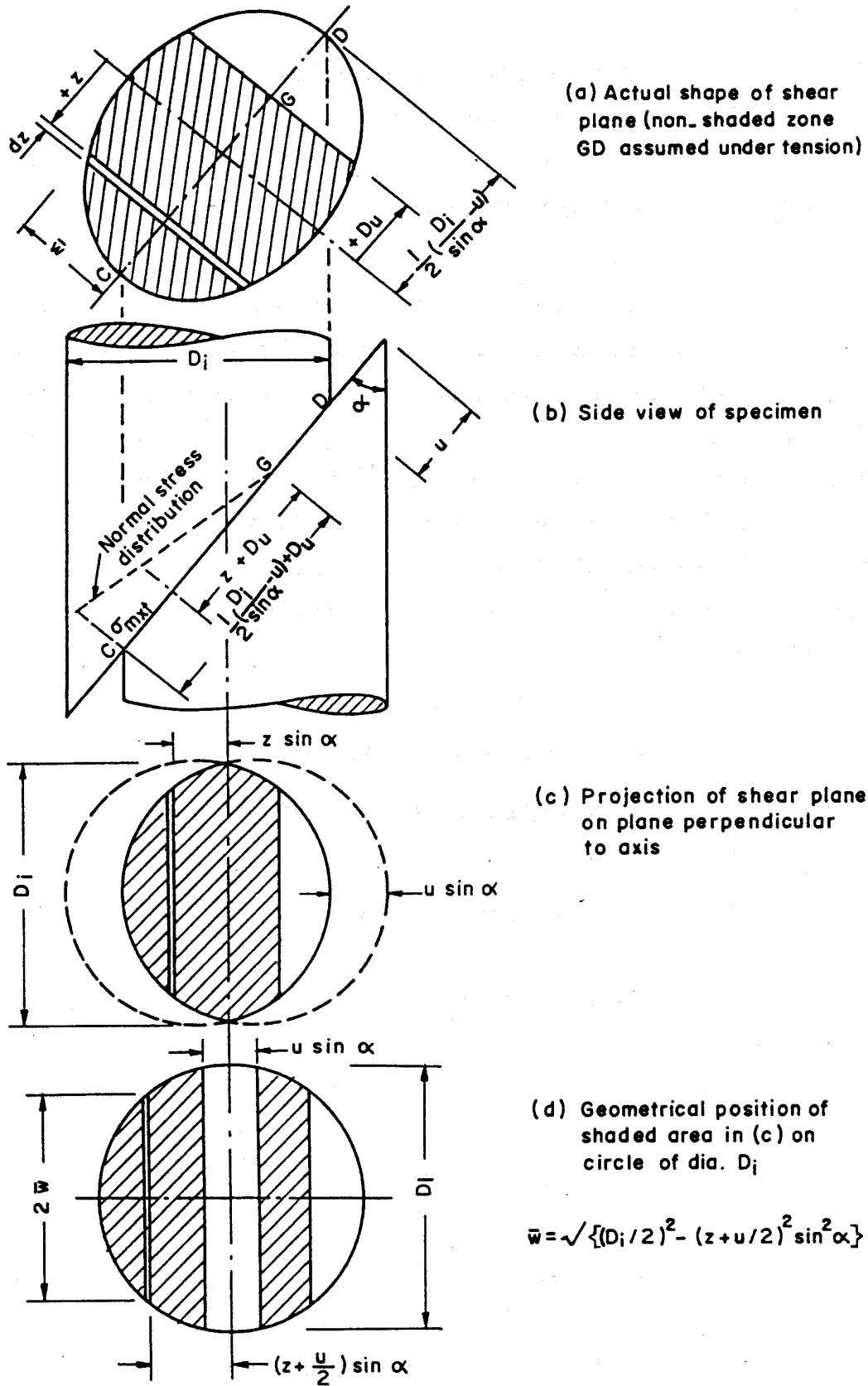


Fig. A1. Geometry of shear plane in the cylwrest assumed partly under tension

where  $M$  is the moment acting on the failure plane, calculated as in Appendix 2, and  $I$  is the moment of inertia of the failure plane given by

$$I = f_{2s} \{3f^2(2\pi - 4\psi + \sin 4\psi) - 32fu \cos^3 \psi + 6u^2(\pi - \psi_{2s})\} / 24 \quad (\text{A8})$$

If  $\sigma_{\min}$  is negative, equations (A1) and (A6) - (A8) are no longer valid, as soil is generally assumed unable to take any tension. For this condition, if the compression zone of the failure plane extends by a distance  $D_u$  beyond the centre-line (Fig. A1(a)), the correct solution can be obtained by iteration from the following equations. These are based on the assumption that  $D_u$  is positive; separate equations needed for when  $D_u$  is negative have been given by Mirata (1981) and are incorporated in the program CYLWEE88 explained in Chapter 3, but are omitted here because this condition is now, with the application of a lateral load after peak strength, highly hypothetical.

$$D_u = \{P_c \{3f^2[4\psi_u - \sin 4\psi_u - 2(4\psi - \sin 4\psi - \pi)] + 32uf(\cos^3 \psi_u - 2 \cos^3 \psi) + 6u^2 J\} - 4|M|E\} / (24|M|J - 4P_c E) \quad (\text{A9})$$

where  $P_c$  is the compressive force equal to the numerator in equation (2.6), and

$$E = 8f \cos^3 \psi_u - 3u(\pi - \psi_{2us}) \quad (\text{A10})$$

$$J = \pi + \psi_{2us} - 2\psi_{2s} \quad (\text{A11})$$

$$\psi_u = \sin^{-1}\{(2D_u + u)(\sin \alpha) / D_i\} \quad (\text{rad}) \quad (\text{A12})$$

$$\psi_{2us} = 2\psi_u + \sin 2\psi_u \quad (\text{A13})$$

If the first estimate  $D_{u1}$  of  $D_u$  to be substituted in equation (A12) is calculated from the following empirical equation, based on actual test results, 2 to 3 iterations are generally sufficient to make the difference between the last value of  $D_u$  calculated by equation (A9) and the previous value less than 0.05 mm.



$$D_{u1} = 3.6 + 0.9 \left\{ 3(d_e / 2 - |M| / P_c) - d_e / 2 \right\} \quad (\text{mm}) \quad (\text{A14})$$

where  $d_e$  is the width of an ‘equivalent rectangle’, which has been found (Mirata, 1981) to have roughly the same flexural properties as the actual failure plane, and is given by

$$d_e = A_c / 0.9D_i \quad (\text{A15})$$

The area  $A_{cp}$  of the failure plane under compression (shaded zone in Fig. A1(a)) is given by

$$A_{cp} = \left\{ A_c - f_{2s} (\psi_{2s} - \psi_{2us}) \right\} / 2 \quad (\text{A16})$$

where  $A_c$  is the area calculated by equation (A1). The average normal and shear stresses can then be calculated by substituting  $A_{cp}$  for  $A_c$  in equations (2.6) and (2.7). The maximum value  $\sigma_{mxt}$  of normal stress for this condition is given by

$$\sigma_{mxt} = 6(2D_u + 2f - u)P_c / (6D_u J + E) f_{2s} \quad (\text{A17})$$

### A1.3 Co-ordinates of the centre of gravity of test mould and soil wedge

The co-ordinates  $(\bar{x}_t, \bar{y}_t)$  of the mobile half TM of the test mould (Fig. 2.2), relative to the centroid of the shear plane of TM are given by

$$\begin{aligned} \bar{x}_t = & \left\{ 8[2h_L - (D_o - D_i) \cot \alpha_n] (h_L + D_i \cot \alpha_n) \right. \\ & \left. + 3(D_o^2 + D_i^2) \cot^2 \alpha_n \right\} / 16h_{di} \end{aligned} \quad (\text{A18})$$

$$\bar{y}_t = \left\{ (D_o^2 + D_i^2) \cot \alpha_n \right\} / 8h_{di} \quad (\text{A19})$$

where

$$h_{di} = 2h_L + D_i \cot \alpha_n \quad (\text{A20})$$

$D_o$  and  $D_i$  are the outer and inner diameters, and  $h_L$  is the minimum height of TM.

The co-ordinates  $(\bar{x}_s, \bar{y}_s)$  of the mobile half of the soil wedge, relative to the centroid  $O_1$  of the initial shear plane (Fig. 2.2) are given by

$$\bar{x}_s = \{16h_s (h_s + D_i \cot \alpha) + 3D_i^2 \cot^2 \alpha\} / 16h_{ds} \quad (\text{A21})$$

$$\bar{y}_s = (D_i^2 \cot \alpha) / 8h_{ds} \quad (\text{A22})$$

where

$$h_{ds} = 2h_s + D_i \cot \alpha \quad (\text{A23})$$

and  $h_s$  = minimum height of the soil wedge.

## APPENDIX 2. MOMENT EQUATIONS

### A2.1 For Analyses A and B

In analysis A, the moment  $M$  acting on the failure plane from the mobile half of the soil wedge is given by the following equations, clockwise moments (Fig. 2.2) being taken as positive. When Analysis B (Chapter 2) is used,  $\delta_x, \delta_y$  in these equations are replaced by  $\delta_{x_0}, \delta_{y_0}$  calculated as in Appendix 3.

$$\begin{aligned} M = & (\bar{y}_1 + \delta_y - \Delta y_{sh}) W \sin \theta - (D + h_{og} - \bar{x}_1) W \cos \theta \\ & + (\delta_y / 2 - \Delta y_{sh}) X' + (D + h_{og} - \delta_x / 2) Y' \\ & + (\delta_y - \Delta y_{sh}) \frac{W_{BC}}{2} \sin \theta - M_B \cos \theta + \delta M_q \end{aligned} \quad (\text{A24})$$

where

$$\delta M_q = -(D + h_{og} - \bar{x}_{q1}) \delta Y_q - (\bar{y}_{q1} + \delta_y - \Delta y_{sh}) \delta X_q \quad (\text{A25})$$

and  $\Delta y_{sh}$  is the amount of shift in the positive  $y$  direction (Figs 1.2 and 2.2), applied to  $P$  during the test, and is calculated from

$$\Delta y_{sh} = \delta_y - \Delta y_{MP} \quad (A26)$$

where  $\Delta y_{MP}$  is the displacement of the centre of the grooved plate LP2 relative to the centroid  $O_1$  of the initial shear plane in the negative  $y$  direction (Figs 1.2 and 2.2);  $h_{og}$  is the distance between the grooves on LP1 and the centroid  $O_1$  of the initial shear plane;  $X', Y'$  are the reactions acting at the centroid  $O_3$  of the shear plane, and equal but opposite to  $X, Y$  calculated by equations (2.1) and (2.2);  $(\bar{x}_1, \bar{y}_1)$  and  $(\bar{x}_{q1}, \bar{y}_{q1})$  are respectively the co-ordinates of the centroid of  $W$  and the point of application of  $Q$  relative to  $O_1$ .

### A2.2 For Analysis C

If the reactions  $X', Y'$  are assumed to act at the centroid of  $A_1B_1$  in Figs 2.1 and 2.3, the following moment equation results.

$$\begin{aligned} M = & -(\bar{y}_{sx} - \Delta\bar{y} - \bar{y})W \sin \theta_r - (\bar{x}_{sy} + \Delta\bar{x} - \bar{x})W \cos \theta_r \\ & - \bar{y}_{xs} X' + \bar{x}_{sy} Y' + (\delta_{yo} - \Delta y_{sh}) \frac{W_{BC}}{2} \sin \theta_r \\ & - M_B \cos \theta_r + \delta M_q \end{aligned} \quad (A27)$$

where

$$\delta M_q = -(\bar{x}_{sy} + \Delta\bar{x} - \bar{x}_q) \delta Y_q + (\bar{y}_{sx} - \Delta\bar{y} - \bar{y}_q) \delta X_q \quad (A28)$$

$(\bar{x}, \bar{y})$  and  $(\bar{x}_q, \bar{y}_q)$  are respectively the co-ordinates of the centroid of  $W$  and the point of application of  $Q$  relative to the centroid of the shearing plane of the mobile half TM of the test mould; and

$$\bar{x}_{sy} = \left( D_b - \frac{\overline{A_1B_1}}{2} \cos \alpha_i \right) \cos \beta \quad (A29)$$

$$\bar{y}_{sx} = \frac{\overline{A_1B_1}}{2} \sin \alpha_r - \left\{ d_{yb} - (\Delta y_P + \Delta y_{RB}) - \beta D_b \right\} \quad (A30)$$

$$\Delta\bar{x} = h_{pp} - \frac{\overline{A_1 B_1}}{2} \cos \alpha_r \quad (\text{A31})$$

$$\Delta\bar{y} = h_{np} - \frac{\overline{A_1 B_1}}{2} \sin \alpha_r \quad (\text{A32})$$

where  $D_b$  is the distance, measured in the  $x$  direction, between the single ball SB and the point  $B_1$ , and remains constant in all wedge shear tests where a hydraulic jack is used, decreases by  $\delta_{x_0}$  for the configuration in Fig. 2.2; and  $h_{np}$ ,  $h_{pp}$  are as defined in Table 2.1 for the different versions of the test.

### APPENDIX 3. ITERATIVE CALCULATION OF $\bar{u}$ , $\bar{v}$ and $\beta$

The test mould TM (Fig. 2.1) is assumed to reach any one position firstly by moving, without rotation, by average shear and normal displacements  $\bar{u}$ ,  $\bar{v}$  (dotted position), and then rotating by  $\beta$  about  $O_3$ , defined as in Analysis A (Chapter 2). The values of  $\bar{u}$ ,  $\bar{v}$ , and  $\beta$  are then obtained by iteration as follows.

If the previously defined  $\delta_x$  and  $\delta_y$  are the values recorded by independently supported dial gauges bearing on points at initial distances  $d_1$  and  $d_2$  respectively, measured from the edge of the initial position of TM and taken as positive when positioned as in Fig. 2.1; and  $\delta_{x_0}$  and  $\delta_{y_0}$  are the corresponding actual displacements of TM if it did not rotate,  $\bar{u}$ ,  $\bar{v}$  are given by

$$\bar{u} = u + \left\{ \overline{O_3 E} \cdot \cos \psi_1 \sin \alpha + \overline{O_3 F} \cdot \sin \psi_2 \cos \alpha \right\} \beta \quad (\text{A33})$$

$$\bar{v} = v + \left\{ \overline{O_3 E} \cdot \cos \psi_1 \cos \alpha - \overline{O_3 F} \cdot \sin \psi_2 \sin \alpha \right\} \beta \quad (\text{A34})$$

where

$$\overline{O_3 E} = N_r / \sin \psi_1 \quad (\text{A35})$$

$$\overline{O_3 F} = D_n / \cos \psi_2 \quad (\text{A36})$$

$$\psi_1 = \tan^{-1} \left\{ N_r / (D_n - d_1 + \delta_{x_0}) \right\} \quad (\text{A37})$$

$$\psi_2 = \tan^{-1} \left\{ (N_r - d_2 - \delta_{yo}) / D_n \right\} \quad (\text{A38})$$

$$D_n = d_{mx} - \delta_{xo} / 2 \quad (\text{A39})$$

$$N_r = d_{my} + \delta_{yo} / 2 \quad (\text{A40})$$

$$\delta_{xo} = \bar{u} \cos \alpha - \bar{v} \sin \alpha \quad (\text{A41})$$

$$\delta_{yo} = \bar{u} \sin \alpha + \bar{v} \cos \alpha \quad (\text{A42})$$

$$\beta = \left( \delta_{yo} - \Delta y_{MP} - \Delta y_P - \Delta y_{RB} \right) / \left( D + h_{og} - \delta_{xo} / 2 \right) \quad (\text{rad}) \quad (\text{A43})$$

$d_{mx}$ ,  $d_{my}$  are as defined in Table 2.1 for the different versions of the test,  $\Delta y_P$  and  $\Delta y_{RB}$  are the amounts of shift, in the positive  $y$  direction, applied to  $P$  relative to the initial centroid  $O_1$  of the shear plane prior to the start of shear and during shear respectively.

Iteration starts by replacing  $\bar{u}, \bar{v}$  in equations (A41) and (A42) by  $u$  and  $v$  given by equations (2.10) and (2.11). Two to three iterations are generally adequate to make the sum of the absolute values of the differences between  $\bar{u}, \bar{v}$  and the corresponding values obtained by the previous iteration less than or equal to 0.1 mm.

#### APPENDIX 4. CALCULATION OF $\overline{A_1 B_1}$ and $\alpha_i$

The co-ordinates ( $x_{A11}, y_{A11}$ ) of  $A_{11}$ , the position of  $A_1$  before rotation by  $\beta$  about  $O_3$ , defined as in analysis A (Chapter 2), and so the length  $\overline{A_1 B_1}$  and the inclination  $\alpha_i$  of the shear plane to the initial direction of  $P$  can be obtained from the geometry of Figs 2.1 and 2.3 as follows.

$$\overline{A_1 B_1} = \left( -2y_{A11} + \overline{O_3 A_{11}} \cdot \beta \cos \psi_a \right) / \sin \alpha_i \quad (\text{A44})$$

$$\alpha_i = \tan^{-1} \left( \frac{-2y_{A11} + \overline{O_3 A_{11}} \cdot \beta \cos \psi_a}{2x_{A11} - \overline{O_3 A_{11}} \cdot \beta \sin \psi_a} \right) \quad (\text{A45})$$

where

$$\overline{O_3 A_{11}} = -y_{A11} / \sin \psi_a \quad (\text{A46})$$

$$\psi_a = \tan^{-1}(-y_{A11} / x_{A11}) \quad (\text{A47})$$

$$x_{A11} = (d_{ax} - \delta_{xo}) / 2 \quad (\text{A48})$$

$$y_{A11} = -(2d_{yb} - \delta_{yo}) / 2 \quad (\text{A49})$$

and  $d_{ax}$  is as defined in Table 2.1 for the different versions of the test.

## APPENDIX 5. DERIVATION OF CURVES IN FIG. 2.4

If equations (2.1) to (2.7) are combined with the Mohr-Coulomb failure criterion,  $\lambda_q = 90^\circ$  is assumed, the significant terms in  $P$  and  $Q$  are eliminated in turn between the new forms of equations (2.6) and (2.7), and differentials taken, the following equations result.

$$\Delta P = \frac{A_c \Delta \sigma}{\cos \phi} \sin(\alpha + \phi) \quad (\text{A50})$$

$$\Delta Q = \frac{A_c \Delta \sigma}{\cos \phi} \cos(\alpha + \phi) - \mu \cdot \Delta P \quad (\text{A51})$$

Eliminating  $\Delta \sigma$  between equations (A50) and (A51)

$$\Delta P = \frac{\sin(\alpha + \phi)}{\cos(\alpha + \phi) - \mu \cdot \sin(\alpha + \phi)} \Delta Q \quad (\text{A52})$$

From equations (A50) and (A52)

$$\frac{A_c}{\cos \phi} \Delta \sigma = \frac{\Delta Q}{\cos(\alpha + \phi) - \mu \cdot \sin(\alpha + \phi)} \quad (\text{A53})$$

## APPENDIX 6. CALCULATOR PROGRAMS FOR THE SIMPLIFIED EVALUATION OF THE WEDGE SHEAR TEST AND FOR KEEPING $\sigma \approx \sigma_f$ AFTER PEAK STRENGTH

### A6.1 Introduction

In this appendix, programs are given for the example of the Casio fx-3800P calculator, having a program memory of 135 steps, and presently (in 1998) available in Turkey for the equivalent of US \$ 28.00. Forms A to E and Programs I and II are for the simplified evaluation of the wedge shear test using equations (2.1) - (2.11), and for the regression of the test results. Forms F and G, and Programs III and IV are for the calculations based on equations (2.16) - (2.20) for keeping the normal stress  $\sigma$  at around its value  $\sigma_f$  at peak strength. For further simplicity, Program I assumes that  $\lambda_q = 90^\circ$ ; if this angle differs significantly from  $90^\circ$ , the exact value of  $\delta X_q$  as given by equation (2.3) may be entered in register K2, and the value of  $\delta_q \cdot \sin \lambda_q$  be fed at step 34 in running Program I, for better accuracy.

For the adjustment of  $Q$  to keep  $\sigma \approx \sigma_f$ , Program III is run only once for any one test, for the values recorded at peak strength (or for a set of values in an earlier test in which the currently aimed  $\sigma$  value has been reached (see, Box 4.2, file 1)); Program IV is then used as many times as needed to adjust  $Q$  to keep  $\sigma \approx \sigma_f$ .

**A6.2 Data sheets for the simplified evaluation of the wedge shear test**

**FORM A. Fixed data for any one test**

Sample tested: .....

Type of test (delete the inapplicable tests): cylwest / iswest / priswest.

Inclination of the main load  $P$  to the horizontal (upward positive),  $\theta = \dots\dots\dots$  deg

Nominal angle of the test mould,  $\alpha_n = \dots\dots\dots$  deg

Weight of movable part of test mould + enclosed soil + grooved plate LP1,  $W = \dots\dots\dots$  kgf

Weight of grooved plate LP2,  $W_{LP} = \dots\dots\dots$  kgf

Weight of ball cage,  $W_{BC} = \dots\dots\dots$  kgf

Constant for converting the main load gauge readings into kgf,  $C_p = \dots\dots\dots$  kgf/div

Constant for converting the lateral load gauge readings into kgf,  $C_q = \dots\dots\dots$  kgf/div

Inclination of the lateral load  $Q$  to the horizontal (downward positive),  $\lambda_1 = \dots\dots\dots$  deg

The component  $W_{qn}$  normal to  $Q$  of the simply supported reaction due to the self weight ( $W_q$ )

of the  $Q$  device,  $W_{qn} \approx \frac{W_q}{2} \cos \lambda_1 = \dots\dots\dots = \dots\dots\dots$  kgf

The simply supported reaction of the  $P$  device, when horizontal, at the grooves on LP1,  
 $M_B / D \approx Total \text{ weight of this unit} / 2 = \dots\dots\dots$  kgf

**FORM B. Readings taken during the test and intermediate calculations**

Time	Reading of $P$ device, $\delta_p$	Reading of $Q$ device, $\delta_q$	Displacement parallel to $P$ , $\delta_x$		Displacement normal to $P$ , $\delta_y$	
			(div)	(cm)	(div)	(cm)



### A6.3 Input / Output forms for the simplified evaluation of the wedge shear test

#### FORM C. Input for Casio fx-3800P Program I attached and the relevant output

Press MODE 7 3 ; MODE .

#### (a) Values to be stored in the memory registers

	Keys to be pressed
M: $\theta$ (from Form A) = ..... (deg) $\longrightarrow$	<span style="border: 1px solid black; padding: 2px;">SHIFT</span> <span style="border: 1px solid black; padding: 2px;">M in</span>
K1: $C_p$ (from Form A) = ..... (kgf/div) $\longrightarrow$	<span style="border: 1px solid black; padding: 2px;">K in</span> <span style="border: 1px solid black; padding: 2px;">1</span>
K2: If $\theta \geq 0$ , $-W_{qn}$ ; if $\theta < 0$ , $W_{qn}$ (from Form A) = ..... (kgf) $\rightarrow$	<span style="border: 1px solid black; padding: 2px;">K in</span> <span style="border: 1px solid black; padding: 2px;">2</span>
K3: $C_q$ (from Form A) = ..... (kgf/div) $\longrightarrow$	<span style="border: 1px solid black; padding: 2px;">K in</span> <span style="border: 1px solid black; padding: 2px;">3</span>
K4: $M_{B/D}$ (from Form A) = ..... (kgf) $\longrightarrow$	<span style="border: 1px solid black; padding: 2px;">K in</span> <span style="border: 1px solid black; padding: 2px;">4</span>
K5: $W$ (from Form A) = ..... (kgf) $\longrightarrow$	<span style="border: 1px solid black; padding: 2px;">K in</span> <span style="border: 1px solid black; padding: 2px;">5</span>
K6: $W_{LP} + W_{BC}$ (from Form A)* = ..... (kgf) $\longrightarrow$	<span style="border: 1px solid black; padding: 2px;">K in</span> <span style="border: 1px solid black; padding: 2px;">6</span>

#### (b) Data to be entered and the output of program I (Press I)

Step	1	2	3	4	5	6	7
Test No.	Enter 1 Reading of $P$ device, $\delta_p$	Press	Output 1 $X$ (kgf)	Press	Enter 2 Reading of $Q$ device, $\delta_q$	Press	Output 2 $Y$ (kgf)
.....	.....	RUN	.....	RUN	.....	RUN	.....
.....	.....	RUN	.....	RUN	.....	RUN	.....
.....	.....	RUN	.....	RUN	.....	RUN	.....
.....	.....	RUN	.....	RUN	.....	RUN	.....
.....	.....	RUN	.....	RUN	.....	RUN	.....
.....	.....	RUN	.....	RUN	.....	RUN	.....
.....	.....	RUN	.....	RUN	.....	RUN	.....
.....	.....	RUN	.....	RUN	.....	RUN	.....

\* In cylwests, if the proving ring dial has been set to zero with the two grooved plates and the ball cage resting on the proving ring, this value should be entered as  $(-W_{LP})$ .

**FORM D. Input for Casio fx-3800P Program II attached and the relevant output**

Press MODE 7 3 ; MODE .

**(a) Values to be stored in the memory registers**

Keys to be pressed

M: For iswests and priswests, inner width of mould,  $b = \dots\dots$  cm

SHIFT M in

For cylwests, inside diameter of mould,  $D_i = \dots\dots$  cm

K1: Initial area of shear plane

For iswests and priswests,  $b.d = \dots\dots\dots$  cm<sup>2</sup>

K in 1

For cylwests,  $\pi D_i^2 / 4.\sin \alpha = \dots\dots\dots$  cm<sup>2</sup>

( $\alpha = \alpha_n$  unless failure takes place along another plane in cylwests.)

K2:  $\sin \alpha = \dots\dots\dots$   K in 2

K in 2

K3:  $\cos \alpha = \dots\dots\dots$   K in 3

K in 3

**(b) Data to be entered and the output of program II (Press II )**

Step	1	2	3	4	5	6	7	8	9	10	11
Test No.	Ent.1 $X$ (kgf)*	Press RUN	Ent.2 $Y$ (kgf)*	Press RUN	Ent.3 $\delta_x$ (cm)#	Press RUN	Ent.4 $\delta_y$ (cm)#	Press RUN	Output 1 $\sigma$ kgf/cm <sup>2</sup>	Press RUN	Output 2 $\tau$ kgf/cm <sup>2</sup>
.....	.....	RUN	.....	RUN	.....	RUN	.....	RUN	.....	RUN	.....
.....	.....	RUN	.....	RUN	.....	RUN	.....	RUN	.....	RUN	.....
.....	.....	RUN	.....	RUN	.....	RUN	.....	RUN	.....	RUN	.....
.....	.....	RUN	.....	RUN	.....	RUN	.....	RUN	.....	RUN	.....
.....	.....	RUN	.....	RUN	.....	RUN	.....	RUN	.....	RUN	.....
.....	.....	RUN	.....	RUN	.....	RUN	.....	RUN	.....	RUN	.....
.....	.....	RUN	.....	RUN	.....	RUN	.....	RUN	.....	RUN	.....
.....	.....	RUN	.....	RUN	.....	RUN	.....	RUN	.....	RUN	.....
.....	.....	RUN	.....	RUN	.....	RUN	.....	RUN	.....	RUN	.....
.....	.....	RUN	.....	RUN	.....	RUN	.....	RUN	.....	RUN	.....

\* From Form C

# From Form B

**FORM E. Fitting envelopes to n pairs of ( $\sigma$ ,  $\tau$ )**

(a) *Fitting an envelope of the form  $\tau_f = c + \sigma \cdot \tan \phi$*

Press MODE 7 4 ; MODE 2 ; SHIFT KAC

Data pair	Ent. 1	Press	Ent. 2	Press											
<i>i</i>	$\sigma$ (kPa)		$\tau$ (kPa)												
1	.....	X <sub>D</sub> , Y <sub>D</sub>	.....	DATA	<p style="text-align: center;"><u>After row <math>i = n</math> is entered</u></p> <table style="width: 100%; border: none;"> <tr> <th style="text-align: left; width: 50%;"><u>Keys to be pressed</u></th> <th style="text-align: left;"><u>Output</u></th> </tr> <tr> <td style="border: none;"><span style="border: 1px solid black; padding: 2px;">SHIFT</span> <span style="border: 1px solid black; padding: 2px;">A</span></td> <td style="border: none;"><math>c =</math> ..... kPa</td> </tr> <tr> <td style="border: none;"><span style="border: 1px solid black; padding: 2px;">SHIFT</span> <span style="border: 1px solid black; padding: 2px;">B</span></td> <td style="border: none;"><math>\tan \phi</math></td> </tr> <tr> <td style="border: none;"><span style="border: 1px solid black; padding: 2px;">SHIFT</span> <span style="border: 1px solid black; padding: 2px;"><math>\tan^{-1}</math></span></td> <td style="border: none;"><math>\phi =</math> ..... deg</td> </tr> <tr> <td style="border: none;"><span style="border: 1px solid black; padding: 2px;">SHIFT</span> <span style="border: 1px solid black; padding: 2px;">r</span></td> <td style="border: none;"><math>r =</math> .....</td> </tr> </table>	<u>Keys to be pressed</u>	<u>Output</u>	<span style="border: 1px solid black; padding: 2px;">SHIFT</span> <span style="border: 1px solid black; padding: 2px;">A</span>	$c =$ ..... kPa	<span style="border: 1px solid black; padding: 2px;">SHIFT</span> <span style="border: 1px solid black; padding: 2px;">B</span>	$\tan \phi$	<span style="border: 1px solid black; padding: 2px;">SHIFT</span> <span style="border: 1px solid black; padding: 2px;"><math>\tan^{-1}</math></span>	$\phi =$ ..... deg	<span style="border: 1px solid black; padding: 2px;">SHIFT</span> <span style="border: 1px solid black; padding: 2px;">r</span>	$r =$ .....
<u>Keys to be pressed</u>	<u>Output</u>														
<span style="border: 1px solid black; padding: 2px;">SHIFT</span> <span style="border: 1px solid black; padding: 2px;">A</span>	$c =$ ..... kPa														
<span style="border: 1px solid black; padding: 2px;">SHIFT</span> <span style="border: 1px solid black; padding: 2px;">B</span>	$\tan \phi$														
<span style="border: 1px solid black; padding: 2px;">SHIFT</span> <span style="border: 1px solid black; padding: 2px;"><math>\tan^{-1}</math></span>	$\phi =$ ..... deg														
<span style="border: 1px solid black; padding: 2px;">SHIFT</span> <span style="border: 1px solid black; padding: 2px;">r</span>	$r =$ .....														
2	.....	X <sub>D</sub> , Y <sub>D</sub>	.....	DATA											
3	.....	X <sub>D</sub> , Y <sub>D</sub>	.....	DATA											
4	.....	X <sub>D</sub> , Y <sub>D</sub>	.....	DATA											
5	.....	X <sub>D</sub> , Y <sub>D</sub>	.....	DATA											
6	.....	X <sub>D</sub> , Y <sub>D</sub>	.....	DATA											
7	.....	X <sub>D</sub> , Y <sub>D</sub>	.....	DATA											
8	.....	X <sub>D</sub> , Y <sub>D</sub>	.....	DATA											
...	.....	X <sub>D</sub> , Y <sub>D</sub>	.....	DATA											
...	.....	X <sub>D</sub> , Y <sub>D</sub>	.....	DATA											

(b) *Fitting an envelope of the form  $\tau_f = \sigma \cdot \tan \phi$*

Enter the data pairs as at (a). Then press Kout 6 ; ÷ ; Kout 1 ; = ;

SHIFT  $\tan^{-1}$ . **Output** =  $\phi$  for envelope forced through the origin = ..... deg

(c) *Fitting an envelope of the form  $\tau_f = a(\sigma')^{b_1}$*

Data pair	Ent. 1	Press	Ent. 2	Press
<i>i</i>	$\sigma$ (kPa)		$\tau$ (kPa)	
1	.....	<span style="border: 1px solid black; padding: 2px;">SHIFT</span> <span style="border: 1px solid black; padding: 2px;">ln</span> <span style="border: 1px solid black; padding: 2px;">X<sub>D</sub>, Y<sub>D</sub></span>	.....	<span style="border: 1px solid black; padding: 2px;">SHIFT</span> <span style="border: 1px solid black; padding: 2px;">ln</span> <span style="border: 1px solid black; padding: 2px;">DATA</span>
2	.....	" " "	.....	" " "
3	.....	" " "	.....	" " "
4	.....	" " "	.....	" " "
5	.....	" " "	.....	" " "
6	.....	" " "	.....	" " "
7	.....	" " "	.....	" " "
8	.....	" " "	.....	" " "
...	.....	" " "	.....	" " "

*After row  $i = n$  is entered*

Keys to be pressed

SHIFT A ; SHIFT  $e^x$

SHIFT B

SHIFT r

Output

The value of the constant  $a =$  .....

The value of the exponent  $b_1 =$  .....

Coefficient of correlation,  $r =$  .....

### A6.4 Input / Output forms for calculations for keeping $\sigma \approx \sigma_f$ after peak strength

#### FORM F. Input for Casio fx-3800P Program III attached and the relevant output

NOTES. (1) Unless defined here, the values needed in the calculation of the fixed data to be entered in the memory registers may be taken from Forms A, C, and D.

(2) The suffix f is used to indicate values at peak strength.

Press MODE 7 3 ; MODE .

#### (a) Values to be stored in the memory registers

K1:  $K_1 = (C_p \cdot \tan \alpha_n) / C_q = (\dots)(\tan \dots) / (\dots) = \dots$  Keys to be pressed  
→ K in 1

K2: For iswests and priswests, where  $d$  = length of shear plane of test mould,

$S_a = 1 / d \cdot \cos \alpha_n = 1 / (\dots \cos \dots) = \dots$   
 For cylwests, where  $D_i$  = inside dia. of the test mould,  
 $S_a = (4 \tan \alpha_n) / \pi \cdot D_i = (4 \tan \dots) / \dots \pi = \dots$  } → K in 2

K3: If  $Q_f > 0$ ,  $K_3 = K_2$ ; if  $Q_f = 0$ ,  $K_3 = K_2 - S \cdot W_{qn} / C_p$ , where  $S$  is defined by equation (2.5), and

$K_2 = \{(W + W_{BC} + W_{LP}) \sin \theta + S \cdot W_{qn} - (W + M_B / D) \cos \theta / \tan \alpha_n\} / C_p$  \*\*  
 $= \{(\dots + \dots + \dots) \sin \dots + (\dots)(\dots) - (\dots + \dots) \cos \dots / \tan \dots\} / \dots$   
 $= \dots$  (to be used in Program IV) → K in 5

$S \cdot W_{qn} / C_p = (\dots)(\dots) / \dots = \dots$   
 If  $Q_f > 0$ ,  $K_3 = K_2 = \dots$  ;  
 if  $Q_f = 0$ ,  $K_3 = K_2 - S \cdot W_{qn} / C_p = (\dots) - (\dots) = \dots$  } → K in 3

#### (b) Data to be entered and the output of program III (Press SHIFT III)

Step	1	2	3	4	5	6	7
Test No.	Enter 1 Reading of $Q$ device, $\delta_{qf}$	Press	Enter 2 Reading of $P$ device, $\delta_{pf}$	Press	Enter 3 $x$ -displacement $\delta_{xf}$ (cm)	Press	Output * $K_4$ (div)
.....	.....	RUN	.....	RUN	.....	RUN	.....

\*  $K_4 = (\delta_{pf} + \delta_{qf} / K_1 - K_3) / (1 - \delta_{xf} \cdot S_a)$ . (Calculated at peak strength only, and stored in K6.)

\*\* If the dial for  $P$  in cylwests has been set to zero with the two grooved plates and the ball cage on top, the expression  $(W + W_{BC} + W_{LP})$  in the equation for  $K_2$  becomes  $(W - W_{LP})$ .

**FORM G. Input for Casio fx-3800P Program IV attached and the relevant output**

Press MODE 7 3 ; MODE .

**(a) Values in memory registers**

The values in registers K1 - K3, and K5 should be those entered before running Program III; the value in K6 is calculated, and entered in this register by running Program III.

**(b) Data to be entered and the output of program IV (Press SHIFT IV )**

Step 1	2	3	4	5
Enter 1 $x$ -displacement $\delta_x$ (cm)	Press	Enter 2 Reading of $P$ device, $\delta_p$ (div)	Press	Output * Reading of $Q$ device, $\delta_q$ (div)
.....	RUN	.....	RUN	.....
.....	RUN	.....	RUN	.....
.....	RUN	.....	RUN	.....
.....	RUN	.....	RUN	.....
.....	RUN	.....	RUN	.....
.....	RUN	.....	RUN	.....
.....	RUN	.....	RUN	.....
.....	RUN	.....	RUN	.....
.....	RUN	.....	RUN	.....
.....	RUN	.....	RUN	.....
.....	RUN	.....	RUN	.....

\* When  $Q$  is changed in order to keep  $\sigma \approx \sigma_f$ ,  $\delta_p$  also changes; so this program may have to be run a number of times at any stage of the test. With experience,  $Q$  may be adjusted anticipating the resultant change in  $\delta_p$ , thus reducing the number of calculations needed. Furthermore, the program may be run and  $Q$  adjusted, without entering the values in the above table.

## PROGRAM I. SIMPLIFIED EVALUATION OF THE WEDGE SHEAR TEST

### Stage I. Evaluation of X and Y in equations\* (2.1) and (2.2)

--- As a check while coding the program, enter first the storage register data at the side, and the values marked with an arrow (←) during coding.

--- To code the program, **press** MODE EXP I

Step	Key	Variable	Example
01	ENT	$\delta_p$	408 ←
02	x		408.000
03	Kout 1	$C_p$	1.365
04	-		556.920
05	(		(01 0.
06	Kout 5	$W$	31.670
07	+		31.670
08	Kout 6		4.450
09	)		36.120
10	x		36.120
11	MR	$\theta$	5.000
12	sin	$\sin \theta$	0.087
13	+		553.772
14	Kout 2	$\delta X_q$	-1.000
15	=	$X$ (kgf)	552.772
16	SHIFT HLT		552.772
17	+		552.772
18	(		(01 0.
19	Kout 5	$W$	31.670
20	+		31.670
21	Kout 6		4.450
22	)		36.120
23	x		36.120
24	MR	$\theta$	5.000
25	sin	$\sin \theta$	0.087
26	-		555.920
27	Kout 2	$\delta X_q$	-1.000
28	=		556.920
29	x		556.920
30	0.0042**	$\mu$	0.0042
31	+		2.339
32	Kout 3	$C_q$	0.338
33	x		0.338
34	ENT	$\delta_q$	710 ←
35	+		242.646
36	(		(01 0.
37	Kout 5	$W$	31.670
38	+		31.670
39	Kout 4	$M_B/D$	9.400
40	)		41.070
41	x		41.070
42	MR	$\theta$	5.000
43	cos	$\cos \theta$	0.996
44	=	$Y$ (kgf)	883.559
45	SHIFT RTN		883.559

### Sample storage data

Press MODE 7 3 ; MODE .

Register	Variable	Example
M	$\theta$ (deg)	5.0
K1	$C_p$ (kgf/div)	1.365
K2	$\delta X_q$ (kgf)	-1.0
K3	$C_q$ (kgf/div)	0.33846
K4	$M_B/D$ (kgf)	9.4
K5	$W$ (kgf)	31.67
K6 <sup>#</sup>	$W_{BC} + W_{LP}$ (kgf)	4.45

\*  $\lambda_q = 90^\circ$  is assumed for these calculations. Thus, from equation (2.3),  
 if  $\theta \geq 0$ ,  $\delta X_q = -W_{qn}$   
 if  $\theta < 0$ ,  $\delta X_q = W_{qn}$   
 and from equation (2.4),  

$$\delta Y_q = Q$$

\*\* The actual value of  $\mu$  should be entered here, and if different from the value given as example, there will be slight differences in the values that follow.

# In cylwests, if the proving ring dial has been set to zero with the two grooved plates and the ball cage bearing on the proving ring, the expression ( $W + W_{BC} + W_{LP}$ ) in equation (2.1) should be ( $W - W_{LP}$ ), and the value in register K6 entered as ( $-W_{LP}$ ).

## PROGRAM II. SIMPLIFIED EVALUATION OF THE WEDGE SHEAR TEST

### Stage II. Evaluation of $\sigma$ and $\tau$ by equations (2.6) to (2.10)

--- As a check while coding the program, enter first the storage register data at the side, and the values marked with an arrow ( $\leftarrow$ ) during coding.

--- To code the program, press MODE EXP II

Step	Key	Variable	Example
01	ENT	X (kgf)	553 $\leftarrow$
02	K in 4		553.000
03	x		553.000
04	Kout 2	$\sin \alpha$	0.500
05	+		276.500
06	ENT	Y (kgf)	284 $\leftarrow$
07	K in 5		284.000
08	x		284.000
09	Kout 3	$\cos \alpha$	0.866
10	=		522.444
11	$\div$		522.444
12	(		(01 0.
13	Kout 1	$A_o$ (cm <sup>2</sup> )	900.000
14	-		900.000
15	(		(02 0.
16	ENT	$\delta_x$ (cm)	8.93 $\leftarrow$
17	x		8.930
18	Kout 3	$\cos \alpha$	0.866
19	+		31.670
20	ENT	$\delta_y$ (cm)	4.58 $\leftarrow$
21	x		4.580
22	Kout 2	$\sin \alpha$	0.500
23	)	$u$ (cm)	10.023
24	x		10.023
25	MR	$b$ (cm)	25.000
26	)	$A_c$ (cm <sup>2</sup> )	649.416
27	K in 6		649.416
28	=	$\sigma$ (kgf/cm <sup>2</sup> )	0.804
29	SHIFT HLT		0.804
30	Kout 4	X (kgf)	553.000
31	x		553.000
32	Kout 3	$\cos \alpha$	0.866
33	-		478.898
34	Kout 5	Y (kgf)	284.000
35	x		284.000
36	Kout 2	$\sin \alpha$	0.500
37	=		336.898
38	$\div$		336.898
39	Kout 6	$A_c$ (cm <sup>2</sup> )	649.416
40	=	$\tau$ (kgf/cm <sup>2</sup> )	0.519
41	SHIFT RTN		0.519

### Sample storage data

Press MODE 7 3; MODE .

Register	Variable	Example
M	For iswests and priswests, $b$ (cm) For cylwests, $D_1$ (cm)	25
K1	$A_o$ (cm <sup>2</sup> )	900
K2	$\sin \alpha$	0.500
K3	$\cos \alpha$	0.866

$A_o$  = initial area of shear plane.

**PROGRAM III. CALCULATIONS FOR KEEPING  $\sigma \approx \sigma_f$  AFTER PEAK STRENGTH**

**Stage I. Calculation of  $K_4$  in equation (A54) \***

--- As a check while coding the program, enter first the storage register data at the side, and the values marked with an arrow ( $\leftarrow$ ) during coding.

--- To code the program, **press** MODE EXP; SHIFT III

Step	Key	Variable	Example
01	ENT	$\delta_{pf}$ (div)	64 $\leftarrow$
02	$\div$		64.000
03	Kout 1	$K_1$	0.726
04	+		88.191
05	ENT	$\delta_{pf}$ (div)	500 $\leftarrow$
06	-		588.191
07	Kout 3	$K_3$	14.040
08	=		574.151
09	$\div$		574.151
10	(		(01 0.
11	1		1
12	-		1.000
13	ENT	$\delta_{xf}$ (cm)	0.552 $\leftarrow$
14	x		0.552
15	Kout 2	$S_a$	0.124
16	)	$F_{af}$	0.931
17	=	$K_4$	616.447
18	K in 6		616.447
19	SHIFT RTN		616.447

Sample storage data

**Press** MODE 7 3; MODE .

Register	Variable	Example
K1	$K_1$ (Form F)	0.7257
K2	$S_a$ (Form F)	0.1243
K3	$K_3$ (Form F)	14.04
K5	$K_2$ (Form F)	14.04
	(for Program IV)	

$$* K_4 = \frac{\delta_{pf} + \delta_{af} / K_1 - K_3}{F_{af}} \quad (A54)$$

where

$$F_{af} = 1 - S_a \delta_{xf} \quad (A55)$$

and other symbols are as defined after equations (2.16) to (2.20).



**PROGRAM IV. CALCULATIONS FOR KEEPING  $\sigma \approx \sigma_f$  AFTER PEAK STRENGTH**

**Stage II. Calculation of reading  $\delta_q$  of device for measuring  $Q$  using equation (A56)\***

--- As a check while coding the program, enter first the storage register data at the side, and the values marked with an arrow ( $\leftarrow$ ) during coding.

--- To code the program, **press** MODE EXP SHIFT IV

Step	Key	Variable	Example
01	ENT	$\delta_x$ (cm)	2.087 $\leftarrow$
02	x		2.087
03	-1		-1
04	x		-2.087
05	Kout 2	$S_a$	0.124
06	+		-0.259
07	1		1
08	=	$F_a$	0.741
09	x		0.741
10	Kout 6	$K_4$	616.447
11	-		456.532
12	ENT	$\delta_p$ (div)	350 $\leftarrow$
13	+		106.532
14	Kout 5	$K_2$	14.040
15	=		120.572
16	x		120.572
17	Kout 1	$K_1$	0.726
18	=	$\delta_q$ (div)	87.499
19	SHIFT RTN		87.499

Sample storage data

**Press** MODE 7 3 ; MODE .

Register	Variable	Example
K1	$K_1$ (Form F)	0.7257
K2	$S_a$ (Form F)	0.1243
K3	$K_3$ (Form F)	14.04
K5	$K_2$ (Form F)	14.04
K6	$K_4$ (Program III)	616.447

\* From equations (2.16) and (A54),

$$\delta_q = K_1 F_a \left( K_4 - \frac{\delta_p - K_2}{F_a} \right)$$

or

$$\delta_q = K_1 (K_4 F_a - \delta_p + K_2) \dots\dots (A56)$$

where  $F_a$  is given by equation (2.17), and other symbols are as defined after equations (2.16) to (2.20).

## REFERENCES

- Aybak, T. (1988). *Improved measurement of shear strength in the in situ wedge shear test*. MS thesis, Middle East Technical University (METU), Ankara.
- Bishop, A.W. & Henkel, D.J. (1962). *Measurement of soil properties in the triaxial test*, p.192. London: Edward Arnold.
- British Standards Institution. (1975). *Methods of test for soils for civil engineering purposes*, BS 1377. London: BSI.
- Cascini, L. (1980). Su alcune prove eseguite con l'Iswest. *Riv. Ital. Geotecn.* **14**, No.1, 63-69.
- Cascini, L. (1983). Alcune osservazioni sulla tecnica Iswest. *Riv. Ital. Geotecn.* **17**, No.1, 19-25.
- Cascini, L. (1985). Un esempio di utilizzazione della tecnica Iswest. *Riv. Ital. Geotecn.* **19**, No.3, 161-167.
- Cascini, L. (1988). Private communication.
- Cascini, L. (1992). Discussion. *Géotechnique* **42**, No. 4, 645-648.
- Charles, J.A. & Watts, K.S. (1980). The influence of confining pressure on the shear strength of compacted rockfill. *Géotechnique* **30**, No. 4, 353-367.
- Esu, F. (1966). Short-term stability of slopes in unweathered jointed clays. *Géotechnique* **16**, No. 4, 321-328.
- Fredlund, D.G. & Rahardjo, H. (1993). *Soil mechanics for unsaturated soils*. New York: Wiley.
- Gökalp, A. (1994). *Investigation of certain problems related with the wedge shear test*. MS thesis, METU, Ankara.
- Gün, F. (1997). *Comparison of the shear strength of statically and dynamically compacted clays*. MS thesis, METU, Ankara.
- Kennard, M.F., Lovenbury, H.T., Chartres, F.R.D. & Hoskins, C.G. (1978). Shear strength specification of clay fills. *Proc. Conf. on Clay Fills*, London, 143-147.
- Khalili, N. & Khabbaz, M.H. (1998). A unique relationship for  $\chi$  for the determination of the shear strength of unsaturated soils. *Géotechnique* **48**, No. 5, 681-687.
- McGown, A., Radwan, A.M. & Gabr, A.W.A. (1977). Laboratory testing of fissured and laminated soils. *Proc. 9th Int. Conf. Soil Mech. Fdn Engng*, Tokyo **1**, 205-210.

- Mirata, T. (1974). The in situ wedge shear test -- a new technique in soil testing. *Géotechnique* **24**, No. 3, 311-332. Corrigenda: *Géotechnique* **24**, No. 4, 698; **25**, No. 1, 157-158; **36**, No. 1, 144; **37**, No. 3, 420; **38**, No.1, 163.
- Mirata, T. (1975). Expansible segments for support of test pit walls. *Proc. Istanbul Conf. Soil Mech. Fdn Engng* **1**, 291-297.
- Mirata, T. (1976). *Short-term stability of slopes in Ankara Clay*. PhD thesis, University of London.
- Mirata, T. (1979). Strength parameters for short term stability problems in stiff fissured unsaturated clays. *Proc. 7th European Conf. Soil Mech. Fdn Engng*, Brighton **3**, 113-114.
- Mirata, T. (1980). Potential of the in situ wedge shear test in landslide forecasting. *Proc. Int. Conf. on Engng for Protection from Natural Disasters*, Bangkok, 593-604.
- Mirata, T. (1981). *Laboratory wedge shear test*. Research report, Department of Civil Engineering, METU, Ankara.
- Mirata, T. (1990). *Developments in wedge shear testing of unsaturated clays and gravels*. Research report, Department of Civil Engineering, METU, Ankara.
- Mirata, T. (1991). Developments in wedge shear testing of unsaturated clays and gravels. *Géotechnique* **41**, No. 1, 79-100. Corrigenda: *Géotechnique* **41**, No. 2, 296; **41**, No. 4, 639; **42**, No. 4, end of p. 648.
- Mirata, T. (1992). Discussion. *Géotechnique* **42**, No. 4, 646-648.
- Mirata, T. & Gökalp, A. (1997). Discussion. *Géotechnique* **47**, No. 4, 887-889.
- Öktem, Ü.E. (1984). *Laboratory wedge shear test for the short term stability of clay fills*. MS thesis, METU, Ankara.
- Mirata, T., Gökalp, A., Şakar, M. (1998). Achieving higher normal stress levels in the prismatic wedge shear test. *Electronic Journal of Geotechnical Engineering*. <http://www.ejge.com/>
- Mirata, T., Varan M., Seçkin, A, Gün, K.F. (1999). Applications of the cylindrical wedge shear test to the study of shear strength of undisturbed and compacted soils. *Electronic Journal of Geotechnical Engineering*. <http://www.ejge.com/>
- Seçkin, A. (1993). *Further study of shear strength measured in the cylindrical wedge shear test*. MS thesis, METU, Ankara.

- Skempton, A.W. (1954). Pore pressure coefficients A and B. *Géotechnique* **4**, No. 4, 143-147.
- Şakar, M. (1997). *Wedge shear testing of clayey gravels under higher normal stresses*. MS thesis, METU, Ankara.
- Tosun, H., Mirata, T., Mollamahmutoğlu, M., Çolakoğlu, N.S. (1999). Shear strength of gravel and rockfill measured in triaxial and prismatic wedge shear tests. *Electronic Journal of Geotechnical Engineering*. <http://www.ejge.com/>
- Vallejo, E.L. (1987). The influence of fissures in a stiff clay subjected to direct shear. *Géotechnique* **37**, No. 1, 69-82.
- Varan, M. (1989). *Use of the cylindrical wedge shear test for the compaction control of clay fills*. MS thesis, METU, Ankara.
- Vaughan, P.R., Hight, D.W., Sodha, V.G. & Walbancke, H.J. (1978). Factors controlling the stability of clay fills in Britain. *Proc. Conf. on Clay Fills*, London, 205-217.

## ABBREVIATIONS

col.	column
crs	centres
cylwest	cylindrical wedge shear test
detl.	detailed output
dia.	diameter
div	division
ent.	enter data
Eq	equation
fl. pl.	failure plane
horiz.	horizontal
incl.	inclination
iswest	in situ wedge shear test
METU	Middle East Technical University
o/w	otherwise
port.	portable frame
priswest	prismatic wedge shear test
p/w	priswest
rad.	radius
sum.	summary table only
triax.	triaxial compression machine

## INDEXES

### Index of boxes

Box	Page	Box	Page	Box	Page
4.1	87	4.3	90	5.2	105
4.2	89	5.1	104	5.3	113

### Index of definition of program variables

VARIABLE	PAGE	ROW	COL.
A	28	7	33
AC	34		23
ACNB	34		24
ACONST	38		
AL	28	7	17
ALFA	46	10	
ALFN	28	7	1
ALFN	42	8	1
ALFNOC	42	8	17
ALPHA	36		55
ALPHAR	36		56
AMPL1L	31	11	9
ANGLQ	35		48
ANPQIN	30	9	41
ANSAVP	35		51
APG	28	2	57
ASPBL1	42	4	41
ASPBL2	42	4	57
AVPRST	36		53
B	28	7	25
BETABC	34		2
BEXPNT	38		
CGDISR	30	10	57
CLRNCE	31	11	41
CLRNCE	42	9	9
COFCOR	38		
COHESN	38		
CONDES	30	9	65
CONDX	28	3	17
CONDY	28	3	25
CONRPB	28	3	41
CONYMP	28	3	33
D	28	7	41
D1	29	8	25
D1	42	8	57
D2	29	8	33
D2	42	8	65
D3	29	8	41
D3	42	9	1
DBPI	27	2	41
DCLPSB	41	4	1
DCOMPU	48		
DDENSL	33	16	
DECLYK(I)	44	12	65
DEFSUP(I)	32	12	55
DENSOL	27	2	49
DENSTL	33	1	
DENSWD	46	2	
DETMDM	29	8	1
DEVIB	35		31
DEVIBA	35		30
DEVIBT	35		32
DEVJNR	35		34
DEVNB	35		36
DEVREC(I)	48		30

VARIABLE	PAGE	ROW	COL.
DEVRPT	35		33
DEVVPI	35		35
DGR	36		57
DH	29	8	65
DH	43	9	25
DH	46	12	
DH1	47	19	
DH2	43	9	33
DIAIN	42	8	9
DIAOUT	43	11	1
DIAROD	30	10	41
DIASSTB	28	3	9
DIFMOM	34		29
DIVPRP	41	2	65
DIVPRQ	28	3	65
DOITRM	47	14	
DP	34		26
DPG	28	2	65
DRPB	35		43
DRPB(I)	31	12	33
DRPB(I)	44	12	33
DSB	33	4	
DSPBL1	42	4	49
DSPBL2	42	4	65
DTMLP2	35		42
DTMLP2(I)	31	12	25
DTMLP2(I)	44	12	25
DVOVDU	36		54
DVRP	46	3	
DXABS	35		40
DXABS(I)	31	12	9
DXABS(I)	44	12	9
DY1ABS	35		41
DY1ABS(I)	31	12	17
DY1ABS(I)	44	12	17
ERUABS	35		37
EXTASC	31	11	49
FRCOEF	27	2	33
GR(I)	32	12	41
GRADQ(I)	32	12	67
GRDQC	35		47
GRINL	41	2	49
GRSBAL	48		47
GRSLO	41	2	57
GS	31	11	33
GS	43	10	9
GS(AS)	33	16	
GS(MD)	33	16	
H2	41	3	17
HDISC	42	8	49
HEMPTY	42	8	41
HIGHDX	40		2
HIGHDY	40		4
HIGHTL	40		6
HOURL(I)	31	12	1

VARIABLE	PAGE	ROW	COL.
HTFSPB	41	4	9
HTFSB	41	4	17
HTFYKS(I)	44	12	57
HTIPWM	30	11	1
HTLC	28	7	49
HTLOWR	43	11	9
HTLOWS	46	10	
HTMOLD	44	11	33
HTQPRP	28	3	49
HTROD	30	10	49
HTSPCR	30	16	
INDEX	34		17
INXDU	48		
IPARA(I)	31	12	8
IPARFL(I)	32	12	48
IPRSDX(I)	31	12	16
IPRSLP(I)	31	12	32
IPRSRP(I)	31	12	40
IPRSY1(I)	31	12	24
JTM	33	13	
L	33	11	
LYOK	42	4	25
MINUTE(I)	31	12	4
P	34		19
PARCUT	42	8	25
PARFPL	29	9	1
PARFPL	29	9	41
PARINC	47	14	
PARLAT	40	1	33
PAROUT	27	1	9
PARREG	27	1	17
PDATCH	27	1	1
PERSMA	47		26
PFIXDR	29	9	17
PFIXDR	43	9	49
PGRDG(I)	32	12	61
PGT45D	31	11	65
PHI	38		
PHILRG	38		
POISNR	27	1	49
PORINL	33	16	
PRCONQ	28	3	57
PSPBDL	43	9	57
PWQRTI	35		50
Q	36		8
RDGNUM	29	9	9
RDGNUM	43	9	65
RDGNUM	43	10	1
RM	46	12	
RMLC	46	1	
RMPR	46	2	
RMV	35		38
RODNUM	30	9	49
SATINL	33	16	
SECMOM	47		25

**Index of definition of program variables (continued)**

VARIABLE	PAGE	ROW	COL.
SIG	38		
SLATLD	35		44
SLATLD(I)	32	12	49
SLRHC	33	13	
SOVERN	34		11
SOVRNB	34		12
SPBAL1(I)	44	12	49
SPBAL2(I)	44	12	69
SPRCON	30	9	57
SS	34		7
SSAVP	35		52
SSNB	34		8
SW	47	13	
T	34		1
T(IMAXP)	36		74
TAUF	38		
TETA	28	7	9
THETA	33	10	
TIMACT	40		1
TKNESS	27	2	1
TLOWDX	40		3
TLOWDY	40		5
TLOWTL	40		7
TLP1MN	27	2	9
TMOM	34		28
TMOMA	34		27
TMOMAH	44	11	65
TMOMAV	44	11	57
TMOMDM	41	3	33
TNNB	34		10
TNSAVE	34		9
TNSAVP	35		51
TNSMAX	34		13
TNSMIN	34		14
TO	29	8	49

VARIABLE	PAGE	ROW	COL.
TYPFRA	40	1	25
TYPQDV	27	1	33
TYPTST	27	1	41
U	34		4
UBAR	34		3
USTRN	34		21
V	34		6
VBAR	34		5
VOIDR	47	18	
VOIDRI	33	16	
VPI	29	8	9
VPIT	34		15
VPIT	43	9	17
VPITT	34		16
VPTI	29	8	17
VSTRN	34		22
W	33	10	
WADDTM	44	11	49
WATCON	31	11	25
WATCON	43	10	17
WBC	27	2	25
WCINL	47	14	
WCOMPS	31	11	17
WD	46	10	
WDM	29	7	65
WHJ	28	3	1
WHJ	41	3	9
WINPUT	30	10	1
WLC	29	7	57
WLP	27	2	17
WLP1	41	2	1
WLP2	41	2	9
WPR	41	3	1
WQ	27	1	25
WQNC	35		49

VARIABLE	PAGE	ROW	COL.
WS	46	10	
WSPPTM	42	8	33
WTFLOW	31	11	57
WTM	46	10	
WTMC	46	13	
WTMEMP	44	11	41
WYK	42	4	33
X1	30	10	9
X1C	33	10	
X1C	47	18	
X1Q	30	10	25
XBARQT	33	13	
XBARQT	43	11	17
XBARS	46	10	
XBARTM	46	10	
XBRTMC	46	13	
XFC	48		58
XFORCE	36		9
XSBTPQ	30	9	25
XTMO1	47	18	
Y1	30	10	17
Y1C	33	11	
Y1C	47	18	
Y1Q	30	10	33
YBARQT	33	13	
YBARQT	44	11	25
YBARS	46	12	
YBARTM	46	12	
YBRTMC	47	13	
YFORCE	36		10
YSBTPQ	30	9	33
YTMO1	47	18	
ZEROF	29	8	57

**Index of definition of symbols**

Symbol	Page	Symbol	Page	Symbol	Page	Symbol	Page
$A_c$	15	$A_{s2}$	53	$C_q$	18	$D_o$	43
$A_{cp}$	145	$a$	38	$c$	2	$D_p$	52
$A_n$	20	$a_1$	113	$c'$	1	$D_{pg}$	49
$A_o$	159	$B$	4	$D$	14	$D_r$	50
$A_p$	52	$b$	15	$D_b$	148	$D_{s1}$	53
$A_{pg}$	49	$b_1$	38	$D_i$	15	$D_{s2}$	53
$A_r$	50	$C_F$	1	$D_{is}$	79	$D_u$	144
$A_{s1}$	53	$C_p$	18	$D_n$	149	$D_{u1}$	144

**Index of definition of symbols (continued)**

Symbol	Page	Symbol	Page	Symbol	Page	Symbol	Page
$D_1$ to $D_3$	60	$h_{pp}$	21	$s$	6	$Y$	14
$d$	15	$h_r$	58	$t$	27	$Y'$	147
$d_{ax}$	21	$h_s$	146	$u$	15	$y_{A11}$	150
$d_e$	145	$h_1$	50	$u_w$	1	$y_{sp}$	50
$d_{mx}$	21	$h_2$	27	$\bar{u}$	16	$\bar{y}$	51
$d_{my}$	21	$I$	144	$\bar{u}_1$	17	$\bar{y}_q$	51
$d_r$	58	$i$	155	$v$	15	$\bar{y}_{q1}$	147
$d_{yb}$	21	$J$	144	$\bar{v}$	16	$\bar{y}_s$	146
$d_1$	148	$K_1$ to $K_3$	18	$W$	14	$\bar{y}_{sx}$	147
$d_2$	148	$K_4$	156	$W_a$	44	$\bar{y}_t$	145
$d_3$	29	$L_y$	58	$W_{BC}$	14	$\bar{y}_{tp}$	51
$d_4$	29	$L_1$ to $L_6$	111	$W_{LP}$	14	$\bar{y}_1$	147
$E$	144	$L_7$ to $L_{22}$	112	$W_q$	152	$z$	143
$F_a$	18	$M$	146	$W_{qn}$	14	$\alpha$	15
$F_{af}$	18	$M_{ah}$	44	$W_{tp}$	50	$\alpha_i$	17
$F_s$	6	$M_{av}$	44	$w$	1	$\alpha_n$	15
$f$	142	$M_b$	14	$w_L$	1	$\alpha_{no}$	17
$f_{2s}$	142	$M_1$	79	$w_P$	1	$\alpha_r$	17
$G_{pg}$	49	$N_r$	149	$\bar{w}$	143	$\beta$	13
$G_r$	50	$n$	155	$X$	14	$\Delta h$	50
$G_s$	31	$n_c$	13	$X'$	147	$\Delta P$	19
$G_{y1}$	53	$n_d$	79	$x_{A11}$	150	$\Delta Q$	19
$G_{y2}$	53	$n_s$	79	$x_b$	41	$\Delta \bar{x}$	148
$h$	33	$P$	14	$x_h$	44	$\Delta y_{MP}$	49
$h_b$	117	$P_c$	144	$x_{sp}$	50	$\Delta y_P$	33
$h_c$	79	$P_{pg}$	49	$\bar{x}$	51	$\Delta y_{RB}$	49
$h_{cg}$	58	$Q$	14	$\bar{x}_q$	51	$\Delta y_{sh}$	147
$h_{di}$	145	$Q_f$	18	$\bar{x}_{q1}$	147	$\Delta \bar{y}$	148
$h_{ds}$	146	$Q_1 ; Q_2$	53	$\bar{x}_s$	146	$\Delta \sigma$	19
$h_l$	145	$r$	155	$\bar{x}_{sy}$	147	$\delta_p$	18
$h_m$	22	$S$	14	$\bar{x}_t$	145	$\delta_{pf}$	18
$h_{np}$	21	$S_a$	21	$\bar{x}_{tp}$	51	$\delta_q$	18
$h_{og}$	147	147	1	$\bar{x}_1$	147	$\delta_{pf}$	18



### Index of definition of symbols (continued)

Symbol	Page	Symbol	Page	Symbol	Page	Symbol	Page
$\delta_x$	15	$\delta\sigma/\sigma$	26	$\sigma_{\min}$	142	$\phi'$	
$\delta_{x0}$	148	$\theta$	14	$\sigma_{\text{mxt}}$	145	$\psi$	142
$\delta_y$	15	$\theta_r$	16	$\sigma'$	3	$\psi_a$	149
$\delta_{y0}$	148	$\lambda_q$	14	$\sigma_3$	1	$\psi_h$	97
$\delta h$	53	$\lambda_1$	51	$\sigma_1'$	9	$\psi_u$	144
$\delta h_1$	53	$\mu$	14	$\sigma_3'$	9	$\psi_1$	148
$\delta h_2$	53	$\nu$	27	$\tau$	14	$\psi_2$	149
$\delta M_q$	146	$\rho$	79	$\tau_f$	9	$\psi_{2s}$	142
$\delta X_q$	14	$\sigma$	14	$\phi$	2	$\psi_{2us}$	144
$\delta Y_q$	14	$\sigma_f$		$\phi_{\text{pw}}$	7		
$\delta\theta$	14	$\sigma_{\max}$	142	$\phi_{\text{tr}}$	7		

### Index of equations

Equation	Page	Equation	Page	Equation	Page
2.1 - 2.5	14	3.3; 3.4	52	A21 - A25	146
2.6 - 2.11	15	3.5; 3.6	53	A26 - A30	147
2.12 - 2.15	17	3.7; 3.8	53	A31 - A37	148
2.16 - 2.20	18	4.1; 4.2	79	A38 - A45	149
2.21	19	A1 - A7	142	A46 - A53	150
3.1	49	A8 - A13	144	A54; A55	160
3.2	50	A14 - A20	145	A56	161

### Index of figures

Figure	Page	Figure	Page	Figure	Page	Figure	Page
1.1	9	2.3	24	4.1	95	4.10	101
1.2	10	2.4	25	4.2; 4.3	96	5.1	117
1.3	11	3.1	57	4.4; 4.5	97	5.2	118
1.4	12	3.2	58	4.6	98	5.3	119
2.1	22	3.3	59	4.7; 4.8	99	5.4	120
2.2	23	3.4; 3.5	60	4.9	100	5.5	121

**Index of figures (continued)**

Figure	Page	Figure	Page	Figure	Page	Figure	Page
5.6; 5.7	122	5.13	128	5.19	134	5.25	140
5.8	123	5.14	129	5.20	135	5.26	141
5.9	124	5.15	130	5.21	136	A1	143
5.10	125	5.16	131	5.22	137		
5.11	126	5.17	132	5.23	138		
5.12	127	5.18	133	5.24	139		

**Index of forms**

Form	Page	Form	Page	Form	Page
1	55	B	152	E	155
2	56	C	153	F	156
A	152	D	154	G	157

**Index of notes**

Note	Page	Note	Page	Note	Page
1; 2	48	16 - 20	51	36 - 42	54
3 - 6	49	21 - 28	52	43 - 46	92
7 - 15	50	29 - 35	53	47, 48	93

**Index of tables**

Table	Page	Table	Page	Table	Page	Table	Page
2.1	21	3.4	36	3.8	40	4.1	94
3.1	27	3.5	38	3.9	45	5.1	111
3.2	33	3.6	38	3.10	46		
3.3	34	3.7	40	3.11	47		